RHEOLOGICAL CHARACTERISATION OF THERMALLY HYDROLYSED WASTE ACTIVATED SLUDGE

A thesis submitted in fulfilment of the requirements for the degree of Doctor of Philosophy

Kevin Hii

B. Eng. (Chemical), RMIT University

School of Engineering

College of Science, Engineering and Health

RMIT University

May 2019

DECLARATION

I certify that except where due acknowledgement has been made, the work is that of the author alone; the work has not been submitted previously, in whole or in part, to qualify for any other academic award; the content of the thesis is the result of work which has been carried out since the official commencement date of the approved research program; any editorial work, paid or unpaid, carried out by a third party is acknowledged; and, ethics procedures and guidelines have been followed.

I acknowledge the support I have received for my research through the provision of an Australian Government Research Training Program Scholarship.

Kevin Hii

April 2019

ACKNOWLEDGEMENT

I would like to express sincere gratitude to my senior supervisor Associate Prof. Nicky Eshtiaghi for her dedicated support and encouragement throughout my PhD candidature, going above and beyond in providing guidance and mentorship.

Additionally, I would like to thank the rest of my supervisory team, Professor Rajarathinam Parthasarathy, Dr. Saeid Baroutian and Dr. Daniel Gapes for their insight and advice throughout the research project.

Special thanks go to the administrative staff from the School of Engineering and technical staff in the Rheology and Materials Processing laboratory, including Dr. Muthu Pannirselvam and Dr. Babu Iyer, for ensuring a safe and healthy journey throughout my candidature. Also, I would like to thank RMIT University for support through APA scholarship.

Furthermore, I would like to thank my fellow PhD colleagues, including Tharaka Bandara, Xuran Du, Md Sakinul Islam, Ehsan Farno, Flora Markis, Veena Bobade, Samira Miryahyaei, Navid Moghadam and Tanmoy Das for their help and encouragement.

Additional thanks go to Patrick Morison, Gurmanpreet Kaler, and Kubra Isguder for providing me the opportunity to support and supervise their journey into the world of research, but more importantly for their assistance in data collection and experimental work.

Mostly, I give thanks to the Universe for boundless Grace; the pioneers who have come before; and my family and friends for their continued support and unconditional love.

PUBLICATIONS

JOURNAL PAPERS

1. **Hii, K.,** Baroutian, S., Parthasarathy, R., Gapes, D. J., & Eshtiaghi, N. (2014). "A review of wet air oxidation and thermal hydrolysis technologies in sludge treatment." Bioresource technology, 155, 289-299
2. **Hii, K.,** Baroutian, S., Parthasarathy, R., Gapes, D. J., & Eshtiaghi, N. (2017). "Rheological measurements as a tool for monitoring the performance of high pressure and high temperature treatment of sewage sludge." Water Research, 114, 254-263
3. **Hii, K**., Farno, E., Baroutian, S., Parthasarathy, R., Eshtiaghi, N., (2019). "Rheological characterization of thermal hydrolysed waste activated sludge." Water Research, 156, 445-455.

PEER-REVIEWED CONFERENCE PAPERS:

1. **Hii, K.,** Parthasarathy, R., Baroutian, S., Gapes, D. J., Eshtiaghi, N., "Hydrothermal Processing of Sludge – A Review", Chemeca, 29Sept.-2nd Oct., Brisbane, Australia 2013
2. **Hii K.,** Parthasarathy, R., Baroutian, S., Gapes, D. J., Eshtiaghi, N., "Changes in waste activated sludge viscosity during thermal treatment", Chemeca Conference 2016, Paper no. 3403844.

CONFERENCE PRESENTATIONS

1. **Hii, K.,** Parthasarathy, R., Baroutian, S., Gapes, D. J., Eshtiaghi, N., "Viscosity of Waste Activated Sludge Under High Temperature and High Pressure Conditions", CHEMECA 2014 Conference, Perth, Australia.
2. **Hii, K.,** Parthasarathy, R., Baroutian, S., Gapes, D. J., Eshtiaghi, N., "Viscosity change of thickened waste activated sludge during thermal hydrolysis", WETT 2015 Water Research Symposium, RMIT University, Melbourne, Australia.
3. **Hii K.,** Parthasarathy, R., Baroutian, S., Gapes, D. J., Eshtiaghi, N., "Changes in waste activated sludge viscosity during thermal treatment", Chemeca Conference 2016, Adelaide, Australia.

4. **Hii K.,** Parthasarathy, R., Baroutian, S., Gapes, D. J., Eshtiaghi, N., "Thermal hydrolysis of secondary sewage sludge and viscosity decrease", 13th IWA Specialized Conference on Small Water and Wastewater Systems, 2016, Athens, Greece.
5. **Hii, K.,** Parthasarathy, R., Baroutian, S., Gapes, D. J., Eshtiaghi, N., "Viscosity reduction of waste activated sludge during thermal hydrolysis", WETT 2016 Water Research Symposium, RMIT University, Melbourne, Australia.
6. **Hii K.,** Parthasarathy, R., Baroutian, S., Gapes, D. J., Eshtiaghi, N., "Viscous behaviour of thickened waste activated sludge during thermal hydrolysis processes", Chemeca Conference 2017, Melbourne, Australia

NOMENCLATURE

COD	chemical oxygen demand (mg/L)
E	FKV model spring constant (Pa)
E_1	FKV model fractional modulus (Pa.s$^{\alpha}$)
E_2	FKV model elastic modulus (Pa).
E_α	Mittag-Leffler function of order α
G'	storage modulus (Pa)
G''	loss modulus (Pa)
k	consistency index (Pa.s^{n})
n	power index for Herschel-Bulkley model
rsCOD	released
S_x	shift factor in the x-axis for master curve
S_y	shift factor in the y-axis for master curve
T	temperature (°C)
TS	total solids concentration (wt%)
t	time (s).
$_0$	parameters of untreated sludge at 25 °C
$_7$	parameters of 7 wt% sludge.
$_f$	parameters of thermally-treated sludge at 25 °C
$_i$	denotes values measured in situ, at elevated conditions
α	FKV model fitting constant (-)
$\dot{\gamma}$	shear rate (s^{-1})
γ	strain (-)
$\eta(\dot{\gamma})$	steady-shear viscosity (Pa.s)
$\eta^*(\omega)$	complex viscosity (Pa.s)
$\eta'(\omega)$	dynamic viscosity (Pa.s)
η_∞	high-shear viscosity (Pa.s)
σ	shear stress (Pa)
σ_c	yield stress (Pa).
τ	respondence time (s)
ω	angular velocity (rad/s)
Γ	*dimensionless shear rate,* $\Gamma = (\eta/\sigma_c).\dot{\gamma}$ (-)

SUMMARY

Hydrothermal sludge processing is a branch of sludge treatment technologies finding increased adoption in modern sewage treatment processes. These technologies involve the use of elevated temperature conditions to desirably alter sludge characteristics in the liquid phase. Benefits of these processes, such as thermal hydrolysis pre-treatment, include increased biogas production during anaerobic digestion, improved sludge dewaterability, sterilization of sludge, and improved transport operations due to desirable rheological enhancements. Sludge rheology plays a significant role in the design and operation of these sludge-handling processes. Despite this, rheological studies related to sludge in hydrothermal processing conditions is very scarce. Therefore, a better understanding of sludge's rheological properties, especially at the high temperature conditions encountered during hydrothermal processing is required for better optimization of these processes.

This study investigates the rheological characteristics of thickened waste activated sludge (WAS) in thermal hydrolysis (TH) processes. Using in-situ rheometric measurements, changes in the sludge's flow properties due to the impact of treatment conditions (temperature, time, and sludge concentration) were examined. These changes were related to the solubilisation of sludge organics, measured by the chemical oxygen demand (COD) of sludge. Based on these observations, equations were derived to predict the rheological properties of sludge at various conditions of TH and its link to COD. Furthermore, the viscoelastic properties of the thickened, untreated and thermally-treated sludges were studied in order to characterize sludge's solid-like properties. A correlation was proposed to associate sludge's viscoelastic data to flow curve data such that oscillatory measurement techniques could be used to collect steady-shear data which are traditionally obtained via rotational measurement.

In-situ rheological measurements revealed WAS behaved as a shear-thinning, yield stress fluid which could be described by the Herschel-Bulkley model. Despite elevated treatment temperatures (80 – 140 °C), Newtonian flow behaviour was not observed at any time in the sludge. The flow behaviour of the sludge at all treatment conditions examined could be described by a single master curve. This means sludge's flow behaviour was governed by a similar network of physical interactions regardless of its concentration or treatment conditions. As a result of TH, the apparent viscosity, η, and Herschel-Bulkley rheological parameters (yield stress, σ_c, and consistency index, k) were reduced irreversibly. The extent of this reduction followed a linear relationship with treatment temperature. The in-situ values of η, σ_c, and k

were up to 92% lower compared to measurements after the thermally-treated sludge is cooled to ambient temperature.

In-situ measurements also showed that η, σ_c, and k reduced gradually during TH at constant temperature, following a logarithmic relationship with treatment duration. This meant the solubilization effects of TH were a time-dependent process. At constant time, reduction of η, σ_c, and k in situ were described by a linear relationship with increasing sludge temperature (80 – 140 °C). At constant treatment time and temperature, η, σ_c, and k were increased with sludge concentration (7 – 13 wt%) following a power-law relationship. The effectiveness of sludge solubilisation during TH was not impacted by varying sludge concentrations, since the reduction of η, σ_c, and k were nearly constant between the different sludge concentrations.

The solubilisation of sludge organics also followed a logarithmic time-dependent behaviour as shown by increasing values of COD in the soluble phase of the sludge during TH. This increase in sludge's soluble COD (sCOD) indicated that the rheological changes observed during TH were due to the disintegration of sludge's network structure. Accordingly, linear correlation existed between the reduction of rheological parameters (η, σ_c, and k) and the increase in sCOD. This correlation indicates the rheological measurement of sludge in situ can be used as a means to monitor the performance of hydrothermal processes.

Viscoelastic measurements of the untreated and thermally treated sludges revealed gel-like behaviour in the linear viscoelastic region. The frequency and creep response of the sludges were described using a fractional Kelvin-Voigt model (FKV). With increasing treatment temperatures, the storage (G') and loss (G'') moduli were reduced linearly, further indicating a weakening of structural components in the sludge, such as extracellular polymeric substances. This is reflected in the decreasing value of energy of cohesion, E_c which describes the strength of the three-dimensional sludge network.

Viscoelastic data, as obtained from dynamic oscillatory measurements of the sludge could be related to the flow curve data of the sludge, as obtained via steady-shear measurements. A modified Cox-Merz relationship related the complex viscosity, $\eta^*(\omega)$, to the steady shear viscosity, $\eta(\dot{\gamma})$, by applying shift factors. More notably, raw values of dynamic viscosity, $\eta'(\omega)$, were nearly equal to $\eta(\dot{\gamma})$ at equivalent shear rates. This meant that oscillatory measurement could readily describe steady-shear, flow data. Besides that, the yield stress of the sludge could also be estimated from the above shift factors and values of G'.

Finally, the engineering implications of this observations and results in this study were discussed, highlighting the significance of correct determination of rheological parameters which are needed in the design and operation of unit operations.

TABLE OF CONTENTS

LIST OF FIGURES

LIST OF TABLES

CHAPTER 1: INTRODUCTION

1.1 PROJECT RATIONALE

Sewage and wastewater treatment operations are a vital part of any large city and play an important role in ensuring the city's sustainable growth and environmental performance. However, increasing urban populations means that wastewater treatment plants (WWTPs) are receiving increasingly larger volumes of wastewater. Subsequently, this leads to increasingly large volumes of wastewater sludge which must be disposed. Sludge management (treatment and disposal) has become an essential component in WWTPs, representing 30-40% capital costs and 50% operating costs (Pilli et al., 2015; Ruffino et al., 2015). However, due to increasingly stringent environmental regulations traditional sludge disposal routes, such as landfilling, are quickly becoming unsustainable. This necessitates applying new strategies and technologies to reduce their amount being landfilled.

Hydrothermal processing is one branch of technologies which has become increasingly favourable for the pre-treatment, treatment and conversion of sludge. These involve the use of elevated temperature and pressure conditions under aqueous conditions to achieve various improvements of sludge characteristics. Hydrothermal processing of organic wastes has three major objectives based on application: (i) enhancement of methanogenic energy production (Baroutian et al., 2012), (ii) degradation and removal of organic compounds from waste and reduction of mass and volume of solid wastes (Strong and Gapes, 2012), and (iii) recovering valuable compounds (Strong et al., 2011; Suárez-Iglesias et al., 2017; Yoshida et al., 2003). In conventional sludge treatment via anaerobic digestion, the implementation of hydrothermal processing, such as thermal hydrolysis pre-treatment (100 - 180 °C), can lead to significant improvements including: increased biogas production (Camacho et al., 2008); improved sludge rheological characteristics (Bougrier et al., 2008); enhanced dewaterability (Neyens and Baeyens, 2003); and positive net energy production in the sludge treatment process (Carrere et al., 2008; Chen et al., 2012; Pérez-Elvira et al., 2008; Sapkaite et al., 2017).

However, despite numerous studies on various aspects of hydrothermal processing technologies, there is a distinct lack of literature about sludge rheology in these processes. An understanding of the hydrodynamic behaviour and rheological properties of sludge is of great importance to the optimization and design of sludge handling processes as noted by several researchers including Bhattacharya (1981), Slatter (2008), Baudez and Coussot (2001), and Mori et al. (2006). Sludge rheological properties such as viscosity, yield stress, and viscoelasticity are design parameters used in heat and mass transfer operations (Pereboom et al., 2014; Seyssiecq et al., 2003), mixing and power requirements (Yang et al., 2009),

transport (Hammadi et al., 2012), dewatering (Lotito et al., 1997) and pumping (Anderson et al., 2008). Generally, the rheology of sludge at ambient conditions and low to moderate concentrations is well studied (Eshtiaghi et al., 2013; Ratkovich et al., 2013); however, their rheological behaviour at the elevated temperature and pressure conditions of hydrothermal processing is not understood (Barber, 2016). A fundamental understanding of the rheology in sludge hydrothermal processing can help to better optimize its design and operation and may potentially be useful for real-time monitoring of these processes.

The current thesis aims to investigate the rheological characteristics and solubilization of sludge during hydrothermal processing, particularly, with regards to the impact of temperature, treatment time, sludge concentration and sludge composition. The relationship between sludge rheological changes (e.g. yield stress, viscosity) and compositional changes (e.g. organic matter solubilization) are investigated, and the influence of treatment parameters (e.g. treatment time and temperature) are also studied. The expected outcome of the research is to develop predictive equations useful for estimation of sludge solubilization and rheological parameters at various sludge thermal treatment conditions, such that they can be used to monitor the performance of these processes.

1.2 PROJECT AIMS

As described previously, the primary objective of this research is the characterisation of sludge rheological behaviour in hydrothermal processing, particularly in non-oxidative temperature ranges of treatment (i.e. thermal hydrolysis, <180 °C), as well as their relation to sludge compositional changes. It is hoped that this improved understanding can lead to better implementation of hydrothermal processing and potentially be used as a method to monitor its performance. The research questions to be addressed are:

1. What is the impact of elevated temperature conditions on the rheological properties (e.g. flow behaviour, apparent viscosity, and yield stress) of thickened waste activated sludge, and how do these rheological parameters evolve as thermal hydrolysis treatment progresses?

2. What is the impact of increasing sludge solids concentration on the rheological behaviour of waste activated sludge during thermal hydrolysis?

3. What is the impact of thermal hydrolysis treatment on the flow behaviour and viscoelastic characteristics of the thermally-treated sludge, and can the viscoelastic properties be correlated with flow characteristics?

4. How is sludge composition changed during thermal hydrolysis, and how is it related to its rheological characteristics?

5. Why does the impact of elevated temperature conditions during thermal hydrolysis result in changes in rheological properties?

1.3 THESIS OUTLINE

Following this introductory chapter, a detailed literature review is presented in Chapter 2 regarding the background of hydrothermal processing technologies, studies on the rheological behaviour of sewage sludge, and studies on the rheology of sewage sludge in thermal treatment processes. The first part of this literature review was published as a peer-reviewed literature review in the Bioresource Journal (Vol: 155, pp: 289-299, 2014). The final part of this chapter presents the gaps of knowledge identified and the areas of investigation in the current research.

Chapter 3 describes the materials and methodology adopted throughout this study. Experimental considerations and rationale for the protocols adopted are discussed, where relevant. The preparation of sludge samples and its physical characterisation are described. The choice of equipment to perform rheological measurements and sludge thermal hydrolysis experiments are also discussed.

Chapter 4 presents the results and discussion addressing research questions 1, 4, and 5. In this chapter, waste activated sludge rheology was measured for the first time in situ at thermal hydrolysis conditions to show a directly the rheological changes sludge has undergone. The impact of treatment temperature and time were described, and rheological changes were correlated with changes in sludge composition. This chapter was published as a peer-reviewed original research paper in Water Research Journal (Vol:114, pp: 3 – 27, 2017).

Chapter 5 presents the results and discussion addressing, in particular, research question 2 but also 1, 3, and 5. In this chapter, the impact of increasing sludge concentrations on the rheological behaviour of waste activated sludge was investigated. A predictive model for estimating sludge rheological parameters

during thermal hydrolysis, which incorporates the impact of temperature, treatment time, and sludge concentration, is presented. The contents of this chapter are published jointly with contents of Chapter 6 in the Water Research Journal (accepted; doi.org/10.1016/j.watres.2019.03.039).

Chapter 6 addresses research question 3 for various concentrations of waste activated sludge. In this chapter, the impact of thermal hydrolysis on the viscoelastic properties thickened waste activated sludge were investigated. The compatibility between viscoelastic measurements and shear flow measurements for thickened sludge were also discussed. The contents of this chapter are published jointly with contents of Chapter 5 in the Water Research Journal (accepted; doi.org/10.1016/j.watres.2019.03.039).

Chapter 7 elaborates on the practical engineering applications of the results presented in this thesis. This chapter highlights how the rheological changes observed in this study can be related to engineering solutions in sludge-handling processes.

Chapter 9 summarizes the conclusions established in this work and their contributions to knowledge. Recommendations and perspectives for further work are also presented.

REFERENCES

Anderson, C.N., Hanna, D.J., Brotherton, R.H., Brower, G.R., Carthew, G.A., Mulbarger, M.C., Playford, W.C., 2008. Chapter 19 - System Design for Sludge Pumping, in: Jones, G.M., Sanks, R.L., Tchobanoglous, G., Bosserman, B.E. (Eds.), Pumping Station Design (Third Edition). Butterworth-Heinemann, Burlington, p. 19.1-19.29. doi:https://doi.org/10.1016/B978-185617513-5.50026-3

Barber, W.P.F., 2016. Thermal hydrolysis for sewage treatment: A critical review. Water Res. 104, 53–71. doi:10.1016/j.watres.2016.07.069

Baroutian, S., Andrews, J., Robinson, M., Smit, A.-M., McDonald, B., Wijeyekoon, S., Gapes, D., 2012. Variations in extractive compounds during hydrothermal treatment of lignocellulosic sludge. Chemeca 2012 Qual. life through Chem. Eng. 23-26 Sept. 2012, Wellington, New Zeal. 1452.

Baudez, J.-C., Coussot, P., 2001. Rheology of aging, concentrated, polymeric suspensions: Application to pasty sewage sludges. J. Rheol. (N. Y. N. Y). 45, 1123–1139. doi:10.1122/1.1392298

Bhattacharya, S.N., 1981. Flow characteristics of primary and digested sewage sludge. Rheol. Acta 20, 288–298.

Bougrier, C., Delgenès, J.P., Carrère, H., 2008. Effects of thermal treatments on five different waste activated sludge samples solubilisation, physical properties and anaerobic digestion. Chem. Eng. J. 139, 236–244. doi:10.1016/j.cej.2007.07.099

Camacho, P., Ewert, W., Kopp, J., Panter, K., Perez-Elvira, S.I., Piat, E., 2008. Combined experiences of thermal hydrolysis and anaerobic digestion – latest thinking on thermal hydrolysis of secondary sludge only for optimum dewatering and digestion. Proc. Water Environ. Fed. 2008, 1964–1978.

doi:10.2175/193864708788733972

Carrere, H., Bougrier, C., Castets, D., Delgenes, J.P., 2008. Impact of initial biodegradability on sludge anaerobic digestion enhancement by thermal pretreatment. J. Environ. Sci. Health. A. Tox. Hazard. Subst. Environ. Eng. 43, 1551–1555. doi:10.1080/10934520802293735

Chen, N., Liu, Y., Liu, N., Wang, S., 2012. Energy balance of thermal hydrolysis and anaerobic digestion on waste activated sludge BT - 2012 World Automation Congress, WAC 2012, June 24, 2012 - June 28, 2012 1–3.

Eshtiaghi, N., Markis, F., Yap, S.D., Baudez, J.C., Slatter, P., 2013. Rheological characterisation of municipal sludge: A review. Water Res. 47, 5493–5510. doi:10.1016/j.watres.2013.07.001

Hammadi, L., Ponton, A., Belhadri, M., 2012. Temperature effect on shear flow and thixotropic behavior of residual sludge from wastewater treatment plant. Mech. Time-Dependent Mater. 17, 401–412. doi:10.1007/s11043-012-9191-z

Lotito, V., Spinosa, L., Mininni, G., Antonacci, R., 1997. The rheology of sewage sludge at different steps of treatment. Water Sci. Technol. 36, 79–85. doi:http://dx.doi.org/10.1016/S0273-1223(97)00672-0

Mori, M., Seyssiecq, I., Roche, N., 2006. Rheological measurements of sewage sludge for various solids concentrations and geometry. Process Biochem. 41, 1656–1662. doi:10.1016/j.procbio.2006.03.021

Neyens, E., Baeyens, J., 2003. A review of thermal sludge pre-treatment processes to improve dewaterability. J. Hazard. Mater. 98, 51–67. doi:10.1016/S0304-3894(02)00320-5

Pereboom, J., Luning, L., Hol, A., van Dijk, L., de Man, A.W.A., 2014. Full scale experiences with TurboTec® continuous thermal hydrolysis at WWTP Venlo (NL) and Apeldoorn (NL), in: Proceedings of Aqua-Enviro 19th European Biosolids and Organic Residuals Conference and Exhibition, Manchester, UK.

Pérez-Elvira, S.I., Fernández-Polanco, F., Fernández-Polanco, M., Rodríguez, P., Rouge, P., 2008. Hydrothermal multivariable approach. Full-scale feasibility study. Electron. J. Biotechnol. 11. doi:10.2225/vol11-issue4-fulltext-14

Pilli, S., Yan, S., Tyagi, R.D., Surampalli, R.Y., 2015. Thermal pretreatment of sewage sludge to enhance anaerobic digestion: a review. Crit. Rev. Environ. Sci. Technol. 45, 669–702.

Ratkovich, N., Horn, W., Helmus, F.P., Rosenberger, S., Naessens, W., Nopens, I., Bentzen, T.R., 2013. Activated sludge rheology: A critical review on data collection and modelling. Water Res. 47, 463–482. doi:10.1016/j.watres.2012.11.021

Ruffino, B., Campo, G., Genon, G., Lorenzi, E., Novarino, D., Scibilia, G., Zanetti, M., 2015. Improvement of anaerobic digestion of sewage sludge in a wastewater treatment plant by means of mechanical and thermal pre-treatments: Performance, energy and economical assessment. Bioresour. Technol. 175, 298–308. doi:10.1016/j.biortech.2014.10.071

Sapkaite, I., Barrado, E., Fdz-Polanco, F., Pérez-Elvira, S.I., 2017. Optimization of a thermal hydrolysis process for sludge pre-treatment. J. Environ. Manage. 192, 25–30. doi:10.1016/j.jenvman.2017.01.043

Seyssiecq, I., Ferrasse, J.-H., Roche, N., 2003. State-of-the-art: rheological characterisation of wastewater treatment sludge. Biochem. Eng. J. 16, 41–56.

Slatter, P., 2008. Pipe flow of highly concentrated sludge. J. Environ. Sci. Heal. Part A 43, 1516–1520.

Strong, P.J., Gapes, D.J., 2012. Thermal and thermo-chemical pre-treatment of four waste residues and the effect on acetic acid production and methane synthesis. Waste Manag. 32, 1669–1677. doi:10.1016/j.wasman.2012.04.004

Strong, P.J., McDonald, B., Gapes, D.J., 2011. Combined thermochemical and fermentative destruction of municipal biosolids: A comparison between thermal hydrolysis and wet oxidative pre-treatment. Bioresour. Technol. 102, 5520–5527. doi:10.1016/j.biortech.2010.12.027

Suárez-Iglesias, O., Urrea, J.L., Oulego, P., Collado, S., Díaz, M., 2017. Valuable compounds from sewage sludge by thermal hydrolysis and wet oxidation. A review. Sci. Total Environ. 584–585, 921–934. doi:10.1016/j.scitotenv.2017.01.140

Yang, F., Bick, A., Shandalov, S., Brenner, A., Oron, G., 2009. Yield stress and rheological characteristics of activated sludge in an airlift membrane bioreactor. J. Memb. Sci. 334, 83–90. doi:10.1016/j.memsci.2009.02.022

Yoshida, Y., Dowaki, K., Matsumura, Y., Matsuhashi, R., Li, D., Ishitani, H., Komiyama, H., 2003. Comprehensive comparison of efficiency and CO2 emissions between biomass energy conversion technologies—position of supercritical water gasification in biomass technologies. Biomass and Bioenergy 25, 257–272.

CHAPTER 2: LITERATURE REVIEW

2.1 A REVIEW OF WET AIR OXIDATION AND THERMAL HYDROLYSIS TECHNOLOGIES IN SLUDGE TREATMENT.

Section 2.1 of this chapter was published in the journal Bioresource Technology

(Vol: 155, P: 289-299, 2014)

Keywords: Thermal hydrolysis; wet air oxidation; wastewater sludge; hydrothermal processing; sludge treatment

Hii, K, Baroutian, S, Parthasarathy, R, Gapes, D, and Eshtiaghi, N,. "A review of wet air oxidation and thermal hydrolysis technologies in sludge treatment." Bioresource technology 155 (2014): 289-299.

2.1.1 ABSTRACT

With rapid world population growth and strict environmental regulations, increasingly large volumes of sludge are being produced in today's wastewater treatment plants (WWTP) with limited disposal routes. Sludge treatment has become an essential process in WWTP, representing 50% of operational costs. Sludge destruction and resource recovery technologies are therefore of great ongoing interest. Hydrothermal processing uses unique characteristics of water at elevated temperatures and pressures to deconstruct organic and inorganic components of sludge. It can be broadly categorized into wet oxidation (oxidative) and thermal hydrolysis (non-oxidative). While wet air oxidation (WAO) can be used for the final sludge destruction and also potentially producing industrially useful by-products such as acetic acid, thermal hydrolysis (TH) is mainly used as a pre-treatment method to improve the efficiency of anaerobic digestion. This paper reviews current hydrothermal technologies, roles of wet air oxidation and thermal hydrolysis in sludge treatment, and challenges faced by these technologies.

2.1.2 INTRODUCTION

Today, rapid world population growth has increased the volume of sewage sludge produced from wastewater treatment plants (WWTP) whilst strict environmental regulations have limited their disposal (Eshtiaghi et al., 2013). The treatment of sludge has therefore become an essential part of today's WWTPs representing up to 50% of operational costs (Kroiss, 2004; Neyens and Baeyens, 2003; Spinosa and Vesilind 2001). As such, methods for sludge destruction and resource recovery are of ongoing interest. In sludge treatment, processing techniques which utilize the principles behind hydrothermal processing have been implemented for different purposes and accomplished different outcomes in the treatment line. Although these methods have achieved varying degrees of success, their relative simplicity and ease of implementation still make them attractive enough to further be investigated for improvement.

Hydrothermal processing refers to technologies involving reactions carried out in an aqueous solvent at elevated temperatures and pressures. This can not only degrade the waste but also potentially produce industrially useful by-products. Since the necessary reactions can be completed in the water phase, the need for removing water from the waste prior to processing is avoided (Baroutian et al., 2013a). Hydrothermal technologies in sludge treatment can be

broadly categorized into two main groups, oxidative techniques and non-oxidative techniques. Catalysts and chemicals may or may not be involved in both cases but the main difference between the techniques is the presence of oxidative agents and subsequently the end-products achieved (Strong et al., 2011). Wet air oxidation (WAO) is representative of the oxidative techniques, and it is usually carried out at high temperatures (>200 °C) in the presence of an oxidant. Non-oxidative techniques, such as thermal hydrolysis (TH), are usually undertaken at a lower temperature range (100 °C – 200 °C) without the addition of oxidants. Although these technologies can appear anywhere on the sludge treatment line, TH is normally used as a pre-treatment step before anaerobic digestion (AD) whereas WAO is used towards the end of the treatment line as a means of final sludge destruction. Although it is a well-proven process for sludge treatment, AD suffers from low efficiency associated with a rate-limiting hydrolysis reaction (Appels et al., 2008). By implementing TH pre-treatment, this hydrolysis step is effectively carried out in a separate reactor under optimal conditions provided by the TH process. Using high temperatures and pressures, the complex molecular compounds and cellular content of sewage sludge is broken down. This releases intracellular content and water, thus making the sludge more digestible. As a result, the digestion efficiency and biogas production during AD is improved. This is particularly effective when treating waste activated sludge that contains bacterial cells, which are not easily biodegradable (Chen et al., 2012). Waste activated sludge is known to be difficult to dewater (Neyens and Baeyens, 2003). Therefore, TH would also help for dewatering of waste activated sludge.

Whereas TH is mainly used as pre-treatment in the sludge treatment line, WAO can be used as the final step in complete sludge destruction. Wet air oxidation works by oxidizing organic and inorganic substances in an aqueous solution using air or oxygen, which is achievable at high temperatures and pressures. The result is that these substances are either broken down into simpler components or converted into water and carbon dioxide with complete oxidation. The technology is comparable with incineration other than the fact that it is completed in the aqueous phase, making it very useful for wastes which are too dilute for incineration, such as sewage sludge. In contrast to incineration however, harmful emissions such as nitrous oxides (NO_x) are not released and WAO can be used to treat toxic waste components. Furthermore, since the

extent of oxidation is controlled by the severity of operating conditions, the WAO can also be controlled to produce useful intermediate products such as acetic acid (Strong et al., 2011).

In the past decade, WAO and TH processes in waste treatment have been reviewed by different authors. For example, the WAO process has been reviewed for the treatment of aqueous wastes and industrial wastes by Debellefontaine and Foussard (2000) which covered topics including its history, industrial examples and reactor design. Similarly, Zou et al. (2007) have also reviewed WAO for waste treatment, covering topics such as catalysts and design. Appels et al. (2008) reviewed anaerobic digestion and briefly reviewed TH as a pre-treatment process. Carerre et al. (2010) also reviewed pre-treatment processes used to improve anaerobic digestion and presented TH as one of the methods. In addition, there are some useful review papers on different aspects of hydrothermal processing techniques (Table 2.1). However, no work has attempted to compare TH and WAO as hydrothermal processes implemented in sludge treatment. This paper presents an overview of the emergence and development of hydrothermal technologies specifically in the field of sludge treatment. In particular TH and WAO are compared, showcasing their fundamental differences in terms of process mechanisms, goals and end-products.

Table 2. 1 – Reviews on non-catalytic wet oxidation (WO) and thermal hydrolysis (TH). Published from 1995 to 2013.

Reference	Technology		Review highlights	Review gaps:
	WAO	TH		
Mishra et al., 1995	X		Industrial applications and miscellaneous applications.	Sludge treatment. Process parameters.
Debellefontaine et al., 1996	X		Oxygen transfer mechanisms, solubility and balance.	Sludge and biological wastes. WAO chemistry.
Foussard et al., 1997	X		Process development challenges.	
Luck, 1999	X		Technical features of various commercial processes. Advantages of catalytic WO.	Non-catalytic WAO.
Imamura, 1999	X		Correlations study on reactivity with carbon content.	Sludge and biological wastes.
Kolaczkowski et al., 1999	X		Kinetics and mass transfer. Industrial applications.	Process parameters.
Debellefontaine & Foussard, 2000	X		Kinetics and mass transfer. Reactor design. Industrial examples.	Non-European facilities.
Zarycki & Imbierowicz, 2001	X		Mathematical modelling. Industrial applications.	Mass transfer as a controlling phenomenon.
Maugans & Ellis, 2002	X		Process commercialization and commercial examples.	Technical aspects.
Oliviero et al., 2003	X		WAO of toxic nitrogen-containing compounds.	Nitrogenous compounds produced in WWTPs.
Neyens & Baeyens, 2003		X	Optimum treatment conditions.	Technical aspects and chemistry.
Bhargava et al., 2006		X	Chemistry and mechanisms of WAO.	Non-catalytic WAO of municipal sludge.
He et al., 2008	X	X	Production of useful chemicals via hydrothermal processing.	Discussion on WAO and TH.
Berardinelli et al., 2008	X		Catalytic and non-catalytic WAO.	Chemistry and technical aspects.
Zhu et al., 2011		X	WAO reaction mechanisms.	
Luan et al., 2012	X		Mechanism and kinetics of WAO. Treatment of refractory pollutants.	Sludge treatment.
Kang et al., 2013	X		Production of value-added chemicals.	Process chemistry.
Tyagi & Lo, 2013	X	X	Resource recovery from sludge. Major factors affecting processes. Advantages and drawbacks of processes.	Major focus not on hydrothermal treatment.

2.1.3 HYDROTHERMAL PROCESSING

The principles behind hydrothermal technologies have long been utilized in many fields and applications besides waste treatment. The term “hydrothermal reactions” has been defined as “any heterogeneous chemical reaction in the presence of a solvent (whether aqueous or non-aqueous) above room temperature and at pressures greater than 1 atm in a closed system (Byrappa and Yoshimura, 2001). However, in the context of this review, hydrothermal treatment generally refers to processes involving reactions carried out in water facilitated by high temperatures and high pressures conditions.

In sludge treatment, hydrothermal processing has four main goals: (i) enhancing anaerobic digestion process, (ii) degrading and removing organic compounds, (iii) reducing waste mass and volume and (iv) recovering valuable compounds (Baroutian et al., 2013a). Water plays an important role in hydrothermal sludge treatment where it not only acts as solvent for the sludge contents but is also a main reactant for the hydrolysis of the organic compounds in sludge (Toor et al., 2011; Brunner, 2009). At the high temperature and high-pressure conditions usually employed in hydrothermal processes, water has a high reactivity and is able to break the chemical bonds in complex molecules and convert them into simpler compounds. This is known as hydrolysis and follows the following reaction (Brunner 2009):

$$A - B + H - OH \rightarrow A - H + B - OH \qquad Eq.2.1$$

The main steps in WWTPs are generally a pre-treatment followed by primary and secondary treatment. During pre-treatment, coarse particles are separated from wastewater by screening. Primary sludge is produced in primary treatment when heavy compounds are settled by gravity in a primary settler. Secondary treatment involves biological treatment and produces a sludge which is highly organic and contains large amounts of microorganisms. The activated sludge process is the most popular method for secondary treatment and produces excess sludge known as waste activated sludge (WAS), which is an aquatic culture of bacteria and other living organisms. It also contains extracellular polymeric substances (EPS) produced by microorganisms in the sludge. The EPS are three-dimensional, gel-like, highly hydrated and often charged biofilm matrices that can be used to accumulate the microorganisms and cells into aggregates known as flocs. The term EPS is generally used to describe a variety of classes of macromolecules found to occur on the cell surface of the microorganisms. These compounds include polysaccharides, proteins, nucleic acids and lipids (Neyens et al., 2004). The EPS found in WAS are predominantly composed of proteins, which may have originated from proteins released from lysed cells and entrapped exoenzymes (Liu and Fang, 2003). Following secondary treatment, the mixture of primary

sludge and WAS are usually treated in anaerobic digesters before disposal and digested sludge is produced during this digestion process. Wastewater sludge is thus a suspension composed of 1 to 5% of the solid waste products generated as a net result of the wastewater treatment process. It is characterized by non-degraded organics, excess bacterial populations and some minerals. The moisture content in sludge is generally very high (75 – 90 wt%) and the dry matter contains 30 – 40 wt% carbon (Bernardi et al., 2010).

Extracellular polymeric substances have been found to bind large volumes of water, making WAS especially difficult to dewater, and meaning sludge volumes cannot be reduced easily. Hydrothermal treatments are able to break down the structure of EPS to liberate bound water and destroy cell walls thus releasing cell contents in the sludge. These changes improve the dewaterability of the sludge and make it more susceptible to anaerobic digestion, and the treated sludge is also sterilized (Neyens and Baeyens, 2003). Hydrothermal technologies for waste treatment emerged more than 50 years ago with the development of the WAO process for treatment of paper mill liquors. An early technology, named the Zimmerman process or Zimpro®, used air at high pressure to cause combustion of organic compounds suspended or dissolved in water. Almost all (95%) of organic matter was removed at temperatures up to 300 °C and at pressures up to 175 bar. The main products were carbon dioxide, nitrogen, ammonia, ash and small amounts of acetic acid. A modified version of this process which operated at lower temperatures (<200 °C) was later used to treat municipal sludge. This process, called low pressure oxidation, involved very little oxidation and is in fact more similar to TH processes (Camacho et al., 2008). However, many plants faced issues with corrosion and high energy costs, and eventually closed down (Odegaard, 2004; Debellefontaine and Foussard, 2000).

A thermal hydrolysis concept can also be found during the 1960s in the form of the Porteous process, which involved applying heat treatment to sludge to improve its dewaterability before incineration (Camacho et al., 2008). The Porteous process operated at higher temperatures (200 °C) than today's thermal hydrolysis processes and resulted in an end product which could be dewatered to 40 – 60% solids content without the aid of chemicals (Hecht and Duvall, 1975). However, technical problems, issues with odour and economic factors have also led to most plants to shut down (Kepp et al., 2000).

The more recent thermal hydrolysis processes developed by Cambi were a result of research work which showed advantages of operating at lower temperatures (150 – 200 °C). The resulting processes were designed around an optimum temperature of 170 °C which gave the best compromise between improved dewaterability at higher temperatures and better digestibility at lower temperatures. Cambi TH processes are the most widely used TH processes at present (Maugans and Ellis, 2002; Camacho et al., 2008).

The main difference between WAO and TH is that oxidation reactions are desired in WAO processes whereas they are not necessary in TH processes; oxidation is achieved by the addition of an appropriate oxidant such as oxygen gas or hydrogen peroxide. The TH process is largely used as a pre-treatment for other processes in the sludge treatment line for its ability to alter sludge properties. As oxidation is an ultimate method for the organic waste destruction, it is typically used as one of the final processes in the sludge treatment line. Typical setups for TH and WAO are illustrated in Figure 2.1 (a) and (b).

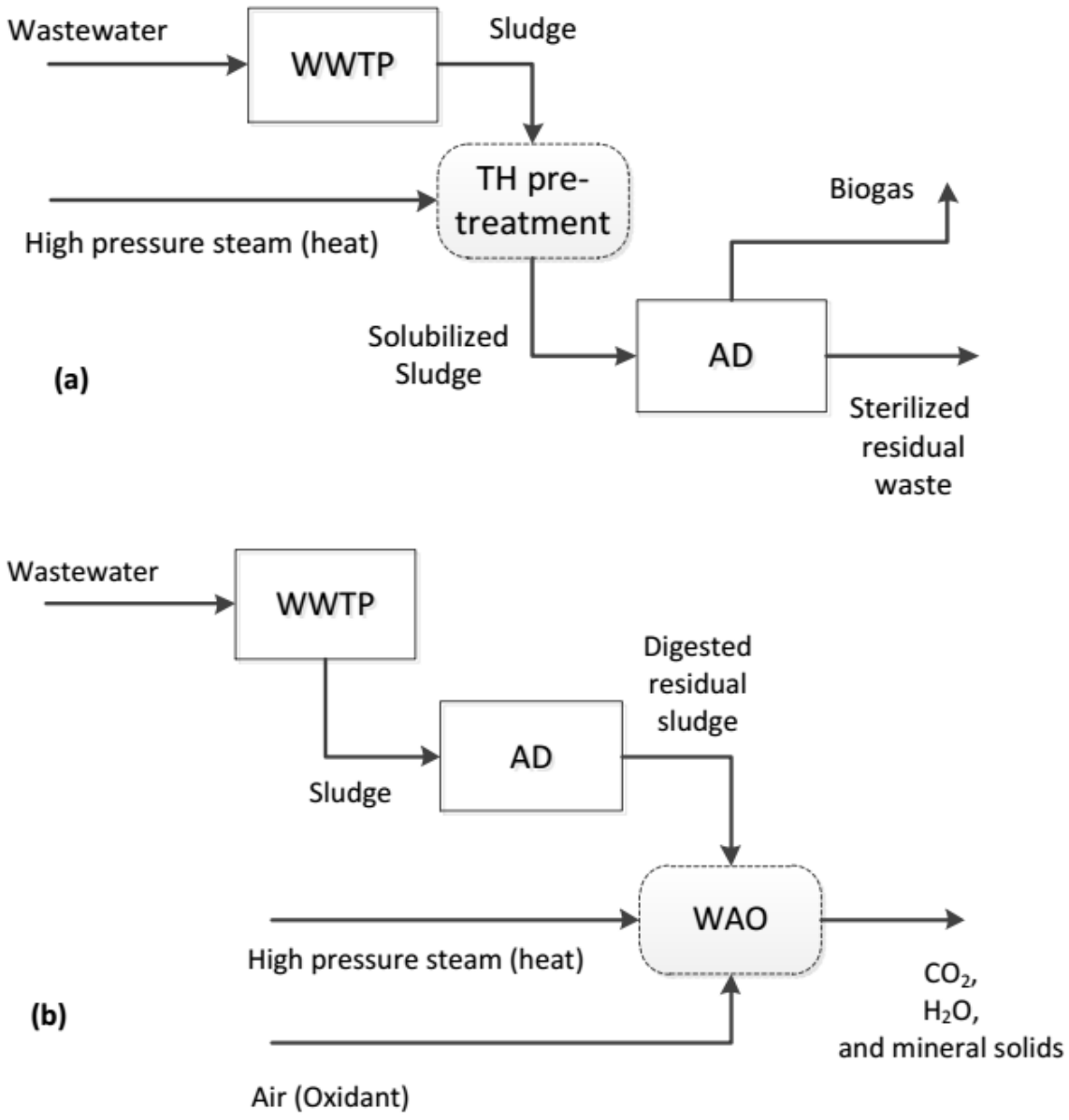

Figure 2. 1 – Typical configuration of thermal hydrolysis (a) and wet air oxidation (b) in a sludge treatment line.

2.1.4 WET AIR OXIDATION (WAO)

Wet oxidation or wet air oxidation technologies were first commercialized for the production of artificial vanilla flavouring and later for destruction of paper-mill sludge and biological sludge. Today, the application of this technology has expanded – most successfully for treatment of industrial wastes such as the caustic solution from scrubbing towers, and for treatment of powdered activated carbon (Maugans

and Ellis, 2002). Other applications include the production of useful products such as acetic acid (Shanableh, 2000), biofuel from microalgae (Alba et al., 2011) and synthesis of methyl methacrylate (Giudici & Maugans, 2000).

The WAO process can be defined as "the oxidation of organic and inorganic substances in an aqueous solution or suspension by means of oxygen or air at elevated temperatures and pressures either in the presence or absence of catalysts" (Zou et al., 2007). The main reactions are similar to incineration, and any substance that can be incinerated can be oxidized in water via WAO. The WAO process is therefore ideal for treating waste liquors, slurries and sludge where the organic matter is very high in concentration compared to water. Another benefit of the WAO process is that nitrous oxide, sulphur dioxide, hydrochloric acid, dioxins, furans, and fly ash are not generated. The WAO process is capable of up 99% conversion of toxic organics to harmless end products. For compounds which that not completely oxidized, intermediate compounds representing up to a quarter of the original mass of the organic matter are formed, such as small carboxylic acids.

Typical conditions for WAO are temperatures between 150 - 320 °C, at 20 – 150 bar and with a residence time 15 – 120 minutes. The type of application is usually determined by the range of temperatures used. Low temperature oxidation (100 – 200 °C) is used for thermal conditioning of municipal and paper industry sludge, whereas medium temperature (200 – 260 °C) oxidation is typically used for treatment of ethylene spent-caustics and some other industrial wastes, as well as for regeneration of powdered activated carbon used in wastewater treatment. Higher temperatures (260 – 320 °C) are used for sludge destruction and treatment of industrial wastewaters including organic industrial wastes such as pharmaceutical wastes and solvents. At the higher end of this temperature range, complete destruction of municipal, pulp and paper and other organic sludge is expected (Giudici & Maugans, 2000). This high temperature range is within the sub-critical region for water where the solubility of salts is reduced. Precipitated salts may be the cause of the corrosion that was a problem for early Zimpro sludge treatment operations. The process of WAO must be undertaken in the aqueous phase so high pressures are required to maintain water as a liquid. Pressurization also increases the concentration of dissolved oxygen and thus increases the oxidation rate (Debellefontaine & Foussard, 2000).

2.1.4.1 KINETICS AND MECHANISM OF WAO

The composition of sewage sludge can vary greatly but the main components are carbohydrates, proteins and lipids. The first stage in the WAO of sludge involves a large proportion of the insoluble organic content being converted into simpler soluble organics compounds (sugars, amino acids, fatty acids, etc.). The smaller molecules are then oxidized into easily biodegradable and oxygenated products (carbon dioxide, inorganic salts and water) (Bernardi et al., 2010). This conversion is achieved through a number of hydrolysis and oxidation reactions occurring in series. These series of reactions are propagated by an organic radical obtained through oxidation of C-H bonds. The organic radicals produced are able to oxidize all organic compounds that contain hydrogen via hydrogen abstraction. The organic compounds are gradually decomposed into more stable intermediates which are finally oxidized to carbon dioxide and water. The overall reaction rate slows down as the easily oxidized compounds are gradually removed and acetic acid and other stable intermediates are formed (Imteaz & Shanableh, 2004).

To simplify the reaction mechanism for WAO, it can be assumed that the destruction of sludge proceeds via two pathways – it can proceed either directly or indirectly. In the direct pathway, all initial relatively unstable intermediates in sludge come into direct contact with oxygen and are converted into carbon dioxide. In the indirect pathway, these initial relatively unstable intermediates first undergo hydrolysis to form relatively refractory intermediates such as acetic acid. These intermediates are later oxidized into carbon dioxide. Based on this simplified reaction scheme, Li (1991) developed a generalized kinetic model for WAO of organic compounds where production of an intermediate such as acetic acid was considered to be the rate-limiting step. The overall reaction rate can be calculated according to a general model (Eq. 2.1), which is true when describing the global reaction rate of any elementary chemical reaction (Debellefontaine and Foussard, 2000; Li et al., 1991). However, sludge contains a complex mixture of compounds. Through the series of reactions involved in WAO, some of the organic compounds are fully oxidized, whereas some are transformed to intermediate products of lower reactivity.

The generalized kinetic model of Li et al. (1991) is given in Eq. 2.2, which describes the change in concentration of organic compounds over time. The concentrations for A and B can be expressed in terms of total organic carbon (TOC), chemical oxygen demand (COD), or total oxygen demand (TOD). This model takes into account the formation and destruction of rate-controlling intermediates, based on the 2-pathway reaction scheme described previously. It was decided that the global rate for WAO depended on the formation rate of final oxidation products as well as the formation and destruction rates of low-

reactivity intermediates. This was due to the relatively high activation energies of these intermediates, which are represented by acetic acid, methanol and ethanol.

$$r_c = k_0 e^{-\frac{E}{RT}} C_i \left(C_{O_2}\right)^b \qquad Eq.\,2.2$$

$$\frac{(A+B)}{(A+B)_0} = \frac{k_2}{k_1+k_2-k_3} e^{-k_3 t} + \frac{k_1-k_3}{k_1+k_2-k_3} e^{-(k_1+k_2)^t} \qquad Eq.\,2.3$$

$$k_i = k_{0,i} e^{-\frac{E_i}{RT}} \left(C_{O_2}\right)^{b_i} \qquad Eq.\,2.4$$

where

r_c = Rate of chemical reaction

k_0 = Pre-exponential factor for the rate of a reaction

E =Activation energy (k/Jmol)

R = Ideal gas constant (8.3145 J/mol.K)

T = Temperature (K)

C_i = Concentration of organic substrate where *i* represents the i^{th} substrate (mol/L)

C_{O2} = Concentration of dissolved oxygen (mol/L)

t = Time (s)

b = Partial order of the reaction with respect to the oxidant

A = Concentration of all initial and intermediate organic compounds other than acetic acid

B = Concentration of acetic acid

k_i = Rate constant for the reaction of a specific compound, *i* (*i* = 1, 2, or 3)

Imteaz and Shanableh (2004) have developed a model for the WAO of wastewater sludge using a simplified first-order reaction scheme. The proposed alternative WAO reaction model aimed to present a more convenient method to describe the oxidation of sludge. Instead of describing the WAO process in terms of oxidation of unstable and stable compounds, the authors simplified the reaction scheme in terms of solubilisation and oxidation of all the COD in sludge. Here, it is assumed that the destruction of COD proceeds via a single pathway involving two reaction steps. Any solid COD in the sludge must first solubilize via hydrolysis before it can come into contact with the oxidants and finally oxidize. The global reaction model proposed is shown in Eq. 2.4:

$$\frac{d(X+Y)}{dt} = -ke^{-\frac{E}{RT}}(X+Y)^m(\mathrm{O})^n \qquad Eq.\,2.5$$

where

(X + Y) = total COD

O = concentration of oxidant

m = order of reaction with respect to organic reactant

n = order of reaction with respect to oxidant

Both models presented here are suitable for describing the WAO process. The model proposed by Li et al. (1991) is more representative of the kinetics of WAO processes. However, it is more complex and requires good understanding of the contents of treated sludge, which may sometimes be impractical. On the other hand, the model proposed by Imteaz and Shanableh (2004) is much simpler but gave some inconsistent predictions in terms of effluent COD.

Several other models have also been proposed however, they are will not be described in detail for the purpose of this review. An early study on WAO of sewage sludge by Ploos van Amstel and Rietema (1973) produced a model which could be used for the design of large-scale reactors. This model assumed that the sludge consisted of three groups of components which were of high reactivity, intermediate reactivity and no reactivity at all. The effect of hydrolysis on the overall conversion was neglected and the reactions were assumed to be first order. When the model results compared to the results obtained from a large scale WAO installation (200 tons per day of dry sludge), the model predicted a COD reduction value with 1% error compared to the actual value.

Verenich et al. (2002; 2003) have developed a lumped kinetic model for WAO treatment of organic wastewaters. The mechanism proposed considered the degradation of organics into end products. The refractory compounds were considered to undergo two parallel reactions. The first one would lead to the formation of oxidation end-products and the second one would lead to organic compounds, which are degraded to biologically oxidizable large molecules. These large molecules will undergo further transformation into smaller biodegradable compounds which are finally be oxidized into end products.

2.1.4.2 WAO TREATMENT CONDITIONS

Wet air oxidation processes typically take place at temperatures between 150 – 320 °C and pressures 20 – 150 bar. Researchers have considered supercritical water technologies as a part of WAO technologies (Fytlili and Zabaniotou, 2008; He et al., 2008; Zou et al., 2007) or as an alternative (Bermejo and Cocero, 2006). Fytlili and Zabanioutou, (2008) described the WAO process as “occurring in two distinctive regimes”,

with the first occurring at sub-critical conditions for water (below 374 °C temperature and 100 bar pressure) and the second occurring at supercritical conditions for water (above 374 °C temperature and 220 bar pressure).

Maugan and Ellis (2002) divided the typical range of WAO temperatures used for various applications, into low (100 – 200 °C), medium (200 – 260 °C) and high (260 – 320 °C). The high temperature range is commonly used for sludge destruction and industrial wastewater treatment. The range of low temperatures is used for sludge-conditioning purposes. However, oxidation is unlikely to occur at low temperatures and these processes are, in fact, thermal hydrolysis processes. The WAO process typically becomes energetically self-sufficient at medium and high temperature ranges.

It has been noted that COD reduction in sludge is primarily a function of temperature and the type of sludge being treated. Up to 20% variation in COD reduction can be identified between primary, secondary and digested sludge when treated under a given reaction temperature, whilst secondary sludge was found to be most resistant to oxidation (Lendormi et al. 2001). Many researchers have highlighted the influence of temperature and reaction time on the performance of WAO (Baroutian et al., 2013b; Chung et al., 2009; Lendormi et al., 2001; Shanableh, 2000). Shanableh (2000) reported that COD removal from the sludge increased as temperature increased in the range of 280 – 460 °C, with 67 – 97% COD reduction achievable. The author noted that COD removal was also dependent on reaction time. However, COD removal was limited to 85% at temperatures below 300 °C (sub-critical water oxidation) even after 1 hour of reaction time. This was due to the generation of thermally resistant by-products, mainly acetic acid and ammonia, at the lower temperatures. At supercritical conditions however, COD removal above 99.9% was possible within 10 minutes of reaction time at 450 °C temperature. Similarly, Lendormi et al. (2001) reported that at temperatures of 240 °C, COD reduction is limited to 70% whereas COD removal efficiencies greater than 80% is achievable at 300 °C without the addition of catalysts.

More recently, Chung et al. (2009) investigated the effects of operational conditions on sludge degradation and organic acids formation. Reaction time and temperature was again found to be important factors affecting liquefaction of volatile solids. The degradation efficiency of sludge and formation of organic acids was improved with longer reaction time and higher temperatures. The high temperatures accelerate sludge dissolution whereas high pressures increased the solubility of the oxidizing agents, such as oxygen – both of which speed up sludge liquefaction. The authors found optimal conditions to be 240 °C temperatures, 60 bar pressure and 30 minutes reaction time.

Baroutian et al., (2013b) examined individual and interactive effects of process variables on the degradation of fermented municipal sludge during wet oxidation. It was found that temperature has the most significant effect on degradation rate throughout. During the near completion stage, the interaction of temperature and oxygen ratio had significant effect on sludge degradation.

In recent years, work has been done on developing wet oxidation under milder conditions and lower pressure (Abe et al., 2013; Abe et al., 2011). Wet air oxidation treatment at 150 °C temperature, 10 bar pressure and 2 hours reaction was able to give a 62% volatile suspended solids (VSS) removal efficiency. This lower pressure WAO process was considered as a sludge pre-treatment process to improve the sludge characteristics for anaerobic digestion. Studies suggested that an excessive concentration of oxygen used in the reaction led to production of recalcitrant soluble organics and toxic compounds and can reduce gas production in anaerobic digestion (Abe et al., 2013). Typically, catalysts will lower reaction temperatures and pressures to be used to achieve the same results as those achieved without catalysts in WAO processes. Refractory compounds such as acetic acid and ammonia also become more susceptible to oxidation (Luck, 1999). Catalytic wet oxidation techniques are beyond the scope of this paper.

2.1.4.3 IMPACT OF WAO ON SLUDGE DIGESTION EFFICIENCY

The Zimpro® process was the first commercial WAO process and several large WAO plants were built in the early 1960s for the treatment of municipal sludge to either improve the dewaterability of sludge or to achieve complete oxidation in the sludge. More than 130 Zimpro® units had been installed around the US and Europe. Most of these were used for conditioning sludge by partially oxidizing the organic fractions such that the sludge flocs are broken to release bound water. Sludge conditioning was performed at 210 – 240 °C, whereas for sludge destruction temperatures of 250 – 270 °C at 85 – 120 bar pressures were used; air was the usual oxidant used (Luck, 1999). Information regarding more recent applications of WAO sludge technologies is relatively scarce despite it often being mentioned for sludge treatment. Some examples of results achieved via WAO are provided in Table 2.2.

Lendormi et al. (2001) studied the application of WAO for treatment of municipal sewage sludge in tests carried out a pilot scale plant. Chemical oxygen demand removal efficiency greater than 80% was achieved at 300 °C without the use of catalysts. However, it was found that at lower temperatures around 240 °C, the process produced foam which impaired the reactor operation. The lower temperatures also generated compounds that are resistant to oxidation.

Genç et al. (2002) investigated WAO for pre-treatment of digested and secondary sludge before aerobic digestion and its effect on the sludge biodegradability. Hydrogen peroxide was used as the oxidant with copper and manganese salts used as catalysts. Temperatures of 120 °C at 2 bar pressure were used to solubilize the sludge organics. The liquid phase organics concentration, measured in terms of total organic carbon (TOC) was found to increase by 16.5 % after 10 minutes, whereas an increase of 66% was achieved after 120 minutes of treatment. The biodegradability was not changed for digested sludge but was increased for activated sludge. The final solids volume was also reduced by 80% after treatment.

Zhu et al. (2004) investigated the digestion of mixture of primary and surplus sludge using wet oxidation without catalysts. WAO experiments were carried out in an autoclave at 250 °C temperature and holding times ranging between 30 to 120 minutes. The volatile suspended solids (VSS) digestion efficiency was around 94-96%. However, the product liquid contained large amounts of organic matter content.

Strong et al. (2011) compared WAO to thermal hydrolysis processes as a pre-treatment for mesophilic anaerobic digestion on a mixture of primary and secondary sludge. Wet air oxidation of Sludge was carried out in a high-pressure reactor at 220 °C temperature, 20 bar pressure and 2 hours reaction time. Volatile suspended solids destruction of 93% and total suspended solids (TSS) destruction of 83% was achieved. The soluble COD found in the product was lower compared to that found in thermal hydrolysis due to the oxidation of these solubilized compounds under WAO. The production of acetic acid was also found to be greater in WAO than thermal hydrolysis.

Abe et al. (2011) compared several pre-treatment methods to improve thermophilic digestion of residual sludge including low pressure wet oxidation. Wet air oxidation experiments were carried out in an autoclave for 2 hours with oxygen supplied in amounts corresponding to 0 – 120% of the theoretical oxygen required for oxidizing the carbon content of the sludge. Volatile suspended solids removal efficiencies of 62% at 150 °C and 94% at 250 °C temperature were achievable and this can be increased when the oxygen supply was increased.

Abe (2013) compared the effectiveness of thermal treatment to WAO under mild conditions for the pre-treatment of secondary sludge before thermophilic anaerobic digestion. Wet air oxidation was carried out in an autoclave under 150 °C temperatures and at 5 – 14 bar pressure for 2 hours. The treatment achieved 77% VSS digestion efficiency and the gas production was highest at 150 °C treatment with 40% of theoretical oxygen supplied.

2.1.4.4 PRODUCTION OF USEFUL BY-PRODUCTS IN WAO

It is well known that the WAO process is able to produce chemical products such as volatile fatty acids (VFA), mainly acetic acid, which can be recovered for use. The production of acetic acid using WAO at sub-critical conditions was investigated by Shanableh (2000) for use as the organic reactants necessary in denitrification processes in WWTPs. The WAO effectively hydrolyses sludge solids but achieves incomplete oxidation of the organic components. This produced COD-rich liquors containing 10% wt/wt acetate, which accounted for up to 80% of soluble COD. Strong et al. (2011) using WAO process at 220 °C was able to obtain a slightly higher production of acetic acid (15% wt/wt). Chung et al. (2009) determined that the formation of organic acids increased with reaction temperature. More organic acids were formed as intermediates when the reaction temperature increases. Acetic acid production increased by four times as temperature was increased from 180 °C to 240°C, at 40-minute reaction time.

He et al. (2008) undertook a comprehensive review on resource recovery from organic wastes using hydrothermal treatment. The author described the mechanism for the formation of various compounds from hydrothermal processing of organic wastes. Acetic acid was identified as the main intermediate product. Jin et al. (2005) suggested a two-step process to improve acetic acid production which consisted both of a hydrothermal reaction process in the absence of oxygen and a reaction process with oxidant supplied afterward. In the first step, the formation of furans is accelerated as the oxidation of these compounds leads to large amounts of acetic acid. In the second step, these furans are further converted to acetic acid by oxidation with fresh supplies of oxygen. The acetic acid obtained was of a high purity.

Aggrey et al. (2011) developed a two-stage hydrothermal process based on the two-step concept proposed by Jin et al. (2005) which is a series combination of TH and WAO processes operated at the same reaction temperature of 220 °C. This process was specifically developed with the intention of maximizing acetic acid production and it was compared to TH at 140 °C and WAO at 220 °C. The WAO process achieved yield and purity of acetic acid of 12% and 38% respectively. On the other hand, the two-stage process achieved 8% yield and purity of 25%.

These works highlight the potential of using WAO to produce acetic acid from sludge. The production of useful chemical products may become an incentive for the implementation of WAO processing in sludge treatment, as research continues on the conditions which affect the production of acetic acid in WAO processing of sludge.

2.1.4.5 COMMERCIAL EXAMPLES OF WAO

Currently, few examples of commercial WAO plants are operational for the treatment of sludge as many of the early plants have shut down due to commercial reasons and technical issues. Debellefontaine (2000) gave an overview of some of the earlier facilities which were made up of technologies such as the Loprox ®, Zimpro ®, Athos™ and VerTech processes.

The Athos process by Veolia Water (Veolia, 2013) is one of the main WAO sludge treatment technologies currently provided commercially. The process operates at temperatures between 250-300 °C, using air or pure oxygen as the oxidant. The process is claimed to produce mineral products, clean gas emissions, and biodegradable liquids. Reference plants are available in Belgium, Italy and France.

Chauzy et al. (2010) reported that he Athos process was in use in a WWTP in North Brussels, Belgium. It is used as a final sludge-destruction process located in the sludge treatment line after the anaerobic digestion of sludge, which was pre-treated by thermal hydrolysis. The process is exothermic and becomes energetically self-sufficient after start-up. The process was also designed so that it was integrated into the plant's energy recovery scheme where the heat produced from WAO is used to produce hot water used to heat buildings and to operate dryer plate filter.

Table 2. 2 – Typical conditions of wet air oxidation and thermal hydrolysis in sludge treatment and their impacts.

Treatment method	Treatment conditions	Treated Material	Outcome	Reference
WAO	240 – 300 °C 50 – 110 bar O_2 oxidant 30 – 76 min	Waste activated sludge (WAS)	83% COD reduction at 300 °C temperature.	Lendormi et al. (2001)
	120 °C 2 bar H_2O_2 oxidant Cu catalyst 10 – 120 min	Mixed primary and activated sludge	16.5 % - 66% increase in liquid phase TOC.	Genç et al. (2002)
	250 °C 30 – 120 bar O_2 oxidant 20 – 120 min	WAS	94 – 96% VSS digestion efficiency; high organic matter content in liquid product.	Zhu et al. (2004)
	150 – 250 °C 10 – 80 bar O_2 oxidant 120 min	WAS	62% VSS removal efficiency at 150 °C and 94% VSS removal efficiency at 250 °C.	Abe et al. (2011)
	220 °C 20 bar Air oxidant 120 min	Mixed primary and secondary sludge	93% VSS destruction; 83% TSS destruction.	Strong et al. (2011)
	150 °C 5 – 14 bar O_2 oxidant 120 min	WAS	77% VSS digestion efficiency at 150°C and 40% theoretical oxygen.	Abe et al. (2013)
TH	62 – 175°C Vapour pressure 15 – 120 min	WAS	Doubled biogas production for temperatures 150 – 175 °C; >60% COD removal efficiency	Li & Noike (1992)
	170 °C 8 bar 60 seconds	WAS mixed with digested sludge	35 – 49% increased methane yield	Dohányos et al. (2004)
	170 °C Vapour pressure 30 min	WAS	Increased biogas production by 40% in half the residence time in mesophilic anaerobic digestion.	Pérez-Elvira et al. (2008)
	170 °C Vapour pressure 0 – 30 min	WAS	50 -75% carbohydrate solubilisation; hydrolysis time greatly improves dewaterability but not solubilisation	Donoso-Bravo et al. (2011)
	170 °C Vapour pressure 60 min	WAS	68% increased biogas production.	Qiao et al. (2011)
	150 – 170 °C 30 min 5 – 8 bar	WAS	24 – 59% increased biogas production in mesophilic anaerobic digestion.	Wilson et al. (2011)
	170 °C Vapour pressure 30 min	WAS	33% increased biogas production time in mesophilic anaerobic digestion.	Pérez-Elvira and Fdz-Polanco (2012)

2.1.4.6 SUPERCRITICAL WATER TECHNOLOGIES

Supercritical water oxidation (SCWO) is basically an evolution of the WAO process where the operating temperature is increased beyond the critical temperature of water. However, because supercritical water behaves very differently to sub-critical water, many of the reactions and mechanisms in SCWO would be different from WAO. The SCWO process has been used for the treatment of various wastes (Brunner, 2009) including sludge, but for the moment in-depth review of SCWO technologies are outside the scope of this paper. Nevertheless, SCWO is showing promise and is being continually developed for application in sludge treatment.

Cabeza et al. (2013) gives one example of SCWO process used in sewage sludge treatment. Here the destruction of sludge was achieved by SCWO in a hydrothermal flame regime, where at operating temperatures above autoignition temperature, the SCWO reaction proceeds in the form of flames. Reaction times can be as little as in the order of milliseconds and the process does not emit hazardous gases, unlike incineration. Furthermore, this technology can successfully achieve destruction of ammonia, which cannot be achieved via WAO alone.

On the other hand, supercritical water gasification (SCWG) is another process similar to SCWO except it occurs in the absence of oxygen, and hence does not involve oxidation. Water splitting, steam reforming, and water-gas shift reactions are the main reactions involved in SCWG. This process has been applied to treat primary sewage sludge (Wilkinson et al., 2012), which results in a vapour product containing water, carbon dioxide, methane and hydrogen. However, the technology is energy intensive compared to traditional AD sludge treatment processes.

2.1.5 THERMAL HYDROLYSIS (TH)

Thermal hydrolysis (TH) and related heat treatment processes have long been used in sludge treatment, although for different purposes. Traditionally, sludge from wastewater treatment processes were simply dewatered and disposed immediately. Thermal hydrolysis was originally used for conditioning the sludge and improving its dewaterability. Early research on TH processes began as early as the 1970s aimed at improving the settleability and filterability of sludge by altering the sludge's physical characteristics. Thermal hydrolysis was found to destroy the structural integrity of microbes in the sludge and cause the lysis of cell walls, which released cell contents. Higher temperatures and treatment times were found to destroy more cell walls and insoluble proteins could also be broken down into more soluble amino acids.

Later, it was realized that combining thermal pre-treatment with anaerobic digestion could potentially improve biogas production and remove odour. Early tests on both the laboratory and pilot-scale showed good results. Anaerobic digestion has today become a promising method for sludge treatment and TH is an important pre-treatment method to improve the efficiency of the process, especially for the digestion of WAS. Essentially, under high temperature conditions (130 – 200 °C), a hydrolysis reaction occurs to break down complex molecules in sludge into simpler compounds. This results in the improved bioavailability of sludge contents for AD (Strong et al., 2011; Li & Noike, 1992).

2.1.5.1 KINETICS AND MECHANISM OF THERMAL HYDROLYSIS

The TH process relates to the thermal decomposition of the sludge contents without the occurrence of oxidation and solid matter becomes soluble. Takamatsu et al. (1970) presented one of the earliest works in establishing a mathematical model to describe thermal decomposition of WAS. Because sludge is composed of very complex compounds, the mathematical model proposed represents the thermal decomposition reaction in terms of four components. These take into account the solid matter, soluble matter (evaporative and non-evaporative) and water. Experiments were carried out on WAS in an autoclave at temperatures 170 - 250 °C, and pressures 60 – 130 bar and without introducing oxygen. The COD in the solids were found to decrease and in the soluble matter, COD was increased. The total COD in the sludge however remained unchanged.

The reactions occurring during thermal decomposition were described by Takamatsu et al. (1970) in terms of solubilisation of solid matter into soluble evaporative matter and soluble non-evaporative matter. The differentiation between evaporative and non-evaporative matter was only relevant within the context of the author's experiment due to limitations in experimental procedure. Evaporative matter was described as matter lost during drying at 120 °C temperature.

Based on the assumption that the rate constants are of the Arrhenius type, the mathematical models for thermal decomposition based on changes in weight was given as:

$$\frac{dA_{wt}}{dt} = -\left(0.37e^{-\frac{249}{T}} + 0.319e^{-\frac{500}{T}}\right)(1 - \xi)A_{Wt} \qquad Eq.\,2.6$$

$$\frac{dB_{Wt}}{dt} = 0.37e^{-\frac{249}{T}}.(1 - \xi).A_{Wt} - \left(1800e^{-\frac{4600}{T}}.B_{Wt}\right) + 0.55e^{\frac{-1260}{T}}.C_{Wt} \qquad Eq.\,2.7$$

$$C_{Wt} = (A_{Wt} + B_{Wt})_{init.} - A_{Wt} - B_{Wt} \qquad Eq.\,2.8$$

where

$\xi = (A_{Wt} + B_{Wt})_{init.}(-0.00457 \times T - 2.323)$;

T = Temperature (K)

$(A_{wt} + B_{wt})_{init.}$ = Initial weight of total solids

and A_{wt}, B_{wt}, C_{wt} are the weights of components *A* (solid matter), B (Soluble non-evaporative matter), and *C* (soluble evaporative matter) in mg/kg-total-sludge.

In their review on subcritical hydrothermal technologies, Toor et al. (2011) have identified a large number of studies on the reaction pathways of components typically found in biomass such as sewage sludge. These components include carbohydrates, lignin, protein and lipids. Based on individual studies on the degradation mechanisms of these components, a basic reaction mechanism in subcritical water was described. The first step of reaction involves depolymerisation of the sludge molecules. This was followed by decomposition of the resultant monomers via cleavage, dehydration, decarboxylation and deamination. The reactive fragments produced are then recombined. Since sludge is a complex waste with varying compositions, the parameters affecting the reaction rates of each individual component in sludge will likely affect the kinetics of the overall process and should be taken into consideration. For example, the authors identified that the hydrolysis of carbohydrates are rapid under hydrothermal conditions, although the hydrolysis rates vary between different types of carbohydrates.

More recently, Imbierowicz and Chacuk (2012) developed a lumped kinetic model for WAS thermohydrolysis which suggested that during heating of WAS, two parallel first-order reactions would occur. The first one related to the thermal destruction and solubilisation of sludge particles to organic carbon while the second parallel reaction produced a new solid phase, which may further decompose into carbon dioxide gas. It was found that reaction temperatures strongly impacted the decrease in the concentration of organic carbon in the solid phase as well as solubilisation of particulate organic matter.

2.1.5.2 TH TREATMENT CONDITIONS

Table 2.2 presents the outcomes of TH sludge treatment under associated treatment conditions. Similar to WAO, treatment time and temperature are the most important parameters which determine the performance of the TH process. Several researchers have performed work over the last few decades to determine the effect of temperature and reaction time on WAS thermal treatment and the best conditions for the process. Most studies have agreed that the optimal range of temperature lies between 160 –

180 °C to achieve increased methane yield in subsequent anaerobic digestion (AD), but at higher temperatures the biodegradability of sludge is reduced sharply (Bougrier et al., 2008).

Li and Noike (1992) investigated the effect of TH pre-treatment on the degradation of WAS in anaerobic digestion in batch and continuous experiments. The pre-treatment temperature ranged between 62 – 175 °C with treatment times between 15 – 60 minutes. It was found that solubilisation generally increased as temperature was increased. More precisely, the solubilisation of carbohydrate and protein were found to increase as the treatment temperature increased from 120 °C to 175 °C. At a given temperature carbohydrate had greatest solubilisation, followed by protein and lipid. This showed that the degree of solubilisation achieved is dependent on the kinds of organic compounds present in WAS. Furthermore, the COD removal efficiency from WAS greatly increased with thermal pre-treatment and increased with temperature between 120 – 170 °C. Above 170 °C, the COD removal efficiency was found to decrease, indicating that an optimum of 170 °C. The author concluded that for a sludge treatment system comprised of TH before anaerobic digestion, the optimal time for TH was between 30 – 60 minutes for increasing methane production from WAS. A reaction temperature between 150 – 175 °C improved anaerobic degradability of WAS and methane production. Furthermore, the retention time necessary for anaerobic digestion can be reduced.

Similarly, Carrere et al. (2010) notes that most studies report optimum TH temperatures between 160 – 180 °C under treatment times of 30 – 60 minutes. Treatment times of 1 minute were also possible in this temperature range (Dohányos et al., 2004) while treatment at much lower temperatures (70 °C) will require up to several days (Gavala et al., 2003, Ferrer et al., 2010). Dwyer et al. (2008) also finds that above 150 °C, no increase in methane production resulted despite increased solubilisation. Treatment temperatures above 170 – 190 °C in fact decrease the biodegradability of sludge.

Recently, Donoso-Bravo et al. (2011) studied the influence of TH reaction time on sewage sludge composition and anaerobic digestion performance. Pre-treatment time was varied between 0 to 30 minutes under treatment temperature of 170 °C. The hydrolysis time was concluded to result in very small improvements with regards to sludge solubilisation but greatly improves its dewaterability.

2.1.5.3 Effect of TH on biogas production

Increased methane and biogas production from anaerobic digestion is the primary goal of TH processes in sludge treatment today because not only are the resources in sludge being recovered, but the energy

which can be produced from the increased methane can be used to make the TH process energetically neutral. This means that identifying the factors which affect methane yield through TH is of great interest.

Haug et al. (1978) finds that for WAS, gas production from anaerobic digestion increases as TH pre-treatment temperatures increased up to 175 °C. At 100 °C, methane production was increased 14% whereas at 175 °C, up to 70% increase could be expected. Above this temperature, inhibitory materials are produced which reduced gas production. For WAS, it was particularly evident that after TH pre-treatment at 175 °C, the sludge contained toxic materials which reduced gas production in anaerobic digestion. This toxicity can be overcome by feeding a diluted sludge containing only 4% solids. Increased methane production was also accompanied by increased VSS reduction. For primary sludge, TH pre-treatment did not increase methane production significantly. Li and Noike (1992) also found that the gas production increased after TH pre-treatment, but the gas production rate decreased with increasing retention time in the anaerobic digester. The gas production increased with increasing temperature between 120 – 170 °C but decreased slightly at 175 °C. The increase of gas production was nearly double for pre-treatment temperatures between 150 – 175 °C.

More recently, Pérez-Elvira et al. (2008) studied TH and anaerobic digestion under mesophilic conditions in a pilot-scale study. Pre-treatment temperatures of 170 °C and reaction time of 30 minutes was used to give a 40% increase in biogas production under half the residence time in anaerobic digestion. In another study pilot-scale study combining TH with mesophilic anaerobic digestion, Pérez-Elvira and Fdz-Polanco (2012) reported a 33% biogas production increase under 17 days residence time. Even at half this residence time, the biogas production was still 24% greater compared to conventional anaerobic digestion. Qiao et al. (2011) investigated the biogas production using different wastes in the lab-scale using hydrothermal pre-treatment at 170 °C temperature and 1-hour reaction time. The biogas production increased 67.8% for municipal sewage sludge after hydrothermal treatment. Wilson et al. (2011) reported biogas production increase between 24 – 59% after thermal pre-treatment at temperatures 150 – 170 °C and 5 – 8 bar pressure when compared with conventional mesophilic anaerobic digestion.

Most researchers generally agree that an optimum temperature for TH lies somewhere around 175 °C, without the addition of catalysts, to increase the solubilisation of sludge solids and to improve the digestibility of the sludge. Temperatures above this would have inhibitory effects in terms of digestibility and biogas production.

2.1.5.4 ENERGY REQUIREMENT OF TH

Thermal hydrolysis processes generally require an input of energy to maintain the reaction temperatures whereas WAO which is exothermic and becomes autothermal at high enough temperatures. In many cases, this energy requirement will impact on the implementation of TH processes in sludge treatment systems. This energy requirement needs to be overcome by the increased rate of biogas production by implementing TH pre-treatment. Careful design of the system to recover excess heat will also be necessary for the TH process to be implemented economically. Haug (1978) performed energy balances for TH and an anaerobic digestion system to treat WAS and mixed primary/secondary sludge. In case of WAS, a 70% increase in gas production rate was expected and required in this system to obtain a net energy production when an anaerobic digestion followed TH pre-treatment. A thorough energy balance study was also carried out by Pérez-Elvira et al. (2008), which considered different configurations of the TH and anaerobic digestion system as well as different options for energy integration. Without implementing an energy integration scheme, it was found that the feed concentration of sludge must be increased (from 3% to 7% total solids) in order to produce enough biogas in the system for the process to become energetically self-sufficient. An energy integration scheme which considered heat recovery from the flash vapor outlet of the TH reactor can lower the required feed concentration. It was also found out that only TH of WAS is beneficial rather than the mixture of primary sludge and WAS to be pre-treated using TH. This scheme can help a 30% increase in biogas production to achieve net energy production.

2.1.5.5 COMMERCIAL EXAMPLES OF TH

Currently, Cambi, a Norwegian company and French company, Veolia Water are the main companies providing TH technologies for sludge treatment. The Cambi process treats sludge under pressure (4.5 bar) at temperatures between 150 – 180 °C and improves both the digestibility and dewaterability of sludge but avoids issues with corrosion and refractory compounds encountered in higher temperature processes. Sludge is first dewatered to 17% dry solids before it is heated using recycled steam. The reaction time is up to 30 minutes and after reaction, the treated sludge is flashed into a flash tank. This technology has been implemented in a large number of wastewater treatment plants globally and especially in Europe.

Veolia Water also provides continuous and batch systems of TH processes combined with anaerobic digestion. These are marketed under the names of Exelys™ and Biothelys™ respectively and currently,

one prototype plant is operating in France using reaction temperature 165 °C, 9 bar pressure and reaction time up to 30 minutes.

2.1.6 UPCOMING TECHNOLOGIES

Many interesting technologies based on the hydrothermal concept are continually being developed for application in sewage sludge treatment. Some of these incorporate ideas from both TH and WAO, blurring the lines between oxidative and non-oxidative hydrothermal processes. One such technology is the advanced thermal hydrolysis (ATH) concept developed by Abelleira et. al (2012). The ATH process can fundamentally be viewed as a modification of the TH process which combines TH with hydrogen peroxide addition. Hydrogen peroxide is a powerful oxidant, and when combined with steam injection used in TH causes a synergistic effect which achieves desirable sludge treatment effects. Like in TH, the ATH process achieves solubilisation of sludge solids and improves sludge dewaterability. However, both solubilisation and dewaterability are markedly better in the ATH process, with solubilisation up to twice as much improved. Furthermore, organic matter removal is achievable due to oxidation reactions occurring (85 - 92% organic matter removal at 170 °C, and stoichiometric hydrogen peroxide dosage). This means ATH process can also potentially be used as a final destruction method, similar to WAO. However, if used as a pre-treatment process to AD, the methane production is not necessarily improved and, in some cases, decreased. Therefore, further research is required to determine the operating conditions which facilitate methane production. ATH is nonetheless a very promising technology as it operates under relatively mild conditions compared to TH and WAO without the addition of catalysts and still achieves comparable results.

On the other hand, a hydrothermal treatment concept has been used to convert sludge into solid residues (Escala et. al 2013; Shi et al., 2013). This hydrothermal treatment involves heating sludge in a water medium up to temperatures of 210 °C and allowing build-up of saturation pressure. Under these conditions the sludge is broken down over a number of reactions including hydrolysis, dehydration, decarboxylation, polymerization and aromatisation. The result is a solid residue, water, and carbon dioxide. The solid residue (hydrochar) can be used as a solid fuel or use as a soil amendment for agricultural application. These technologies are more or less similar to TH although they operate at higher temperatures and generally longer reaction times. These technologies are intended as final solutions for sludge treatment rather for improvement of current sludge treatment lines.

2.1.7 FUTURE WORK

Hydrothermal processing technologies have been shown to provide significant benefits and improvements to existing sludge treatment methods. Thermal hydrolysis greatly enhances anaerobic digestion with potential to increase biogas production by 40% at a half the residence time (Perez-Elvira et al. 2008). The rheological characteristics of sludge are also improved, and dewatering is enhanced (Ahn et al., 2008; Chauzy et al. 2007). On the other hand, WAO is a very effective sludge reduction process which can also be used to convert wastewater sludge into useful products.

However, both TH and WAO are energy-intensive processes which may make them economically infeasible for sludge treatment. Further work should be focused on methods to make them less energy intensive. Several research works such as those by Pérez-Elvira and Fdz-Polanco (2012) have investigated ways to integrate these processes into the overall sludge treatment line that optimizes the recycling of excess heat. This was done by looking at different configurations of the processes within the overall treatment process. This will be especially useful for WAO processes since the oxidation reactions are exothermic and the excess heat can be recovered for use elsewhere.

Thermal hydrolysis has been implemented commercially successfully, however further work needs to be done on describing the process and reaction kinetics. This can help to further optimize the process which may lead to increased biogas yields and reduced energy requirements.

Wet air oxidation has historically suffered from issues with corrosion at high operating temperatures. Catalytic WAO may be investigated in detail to help solve this issue by allowing milder operating conditions. The production of acetic acid has also shown potential benefit for further commercial development of WAO. Further work on maximizing acetic acid production following Jin et al.'s study (2005) would be beneficial.

2.1.8 CONCLUSION

Hydrothermal technologies involving high temperature and high-pressure reactions in water play increasingly substantial roles in sludge treatment. Wet air oxidation (oxidative) is mainly used for final sludge destruction whereas TH (non-oxidative) is used as a pre-treatment method to improve subsequent sludge treatment processes. The optimal TH temperature range is between 170 - 180°C, increasing biogas production by 40%. The TH and WAO processes have been reviewed with regards to their development

in sludge treatment, reaction kinetics, commercial examples, operational specifics and unique characteristics. Differences and similarities between both processes were presented. Future works for improving both processes were recommended.

2.2 LITERATURE REVIEW ON SLUDGE RHEOLOGY.

2.2.1 RHEOLOGY

Rheology refers to the study of flow and deformation of materials. All materials can be characterized rheologically as being in between two extremes of behaviour: ideally viscous liquids and ideally elastic solids. All real materials behave with a combination of both viscous and elastic portions. Hence, they are described as having viscoelastic behaviour. Rheological experiments reveal information about the flow behaviour of liquids and also the deformation behaviour of solids. Rheometry describes the system of measurements used to collect rheological data, including measuring systems, instruments, and test and methods of analysis. Different types of tests are used for obtaining different rheological information from liquids and solids. Tests are generally categorized into rotational and oscillatory types. Viscous behaviour is generally described using rotational tests, whereas viscoelastic behaviour is evaluated using creep tests, relaxation tests, and oscillatory tests (Mezger, 2006).

2.2.1.1 ROTATIONAL TESTS AND FLOW BEHAVIOUR

In rotational testing, a sample is sheared between two surfaces to simulate laminar flow conditions to determine its resistance to flow (Coussot, 2005; Mezger, 2006). In rotational testing, it is defined the shear stress:

$$\sigma = \frac{F}{A} \qquad Eq.2.9$$

Where σ is the shear stress (Pa); F is the shear force (kg·ms^{-2}); and A is the shear area (m^2).

Similarly, it is defined for the shear rate:

$$\dot{\gamma} = \frac{dv}{dh} \qquad Eq.2.10$$

Where $\dot{\gamma}$ is the shear rate (s^{-1}); v is the velocity (ms^{-1}) of the fluid in the shear direction; h is the vertical distance between the shearing surfaces, perpendicular to the direction of shear. In laminar flow conditions, there is a linear velocity distribution across h. Thus, the shear rate is also described as the velocity gradient across the shearing gap.

Finally, it can be defined the shear viscosity:

$$\eta = \frac{\sigma}{\dot{\gamma}} \qquad Eq.2.11$$

Where η is the shear viscosity (Pa.s), which is a material constant describing the material's resistance to flow.

2.2.1.1.1 FLOW CURVE MEASUREMENTS

Flow curves present the results from rotational measurements in terms of the shear stress as a function of shear rate on the tested material. From the flow curves, shear viscosity can be determined as well as Newtonian, or non-Newtonian fluid behaviour (Figure 2.1).

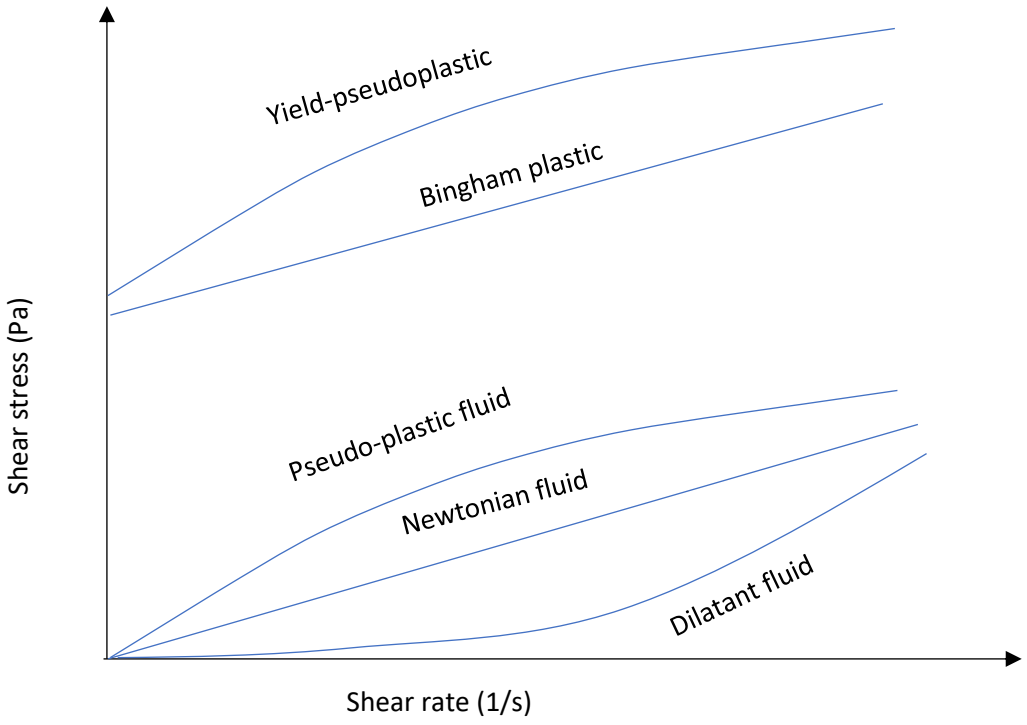

Figure 2. 2 – Flow behaviour of fluids (Chhabra and Richardson, 2008).

2.2.1.2 OSCILLATORY TESTS AND VISCOELASTIC BEHAVIOUR

In oscillatory tests, a sample is deformed homogeneously between two surfaces back-and-forth, resulting in harmonic-periodic motion and the strain and stress are recorded (Mezger, 2006).

For ideally elastic materials, samples comply with Hooke's law, as follows:

$$\sigma(t) = G^* \cdot \gamma(t) \qquad Eq.2.12$$

Where *G** is the complex shear modulus (Pa); *t* is time (s); *γ* is sample deformation or strain (%). Here, *G** can be imagined as the material's resistance to deformation. In oscillatory motion, the *σ(t)*-curve and *γ(t)*-curve can be described by sine curves and occur simultaneously. That is, the strain response in an ideally elastic material occurs immediately at a given stress, or vice-versa, without delay. Therefore, the *σ(t)* and *γ(t)*-curves are described as being "in phase".

For ideally viscous materials, samples comply with Newton's law, as follows:

$$\sigma(t) = \eta^* \cdot \dot{\gamma}(t) \qquad Eq.2.13$$

Where η^* is the complex viscosity (Pa.s), which can be imagined as the viscoelastic flow resistance of the sample. In oscillatory motion, there is a delay between the *σ(t)* and *γ(t)*-curves of 90°. This delay is termed the phase-shift angle, δ (°).

For viscoelastic materials, 0° < δ < 90°, and it can be defined for G*:

$$|G^*| = \sqrt{(G')^2 + (G")^2} \qquad Eq.2.14$$

Where *G'* is the storage modulus (Pa) and *G"* is the loss modulus (Pa). The G' is a measure of deformation energy stored by the sample during shearing, which is used to reverse the deformation of the sample partially or completely; it represents the elastic behaviour of a material. The G" is a measure of the unrecoverable deformation energy used by the sample during shearing due to energy loss to frictional heating; it represents the viscous behaviour of a material (Mezger, 2006). It is defined:

$$G' = \left(\frac{\tau_A}{\gamma_A}\right) \cdot cos\delta \qquad Eq.2.15$$

$$G" = \left(\frac{\tau_A}{\gamma_A}\right) \cdot sin\delta \qquad Eq.2.16$$

Where τ_A and γ_A are the amplitude stress (Pa) and amplitude strain (%), respectively.

2.2.1.2.1 AMPLITUDE SWEEP TEST

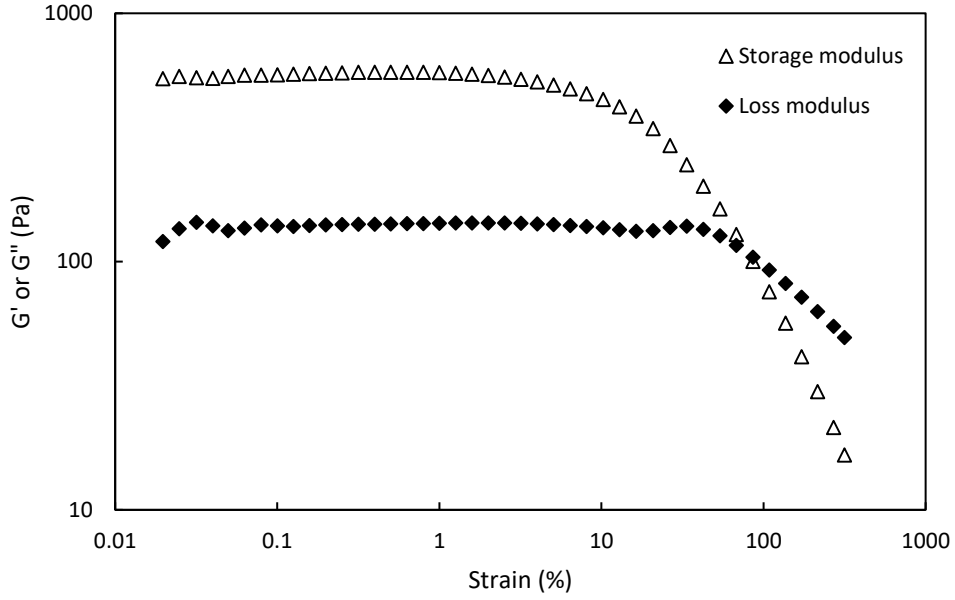

Figure 2.2 – Amplitude sweep for sludge at 10 rad/s.

The amplitude sweep test is an oscillatory test performed by applying variable amplitudes, while keeping the oscillation frequency constant. Results of the amplitude sweep are generally plotted in logarithmic scale with *G'* or *G"* against strain, as in Figure 2.2. The amplitude sweep test reveals the structural character of a sample. At low strain values, both *G'* and *G"* exhibits constant values. This plateau region is termed the linear viscoelastic range (LVE). The limiting value at which the LVE range is exceeded is termed the "yield point" and is the point at which the curve of *G'* or *G"* first deviates the plateau values. This value can be pre-defined as the tolerated range at which values are deviated from the plateau value (e.g. 5 – 10% deviation). Typically, amplitude sweep tests mostly are used to determine the LVE region of a sample. In the LVE region, if *G'>G"* then the sample exhibits weak gel structure. If *G">G'*, then viscous behaviour dominates and samples exhibit character of liquids and tend to flow and show no stability (Mezger, 2006).

2.2.1.2.2 FREQUENCY SWEEP TEST

In frequency sweep tests, the amplitude strain is kept constant while oscillation frequency is varied. Typically, frequency sweeps are performed to investigate the time-dependent deformation behaviour of

samples. Short-term behaviour is simulated by high oscillation frequencies, while long-term behaviour is simulated by low frequencies. The frequency sweep must be performed in the LVE region, as determined by amplitude sweep tests (Mezger, 2006).

2.2.2 WASTEWATER SLUDGE

Sludge refers to the unwanted by-product generated in modern wastewater treatment plants (WWTP). It is a complex material and is notably difficult to characterize (Seyssiecq et al., 2003), but can be described as a suspension of inorganic and organic solids suspended in a liquid of a variety of dissolved solids. The treatment and disposal of sludge often requires over 50% of the operating costs in WWTPs (Spinosa and Vesilind, 2001). Typically, in modern WWTPs sludge originates from primary treatment and secondary treatment, which are part of the sequence of operations used to treat wastewater. Primary sludge, secondary sludge and anaerobically digested sludges are the three main types of sewage sludge.

In primary treatment, primary sludge is produced as a result of removal of settleable solids in the primary clarifier or settling tank. Primary sludge contains the solid material separated from the incoming sewage to WWTPs. It typically contains large amounts of identifiable solid matter and pathogenic organisms. Following primary treatment, the wastewater undergoes secondary treatment. The activated sludge process is the most popular secondary treatment method, where wastewater is mixed with active biomass resulting in the reduction of biological oxygen demand, but an excess growth of biomass. This biomass must be disposed of, and composes secondary sludge, or waste activated sludge (WAS) (Spinosa and Vesilind, 2001). Secondary sludge contains solids but also microorganisms produced during secondary treatment. WAS is significantly different from primary sludge; it is a biological suspension of organic particulates and bacteria held together in flocs of gel-like biofilm matrices called extracellular polymeric substances (EPS) (Li and Ganczarczyk, 1990; Neyens et al., 2004). Digested sludge comprises the stabilized primary and secondary solids produced in anaerobic fermentation.

In sludge, but particularly WAS, EPS are large molecular weight components which originate from bacterial secretion, cell lysis, exocellular constituents, and organic matter in wastewater (Urbain et al., 1993; Wingender et al., 1999). It is considered that EPS contribute greatly to the structural properties and flocculation of sludge (Dong et al., 2011). Furthermore, the hydrophobicity, surface properties and charge density are altered by its presence; sludge dewatering is also affected by presence of EPS since they are able to entrap large volumes of water (Mikkelsen and Keiding, 2002). Hence, rheological properties are

also affected by EPS concentration in sludge flocs (Mikkelsen and Keiding, 2002; Raszka et al., 2006; Urbain et al., 1993).

Due to its inherently low biodegradability and dewatering characteristics, WAS is the sludge type frequently encountered in TH processes (Barber, 2016; Bougrier et al., 2007; Camacho et al., 2008). It is also often encountered in WAO processes (Strong et al., 2011; Suárez-Iglesias et al., 2017; Urrea et al., 2017).

2.2.3 GENERAL SLUDGE RHEOLOGY

Rheological characterisation of sludge is a very useful tool in sludge-handling processes such as transportation, stirring, settling, disposal, and mass oxygen transfer; it allows prediction and estimation of sludge behaviour during these processes and are used in heat and mass transfer calculations (Bandrés et al., 2009). Generally, sludge can be represented as a water-based suspension containing suspended particles, fibrous material and dissolved substances (Baroutian et al., 2013). Sludge characteristics tend to vary depending on wastewater source, treatment process, chemical additives (e.g. polymers) and mechanical operations. Hence its fluid behaviour also varies accordingly (Seyssiecq et al., 2003).

The rheological behaviour of only very dilute sludges is Newtonian but is generally non-Newtonian at increasing solids concentration (Dentel, 1997; Sanin, 2002; Spinosa and Vesilind, 2001). Sludge viscosity is affected by its temperature, particle size distribution, extracellular polymeric substances, and solids concentration (Forster, 1982). Waste activated sludge (WAS) has been identified showing either plastic (Dick, 1986; Dick and Ewing, 1967) or pseudoplastic (Behn, 1962; Moeller and Torres, 1997) behaviour. Wastewater sludges also possess viscoelastic properties (Ayol et al., 2006; Jean Christophe Baudez et al., 2013). Due to its non-Newtonian nature, the shear stress of sludge is not linearly proportional to the shear rate. This has led to difficulty in its rheological characterisation, since its rheological properties cannot be simply related to a single parameter, such as the viscosity (Seyssiecq et al., 2003). The rheological characterisation of sludges have been performed using a range of devices and methods, including capillary rheometers (Behn, 1962; Slatter, 1997) and rotational rheometers (Forster, 1982; Lotito et al., 1997; Mori et al., 2006) but there is no conclusive argument for choosing one over the other.

Sludge's rheological properties have been shown to be strongly correlated to structural and surface characteristics of bio aggregates (Li and Yu, 2011). The colloidal properties of sludge solids Is believed to be the primary contributor to its non-Newtonian characteristics (Hiemenz and Rajagopalan, 1997).

Rheological behaviour of colloidal dispersions has been summarized as being dependent on (Shaw, 1992): dispersion medium viscosity, solids concentration, particle size and shape, and inter-particle or particle-dispersion medium interactions. In terms of WAS, the dispersion medium is considered to be water, a Newtonian fluid of constant viscosity. The impact of solids concentration on WAS rheology is well studied (Dick and Buck, 1985; Dick and Ewing, 1967; Lotito et al., 1997). On the other hand, the impact of particle size and shape is difficult to characterize since WAS has a broad particle size distribution, which also changes with time and physical and chemical factors like shear stresses or solution chemistry (Sanin, 2002). The inter-particle and particle-dispersion medium interactions have not been well studied for sludge.

A wide variety of rheological models have been used to describe sludge rheological behaviour. The power-law, or Ostwald model (Eq. 2.17) is frequently encountered (Ayol et al., 2006; Behn, 1962; Lotito et al., 1997; Valioulis, 1980), as well as the Bingham model (Eq.2.18) (Frost and Owens, 1982; Khalili Garakani et al., 2011; Sozanski et al., 1997). For thicker sludges, Herschel-Bulkley model (Eq. 2.19) appropriately describes flow behaviour at a wide range of shear rates (Baudez et al., 2011) and is commonly used for sludge (Tixier et al., 2003). The Sisko (Eq. 2.20) and Casson (Eq. 2.21) equations have also been used (Baudez, 2008; Seyssiecq et al., 2003).

$$\tau = K\dot{\gamma}^n \qquad Eq.2.17$$

$$\tau = \tau_y + K\dot{\gamma} \qquad Eq.2.18$$

$$\tau = \tau_y + K\dot{\gamma}^n \qquad Eq.2.19$$

$$\tau = \eta_\infty\dot{\gamma} + K\dot{\gamma}^n \qquad Eq.2.20$$

$$\sqrt{\tau} = \sqrt{\tau_y} + \sqrt{\eta\dot{\gamma}} \qquad Eq.2.21$$

In the case of non-Newtonian fluids, the "flow-index", $n < 1$ in equations 2.17, 2.19 and 2.20 describes shear-thinning behaviour. Equations 2.18, 2.19 and 2.21 incorporate a yield stress value, τ_y, which must be exceeded in order to initiate flow. The existence of a yield stress is generally believed to be due to the resistance of solid particles to deformation. In suspensions, the yield stress has also been linked to the presence of a three-dimensional interconnected floc network (Hoover et al., 2001), and corresponds to the stress which must be applied to overcome Van-Der-Waals forces of cohesion. Generally, the yield stress value increases with increasing solid fraction, but decreases as sludge flocs are disrupted under shear (Seyssiecq et al., 2003; Spinosa et al., 1989).

Most sludges also exhibit thixotropic nature, which relates to its time-dependent behaviour. This is mostly related to the tendency of sludges to flocculate. As such, the shearing history of sludge also contributes to its rheological response. For example, if the sludge has not been sheared, the particles are strongly flocculated, leading to high viscosity. But if the sludge had been previously pre-sheared, the particles become disrupted, which leads to lower viscosity values. In practice, this means during rheological measurements, the thixotropic characteristics must be considered since introducing sludge samples to the rheometer will impose a history of shearing. Therefore, samples are generally submitted to a pre-shear phase before rheological measurements. This ensures all samples receive the same degree rearrangement of their internal structure before characterisation (Seyssiecq et al., 2003). The power required to maintain flow in a flocculant suspension (Colin, 1970; Michaels and Bolger, 1962) is used to: disrupt large-scale floc network and overcome yield stress; overcome viscous resistance; and continuously disrupt bonds between groups of particles in aggregates.

Table 2.3 presents some of the developments and major studies relevant to sewage sludge rheology in recent decades.

Table 2. 3 – Development of studies regarding the rheological behaviour of sewage sludge.

Author(s)	Sludge type	Sludge concentration and temperatures	Main rheological observations
Bhattacharya (1981)	*Primary*	3.77 – 7.48 wt%	Non-Newtonian behaviour in both primary and digested sludge, exhibiting yield stress. Primary sludge is shear-thinning, but digested sludge was shear-thickening. Flow behaviour expressed by yield power-law and parabolic model at various temperatures (9 – 37 °C). Yield stress varied exponentially with concentration and linearly with temperature for primary sludge.
	Digested	1.13 – 4.14 wt% (9 – 37 °C)	
Forster (1983)	*WAS*	18.5 – 26.3 g/L	Surface components significantly determine sludge viscosity. Polysaccharides and proteins are the most important surface polymers for WAS, whereas lipopolysaccharides and proteins are important for digested sludge. Bound water content also determines sludge rheology. Volatile fatty acids in digested sludge do not affect rheology.
	Digested	27.3 – 35.6 g/L (45 °C)	

Author(s)	Sludge type	Sludge concentration and temperatures	Main rheological observations
Lotito et al. (1997)	*WAS* *Raw mixed* *Digested* *Dewatered*	0.56 – 5.4% 2.2 – 8.2% 1.2 – 7.6% 1.3 – 9% (20 °C)	All sludges described by Bingham and Power-law models, but Power-law model showed slightly better R^2 values overall. Rheological parameters showed power-law relationship with sludge concentration. For Bingham model, apparent viscosity correlated more strongly than yield stress to concentration; for Power-law model, consistency index correlated more strongly than flow index to concentration. Relationship between rheological parameters with sludge concentration were not equally described for all sludge types, suggesting other parameters besides sludge concentration dominate sludge rheology. For example, extracellular polymers in WAS. Results suggested at concentrations above 8-10%, rheological behaviour possibly changed from liquid to plastic behaviour.
Moeller and Torres (1997)	*Primary* *WAS* *Digested*	1 – 1.5% 1% 3% (N/A)	Sludges showed shear-thinning, Power-law behaviour, with *n*-value 0.4 – 0.7. No yield stress detected, possibly due to low sludge concentrations. Sludge concentration was linearly correlated with *k*-values, but not with *n*-values. Chemical and biological oxygen demand (BOD and COD) were not strongly correlated with *k* and *n*, neither did volatile suspended solids (VSS). Total suspended solids (TSS) correlated linearly with *n*, but not with *k.*
Riley and Forster (2001)	*WAS* *Digested*	<3% <7% (20 °C)	Yield stress of digested sludge and WAS increased with sludge concentration, described by an exponential relationship or polynomial equation. Yield stress of WAS were an order of magnitude greater than digested sludges; yield stress of WAS 2.3 – 3.8 Pa compared to 0.13 – 0.23 Pa for digested sludge, at 4% concentration). Surface charge and bound water content of digested sludges were lower than WAS. Results suggest some parameter other than bound water content determines yield stress.
Forster (2002)	*WAS* *Digested*	1 – 5% TSS 2 – 7% TSS (20 °C)	All sludges exhibited non-Newtonian behaviour with yield stress. For WAS concentrations below 1.1 %, yield stress was negligible, suggesting a critical solids concentration for occurrence of yield stress. WAS yield stress followed power-law relationship with solids concentration. Iron dosing and polymer addition reduced WAS yield stress. Digested sludge showed

Author(s)	Sludge type	Sludge concentration and temperatures	Main rheological observations
			exponential relationship between yield stress and solids concentration. Surface charge of sludges were related logarithmically to yield stress; higher surface charges are associated with higher yield stress. Similarly, bound water content was also logarithmically related to sludge yield stress.
Sanin (2002)	*WAS*	0.2 – 1.8 % (25 °C)	WAS rheological behaviour best described by Power-law model. *K*-value increased with solids concentration; *n*-value decreased with increasing solids concentration. Apparent viscosity increased exponentially with solids concentration. Apparent viscosity increased at increasing pH. Decrease in sludge viscosity correlates with the removal of extracellular polymers from the sludge, which are suspected to act as glues holding sludge particles together.
Tixier et al. (2003)	*WAS*	0 - 22 g/L TSS (20 °C)	WAS showed shear-thinning behaviour. Limit viscosity increased with TSS following an exponential relationship. At fixed TSS, limit viscosity varied depending on sludge origin. Increasing sludge volume index (SVI) was correlated with increasing limit viscosity. Filamentous sludge showed higher hysteresis area in rheograms, even at low TSS concentration, compared to low-filamentous sludge.
Guibaud et al. (2004)	*WAS*	<10 g/L TSS (20 °C)	WAS exhibited minor thixotropic behaviour. Rheological behaviour best described by Bingham model. Sludge viscosity and yield stress increased with TSS following an exponential relationship. Viscosity of sludge supernatant is close to water and did not vary depending on sludge origin.
Mori et al. (2006)	*WAS*	2.5 – 57 g/L TSS (20 °C)	Sludges best described by Herschel-Bulkley model. Yield stress and *k*-value increased exponentially with TSS. Flow index, *n*, decreased linearly with TSS. Yield stress values obtained from oscillatory measurements (static yield stress) were comparable to flow measurement (dynamic yield stress). The critical strain value (~11%) remained largely constant in the range of concentrations studied. The energy of cohesion (a measure of inter-particle interaction) was calculated and shown to increase exponentially with TSS.

Author(s)	Sludge type	Sludge concentration and temperatures	Main rheological observations
Baudez et al. (2011)	*Digested*	2.6 – 4.9 % (25 °C)	Sludge exhibited linear viscoelastic response at low shear stresses, modelled by a generalized Kelvin-Voigt model. As sludge flowed in the liquid regime, the behaviour could be described by Herschel-Bulkley or power-law models at low to intermediate shear rates, and Bingham model at high shear rates. Despite varying sludge concentrations, sludge flow curves were similar, indicating similarity of network interactions within the sludge at different concentrations. Yield stress and Bingham viscosity increased with solid concentration following a power-law and exponential relationship, respectively.
Baroutian et al. (2013)	*Primary and WAS mixture (40:60)*	4.3 – 9.8% (25 – 55 °C)	NMR analysis revealed protein as the dominant sludge component and carbohydrates (cellulosic) were the second largest. Herschel-Bulkley model described sludge rheology with average error 3.25 – 6.22%. Yield stress followed linear relationship with solids concentration and exponential relationship with inverse of temperature. Herschel-Bulkley coefficient, *k*, decreased linearly with temperature but *n* was kept constant across the temperatures investigated. Furthermore, *k* and *n* showed logarithmic and power-law relationship, respectively, with solids content.
Yuan and Wang (2013)	*WAS*	54 g/L TSS (25 °C)	Proteins and polysaccharide are major constituents of sludge extracellular polymeric substances (EPS). Despite extraction of EPS, sludge exhibited non-Newtonian behaviour; thixotropy; and in the LVE region, G'>G". After extraction of loosely-bound EPS, sludge exhibited greater thixotropy – implying sludge containing tightly-bound EPS exhibited stronger network structure. Tightly-bound EPS greatly influenced thixotropy, viscous properties, interactions between flocs and aggregates, cohesion energy, and elasticity.
Markis et al. (2014)	*Primary* *WAS*	2.8 – 8.2% 2.8 – 9.2% (20 °C)	Primary and secondary sludge behaved as shear-thinning, yield stress fluids described by Herschel-Bulkley model. Sludge flow curves could be described by a single master curve. Primary sludge exhibited thixotropy, being dependent on shear history. Secondary sludge exhibited time-dependent behaviour whereby restructuration of the sludge occurred with increasing time of rest. Below the yield stress the

Author(s)	Sludge type	Sludge concentration and temperatures	Main rheological observations
			sludges displayed viscoelastic behaviour. However, primary sludge yielded abruptly but secondary sludge transitioned smoothly into the liquid regime. For both sludges, the relationship between apparent viscosity, yield stress, and consistency index with increasing sludge concentration were described by exponential, power-law, and power-law, respectively.
Eshtiaghi et al. (2016)	*WAS* *Digested* *Mixed WAS and digested*	1.4 – 7% 1.5 – 7% 1.8 – 7%	Secondary, digested and mixtures of these sludges showed shear-thinning, yield stress behaviour. The addition of digested sludge into WAS at constant solids concentration caused an exponential increase in apparent viscosity and yield stress. Sludge flow curves were described by a single master curve based on Herschel-Bulkley model.
Markis et al. (2016)	*Mixed primary and WAS*	2.5 – 7% (20 °C)	Mixed sludge showed shear-thinning, yield stress behaviour described by a single master curve based on Herschel-Bulkley model. Apparent viscosity of mixed sludge increased with increasing fraction of WAS volume which suggested the colloidal components of primary sludge become entangled in secondary sludge's gel-like network structure.
Feng et al. (2016)	*Digested*	28.3 – 26.5 g/L TSS (35 °C)	Herschel-Bulkley model best described sludge behaviour, showing thixotropic behaviour. Sludge viscosity and TSS showed strong linear positive correlation; whereas viscosity and EPS concentration showed negative correlation.
Yuan et al. (2017)	*WAS*	35 g/L TSS (25 °C)	Before and after EPS extraction, sludge showed shear-thinning, thixotropic behaviour. Sludge viscosity and thixotropy increased with TSS. In descending order, the viscosity, hysteresis area, yield stress, cohesion energy, and shear modulus (*G*) followed: WAS after extraction of loosely-bound EPS > raw WAS > WAS after extraction of tightly-bound EPS > WAS after slime extraction. This meant sludge flocs showed stronger interactions after extraction of loosely-bound EPS.

2.2.4 SLUDGE RHEOLOGY IN THERMAL PROCESSES

Despite being an important parameter in the design and operation of hydrothermal processes such as Thermal Hydrolysis (TH), the rheological behaviour of sludge during these processes has not been studied in great detail (Barber, 2016). As shown in Table 2.3, most studies on sludge rheology are focused on non-thermally treated sludges at ambient to moderate conditions (20 – 70 °C) and are related to its application in activated sludge processes and anaerobic or aerobic digestion. Mainly, there is a lack of studies on sludge rheology at the elevated temperature and pressure conditions encountered in hydrothermal processes. Furthermore, the majority of available studies of rheology in sludge thermal processing have been done post-thermal treatment and is only indicative of the final behaviour of the thermally-treated sludge.

In hydrothermal processing, the primary factors which might influence sludge's rheological properties are the elevated temperature and pressurized conditions, as well as the change in sludge's composition due to chemical changes and solubilization effects. The influence of temperature has been well studied. For example, it has been shown that temperature has a significant influence on sewage sludge viscosity (Manoliadis and Bishop, 1984). The relationship between apparent viscosity and sludge temperature (5-30 °C) has been described by the Arrhenius equation; yield stress and Herschel-Bulkley flow index, *n*, increased, while consistency index, *k*, decreased with temperature (Hammadi et al., 2012). On the other hand, it has also been shown that the yield stress and Bingham viscosity decreased with temperature (10 - 60 °C) in digested sludge (Baudez et al., 2013b). It was suggested that sludge flocs became less dense and compact at higher temperature, either due to an increase in the number of voids in the flocs, or due to an increase in floc surface area. This causes a modification of sludge structure which was also irreversible, and termed 'thermal history' (Baudez et al., 2013b). It has also been pointed out that increasing temperatures causes dissolution of organic and inorganic sludge components (Appels et al., 2010; Paul et al., 2006). Then, the argument was made that the change of viscosity or yield stress with temperature based on Arrhenius equation would be inaccurate, since the activation energy would change as sludge composition changes due to thermal treatment (Baudez et al., 2013b). The viscoelastic properties have also been shown to be proportional to the decrease in water viscosity due to the effect of thermal motion at increasing temperatures (Baudez et al., 2013a). Table 2.3 also lists some studies which related the changes in rheological parameters, like yield stress, to temperature. The impact of pressure on sludge rheology is not studied, however it is considered to be negligible since the pressures

encountered are relatively low (<10 bar, in the case of TH); for water, the viscosity would only increase at pressures well above 1000 bar (Barnes, 2000).

In the case of TH, it has been reported that the resultant effect of hydrolysis was to effectively change sludge rheological behaviour such that it behaved as if it were less concentrated. For example, a thermally hydrolysed 12 wt% mixed primary and secondary sludge is comparable to digested sludge at 7-8 wt% (Cumiskey et al., 2003). The viscosity reduction in thermally-treated sludge has been uniformly observed in all studies related to sludge thermal treatment. Verma et al. (2007) investigated the pre-treatment of wastewater sludge (10 – 50 g/L) in thermal (120 °C, 30 min) and thermal alkaline (120 °C, 15 min, pH = 10.25) treatment and found apparent viscosity decreased by 6-22% and 13-42% for thermal and thermal alkaline treatment, respectively. A higher viscosity drop was observed in the higher sludge concentration ranges. The apparent viscosity was related to sludge concentration exponentially in both raw and treated sludges. Non-Newtonian, Power-law behaviour was observed in the sludges, but thermally treated and alkaline thermally treated sludge tended towards Newtonian behaviour. The consistency index, *k*, decreased whereas the flow index, *n*, increased due to thermal treatment. Table 2.4 presents a number of studies related to sludge thermal treatment in which changes to sludge rheology were presented, but not the main focus.

Only in recent years interest has been increasing for detailed rheological study for sludge thermal treatment. Feng et al. (2014) studied the rheological behaviour in raw and thermally treated (170 °C, 60 min) WAS (10 – 187 g/L) obtained in a lab-scale reactor. The sludges displayed Herschel-Bulkley flow behaviour, thixotropy, and viscoelasticity. As a result of TH, the Herschel-Bulkley parameters *k* decreased significantly while *n* increased, showing increasingly Newtonian behaviour. These parameters were correlated with sludge concentration by exponential relationship, and with temperature by an Arrhenius-type equation. Storage modulus, *G'*, decreased by 92.5% after TH. Urrea et al. (2015) studied WAS (23.3 g/L TSS) rheology during TH (160 – 200 °C, 0 – 250 min) by sampling sludge at different periods. Initially, sludge behaved as a Bingham plastic, but showed Newtonian behaviour at the end of treatment. The temperature-dependence of the treated sludge viscosity was described by an Arrhenius-type equation. Zhang et al. (2017) performed laboratory test for TH at low (60 – 90 °C and high temperature (120 – 180 °C) on mechanically dewatered sludge (14.2 – 18.2 wt%) and attempted to correlate sludge organic solubilization with viscoelastic properties. Treated sludge exhibited viscoelastic properties, and *G'* was linearly correlated to soluble proteins, polysaccharides and chemical oxygen demand (COD) in low temperature TH, but showed logarithmic relationship for high temperature TH.

Additional literature review on TH sludge rheology is provided in the subsequent results and discussion chapters, provided alongside discussion which are relevant within the context of that chapter.

Table 2. 4– Impact of hydrothermal treatment on sludge rheology.

Author	Pre-treatment conditions and sludge type	Rheological measurement temperature	Impact on sludge rheology
Dote et al. (1993)	*150 – 300 °C* *0 – 60 min* *Dewatered sludge* *(1.2 – 12.7 wt%)*	6 – 30 °C	Treated sludge showed Power-law behaviour. Sludge viscosity decreased after thermal treatment. Apparent viscosity of treated sludge decreased with measurement temperature by 20 – 30% when temperature increased from 6 – 30 °C.
Bougrier et al. (2006)	*170 – 190 °C* *30 – 60 min* *WAS* *(20 g/L)*	N/A	Shear stress response (flow curves) decreased for treated sludge. Apparent viscosity (100 s^{-1}) decreased by 91%. Treated sludge showed Newtonian behaviour compared to Power-law behaviour of untreated sludge. *K* decreased by a factor of 100, but *n* increased from 0.42 – 0.89.
Urrea et al. (2014)	*160 – 200 °C* *0 – 200 min* *WAS* *(32.25 g/L)*	5 – 100 °C	Raw WAS showed Bingham behaviour, but Herschel-Bulkley behaviour was observed during treatment. Apparent viscosity (25 °C) reduced by two orders of magnitude after treatment regardless of treatment temperature. After treatment sludge showed Newtonian flow behaviour. Sludge temperature did not have a marked effect on apparent viscosity of treated sludge.
Bougrier et al. (2008)	*90 – 210 °C* *30 min* *WAS* *(14.8 – 33.7 g/L)*	N/A	Apparent viscosity of treated sludge (50 s^{-1}) decreased 30% after thermal treatment. Apparent viscosity decreased with increasing treatment temperature up to 150 °C but remained constant at higher treatment temperatures.
Pérez-Elvira et al. (2008)	*170 °C* *30 min* *Primary, WAS, mixed* *(3 – 11 wt%)*	N/A	After TH, sludge viscosity reduced by 70%.
Perez-Elvira et al. (2010)	*170 °C* *30 min* *Mixed sludge* *(35 g/L)*	25 °C	Apparent viscosity of TH sludge was 70% lower than non-treated sludge. Treated sludge showed shear-thinning behaviour.

Author	Pre-treatment conditions and sludge type	Rheological measurement temperature	Impact on sludge rheology
Pérez-Elvira et al. (2011)	*170 °C* *30 min* *Mixed sludge* *(30.5 -58.3 g/L)*	25 °C	Sludge behaved as non-Newtonian fluid. Apparent viscosity radically decreased after TH.
Liu et al. (2012)	*175 °C* *60 min* *WAS* *(0.08 wt%)*	N/A	Apparent viscosity reduced by 95% after TH.
Carvajal et al. (2013)	*55 °C* *12-24 h* *WAS* *(2.3 – 8 g/L)*	20 °C	Sludge flow behaviour described by Herschel-Bulkley model. Yield stress reduced by 82%. *K* decreased by 10%.
Pereboom et al. (2014)	*140 – 160 °C* *30 – 60 min* *WAS* *(6 – 11 wt%)*	15 – 100 °C	For raw WAS, temperature strongly reduces viscosity between 15 – 60 °C, but the effect is less pronounced at higher temperatures. After TH, the apparent viscosity (50 s^{-1}) reduced by 98%.
Farno et al. (2014)	*50 – 80 °C* *1 – 30 min.* *Digested sludge* *(2.2 wt%)*	20 – 80 °C	Sludge rheology showed partial irreversibility due to thermal treatment. Apparent viscosity and yield stress of sludge decreased with increasing temperature and duration of heating. Soluble COD of sludge was irreversibly increased after thermal treatment and this increase of COD was proportional to the decrease of yield stress and increase of infinite viscosity of treated sludge.
Farno et al. (2015)	*50 – 80 °C* *1 – 60 min* *Digested sludge* *(3 – 7.2 wt%)*	20 – 80 °C	Higher sludge concentrations, higher temperature and longer duration led to a greater extent of irreversible change in treated sludge rheology. Sludge apparent viscosity, yield stress and COD solubilisation followed a logarithmic relationship with treatment duration. Linear relationship existed between COD solubilisation and reduction of yield stress and apparent viscosity. Sludge flow curves were described by a modified Herschel-Bulkley model and all curves could be described by a single master curve. Increased soluble COD suggests the rheological changes were due related to structural and compositional changes of sludge due to COD solubilisation.

Author	Pre-treatment conditions and sludge type	Rheological measurement temperature	Impact on sludge rheology
Farno et al. (2016a)	*50 – 80 °C* *1 – 60 min* *WAS* *(6.1 – 9.9 wt%)*	20 – 80 °C	The rate of yield stress and infinite viscosity reductions due to thermal treatment were linearly proportional to the rate of organic matter solubilisation. Sludge flow curves were described by a single master curve based on a modified Herschel-Bulkley model. Yield stress and infinite viscosity decreased irreversibly with increasing temperatures, temperature of thermal history, and duration of treatment.
Xue et al. (2015)	*120 – 180 °C* *15 – 180 min* *WAS* *(16.7 wt%)*	25 °C	Apparent viscosity reduced by 96 – 99% depending on treatment temperature.
Farno et al. (2016b)	*50 – 80 °C* *1 – 60 min* *WAS* *(6.1 wt%)*	20 – 80 °C	Storage (*G'*) and loss (*G"*) moduli decreased linearly with treatment temperature and duration. The impact of temperature was comparable to the impact of treatment duration on sludge's storage *G'* and *G"*. Higher temperature treatment at shorter duration had similar impact on viscoelastic properties of sludge as low-temperature thermal treatment at longer duration. Linear relationship existed between soluble COD increase and decrease of *G'* and *G"*. A Rutgers-Delaware approach could be used to relate viscous properties to viscoelastic properties of the untreated and thermally treated sludges.
Liao et al. (2016)	*60 – 80 °C* *15 – 90 min* *Dewatered sludge* *(9.1 – 16.6 wt%)*	N/A	Sludge behaviour modelled as Power-law fluid. Sludge apparent viscosity decreased 48.6%. *k* decreased 17 – 64%.
Farno et al. (2018)	*50 – 80 °C* *1 – 60 min* *WAS* *(6.1 wt%)*	20 – 80 °C	Frequency and creep test results for untreated and thermally-treated sludges were well described by a fractional Kelvin-Voigt model. Fractional Kelvin-Voigt model was better than traditional Kelvin-Voigt model in describing creep data at lower strain rates.

2.3 GAPS OF KNOWLEDGE AND RESEARCH QUESTIONS.

Rheological knowledge of sludge behaviour is paramount to optimization of sludge-handling operations. This invariably includes hydrothermal sludge processing units, as a more detailed rheological study can help improve operation of the processes (Barber, 2016) as well as improve energy balance around the entire sludge treatment system (Pérez-Elvira and Fdz-Polanco, 2012). Although some rheological studies have been performed, this literature survey has revealed several gaps still existed and arguments to be made with regards to the existing body of knowledge. In particular, most of the rheology studies were carried out on sludge only post-treatment, and mostly at ambient conditions. Since the thermal history of the sludge significantly impacts its rheology (Farno et al., 2016), it is based on assumption to relate the rheology of post-treated sludge to the true sludge behaviour during hydrothermal processes. Notably, most rheology studies available were conducted in context of how it affects the downstream processes such as dewatering and anaerobic digestion, rather than how it affects the hydrothermal processing units themselves. Only limited number of studies have investigated sludge in the moderate to high concentration ranges (5 – 15 wt%) typically encountered in hydrothermal processing, and studies on viscoelasticity of sludge are relatively scarce and recent.

In that regard, the current study aims to investigate, particularly, the in-situ rheological behaviour of sludge in TH processes. Furthermore, the potential for using the rheological observations as a means to indirectly monitor TH performance is also examined by linking rheological properties to compositional changes of sludge during thermal treatment process. To achieve this, the following areas of investigation are presented in this thesis:

- Detailed study of rheological changes of WAS during TH processes using in-situ rheometry methods.
- Detailed study of the compositional changes of WAS during TH using a lab-scale reactor.
- Correlating rheological changes observed to the compositional changes of WAS during TH.
- Investigation on the impact of sludge concentration on its flow behaviour and viscoelasticity.
- Developing mathematical models to predict rheological changes of sludge in TH at various TH conditions, including temperature, time, and sludge concentration.

REFERENCES

Abe, N., Tang, Y.-Q., Iwamura, M., Morimura, S. & Kida, K. 2013. Pretreatment followed by anaerobic digestion of secondary sludge for reduction of sewage sludge volume. Water Science & Technology, 67, 2527-2533.

Abe, N., Tang, Y.-Q., Iwamura, M., Ohta, H., Morimura, S. & Kida, K. 2011. Development of an efficient process for the treatment of residual sludge discharged from an anaerobic digester in a sewage treatment plant. Bioresource technology, 102, 7641-7644.

Abelleira, Jose, Sara I. Pérez-Elvira, Juan R. Portela, Jezabel Sánchez-Oneto, and Enrique Nebot, 2012, Advanced Thermal Hydrolysis: Optimization Of A Novel Thermochemical Process To Aid Sewage Sludge Treatment, *Environmental science & technology* 46, no. 11, p6158-6166.

Aggrey, A., Dare, P., Lei, R., & Gapes, D. , 2011. Evaluation of a two-stage hydrothermal process for enhancing acetic acid production using municipal biosolids. Water Science & Technology, 65(1), 149-155.

Appels, L., Baeyens, J., Degrève, J. & Dewil, R. 2008. Principles and potential of the anaerobic digestion of waste-activated sludge. Progress in Energy and Combustion Science, 34, 755-781.

Appels, L., Degrève, J., Van der Bruggen, B., Van Impe, J., Dewil, R., 2010. Influence of low temperature thermal pre-treatment on sludge solubilisation, heavy metal release and anaerobic digestion. Bioresour. Technol. 101, 5743–5748. doi:10.1016/j.biortech.2010.02.068

Ayol, A., Filibeli, A., Dentel, S.K., 2006. Evaluation of conditioning responses of thermophilic-mesophilic anaerobically and mesophilic aerobically digested biosolids using rheological properties. Water Sci. Technol. 54, 23–31. doi:10.2166/wst.2006.543

Bandrés, I., Giner, I., Aldea, M.E., Cea, P., Lafuente, C., 2009. Experimental and predicted viscosities of binary mixtures of cyclic ethers with 1-chloropentane or 1-chlorohexane at 283.15, 298.15, and 313.15K. Thermochim. Acta 484, 22–26. doi:https://doi.org/10.1016/j.tca.2008.11.009

Barber, W.P.F., 2016. Thermal hydrolysis for sewage treatment: A critical review. Water Res. 104, 53–71. doi:10.1016/j.watres.2016.07.069

Barnes, H.A., 2000. A handbook of elementary rheology. Institute of non-Newtonian Fluid Mechanics, University of Wales.

Baroutian, S., Eshtiaghi, N., Gapes, D.J., 2013. Rheology of a primary and secondary sewage sludge mixture:

dependency on temperature and solid concentration. Bioresour. Technol. 140, 227–233.

Baroutian, S., Robinson, M., Smit, A-M., Wijeyekoon, S., Gapes, D., 2013a. Transformation and removal of wood extractives from pulp mill sludge using wet oxidation and thermal hydrolysis, Bioresource Technology, doi: http://dx.doi.org/10.1016/j.biortech.2013.07.098

Baroutian, S., Smit, A-M., Gapes, D., 2013b. Relative influence of process variables during non-catalytic wet oxidation of municipal sludge, Bioresource Technology, Volume 148, Pages 605-610, doi: http://dx.doi.org/10.1016/j.biortech.2013.08.160.

Baudez, J.C., 2008. Physical aging and thixotropy in sludge rheology. Appl. Rheol. 18, 1–8.

Baudez, J.C., Gupta, R.K., Eshtiaghi, N., Slatter, P., 2013a. The viscoelastic behaviour of raw and anaerobic digested sludge: Strong similarities with soft-glassy materials. Water Res. 47, 173–180. doi:https://doi.org/10.1016/j.watres.2012.09.048

Baudez, J.C., Markis, F., Eshtiaghi, N., Slatter, P., 2011. The rheological behaviour of anaerobic digested sludge. Water Res. 45, 5675–5680. doi:http://dx.doi.org/10.1016/j.watres.2011.08.035

Baudez, J.C., Slatter, P., Eshtiaghi, N., 2013b. The impact of temperature on the rheological behaviour of anaerobic digested sludge. Chem. Eng. J. 215–216, 182–187. doi:10.1016/j.cej.2012.10.099

Behn, V.C., 1962. Experimental determination of sludge-flow parameters. J. Sanit. Eng. Div. 88, 39–54.

Berardinelli, S., Resini, C., & Arrighi, L., 2008, Technologies for the removal of phenol from fluid streams: a short review of recent developments. Journal of Hazardous Materials, 160(2), 265-288.

Bermejo, M. D., & Cocero, M. J., 2006. Supercritical water oxidation: a technical review. AIChE Journal, 52(11), 3933-3951.

Bernardi, M., Cretenot, D., Deleris, S., Descorme, C., Chauzy, J., & Besson, M., 2010. Performances of soluble metallic salts in the catalytic wet air oxidation of sewage sludge. Catalysis Today, 157(1), 420-424.

Bhargava, S. K., Tardio, J., Prasad, J., Föger, K., Akolekar, D. B., & Grocott, S. C., 2006, Wet oxidation and catalytic wet oxidation. Industrial & engineering chemistry research, 45(4), 1221-1258.

Bougrier, C., Delgenes, J. P. & Carrère, H. 2008. Effects of thermal treatments on five different waste activated sludge samples solubilisation, physical properties and anaerobic digestion. Chemical Engineering Journal, 139, 236-244.

Bhattacharya, S.N., 1981. Flow characteristics of primary and digested sewage sludge. Rheol. Acta 20, 288–298.

Bougrier, C., Albasi, C., Delgenès, J.P., Carrère, H., 2006. Effect of ultrasonic, thermal and ozone pre-treatments on waste activated sludge solubilisation and anaerobic biodegradability. Chem. Eng. Process. Process Intensif. 45, 711–718. doi:10.1016/j.cep.2006.02.005

Bougrier, C., Delgenès, J.P., Carrère, H., 2007. Impacts of thermal pre-treatments on the semi-continuous anaerobic digestion of waste activated sludge. Biochem. Eng. J. 34, 20–27. doi:10.1016/j.bej.2006.11.013

Bougrier, C., Delgenès, J.P., Carrère, H., 2008. Effects of thermal treatments on five different waste activated sludge samples solubilisation, physical properties and anaerobic digestion. Chem. Eng. J. 139, 236–244. doi:10.1016/j.cej.2007.07.099

Brunner, G., 2009. Near critical and supercritical water. Part I. Hydrolytic and hydrothermal processes. The Journal of Supercritical Fluids, 47(3), 373-381.

Byrappa, K. & Yoshimura, M. 2001. Handbook of hydrothermal technology, Access Online via Elsevier.

Cabeza, P., J. P. S. Queiroz, S. Arca, C. Jiménez, A. Gutiérrez, M. D. Bermejo, and M. J. Cocero, 2013, Sludge Destruction By Means Of A Hydrothermal Flame. Optimization Of Ammonia Destruction Conditions, Chemical Engineering Journal 232 , p1-9.

Camacho, P., Ewert, W., Kopp, J., Panter, K., Perez-Elvira, S. & Piat, E. 2008. Combined experiences of thermal hydrolysis and anaerobic digestion latest thinking on thermal hydrolysis of secondary sludge only for optimum dewatering and digestion. Proceedings of the water environment federation, 2008, 1964-1978.

Camacho, P., Ewert, W., Kopp, J., Panter, K., Perez-Elvira, S.I., Piat, E., 2008. Combined experiences of thermal hydrolysis and anaerobic digestion – latest thinking on thermal hydrolysis of secondary sludge only for optimum dewatering and digestion. Proc. Water Environ. Fed. 2008, 1964–1978. doi:10.2175/193864708788733972

CAMBI. 2012. Biosolids Treatment [Online]. Norway: CAMBI. Available: http://www.cambi.no/wip4/plant.epl?cat=10643&id=156450 [Accessed 9 JUL 2013].

Carrere, H., Dumas, C., Battimelli, A., Batstone, D., Delgenes, J., Steyer, J. & Ferrer, I. 2010. Pretreatment methods to improve sludge anaerobic degradability: a review. Journal of hazardous materials, 183, 1-15.

Carvajal, a., Peña, M., Pérez-Elvira, S., 2013. Autohydrolysis pretreatment of secondary sludge for anaerobic digestion. Biochem. Eng. J. 75, 21–31. doi:10.1016/j.bej.2013.03.002

Chauzy, J., Martin, J., Cretenot, D. & Rosiere, J. 2010. Wet air oxidation of municipal sludge: return experience of the North Brussels Waste Water Treatment Plant. Water Practice & Technology, 5.

Chen, N., Liu, Y., Liu, N. & Wang, S. 2012. Energy balance of thermal hydrolysis and anaerobic digestion on waste activated sludge. World Automation Congress (WAC), . IEEE, 1-3.

Chhabra, R.P., Richardson, J.F., 2008. Non-Newtonian fluid behaviour. Non-newtonian flow Appl. Rheol. 1–55.

Chung, J., Lee, M., Ahn, J., Bae, W., Lee, Y. W., & Shim, H., 2009. Effects of operational conditions on sludge degradation and organic acids formation in low-critical wet air oxidation. Journal of hazardous materials, 162(1), 10-16.

Colin, F., 1970. Application de techniques rhéologiques à l'étude des boues résiduaires. Cent. Belge d'Etude Doc. des Eaux 317, 178–187.

Coussot, P., 2005. Rheometry of pastes, suspensions, and granular materials: applications in industry and environment. John Wiley & Sons.

Cumiskey, A., Dawson, M., Tillitson, M., 2003. Thick Solids Digestion - Research, Design and Validation of Key Process Unit Operations, in: Proceedings of the Water Environment Federation. pp. 1415–1432.

Debellefontaine, H. & Foussard, J. N. 2000. Wet air oxidation for the treatment of industrial wastes. Chemical aspects, reactor design and industrial applications in Europe. Waste management, 20, 15-25.

Debellefontaine, H., Chakchouk, M., Foussard, J. N., Tissot, D., & Striolo, P., 1996, Treatment of organic aqueous wastes: Wet air oxidation and wet peroxide oxidation, Environmental pollution, 92(2), 155-164.

Dentel, S.K., 1997. Evaluation and role of rheological properties in sludge management. Water Sci. Technol. 36, 1–8. doi:https://doi.org/10.1016/S0273-1223(97)00662-8

Dick, R.I., 1986. Rheology of Biological Wastewater Suspensions. Rep. to Natl. Sci. Found.

Dick, R.I., Buck, J.H., 1985. Measurement of activated sludge rheology, in: Environmental Engineering. ASCE, pp. 539–545.

Dick, R.I., Ewing, B.B., 1967. The rheology of activated sludge. J. (Water Pollut. Control Fed. 543–560.

Dohányos, M., Zbransk, J., Kutil, J. & Jenek, P. 2004. Improvement of anaerobic digestion of sludge. Water Science & Technology, 49, 89-96.

Dong, Y.J., Wang, Y.L., Feng, J., 2011. Rheological and fractal characteristics of unconditioned and conditioned water treatment residuals. Water Res. 45, 3871–3882. doi:https://doi.org/10.1016/j.watres.2011.04.042

Donoso-Bravo, A., Pérez-Elvira, S., Aymerich, E. & Fdz-Polanco, F. 2011. Assessment of the influence of thermal pre-treatment time on the macromolecular composition and anaerobic biodegradability of sewage sludge. Bioresource technology, 102, 660-666.

Dote, Y., Yokoyama, S.-Y., Minowa, T., Masuta, T., Sato, K., Itoh, S., Suzuki, A., 1993. Thermochemical liquidization of dewatered sewage sludge. Biomass and Bioenergy 4, 243–248. doi:http://dx.doi.org/10.1016/0961-9534(93)90081-E

DWyer, J., Starrenburg, D., Tait, S., Barr, K., Batstone, D. J. & Lant, P. 2008. Decreasing activated sludge thermal hydrolysis temperature reduces product colour, without decreasing degradability. Water research, 42, 4699-4709.

Escala, M., T. Zumbühl, Ch Koller, R. Junge, and R. Krebs, 2012, Hydrothermal Carbonization as an Energy-Efficient Alternative to Established Drying Technologies for Sewage Sludge: A Feasibility Study on a Laboratory Scale, Energy & Fuels 27, no. 1, p454-460

Eshtiaghi, N., Markis, F., Zain, D., Mai, K.H., 2016. Predicting the apparent viscosity and yield stress of digested and secondary sludge mixtures. Water Res. 95, 159–164. doi:10.1016/j.watres.2016.03.002

Eshtiaghi N., Markis, F., Yap, S.D.,Baudez, J.C. , Slatter, P.Rheological characterisation of municipal sludge: a review, Water Research, In press,2013, doi: 10.1016/j.watres.2013.07.001

Farno, E., Baudez, J.C., Eshtiaghi, N., 2018. Comparison between classical Kelvin-Voigt and fractional derivative Kelvin-Voigt models in prediction of linear viscoelastic behaviour of waste activated sludge. Sci. Total Environ. 613–614, 1031–1036. doi:10.1016/j.scitotenv.2017.09.206

Farno, E., Baudez, J.C., Parthasarathy, R., Eshtiaghi, N., 2016a. Impact of thermal treatment on the rheological properties and composition of waste activated sludge: COD solubilisation as a footprint of rheological changes. Chem. Eng. J. 295, 39–48. doi:10.1016/j.cej.2016.03.022

Farno, E., Baudez, J.C., Parthasarathy, R., Eshtiaghi, N., 2016b. The viscoelastic characterisation of thermally-treated waste activated sludge. Chem. Eng. J. 304, 362–368. doi:10.1016/j.cej.2016.06.082

Farno, E., Baudez, J.C., Parthasarathy, R., Eshtiaghi, N., 2015. Impact of temperature and duration of thermal treatment on different concentrations of anaerobic digested sludge: Kinetic similarity of organic matter solubilisation and sludge rheology. Chem. Eng. J. 273, 534–542. doi:10.1016/j.cej.2015.03.097

Farno, E., Baudez, J.C., Parthasarathy, R., Eshtiaghi, N., 2014. Rheological characterisation of thermally-treated anaerobic digested sludge: Impact of temperature and thermal history. Water Res. 56, 156–161. doi:10.1016/j.watres.2014.02.048

Feng, G., Liu, L., Tan, W., 2014. Effect of thermal hydrolysis on rheological behavior of municipal sludge. Ind. Eng. Chem. Res. 53, 11185–11192. doi:10.1021/ie501488q

Feng, X., Tang, B., Bin, L., Song, H., Huang, S., Fu, F., Ding, J., Chen, C., Yu, C., 2016. Rheological behavior of the sludge in a long-running anaerobic digestor: Essential factors to optimize the operation. Biochem. Eng. J. 114, 147–154. doi:10.1016/j.bej.2016.06.022

Ferrer, I., Vázquez, F. & Font, X. 2010. Long term operation of a thermophilic anaerobic reactor: process stability and efficiency at decreasing sludge retention time. Bioresource technology, 101, 2972-2980.

Forster, C.F., 1982. Sludge surfaces and their relation to the rheology of sewage sludge suspensions. J. Chem. Technol. Biotechnol. 32, 799–807.

Forster, C.F., 1983. Bound water in sewage sludges and its relationship to sludge surfaces and sludge viscosities. J. Chem. Technol. Biotechnol. Biotechnol. 33, 76–84.

Forster, C.F., 2002. The rheological and physico-chemical characteristics of sewage sludges. Enzyme Microb. Technol. 30, 340–345. doi:10.1016/S0141-0229(01)00487-2

Frost, R.C., Owens, J.A., 1982. A method of estimating viscosity and designing pumping systems for thickened heterogeneous sludges, in: Proc. 8th Int. Conf. Hydr. Trans. Solids in Pipes, Johannesburg. pp. 485–501.

Fytili, D., & Zabaniotou, A., 2008. Utilization of sewage sludge in EU application of old and new methods—a review. Renewable and Sustainable Energy Reviews, 12(1), 116-140.

Gavala, H. N., Yenal, U., Skiadas, I. V., Westermann, P. & Ahring, B. K. 2003. Mesophilic and thermophilic anaerobic digestion of primary and secondary sludge. Effect of pre-treatment at elevated temperature. Water Research, 37, 4561-4572.

Genç, N., Yonsel, Ş., Dağaşan, L. & Onar, A. N. 2002. Wet oxidation: a pre-treatment procedure for sludge. Waste Management, 22, 611-616.

Giudici, D., & Maugans, C., 2000. Improvement of Industrial Synthesis of Methyl Methacrylate Application of a Wet Air Oxidation Process (WAO). La Chemica e L'Industria.

Guibaud, G., Dollet, P., Tixier, N., Dagot, C., Baudu, M., 2004. Characterisation of the evolution of activated sludges using rheological measurements. Process Biochem. 39, 1803–1810. doi:10.1016/j.procbio.2003.09.002

Hammadi, L., Ponton, A., Belhadri, M., 2012. Temperature effect on shear flow and thixotropic behavior of residual sludge from wastewater treatment plant. Mech. Time-Dependent Mater. 17, 401–412. doi:10.1007/s11043-012-9191-z

Haug, R. T., Stuckey, D. C., Gossett, J. M. & MCCARTY, P. L. 1978. Effect of thermal pretreatment on digestibility and dewaterability of organic sludges. Journal (Water Pollution Control Federation), 73-85.

He, W., Li, G., Kong, L., Wang, H., Huang, J. & Xu, J. 2008. Application of hydrothermal reaction in resource recovery of organic wastes. Resources, Conservation and Recycling, 52, 691-699.

Hecht, N. L., Duvall, D. S., 1975, Characterization and utilization of municipal and utility sludges and ashes, Volume 1, National Environmental Research Center, Office of Research and Development, U.S.Environmental Protection Agency

Hiemenz, P.C., Rajagopalan, R., 1997. Principles of Colloid and Surface Chemistry, revised and expanded. CRC press.

Hoover, S.R., Cashman, K. V, Manga, M., 2001. The yield strength of subliquidus basalts—experimental results. J. Volcanol. Geotherm. Res. 107, 1–18.

Imamura, S., 1999, Catalytic and Noncatalytic Wet Oxidation. Ind Eng Chem Res 38(5): 1743-1753.

Imbierowicz, M. & Chacuk, A. 2012. Kinetic model of excess activated sludge thermohydrolysis. Water Research.

Imteaz, M. A., & Shanableh, A. 2004. , Kinetic model for the water oxidation method for treating wastewater sludges. Developments in Chemical Engineering and Mineral Processing, 12(5‐6), 515-530.

Jin, F., Zhou, Z., Moriya, T., Kishida, H., Higashijima, H. & Enomoto, H. 2005. Controlling hydrothermal reaction pathways to improve acetic acid production from carbohydrate biomass. Environmental science & technology, 39, 1893-1902.

Kang, S., Li, X., Fan, J., & Chang, J., 2013, Hydrothermal conversion of lignin: A review. Renewable and Sustainable Energy Reviews, 27, 546-558.Kepp, U., Machenbach, I., Weisz, N. & Solheim, O. 2000. Enhanced stabilisation of sewage sludge through thermalhydrolysis-three years of experience with full scale plant. Water Science & Technology, 42, 89-96.

Khalili Garakani, A.H., Mostoufi, N., Sadeghi, F., Hosseinzadeh, M., Fatourechi, H., Sarrafzadeh, M.H., Mehrnia, M.R., 2011. Comparison between different models for rheological characterization of activated sludge. Iran. J. Environ. Heal. Sci. Eng. 8, 255–264.

Kolaczkowski, S. T., Plucinski, P., Beltran, F. J., Rivas, F. J., & McLurgh, D. B., 1999, Wet air oxidation: a review of process technologies and aspects in reactor design. Chemical Engineering Journal, 73(2), 143-160.

Kroiss, H. 2004. What is the potential for utilizing the resources in sludge? Water Science & Technology, 49, 1-10.

Lendormi, T., Prevot, C., Doppenberg, F., Foussard, J., & Debellefontaine, H. , 2001. Subcritical wet oxidation of municipal sewage sludge: comparison of batch and continuous experiments. Water Science & Technology, 44(5), 161-169.

Li, D.D.-H., Ganczarczyk, J.J., 1990. Structure of activated sludge floes. Biotechnol. Bioeng. 35, 57–65. doi:10.1002/bit.260350109

Li, L., Chen, P., & Gloyna, E. F., 1991. Generalized kinetic model for wet oxidation of organic compounds. AIChE Journal, 37(11), 1687-1697.

Li, W.-W., Yu, H.-Q., 2011. Physicochemical characteristics of anaerobic H2-producing granular sludge. Bioresour. Technol. 102, 8653–8660. doi:https://doi.org/10.1016/j.biortech.2011.02.110

Li, Y.-Y. & Noike, T. 1992. Upgrading of anaerobic digestion of waste activated sludge by thermal pretreatment. Water Science & Technology, 26, 857-866.

Liao, X., Li, H., Zhang, Y., Liu, C., Chen, Q., 2016. Accelerated high-solids anaerobic digestion of sewage sludge using low-temperature thermal pretreatment. Int. Biodeterior. Biodegradation 106, 141–149.

doi:10.1016/j.ibiod.2015.10.023

Liu, X., Wang, W., Gao, X., Zhou, Y., Shen, R., 2012. Effect of thermal pretreatment on the physical and chemical properties of municipal biomass waste. Waste Manag. 32, 249–255.

Lotito, V., Spinosa, L., Mininni, G., Antonacci, R., 1997. The rheology of sewage sludge at different steps of treatment. Water Sci. Technol. 36, 79–85. doi:http://dx.doi.org/10.1016/S0273-1223(97)00672-0

Luan, M., Jing, G., Piao, Y., Liu, D. Jin, L., 2012, Treatment of refractory organic pollutants in industrial wastewater by wet air oxidation, Arabian Journal of Chemistry, ISSN 1878-5352, doi: http://dx.doi.org/10.1016/j.arabjc.2012.12.003.

Luck, F., 1999. Wet air oxidation: past, present and future. Catalysis today, 53(1), 81-91.

Manoliadis, O., Bishop, P.L., 1984. Temperature Effect on Rheology of Sludges. J. Environ. Eng. 110, 286–290. doi:10.1061/(ASCE)0733-9372(1984)110:1(286)

Markis, F., Baudez, J.C., Parthasarathy, R., Slatter, P., Eshtiaghi, N., 2016. The apparent viscosity and yield stress of mixtures of primary and secondary sludge: Impact of volume fraction of secondary sludge and total solids concentration. Chem. Eng. J. 288, 577–587. doi:10.1016/j.cej.2015.11.107

Markis, F., Baudez, J.C., Parthasarathy, R., Slatter, P., Eshtiaghi, N., 2014. Rheological characterisation of primary and secondary sludge: Impact of solids concentration. Chem. Eng. J. 253, 526–537. doi:10.1016/j.cej.2014.05.085

Maugans, C. B. & Ellis, C. 2002. Wet air oxidation: a review of commercial sub-critical hydrothermal treatment. IT3, 2, 13-17.

Mezger, T.G., 2006. The Rheology Handbook: For Users of Rotational and Oscillatory Rheometers, Coatings compendia. Vincentz Network.

Michaels, A.S., Bolger, J.C., 1962. The plastic flow behavior of flocculated kaolin suspensions. Ind. Eng. Chem. Fundam. 1, 153–162.

Mikkelsen, L.H., Keiding, K., 2002. Physico-chemical characteristics of full scale sewage sludges with implications to dewatering. Water Res. 36, 2451–2462. doi:https://doi.org/10.1016/S0043-1354(01)00477-8

Mishra, V. S., Mahajani, V. V., Joshi, J. B., 1995, Wet Air Oxidation, Ind Eng Chem Res., 34(1), 2 – 48, doi: http://dx.doi.org/10.1021/ie00040a001.

Moeller, G., Torres, L.G., 1997. Rheological characterization of primary and secondary sludges treated by both aerobic and anaerobic digestion. Bioresour. Technol. 61, 207–211.

Mori, M., Seyssiecq, I., Roche, N., 2006. Rheological measurements of sewage sludge for various solids concentrations and geometry. Process Biochem. 41, 1656–1662. doi:10.1016/j.procbio.2006.03.021

Neyens, E. & Baeyens, J. 2003. A review of thermal sludge pre-treatment processes to improve dewaterability. Journal of Hazardous Materials, 98, 51-67.

Neyens, E., Baeyens, J., Dewil, R., De Heyder, B., 2004. Advanced sludge treatment affects extracellular polymeric substances to improve activated sludge dewatering. J. Hazard. Mater. 106, 83–92. doi:10.1016/j.jhazmat.2003.11.014

Ødegaard, H., 2004. , Sludge minimization technologies- An overview. Water Science & Technology, 49(10), 31-40.

Oliviero, L., Barbier, J., & Duprez, D., 2003, Wet air oxidation of nitrogen-containing organic compounds and ammonia in aqueous media. Applied Catalysis B: Environmental, 40(3), 163-184.

Paul, E., Camacho, P., Lefebvre, D., Ginestet, P., 2006. Organic matter release in low temperature thermal treatment of biological sludge for reduction of excess sludge production. Water Sci. Technol. 54, 59–68. doi:10.2166/wst.2006.547

Pereboom, J., Luning, L., Hol, A., van Dijk, L., de Man, A.W.A., 2014. Full scale experiences with TurboTec® continuous thermal hydrolysis at WWTP Venlo (NL) and Apeldoorn (NL), in: Proceedings of Aqua-Enviro 19th European Biosolids and Organic Residuals Conference and Exhibition, Manchester, UK.

Pérez-Elvira, S. & Fdz-Polanco, F. 2012. Continuous thermal hydrolysis and anaerobic digestion of sludge. Energy integration study. Water Science & Technology, 65, 1839-1846.

Pérez-Elvira, S. I., Fernández-Polanco, F., FERNÁNDEZ-POLANCO, M., RODRÍGUEZ, P. & ROUGE, P. 2008. Hydrothermal multivariable approach: Full-scale feasibility study. Electronic Journal of Biotechnology, 11, 7-8.

Pérez-Elvira, S.I., Fdz-Polanco, F., 2012. Continuous thermal hydrolysis and anaerobic digestion of sludge. Energy integration study. Water Sci. Technol. 65, 1839–1846. doi:10.2166/wst.2012.863

Perez-Elvira, S.I., Fdz-Polanco, M., Fdz-Polanco, F., 2010. Increasing the performance of anaerobic digestion: Pilot scale experimental study for thermal hydrolysis of mixed sludge. Front. Environ. Sci. Eng. China 4, 135–141. doi:10.1007/s11783-010-0024-5

Pérez-Elvira, S.I., Fdz-Polanco, M., Fdz-Polanco, F., 2011. Enhancement of the conventional anaerobic digestion of sludge: Comparison of four different strategies. Water Sci. Technol. 64, 375–383. doi:10.2166/wst.2011.593

Pérez-Elvira, S.I., Fernández-Polanco, F., Fernández-Polanco, M., Rodríguez, P., Rouge, P., 2008. Hydrothermal multivariable approach. Full-scale feasibility study. Electron. J. Biotechnol. 11. doi:10.2225/vol11-issue4-fulltext-14

Ploos Van Amstel, J.J.A., Rietema, K. 1973. Wet-air oxidation of sewage sludge. Part II: The oxidation of real sludges. Chemie Ingenieur Technik, 45, 1205-1211.

Qiao, W., Yan, X., Ye, J., Sun, Y., Wang, W. & Zhang, Z. 2011. Evaluation of biogas production from different biomass wastes with/without hydrothermal pretreatment. Renewable Energy, 36, 3313-3318.

Raszka, A., Chorvatova, M., Wanner, J., 2006. The role and significance of extracellular polymers in activated sludge. Part I: Literature review. Acta Hydrochim. Hydrobiol. 34, 411–424. doi:10.1002/aheh.200500640

Riley, D.W., Forster, C.F., 2001. The physico-chemical characteristics of thermophilic aerobic sludges. J. Chem. Technol. Biotechnol. 76, 862–866. doi:10.1002/jctb.456

Sanin, D.F., 2002. Effect of solution physical chemistry on the rheological properties of activated sludge. Water SA 28, 207–212. doi:10.4314/wsa.v28i2.4886

Seyssiecq, I., Ferrasse, J.-H., Roche, N., 2003. State-of-the-art: rheological characterisation of wastewater treatment sludge. Biochem. Eng. J. 16, 41–56.

Shanableh, A. & Shimizu, Y. 2000. Treatment of sewage sludge using hydrothermal oxidation technologyapplication challenges. Water science and technology, 41, 85-92.

Shanableh, A. 2000. Production of useful organic matter from sludge using hydrothermal treatment. Water Research, 34, 945-951.

Shaw, D.J., 1992. Introduction to colloid and surface chemistry (colloid and surface engineering). Oxford Butterworth-Heinemann.

Shi, Wansheng, Chunguang Liu, Youju Shu, Chuanping Feng, Zhongfang Lei, and Zhenya Zhang, 2013, Synergistic Effect Of Rice Husk Addition On Hydrothermal Treatment Of Sewage Sludge: Fate And Environmental Risk Of Heavy Metals, *Bioresource technology* 149, p 496-502.

Slatter, P.T., 1997. The rheological characterisation of sludges. Water Sci. Technol. doi:10.1016/S0273-1223(97)00663-X

Sozanski, M.M., Kempa, E.S., Grocholski, K., Bien, J., 1997. The rheological experiment in sludge properties research. Water Sci. Technol. 36, 69–78.

Spinosa, L. & Vesilind, P. A. 2001. Sludge into biosolids: processing, disposal and utilization, IWA publishing.

Spinosa, L., Santori, M., Lotito, V., 1989. Rheological characterization of sewage sludges. Recycl. von klarschlamm 2, 177.

Strong, P., Mcdonald, B. & Gapes, D. 2011. Combined thermochemical and fermentative destruction of municipal biosolids: A comparison between thermal hydrolysis and wet oxidative pre-treatment. Bioresource technology, 102, 5520-5527.

Strong, P.J., McDonald, B., Gapes, D.J., 2011. Enhancing denitrification using a carbon supplement generated from the wet oxidation of waste activated sludge. Bioresour. Technol. 102, 5533–5540. doi:10.1016/j.biortech.2010.12.025

Suárez-Iglesias, O., Urrea, J.L., Oulego, P., Collado, S., Díaz, M., 2017. Valuable compounds from sewage sludge by thermal hydrolysis and wet oxidation. A review. Sci. Total Environ. 584–585, 921–934. doi:10.1016/j.scitotenv.2017.01.140

Takamatsu, T., Hashimoto, I., & Sioya, S., 1970. , Model identification of wet-air oxidation process thermal decomposition. Water Research, 4(1), 33-59.

Tixier, N., Guibaud, G., Baudu, M., 2003. Determination of some rheological parameters for the characterization of activated sludge. Bioresour. Technol. 90, 215–220. doi:http://dx.doi.org/10.1016/S0960-8524(03)00109-3

Toor, S. S., Rosendahl, L., & Rudolf, A., 2011. Hydrothermal liquefaction of biomass: A review of subcritical water technologies. Energy, 36(5), 2328-2342.

Tyagi, V. K., & Lo, S. L., 2013, Sludge: A waste or renewable source for energy and resources recovery?. Renewable and Sustainable Energy Reviews, 25, 708-728.

Urbain, V., Block, J.C., Manem, J., 1993. Bioflocculation in activated sludge: an analytic approach. Water Res. 27, 829–838. doi:https://doi.org/10.1016/0043-1354(93)90147-A

Urrea, J.L., Collado, S., Laca, A., Díaz, M., 2014. Wet oxidation of activated sludge: Transformations and mechanisms. J. Environ. Manage. 146, 251–259. doi:10.1016/j.jenvman.2014.07.043

Urrea, J.L., Collado, S., Laca, A., Díaz, M., 2015. Rheological behaviour of activated sludge treated by thermal hydrolysis. J. Water Process Eng. 5, 153–159. doi:10.1016/j.jwpe.2014.06.009

Urrea, J.L., Collado, S., Oulego, P., Díaz, M., 2017. Formation and degradation of soluble biopolymers during wet oxidation of sludge. ACS Sustain. Chem. Eng. 5, 3011–3018.

Valioulis, I., 1980. Relationship between settling, dewatering and rheological properties of activated sludge. Master Sci. Thesis, Cornell Univ., Ithaca, New-York, USA.

VEOLIA. 2013. Sludge & Biosolids [Online]. Veolia Water Solutions & Technologies. Available: http://www.veoliawaterst.com/municipalities/sludge-biosolids/ [Accessed 9 JUL 2013].

Verenich, S., Kallas, J. 2002. Wet oxidation lumped kinetic model for wastewater organic burden biodegradability prediction. Environmental Science and Technology, 36(15), 3335-3339.

Verenich, S., Laari, A., Kallas, J. 2003. Parameter estimation and sensitivity analysis of lumped kinetic models for wet oxidation of concentrated wastewaters. Industrial and Engineering Chemistry Research, 42(21), 5091-5098.

Verma, M., Brar, S.K., Riopel, A.R., Tyagi, R.D., Surampalli, R.Y., 2007. Pre-treatment of wastewater sludge--biodegradability and rheology study. Environ. Technol. 37–41. doi:10.1080/09593332808618788

Wetox, 2010, Waste to water & recovered resources [Online], Wetox, Available: http://www.wetox.co.nz/index.html [Accessed 9 JUL 2013]

Wilkinson, N., Wickramathilaka, M., Hendry, D., Miller, A., Espanani, R., & Jacoby, W., 2012, Rate Determination Of Supercritical Water Gasification Of Primary Sewage Sludge As A Replacement For Anaerobic Digestion, Bioresource Technology 124, p269-275

Wilson, C. A., Tanneru, C. T., Banjade, S., Murthy, S. N. & Novak, J. T. 2011. Anaerobic digestion of raw and thermally hydrolyzed wastewater solids under various operational conditions. Water Environment Research, 83, 815-825.

Wingender, J., Neu, T.R., Flemming, H.C., 1999. What are bacterial extracellular polymeric substances?, in: Microbial Extracellular Polymeric Substances. Springer, Berlin, Heidelberg, pp. 1–19.

Xue, Y., Liu, H., Chen, S., Dichtl, N., Dai, X., Li, N., 2015. Effects of thermal hydrolysis on organic matter solubilization and anaerobic digestion of high solid sludge. Chem. Eng. J. 264, 174–180.

Yuan, D., Wang, Y., 2013. Influence of extracellular polymeric substances on rheological properties of activated sludge. Biochem. Eng. J. 77, 208–213.

Yuan, D., Wang, Y., Qian, X., 2017. Variations of internal structure and moisture distribution in activated sludge with stratified extracellular polymeric substances extraction. Int. Biodeterior. Biodegradation 116, 1–9.

Zarzycki, R. and M. Imbierowicz, 2001, Mechanism and mathematical modeling of wet oxidation processes, Ecological Chemistry and Engineering 8: 1205-1220.

Zhang, J., Xue, Y., Eshtiaghi, N., Dai, X., Tao, W., Li, Z., 2017. Evaluation of thermal hydrolysis efficiency of mechanically dewatered sewage sludge via rheological measurement. Water Res. 116, 34–43. doi:10.1016/j.watres.2017.03.020

Zhu, G., Zhu, X., Fan, Q., & Wan, X., 2011, Recovery of biomass wastes by hydrolysis in sub-critical water. Resources, Conservation and Recycling, 55(4), 409-416.

Zhu, Y., Shigematsu, T., Kai, L., Ikbal, Morimura, S., Yamagata, M., Kida, K. 2004. Complete Digestion of Sewage Sludge Using Wet-Oxidation and Subsequently Simultaneous Removal of Residual NH4+ and Volatile Fatty Acids by Biological Treatment. Japanese Journal of Water Treatment Biology, vol. 40, 89-96.

Zou, L. Y., Li, Y., & Hung, Y. T., 2007. Wet air oxidation for waste treatment (pp. 575-610). Humana Press.

CHAPTER 3: MATERIALS AND METHODS

CHAPTER 3: MATERIALS AND METHODS

The experimental work in this thesis aims to characterize the rheological and physico-chemical changes in sewage sludge due to hydrothermal processes, as well as its relationship with processing conditions. To this end, various rheological measurements were performed which described sludge's flow behaviour and viscoelastic properties. These measurements were carried out at varying conditions such that the role of process parameters, including treatment temperature, duration and sludge concentration could be evaluated. Besides that, changes in sludge composition were investigated by examining samples of hydrothermally treated sludge obtained from a lab-scale reactor. This was done to establish whether a correlation existed between sludge composition and rheological parameters, which helped determine possible explanations for the changes observed. Data collected from these tests were analysed and formed the basis for subsequent results and discussion chapters. This chapter describes the experimental methodology and protocols adopted throughout this thesis. Experimental considerations and limitations are described, where relevant. In the subsequent results and discussion chapters, the experimental methods which are relevant to the contents of that chapter are also reiterated in summary.

3.1 SAMPLE PREPARATION

3.1.1 SLUDGE TYPE

Waste activated sludge (WAS) has been established as being the most relevant sludge type for undergoing thermal hydrolysis (TH) pre-treatment (Bougrier et al., 2007; Pinnekamp, 1989). This is due to its high carbohydrate and protein content, which would benefit from the solubilization effects of TH and lead to anaerobic digestion enhancements (Barber, 2016; Wilson and Novak, 2009). In comparison, other sludge types such as primary sludge, which are already inherently easily biodegradable, would not benefit from TH and would diminish cost-effectiveness if pre-treated (Pérez-Elvira et al., 2008). Therefore, WAS is the focal sludge type for the purposes of this experimental work.

3.1.2 SLUDGE SAMPLING

Samples of WAS were collected from Mount Martha wastewater treatment plant (Mornington Peninsula, Victoria) where sludge is thickened via dissolved air flotation without polymer dosing. Due to its organic nature, samples were stored at 4 °C for 30 days upon collection before they were used for experiments.

This ensured biological activity was stabilized during experiments which helped to minimize variations in the sludge composition and maintain sample consistency between experiments (Baudez et al., 2011; Curvers et al., 2009).

3.1.2.1 SLUDGE THICKENING

Sludge samples had initial total solids (TS) concentration of 3.5 wt% upon collection. These were thickened to achieve higher TS values required for experiments. Initially, sludge was thickened via vacuum filtration, as this was believed to impose minimal sample stresses. However, this was found to be impractical and rarely achieved TS values greater than 9 wt%. As such, sludge samples were thickened via centrifugation as follows:

1. 3.5 wt% WAS samples were inserted into polypropylene centrifuge bottles.
2. Centrifuge temperature was configured to maintain a constant temperature at 4 °C during centrifugation. This was achieved via the environment control system built into the centrifuge.
3. Bottled samples were centrifuged at 9000 rpm (13,700 G) for 20 minutes.
4. Centrate was collected from centrifuged sludge and stored.
5. Thickened sludge was then centrifuged again at 9000 rpm (13,700 G) for 20 minutes.
6. Steps 4 – 5 were repeated such that the centrifugation time of sludge totalled 2 hours.
7. Thickened sludge (Figure 3.1) and collected centrate (sludge liquor) were stored separately at 4 °C.

Then, the centrifuge-thickened sludge was diluted using the collected sludge liquor or the original, unthickened sludge (3.5 wt%) to achieve a range of sludge concentrations (7 – 13 wt%). The TS of sludge was determined as described in 3.2.1.1.

3.1.2.1.1 EFFECT OF CENTRIFUGATION ON SLUDGE SOLUBILIZATION

Since centrifugation thickening of the sludge was necessary to achieve the required sludge concentrations in this work, it was investigated whether the high stresses involved affected the sludge characteristics. Primarily, the quantity of organic content (measured as soluble chemical oxygen demand, sCOD) in the soluble phase of the sludge was compared between different centrifugation parameters and non-centrifuged sludge. These were:

1) 2 – step filtration: whereby 3% sludge was filtered firstly through a 6 µm filter followed by filtration through a 0.45 µm filter to obtain sludge liquor.
2) Centrifugation at 4400 rpm (2300 G) for 20 minutes to obtain sludge liquor.
3) Centrifugation at 6000 rpm (4340 G) for 20 minutes to obtain sludge liquor.
4) Centrifugation at 10, 000 rpm (12,100 G) for 1 minute, 5 minutes, 10 minutes, and 20 minutes to obtain sludge liquor.

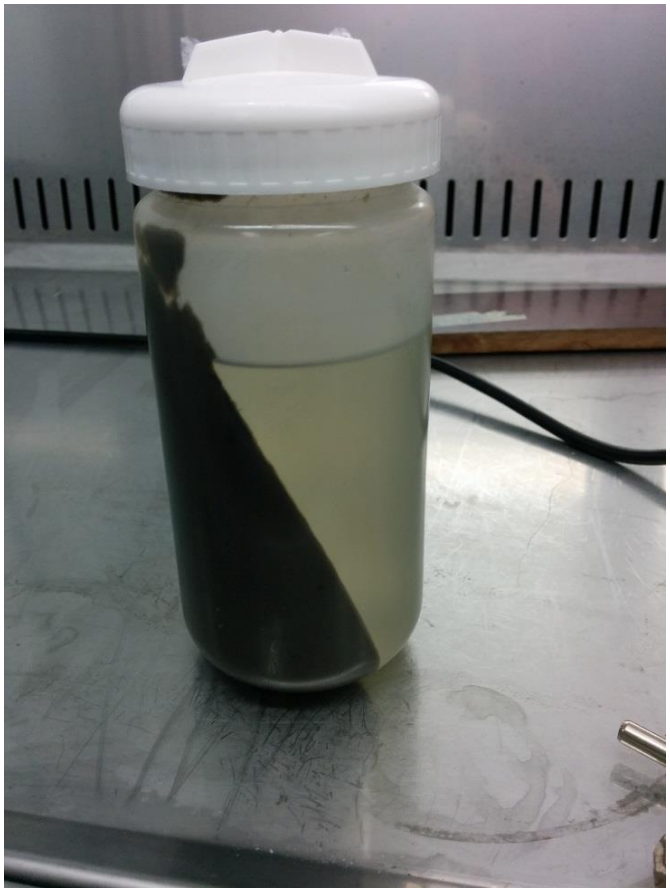

Figure 3. 1 – Polypropylene centrifuge bottles used to thicken waste activated sludge via centrifuge, showing thickened sludge separated from sludge liquor.

The sludge liquor obtained were analysed for sCOD as described in 3.2.2.2. It was observed (Figure 3.2) that centrifugation did not significantly affect the sCOD content in the sludge liquor. In most cases, sCOD in the centrifuged sludge was very similar to the non-centrifuged sludge. Variation in the sCOD values between the centrifuged and non-centrifuged sludge are also consistent with inherent errors arising from the COD method and variations in sample characteristics. The results indicate the centrifuging stresses

are not significant to cause rupture of cells (therefore change in soluble organic content). Besides that, all samples used for this study were centrifuged equally during sludge preparation; so, any changes due to centrifugation effects would be equally present in all samples used for this study.

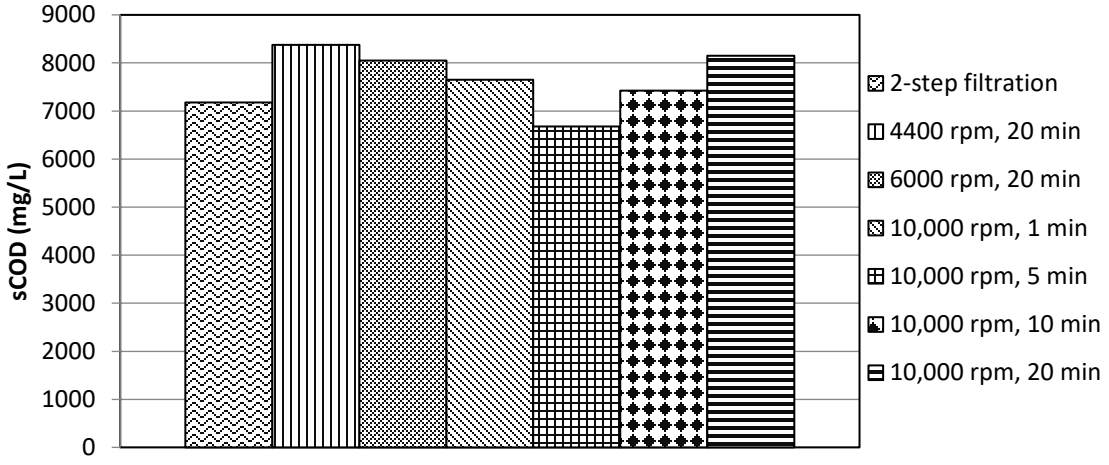

Figure 3. 2 – Effect of centrifugation on the soluble chemical oxygen demand (sCOD) of 3 wt% waste activated sludge compared to non-centrifuged sludge (2-step filtration).

3.2 SLUDGE CHARACTERIZATION

3.2.1 SLUDGE SOLIDS CHARACTERIZATION

The solids content of sludge was characterized based on procedures established in Standard Methods (APHA, 1992) for total solids (TS, wt%), volatile solids (VS, wt%), total suspended solids (TSS, wt%), and volatile suspended solids (VSS, wt%).

3.2.1.1 TOTAL SOLIDS CONCENTRATION

The TS content was determined gravimetrically for all sludge samples as follows:

1. Ceramic evaporating dishes were cleaned and ignited at 550 °C for at least 1 hour, and the mass of the dish was weighed after cooling in a sealed desiccator.
2. Sludge samples were mixed at 500 rpm using a mechanical mixer for 5 minutes.
3. Samples of wet sludge were transferred onto dishes and weighed.

4. Wet sludge samples were placed into a drying oven at 105 °C for 24 hours or until constant mass is attained.
5. The dried sample was weighed, and TS was calculated as follows:

$$TS\ (\%) = \frac{(mass\ of\ dried\ sludge - mass\ of\ dish)}{(mass\ of\ wet\ sludge - mass\ of\ dish)} * 100$$

3.2.1.2 VOLATILE SOLIDS CONCENTRATION

The VS content of sludge was determined using dried sludge samples produced during TS measurement, as follows:

1. Dried sludge samples were weighed as in step 5 of 3.2.1.1.
2. Dried sludge samples were placed inside a furnace and ignited at 550 °C for 2 hours.
3. Ignited samples were removed from furnace and placed in a desiccator to cool to room temperature.
4. Ignited sample residue was weighed, and VS calculated as:

$$VS\ (\%) = \frac{(mass\ of\ dried\ sludge - mass\ of\ sludge\ ash)}{(mass\ of\ dried\ sludge)} * 100$$

3.2.1.3 TOTAL SUSPENDED SOLIDS CONCENTRATION

Due to the highly concentrated nature of the sludge used in this study, samples must be diluted in order to determine its TSS content. The TSS content was determined as follows:

1. A small sheet of plastic film was placed on an analytical balance which was then zeroed.
2. A pea-sized amount of thickened sludge sample was transferred onto the plastic sheet using a spatula and weighed.
3. The weighed sludge sample was transferred together with the plastic sheet into a beaker containing a pre-determined volume of deionized water. The volume of water was determined such that the sludge sample would be effectively diluted up to a factor of 20 once mixed. The density of sludge was previously determined to be comparable to the density of water at room temperature with negligible variation.

4. A magnetic stirrer was used to mix the sludge and deionized water until uniform. The plastic film sheet was removed, ensuring no sludge residue remained on the sheet.
5. Borosilicate glass fibre filters (1.5 µm pore size), which were factory prewashed and weighed according to Standard Methods (ProWeigh Filters, Environmental Express), were placed onto a vacuum filter apparatus and wetted with deionized water.
6. Diluted sludge samples were completely filtered through filter apparatus via vacuum, washing 3 times with 10 mL deionized water.
7. Filter paper was carefully removed after all traces of water were removed by suction and placed in an oven to dry at 105 °C for 24 hours.
8. Dried samples were cooled in a desiccator then quickly weighed using an analytical balance.
9. TSS was calculated as:

$$TSS\ (\%) = \frac{(mass\ of\ dried\ sample\ and\ filter - mass\ of\ filter)}{(mass\ of\ original\ sample)} * 100$$

3.2.1.4 VOLATILE SUSPENDED SOLIDS CONCENTRATION

The VSS content was determined using the dried samples produced during TSS measurement, as follows:

1. Dried sludge samples were weighed as in step 8 of 3.2.1.3.
2. Dried sample on glass filter paper was transferred onto ceramic dishes and ignited in a furnace at 550 °C for 2 hours.
3. Samples were removed from furnace and placed into desiccator to cool to room temperature.
4. Ignited samples were weighed on glass filter papers using an analytical balance.
5. VSS was calculated as:

$$VSS\ (\%) = \frac{(mass\ of\ dried\ sample - mass\ of\ ashed\ sample)}{(mass\ of\ dried\ sample)} * 100$$

3.2.2 SLUDGE COMPOSITION CHARACTERIZATION

Changes in sludge composition due to hydrothermal processing must be determined in order to establish whether these changes are related to the sludge rheology. However, sludge is a complex heterogeneous

biological suspension composed of various organic compounds, including carbohydrates, proteins, lipids, as well as other materials such as lignin and fibres (Li and Noike, 1992; Toor et al., 2011). This makes quantifying compositional changes based on any specific sludge component particularly challenging since the characteristics of sludge in the real world tend to vary greatly, depending on factors such as sample origin and time of collection. Therefore, the investigated parameters must be quantifiable and consistent between samples, as well as being representative of the changes occurring due to hydrothermal treatment. As revealed in the literature review for hydrothermal processes (Chapter 2), sludge organics undergo solubilization during treatment. Furthermore, in the range of experimental temperatures investigated (no more than 150 °C), sludge solids undergo thermal decomposition without occurrence of oxidation (i.e. thermal hydrolysis). Thus, the primary performance indicator to be considered, within the scope of this study, is the extent of organic matter solubilization. Chemical parameters which are commonly used to reflect the soluble organic content of sludge include: soluble chemical oxygen demand (sCOD), soluble proteins, and soluble polysaccharides. There is currently no generalized method for evaluating the performance of thermal hydrolysis (TH) processes but chemical oxygen demand (COD), and sCOD are very frequently reported in literature (Pilli et al., 2015). COD is defined as the amount of a specified oxidant that reacts with a sample under controlled conditions (APHA, 1992). In the case of WAS, it provides a measure of its organic content. Since COD does not distinguish between organic compounds, it provides a very practical method for quantifying the solubilization of sludge organics, regardless of variations in sludge composition. For these reasons, the characterization of sludge composition in this thesis was based around COD measurement. The methods of characterization are described in the following section.

3.2.2.1 TOTAL CHEMICAL OXYGEN DEMAND

Measurements of COD were carried out using commercial COD test kits from HACH Pacific (High Range Plus; Method 8000; using DR 5000 Spectrophotometer and DRB200 Single Block Reactor). Since sludge can be categorized into two phases: particulate and soluble phases, the total COD (tCOD) measurement describes the sum of organic content present in both phases of the sludge. Total COD measurement was performed as follows:

1) A sludge sample of known mass was diluted up to 20 times by mixing with deionized water using a magnetic stirrer.

2) 0.2 mL sample of diluted sludge was pipetted into vials containing COD digestion reagent and gently shaken to mix.
3) 0.2 mL of deionized water was also pipetted into a vial containing COD digestion reagent to produce a blank.
4) The vials were placed into the reactor (DRB200) preheated to 150 °C and heated for 2 hours.
5) Vials were cooled in the reactor until 120 °C and removed to cool in a cooling rack to room temperature.
6) Spectrophotometer program for COD measurement was started and the blank COD vial was inserted to zero the spectrophotometer.
7) Vials containing reacted sludge samples were placed into spectrophotometer and the COD value (mg/L) was recorded.
8) COD values were multiplied by their respective dilution factors to obtain true values.
9) COD measurement was performed in triplicate per sample in separate reagent vials and values averaged.

3.2.2.2 Soluble chemical oxygen demand

Measurement of the soluble COD was performed on the sludge liquor to determine the organic content of sludge which has been solubilized. Here, the soluble phase of sludge is defined as the sludge which passes a 0.45 µm filter. The sCOD measurements were performed as follows:

1) Sludge samples were centrifuged for 20 minutes at 10,000 rpm (12,100 G).
2) Then, the centrate (sludge liquor; Figure 3.3) was filtered through a mixed cellulose ester membrane (0.45 µm pore size) via vacuum.
3) The filtered liquor was collected (Figure 3.4) and diluted up to 40 times by mixing with deionized water using a magnetic stirrer.
4) COD of the diluted filtered liquor was determined as steps 2 – 9 in 3.1.4.1.

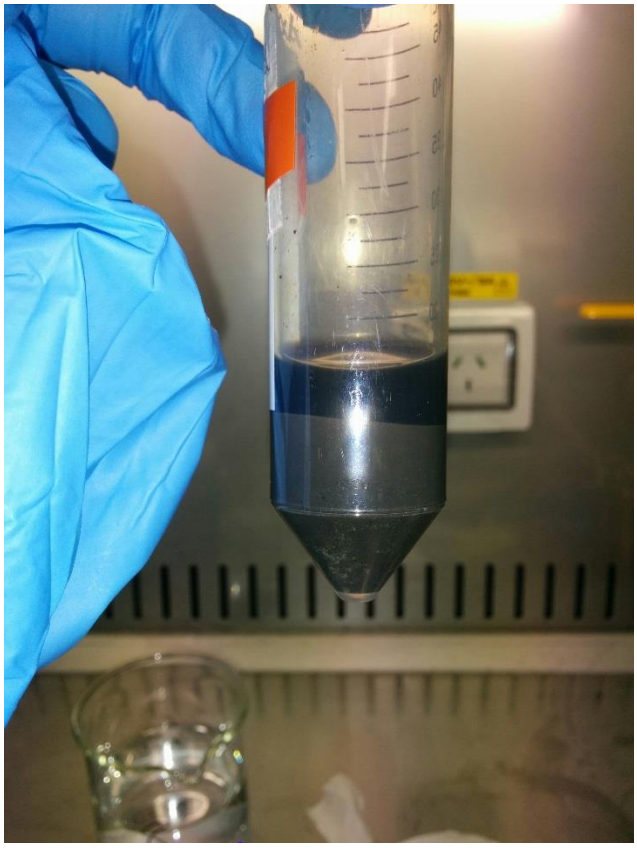

Figure 3. 3 – Centrifuged thermally treated sludge sample; sludge liquor is separated from sludge cake and filtered to determine soluble chemical oxygen demand.

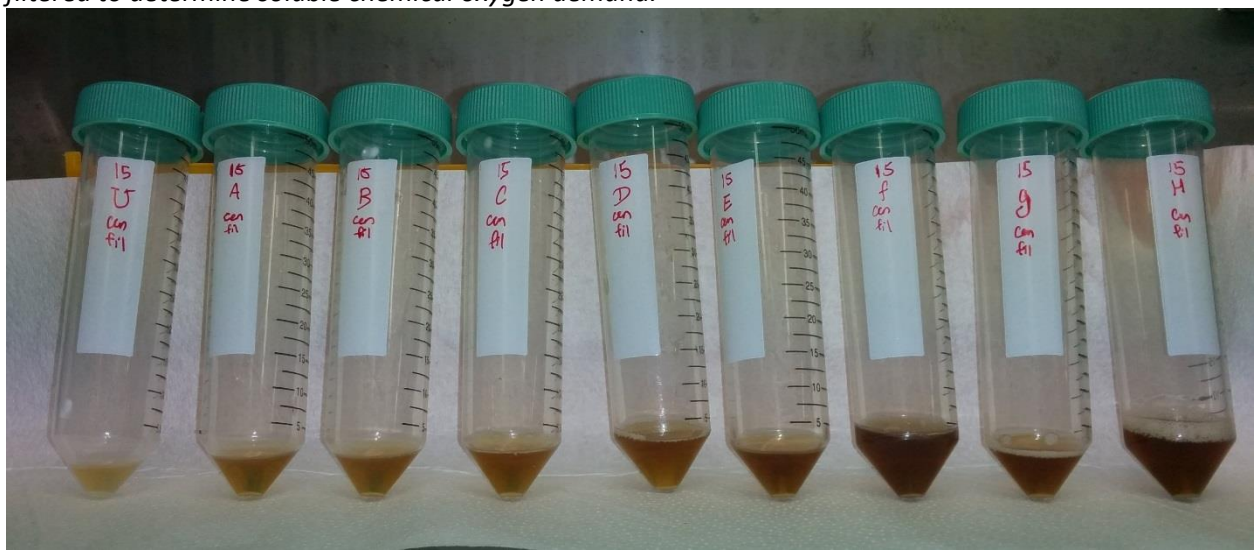

Figure 3. 4 – Sludge liquor collected from thermally treated sludge after filtration (0.45 µm) to be used for soluble chemical oxygen demand measurement; (left) liquor of untreated sludge; second from left to right shows liquor from sludge thermally treated at constant temperature (100 °C) at increasing treatment times (0, 3, 6, 15, 25, 35, 45, 60 minutes), showing greater intensity of liquor colour at higher treatment times.

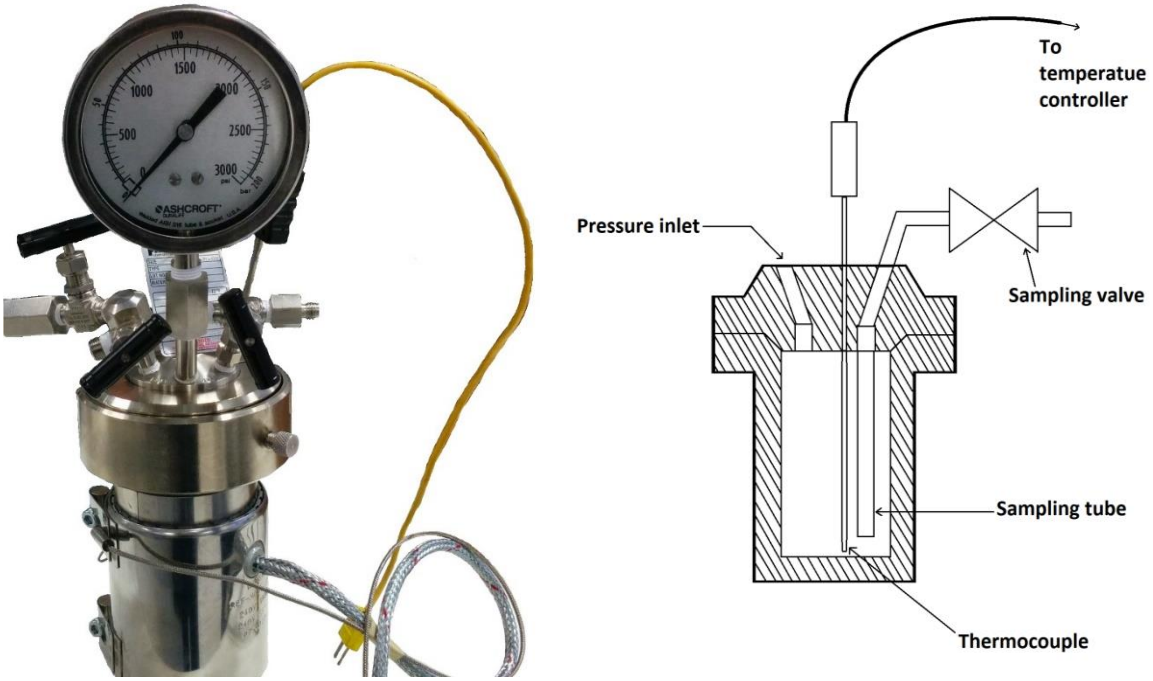

Figure 3. 5 – (Left) pressure vessel for thermal hydrolysis reaction; (right) diagrammatic representation of the pressure vessel.

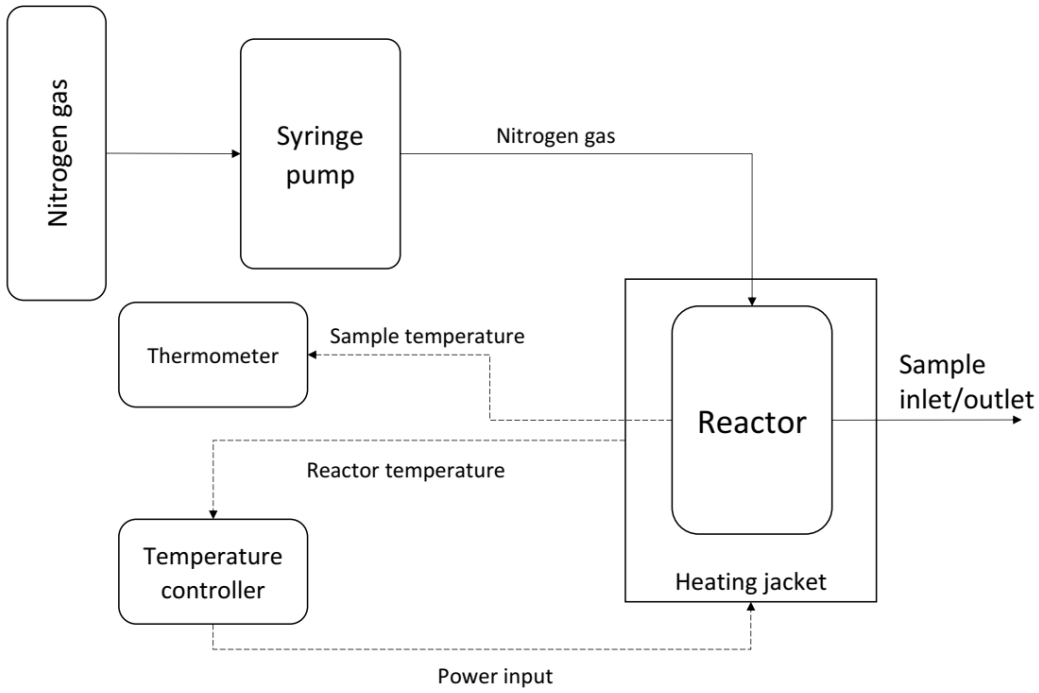

Figure 3. 6 – Diagrammatic representation of reactor setup for thermal hydrolysis of sludge.

3.3 SLUDGE THERMAL HYDROLYSIS

3.3.1 THERMAL HYDROLYSIS REACTOR

Sludge thermal hydrolysis (TH) was performed in a lab-scale reactor in order to obtain samples for solubilisation characterization. The reactor used was a 100 mL stainless steel pressure vessel (Parr 4791 series, split ring-type) with a detachable head (Figure 3.5). The detachable head, which is used to seal the vessel, is equipped with four separate openings for connecting a sampling valve, a safety rupture disc, a pressure gauge, and a thermocouple. Once assembled, a flouroelastomeric gasket provides an airtight seal. The pressure vessel has maximum operating temperature of 250 °C and maximum operating pressure of 207 bar. A sampling tube is attached to the sampling valve connector on the inner side of the vessel to allow real-time sampling of sludge. Heating was provided via a heating jacket (Hotco Rollband series). A temperature controller regulates heating via a thermocouple attached to the outer surface of the vessel. A separate thermocouple was connected on the inside of the vessel to monitor sample temperature. During operation, a syringe pump was used to pressurize the vessel using nitrogen gas. A diagrammatic representation of the reactor setup during operation is illustrated in Figure 3.6.

3.3.2 THERMAL HYDROLYSIS REACTION

Thermal hydrolysis of sludge was carried out under conditions simulating those used in full-scale processes. Sludge was heated to the desired treatment temperature and held constant for 60 minutes under pressurized nitrogen environment. Nitrogen prevents oxidation of sludge contents and pressurization ensured that sludge remained in the liquid phase. During the 60-minute treatment period, samples of sludge were obtained periodically to be used for COD characterization. The TH reactions were carried out as follows:

1) Thickened sludge samples were mixed using a mechanical mixer for 5 minutes at 500 rpm.
2) 90 mL of sludge was introduced into the reactor via the sampling tube using a syringe. The syringe was modified to allow a secure attachment to the sample inlet valve of the reactor (Figure 3.7). This allowed the sludge to fill reactor from the bottom of the vessel. This prevents any air bubbles being trapped within the sludge, especially for thickened sludge.
3) The reactor was sealed by securing the vessel head to the body, during which the sample thermocouple and sampling tube were submerged into the sludge. The thermocouple was positioned such that it was only in contact with the sludge and located near the sampling tube.

4) The syringe pump was filled with nitrogen gas using a nitrogen gas bottle and then connected to the sealed reactor.
5) Air was purged from the reactor by pressurization and venting cycles.
6) The reactor was pressurized to 5 bar pressure using nitrogen gas, which was maintained by the syringe pump.
7) The heating jacket was attached to the pressure vessel and the vessel was heated to 25 °C. The sample was allowed to equilibrate for 5 minutes once it reached 25 °C.
8) Then, the reactor temperature was raised to the set point temperature (80 – 145 °C) using the temperature controller. A stopwatch was used to record the amount of time required for the sample to reach set point temperature.
9) 5 mL sludge samples were collected periodically during the heat up period by opening the sampling valve and collecting sludge samples in sealable containers. Once collected, the sample containers were immediately submerged into an ice bath to rapidly cool. Cooled samples were immediately placed in 4 °C refrigerator. The syringe pump automatically adjusts to maintain constant 5 bar pressure in the reactor.
10) Once sample temperature reached set point temperature, the temperature was held constant for 60 minutes.
11) During the 60-minute treatment period, 5 mL sludge samples were collected periodically, as in step 9.
12) Sludge characterization (tCOD, sCOD, TS, TSS, VS, and VSS) was carried out on collected samples as per Section 3.2.

3.4 SLUDGE RHEOLOGICAL CHARACTERIZATION

Rheological testing comprised most of the experimental work carried out in this thesis. Measurements were made primarily to characterize sludge's flow behaviour and viscoelastic characteristics. Particularly, the characterization of sludge's rheological properties in situ during hydrothermal processing was of interest since this had not been done in any published literature. In-situ rheological measurement of hydrothermally processed sludge traditionally posed many practical challenges largely due to the elevated temperature and pressurized conditions of the processes. However, the recent availability of commercial accessories which allow rheological measurements at pressurized environments has made some of these

measurements possible. The following sections describe the developmental process of the rheometric techniques, and the protocols eventually adopted in this experimental work.

3.4.1 RHEOMETER

All rheological tests in this thesis were performed on a controlled-stress rheometer (HR-3, TA Instruments; Figure 3.8). The rheometer is equipped with a variety of geometries, including: concentric cylinder geometry adhering to DIN 53019 specifications (inner diameter: 28 mm, outer diameter: 30.4 mm, length: 42 mm), vane geometry with serrated cup (inner diameter: 29 mm, outer diameter: 32 mm, length 44 mm), and parallel plate geometry (40 mm diameter). In the case of the concentric cylinder and vane geometries, sample temperature was controlled using a water jacket utilizing Peltier elements for heating and circulating water for cooling. For the parallel plate geometries, heating and cooling are achieved through the bottom plate via Peltier elements and circulating water. The rheometer was also equipped with a pressure cell accessory to enable measurement of samples under pressurized conditions.

3.4.1.1 RHEOMETER PRESSURE CELL

The pressure cell was used when performing rheological measurements at high temperature and pressurized conditions to simulate conditions encountered in hydrothermal processing. It was capable of operating at maximum temperature 150 °C, and heating was supplied by a water-cooled Peltier jacket. The pressure cell is made up of the pressure cell cup, the rotor assembly, and the magnet assembly, illustrated in (Figure 3.9). In operation, the pressure cell performs as a concentric cylinder geometry, with rotor (26 mm diameter, 44 mm length) and cup (28 mm diameter). Due to the enclosed nature of the pressure cell, the rotor (bob) is not physically connected to the rheometer. Rather, connection was achieved via magnetic coupling. During operation, pressurization was achieved using a syringe pump.

Figure 3. 7 – Modified syringe connected to sample inlet valve of pressure vessel to allow sludge to be loaded into reactor from the bottom of the vessel.

Figure 3. 8 – Rheometer (HR3, TA Instruments) with pressure cell attached for measuring sludge at high temperature and high-pressure conditions.

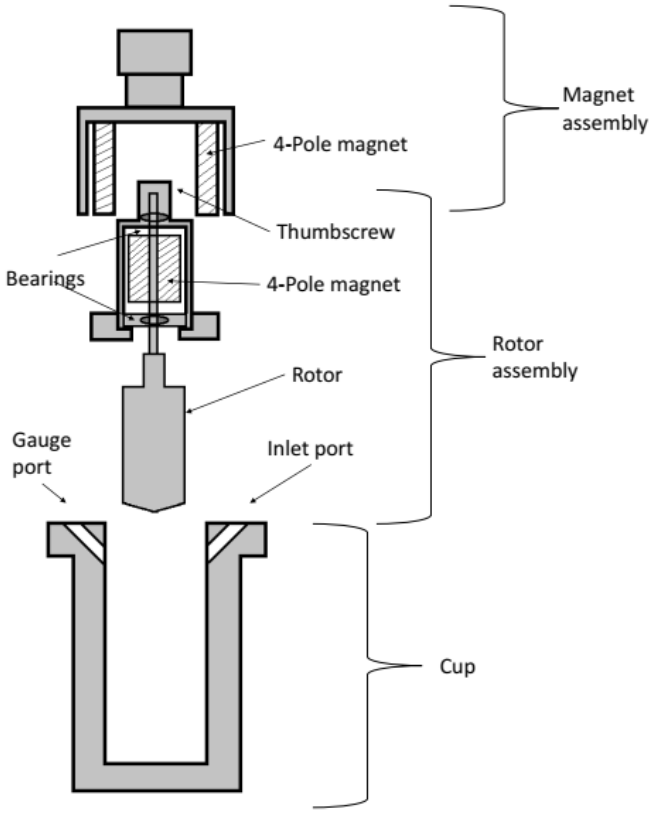

Figure 3. 9 – Illustration of pressure cell components.

3.4.1.1.1 PRESSURE CELL ERROR MINIMIZATION

It was observed during preliminary testing that the pressure cell frequently produced unreliable results. This was often the case when measurements were performed at high temperatures. For example, flow curves measured at high temperatures may produce a lot of noise in the data or be evidently inconsistent (Figure 3.10). It was suspected that these errors are primarily due to the pressure cell, since they were not present when using the concentric cylinder geometries at lower temperatures (<80 °C). One possible source of error was from the magnetic coupling between the rotor and the rheometer (Figure 3.9). Since the rotor is not physically connected to the rheometer, there were likely flaws in the transmission of shearing forces from the rotor to the rheometer sensors. More importantly, the magnets used to achieve the coupling are of relatively high mass. This adds to the inertia of the rotor and makes measurement at low shear rates prone to error. Another source of error was friction between the rotor shaft and the bearings used to keep the rotor in alignment. Notably, it was observed at the end of experiments droplets of water would sometimes collect around the bearings (Figure 3.11) – likely due to condensation. Also, the bearings would sometimes show stains of sludge samples likely resulting from the sludge being

splashed during measurement. To overcome these errors, certain steps and precautions were adopted during the loading of sample and pre-preparations:

1) Prior to assembling the pressure cell, the components which make up the rotor assembly were thoroughly cleaned and dried. The bearings were cleaned under soapy water using a pipe brush and the rotor shaft was cleaned by wiping with alcohol. After cleaning, the rotor assembly components were dried in an oven at 105 °C for at least 10 minutes. This helped to ensure minimal friction arising from the bearings.
2) Exactly 10 mL of sample was loaded during each measurement. Samples were injected using a syringe directly into the unsealed pressure cell cup from the bottom of the cup to ensure no gas bubbles are entrapped in the samples. This ensures the pressure cell is correctly filled every time and avoids sample splashes due to over-filling.
3) After sample loading, the pressure cell was sealed carefully without rotating the rotor, ensuring no sample overflow. Once sealed, the rotor was operated to shear the sample for 5 minutes at shear rate 10 s^{-1}. This ensured the sample was properly distributed in the measuring gap.
4) Once sealed, the thumbscrew at the top of the rotor assembly (Figure 3.9) was removed. Then, the pressure cell was connected to a nitrogen gas-filled syringe pump and the inlet valve was opened to allow pressurized nitrogen gas to enter the pressure cell and exit from the opened thumbscrew. This was done to effectively "flush" the bearings and remove any excess moisture.
5) Finally, the thumbscrew is reassembled, and the pressure cell is sealed properly. Measurements protocols were then commenced normally.

The above steps were applied each time during measurements using the pressure cell, regardless of test-type and conditions.

3.4.2 IN-SITU RHEOMETRIC METHODS

As previously highlighted, one of the major goals of this experimental work was the in-situ measurement of sludge rheological properties during hydrothermal treatment. The objective was to obtain a real-time depiction of the rheological changes occurring due to hydrothermal treatment. In hydrothermal processes, solubilization of sludge is accomplished by holding the sludge at a fixed temperature over time. One way to measure these changes was by producing flow curves at constant temperature over time. Flow curve generation was the most practical solution since it described the general rheological behaviour and

provides useful parameters such as yield stress and viscosity. Described below are the considerations and development of the in-situ rheometric methods adopted in this thesis.

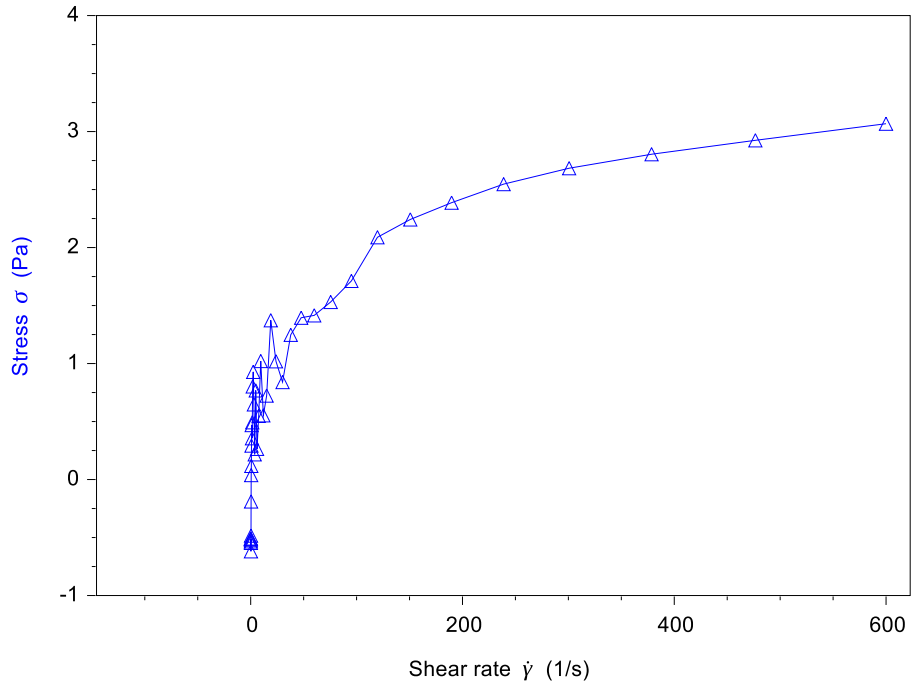

Figure 3. 10 – Flow curve produced using pressure cell measuring 7wt% waste activated sludge exhibiting a lot of noise in the data.

Figure 3. 11 – Pressure cell bearing exhibiting signs of condensation, suspected to increase bearing friction and affect measurement results.

3.4.2.1 CONSTANT SHEAR RATE PEAK HOLD METHOD

One of the challenges considered during development of the test protocol was the time-dependent nature of the sludge undergoing thermal treatment – sludge is solubilized irreversibly as thermal treatment proceeds. As in-situ measurement had not been done before, it was unknown whether sludge rheological changes would occur instantaneously upon reaching treatment temperatures, or whether they proceeded slowly overtime. In case of the latter, the rate of rheological changes was also uncertain. It has been shown that the solubilization of sludge at high temperature is a time-dependent process (Everett, 1972; Imbierowicz and Chacuk, 2012), so the sludge may not be at an equilibrium state during measurement. That is, the time taken for measuring each data point must be considered so they account for the irreversible changes of the sludge during the time taken to measure each data point.

An initial solution proposed for overcoming this was to obtain a continuous curve of shear stress data over time, at a constant shear rate. Then, the shear rate would be varied, and the test repeated on a new sample. This way, the flow curve would be generated manually using shear stress data obtained at various shear rates. One advantage to this was that since the shear stress data was obtained continuously, it is theoretically possible to generate a flow curve for any point in time during thermal treatment. This way, any significant changes occurring within a small timeframe would be observable. The method for the peak hold method at constant shear rate was as follows:

1) Without sample, the pressure cell was heated to set point temperature (80 °C) and a constant shear rate was applied (100 s^{-1}) for 5 minutes. The average torque (µN.m) was divided by the average velocity (rad/s) to obtain the friction correction factor. This value was used to correct the raw data for friction of the pressure cell.
2) After sample loading, pressure cell was sealed, and air was removed by pressurization and venting cycles using nitrogen gas at 5 bar pressure applied via syringe pump. Then sludge was pressurized to 5 bar with nitrogen gas.
3) Sludge was heated to set point temperature (80 °C).
4) Once set point temperature was reached, a constant shear rate was applied to sludge (100 s^{-1}).
5) Shear stress was recorded continuously, with sampling interval of 1 data point per second over 60 minutes.
6) Sample was removed, and the test is repeated using a new sample, varying set point temperature (80 – 145 °C) and shear rate (100 – 600 s^{-1}).

However, it was found that the flow curves manually produced this way would not give consistent or reliable results (Figure 3.12). This was most likely because the measurement for each shear rate was obtained from separate samples, which contain variations unavoidable between each sample. On the other hand, a great number of shear stress data points would be required to produce a more complete flow curve. This was impractical to carry out within the scope of this thesis, so another method was considered.

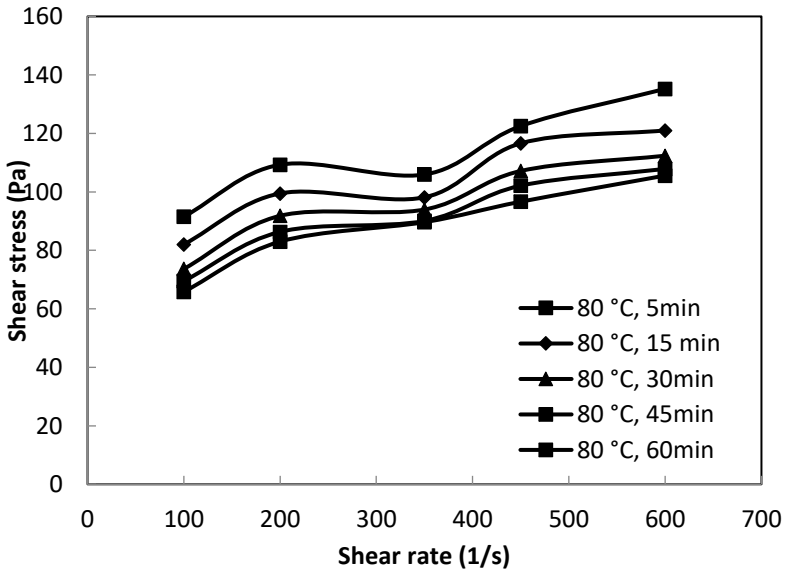

Figure 3. 12 – Flow curves for 7 wt% waste activated sludge thermally treated at 80 °C at different treatment times, generated manually via constant shear rate peak hold method.

3.4.2.2 In-situ flow curve generation method

From the peak hold data generated previously, it was observed that the apparent viscosity of sludge (Figure 3.13) decreased rapidly initially but gradually plateaued over time. This indicated, the rate of rheological changes would be high during the initial 10 – 15 minutes of treatment but negligible at longer treatment times. Then, if a complete flow curves could be generated within a short time period, this may limit the errors arising from measuring the transient properties of sludge. As such, it was decided to generate flow curves periodically while the sludge was held at constant temperature over time. The method was carried out as follows:

1) Sample was loaded, as described in 3.4.1.1.1.

2) Air was purged from the pressure cell by pressurization and venting cycles using nitrogen gas at 5 bar pressure applied via syringe pump. Then sludge was pressurized to 5 bar with nitrogen gas.
3) Sludge was heated to 25 °C and equilibrated for 5 minutes.
4) Sludge was pre-sheared at shear rate 675 s^{-1} (maximum shear rate producible on the pressure cell) for 20 minutes to erase sample shear history. Then the sludge was equilibrated at zero shear for 2 minutes.
5) Flow curve was generated at 25 °C via a logarithmic sweep of decreasing shear rates (600 – 0.1s^{1}). Time taken to produce the complete flow curve averaged around 120 s for 10 data points per decade. This produced the flow curve describing the untreated sludge.
6) Sludge was heated to the set point temperature (80 °C), heating times averaged 10 – 15 minutes.
7) Once set point temperature was reached, sludge was pre-sheared at 675 s^{-1} for 2 minutes followed by 1 minute of equilibration at rest.
8) Sludge was held at set point temperature for 60 minutes.
9) Periodically, flow curves were generated during the constant temperature period. Flow curves were generated via logarithmic sweep of decreasing shear rates (600 – 0.1 s^{-1}). Prior to each flow curve measurement, intermediate pre-shearing was applied (675 s^{-1} shear rate for 2 minutes followed by 1-minute equilibration).
10) After 60 minutes at constant set point temperature, sludge was cooled down to 25 °C. Flow curve was generated as in step 9 to characterize the rheology for thermally treated sludge.
11) Measurements were repeated varying treatment temperature and sludge concentration.

This method was found to be much more reliable for producing consistent results. As such, this method was adopted for in-situ rheometric measurements performed in this thesis.

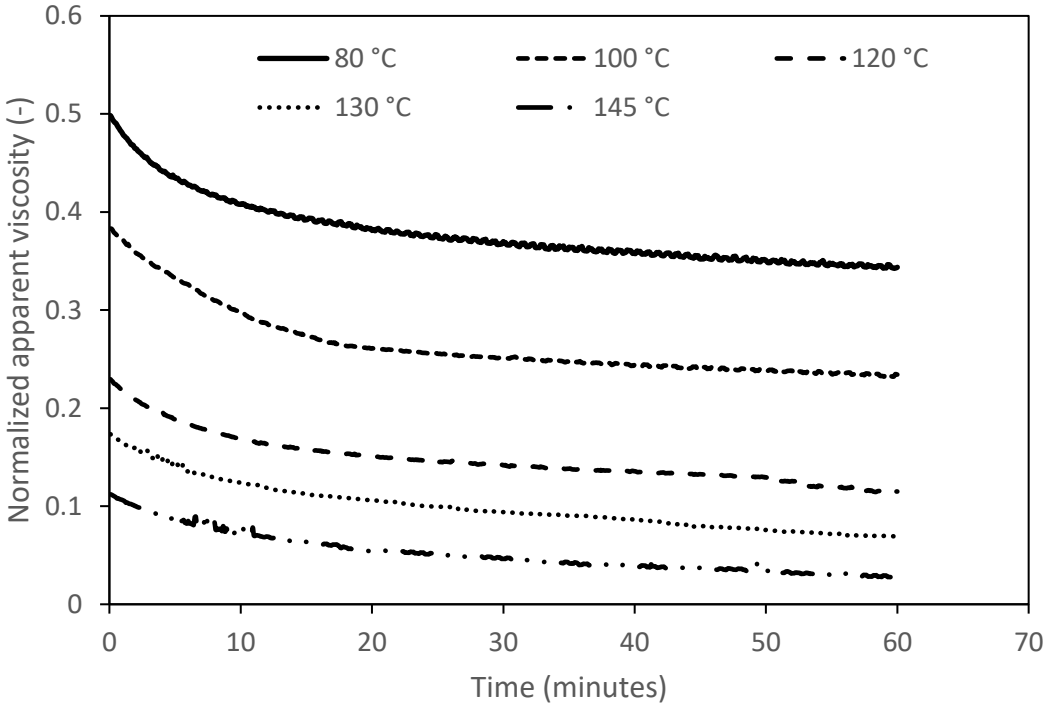

Figure 3. 13 – Apparent viscosity of sludge measured using the constant shear rate (100 s^{-1}) peak hold method at different temperatures, held constant for 60 minutes.

3.4.2.3 SLIPPAGE EFFECTS

It was observed that flow curves generated in the concentric cylinder geometries when measuring sludge produced a secondary curve trend at low shear rates (Figure 3.14). This was true for all concentrations of sludge measured and at all temperatures considered. It was suspected that this was a result of slippage effects at low shear rate values. This phenomenon was investigated by comparing flow curves produced using the regular concentric cylinder geometries versus flow curves generated using the concentric cylinders with sandpaper attached. The concentric cylinder with sandpaper attached can be seen in Figure 3.15 and was produced by attaching strips of sandpaper (400 grit) laterally along the rotor bob. This reduces likelihood of slippage along the rotor surface. As shown in Figure 3.14, attaching the flow curve generated using the sandpaper-attached rotor produced a distinctly continuous curve trend, which is comparable to other shear-thinning materials. Since it was impractical to achieve a reliable roughened surface in the pressure cell, the low shear rate data produced during flow curve generation were disregarded and assumed to be erroneous. Only the high shear rate data were considered for analysis.

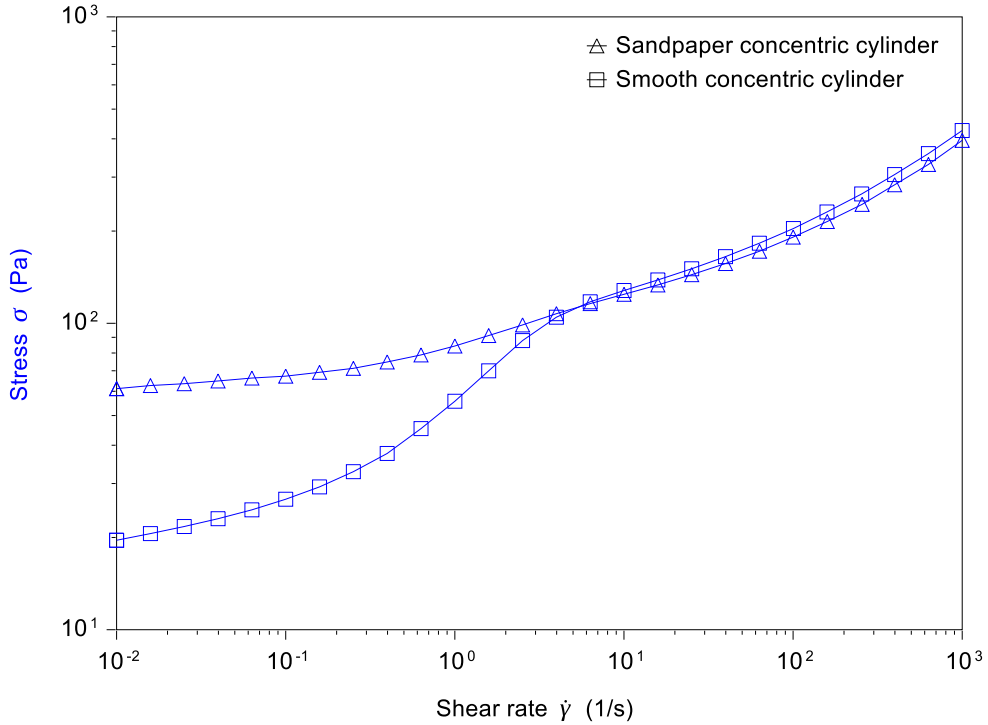

Figure 3. 14 – Flow curves for 7 wt% waste activated sludge produced using the concentric cylinder with and without attaching sandpaper to eliminate slippage effects.

Figure 3. 15 – Concentric cylinder rotor with sandpaper attached to the shearing surface to reduce slippage effects.

3.4.3 VISCOELASTIC CHARACTERIZATION

The viscoelastic properties were measured to characterize the solid-like properties of sludge. However, in-situ measurements requiring the use of the pressure cell were not possible. This was due to the incapability of the pressure cell to produce useful results from oscillatory measurements. Since viscoelastic measurements required the rotor to oscillate at high frequencies, the high inertia of the rotor would produce noisy data. For example, the strain sweep results for sludge measured in the pressure cell produced illegible curve trends (Figure 3.16). As such, viscoelastic characterization was performed using traditional geometries at ambient conditions.

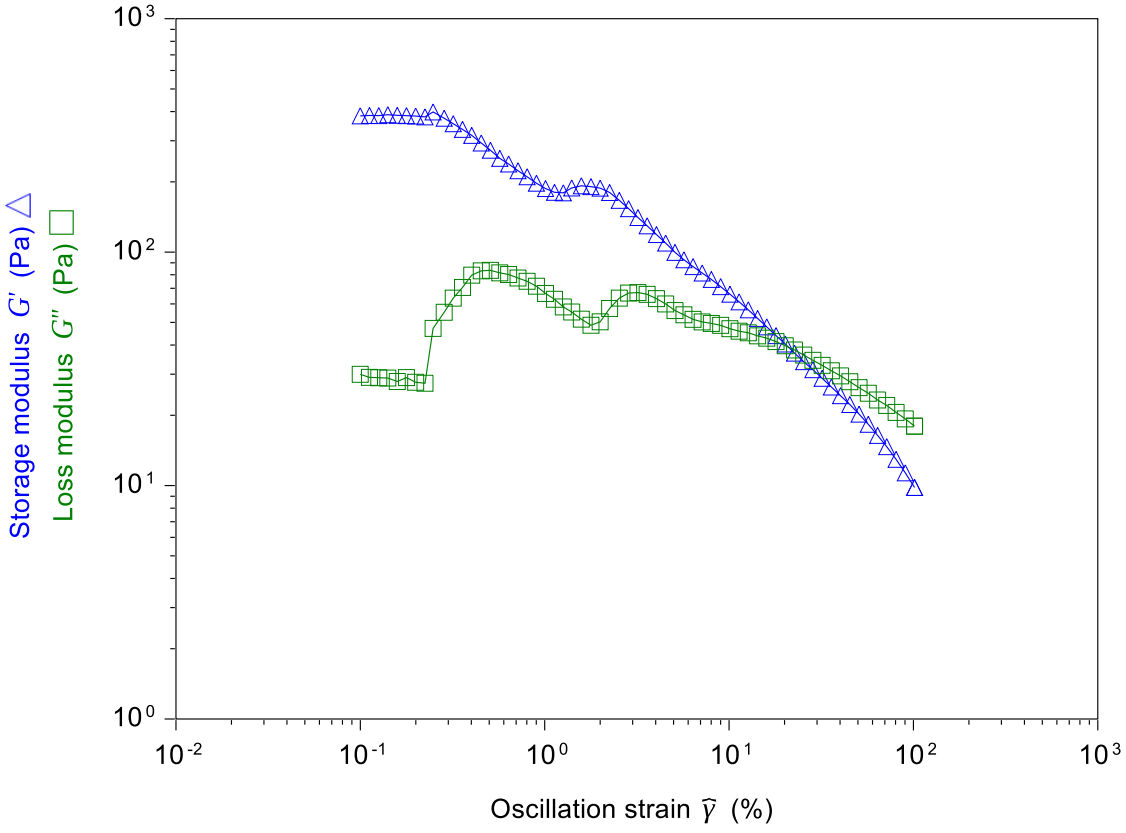

Figure 3. 16 – Strain sweep results obtained from measuring 11 wt% waste activated sludge using the pressure cell geometry, showing erroneous results.

3.4.3.1 Viscoelastic measurement geometries

The suitability of geometries chosen to perform viscoelastic measurements were taken into consideration, since measurement of sludge posed some practical challenges.

3.4.3.3.1 CONCENTRIC CYLINDER GEOMETRY

Concentric cylinder geometry was initially considered for performing the viscoelastic tests for sludge. The main advantage was consistency of geometry with the in-situ tests performed in the pressure cell, which also operated as concentric cylinder geometries. However, since it exhibited slippage effects for sludge at low shear rates (as described in 3.4.2.3), this prevented oscillatory tests performed at low frequency ranges. Slippage on the concentric cylinder geometry could not be reliably prevented in a consistent manner. Hence oscillatory test data obtained using concentric cylinder geometry were not considered for further analysis.

3.4.3.3.2 VANE GEOMETRY

Vane geometry was considered as it avoids the issues of slippage encountered in concentric cylinders, but fundamentally operates on an equivalent basis as the concentric cylinders (Mezger, 2006). The vane geometry consists of four spindles arranged perpendicularly to each other and aligned along the length of the rotor (effective rotor diameter 28 mm, length 42 mm, cup diameter 30.4 mm). However, it was observed that the vane geometry fails when measuring sludge at increasingly higher sludge concentrations. For example, at 12 wt% solids concentration, the sludge could not be distributed evenly into the rheometer cup due to its thickness. As the vane rotor rotates, much of the sludge would cling onto the rotor and a gap effectively forms between the rotor and the shearing surface – hence, no effective shearing occurred (Figure 3.17). Oscillatory test data obtained from vane geometry were not considered for further analysis.

3.4.3.3.2 CONE AND PLATE GEOMETRY

The cone and plate geometry was initially considered as it provides a constant shear rate within the entire shearing gap (Mezger, 2006). The geometry consists of a conical upper rotor (60 mm diameter, 2 ° cone angle, 53 µm truncation gap) and flat bottom plate. However, slippage still existed since the plate surfaces

were smooth. More significantly, the geometry was unsuitable for sludge as it is incapable of accommodating for larger particle sizes due to the small truncation gap.

3.4.3.3.3 Parallel plate geometry

The parallel plate geometry consists of a rotating flat upper plate (40 mm diameter) and a static, flat lower plate. It avoids the particle size limitations of the cone and plate geometry and slippage effects can be easily overcome. However, one drawback is the shear rate imposed on a sample varies along the radius of the plate. Then, the recorded shear rate is only a representative value. However, it was the most reliable geometry for producing consistent results required within the scope of this study. Slippage effects were eliminated by attaching sandpaper (400 grit) to the measuring surfaces. Thus, parallel plate geometry was chosen for performing viscoelastic tests.

Figure 3. 17 – Viscoelastic measurement of 12 wt% waste activated sludge using vane geometry, showing the thickened sludge did not shear properly due to formation of gap between the rotor and the shearing surface of the cup.

3.4.3.2 Amplitude sweep tests

Amplitude sweep tests were performed to determine the linear viscoelastic region (LVE) of the sludge and its gel-like characteristics, as follows:

1) Sludge samples were loaded onto the lower plate and heated to 25 °C to equilibrate at rest for 5 minutes.
2) Upper plate was lowered into the sample such that the measuring gap was 1 mm. Sample overfill was not removed.
3) Sample was pre-sheared at 1000 s^{-1} for 5 minutes followed by 2 minutes equilibration at rest. While the sample was rested, the sample overflow was carefully trimmed and removed. Trimming the excess sample at this stage prevented edge effects during pre-shearing of the sludge, which tended to occur at higher sludge concentrations.
4) Logarithmic sweep of strain from 0.01 – 100 % at 20 points per decade was performed at constant angular frequency of 10 rad/s.

3.4.3.3 Frequency sweep tests

Frequency sweep tests were performed to determine the time-dependent characteristics of the sludge and its gel-like characteristics, as follows:

1) Steps 1 – 3 of 3.4.3.2 was performed.
2) Logarithmic sweep of angular frequency from 1 – 100 rad/s at 10 points per decade was performed at constant strain of 0.1 %.

3.4.3.4 Creep tests

The creeping behaviour of the sludge was evaluated by creep tests as follows:

1) Steps 1 – 3 of 3.4.3.2 was performed.
2) Step stress was imposed on the sludge for 180 s and the strain response was recorded over time. Stress values imposed on the sludge was dependent on sludge type and determined based on the LVE region of the sludge from amplitude sweep results. The step stress was imposed as a raw torque value on the rheometer.

3.4.3.5 YIELD STRESS DETERMINATION

Yield stress was determined directly for sludge samples using the parallel plate geometry by performing a stress ramp, as follows:

1) Steps 1 – 3 of 3.4.3.2 was performed.
2) A linear ramp of torque was applied for 60 s. The range of torque values was determined using amplitude sweep results and chosen as the range of equivalent stress values 1 – 2 decades above and below the transition from LVE region of the sludge.
3) Yield stress was determined by "tangent crossover method" by plotting stress/deformation in logarithmic scale and fitting two straight lines on the two curve intervals (Figure 3.18) that result from the data (Mezger, 2006).

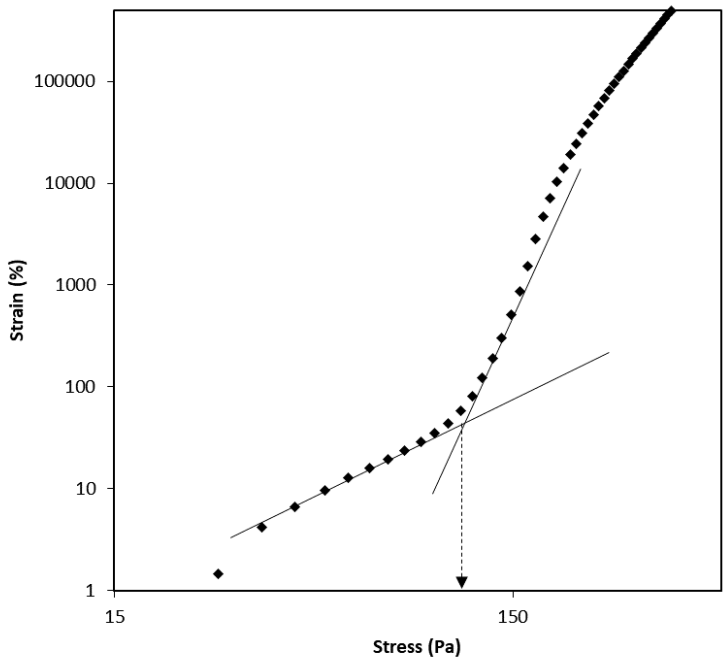

Figure 3. 18 – Yield stress determination from stress ramp curve using the tangent crossover method for thermally treated sludge (9 wt% at 100 °C).

REFERENCES

APHA, 1992. Standard Methods for the Examination of Water and Wastewater.

Barber, W.P.F., 2016. Thermal hydrolysis for sewage treatment: A critical review. Water Res. 104, 53–71. doi:10.1016/j.watres.2016.07.069

Baudez, J.C., Markis, F., Eshtiaghi, N., Slatter, P., 2011. The rheological behaviour of anaerobic digested sludge. Water Res. 45, 5675–5680. doi:http://dx.doi.org/10.1016/j.watres.2011.08.035

Bougrier, C., Delgenes, J.P., Carrere, H., 2007. Impacts of thermal pre-treatments on the semi-continuous anaerobic digestion of waste activated sludge. Biochem. Eng. J. 34, 20–27.

Curvers, D., Saveyn, H., Scales, P.J., Van der Meeren, P., 2009. A centrifugation method for the assessment of low pressure compressibility of particulate suspensions. Chem. Eng. J. 148, 405–413. doi:http://dx.doi.org/10.1016/j.cej.2008.09.030

Everett, J.G., 1972. Dewatering of wastewater sludge by heat treatment. Water Pollut. Control Fed. 92–100.

Imbierowicz, M., Chacuk, A., 2012. Kinetic model of excess activated sludge thermohydrolysis. Water Res. 46, 5747–5755. doi:10.1016/j.watres.2012.07.051

Li, Y.-Y., Noike, T., 1992. Upgrading of Anaerobic Digestion of Waste Activated Sludge by Thermal Pretreatment. Water Sci. Technol. 26, 857–866.

Mezger, T.G., 2006. The Rheology Handbook: For Users of Rotational and Oscillatory Rheometers, Coatings compendia. Vincentz Network.

Pérez-Elvira, S.I., Fernández-Polanco, F., Fernández-Polanco, M., Rodríguez, P., Rouge, P., 2008. Hydrothermal multivariable approach. Full-scale feasibility study. Electron. J. Biotechnol. 11. doi:10.2225/vol11-issue4-fulltext-14

Pilli, S., Yan, S., Tyagi, R.D., Surampalli, R.Y., 2015. Thermal pretreatment of sewage sludge to enhance anaerobic digestion: a review. Crit. Rev. Environ. Sci. Technol. 45, 669–702.

Pinnekamp, J., 1989. Effects of thermal pretreatment of sewage sludge on anaerobic digestion. Water Sci. Technol. 21, 97–108.

Toor, S.S., Rosendahl, L., Rudolf, A., 2011. Hydrothermal liquefaction of biomass: A review of subcritical water technologies. Energy 36, 2328–2342. doi:10.1016/j.energy.2011.03.013

Wilson, C.A., Novak, J.T., 2009. Hydrolysis of macromolecular components of primary and secondary wastewater sludge by thermal hydrolytic pretreatment. Water Res. 43, 4489–4498. doi:10.1016/j.watres.2009.07.022

CHAPTER 4:

RHEOLOGICAL MEASUREMENTS AS A TOOL FOR MONITORING THE PERFORMANCE OF HIGH PRESSURE AND HIGH TEMPERATURE TREATMENT OF SEWAGE SLUDGE

This chapter was published in Water Research Journal

(Vol: 114, pp: 3 – 27, 2017)

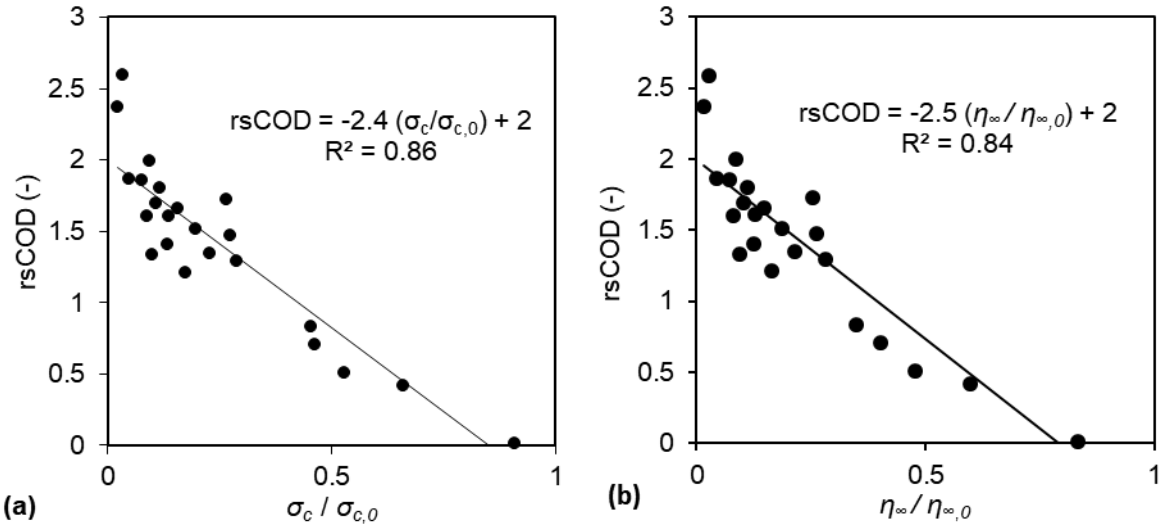

Keywords: Thermal hydrolysis; sewage sludge rheology; yield stress; apparent viscosity; waste activated sludge.

Hii, K, Parthasarathy, R, Baroutian, S, Gapes, D. J., Eshtiaghi, N., 2017, Rheological measurements as a tool for monitoring the performance of high pressure and high temperature treatment of sewage sludge. Water Research Journal 114: 3-27.

4.1 ABSTRACT

Hydrothermal processing plays a significant role in sewage sludge treatment. However, the rheological behaviour of sludge during these processes is not fully understood. A better understanding of the sludge rheology under hydrothermal processing conditions can help improve process efficiency. Moreover, sludge rheology is easier to measure than chemical analyses. If a relationship could be established, it provides a possibility of using rheological measurement as a basis for monitoring the performance of hydrothermal processing. The rheological changes in thickened waste activated sludge (7 wt%) was investigated using a pressure cell-equipped rheometer during 60-min thermal hydrolysis (TH) at various temperatures (80-145 °C) and constant pressure (5 bar). Changes in the soluble chemical oxygen demand (COD) were measured using a separate reactor with a similar operating condition. The sludge behaved as a shear-thinning fluid and could be described by the Herschel-Bulkley model. At constant temperature, the yield stress and high-shear (600 s^{-1}) viscosity of sludge decreased logarithmically over 60 min. At constant time, the yield stress and the high-shear viscosity decreased linearly with increasing TH temperature and these values was much less than corresponding properties after treatment and cooling down to 25 °C. The soluble COD of sludge also increased logarithmically over 60 min at constant temperature and increased linearly with increasing temperature at constant time. Furthermore, the yield stress and high-shear viscosity reduction showed a linear correlation with the increase in soluble COD.

4.2 INTRODUCTION

Implementing hydrothermal processing technologies such as thermal hydrolysis (TH) in sewage sludge treatment has become increasingly popular. The elevated temperature conditions (above 100 °C) used in this process improves sludge treatment outcomes; however, the rheology of sludge under these conditions is not fully understood even though it plays a key role in optimizing these processes (Barber, 2016). Therefore, a better understanding on the rheological behaviour of sludge during hydrothermal processing can help improve its design and operation. Furthermore, the performance indicators in hydrothermal processing, such as sludge solubilisation, cannot be easily measured during operation, whereas in-situ rheological measurements are potentially easier to perform (Konigsberg et al., 2013). As such, the rheology of sludge could potentially be useful in describing the performance of hydrothermal processing operations if a relationship between rheological properties and reaction performance indicators (e.g. COD) could be established.

Thermal hydrolysis is among the more popular hydrothermal processing technologies used in sewage sludge treatment today (Hii et al., 2014). It is primarily used to enhance the anaerobic digestion process whereby incoming sludge is heated to high temperatures for a given amount of time before being fed into the anaerobic digester. The TH pre-treatment causes partial solubilisation of sludge contents and the reduction of the sludge apparent viscosity which in turn ultimately lead to enhancements of the subsequent anaerobic digestion process. Thermal hydrolysis improves digestion efficiency, increases biogas production and reduces sludge volumes while it also allows increased organic loading rates (Appels et al. 2008; Carrère et al., 2010; Morgan-Sagastume et al., 2011). Thermal hydrolysis typically operates at 160 – 180 °C although lower temperature ranges (60 – 150 °C) have also been reported (Abe et al., 2013; Bougrier et al., 2006; Gavala et al., 2003; Hammadi et al., 2012). Typical treatment times range from 30 – 60 minutes (Donoso-Bravo et al., 2011; Kepp et al., 2000; Li and Noike, 1992) but treatment time as low as 60 seconds have also been reported (Dohanyos et al., 2004).

Thermal hydrolysis has been found to be more effective when used on waste activated sludge (WAS) (Perez-Elvira et al., 2008; Bougrier et al., 2007) which is known to have poor biodegradability. Waste activated sludge is a biological suspension of bacteria and organic particulates, which are held together in gel-like biofilm matrices called extracellular polymeric substances (EPS) (Li & Ganczarczyk, 1990; Neyens et al., 2004). It is understood that EPS makes up a significant portion in WAS, representing up to 80 % of its mass (Frolund et al., 1996). Recently, it has been shown that the presence of EPS content and solids content correlates strongly with the rheological behaviour of WAS (Feng et al, 2014; Feng et al. 2016).

It is known that TH reduces the apparent viscosity of treated sludge. However, comprehensive rheological studies on TH treated sludge is relatively scarce. Bougrier et al. (2008) reported shear-thinning behaviour in thermally treated WAS where the apparent viscosity decreased with increasing treatment temperature up to 150 °C, above which it remained constant, suggesting a 150 °C threshold temperature for changes in sludge physical characteristics. Perez-Elvira et al., (2010) also reported shear-thinning behaviour in treated sludge with 70% decrease in sludge viscosity after TH at 170 °C and 30 minutes. The changes were attributed to reduced inter-floc resistance due to breakage of sludge floc structure during TH. Carvajal et al. (2013) performed a thermal treatment process at low temperatures (55 °C, 24 hours) on WAS and reported that the yield stress of treated sludge was decreased by 82 %.

Recently, Feng et al. (2014) investigated the rheological properties of WAS after thermal treatment at 170 °C for 60 minutes. It was found that the shear-thinning behaviour and thixotropic property of sludge became less apparent after TH. The storage modulus was also decreased by 92.5 % following TH. Sludge

solids concentration was found to have a significant impact on the rheology of both treated and untreated sludge. Similarly, Feng et al. (2014b) reported that the behaviour of 5.4 wt% WAS changed from a Herschel-Bulkley fluid to a Newtonian fluid following 1-hour TH at 170 °C. The storage modulus also decreased significantly, and treated sludge was predominantly described by viscous forces. These changes were attributed to the destruction of floc and hydrolysis of macromolecular components. Urrea et al. (2015) investigated the rheological changes of 2.33 wt% WAS due to TH at 160 – 200 °C and 40 – 80 bar. It was found that untreated sludge behaved as a Bingham plastic material. During the initial stages of TH, the authors reported that the sludge behaviour became pseudoplastic, whereas by the end of the treatment period, they observed that the sludge behaved as a Newtonian fluid. The changes observed were attributed to destruction of flocs and release of polymers due to cell lysis. They also showed that the reduction of total suspended solids was the main contributor of the observed changes in rheological properties of sludge, leading to Newtonian behaviour.

During TH, it is believed that the heating of sludge causes microorganism cell walls to rupture, EPS to become degraded, and particulate organic compounds be converted into lower molecular weight compounds (Bougrier et al., 2008; Everett, 1972; Neyens & Baeyens, 2004; Neyens & Baeyens, 2003). However, more systematic studies on the reaction mechanisms and kinetics involved in sludge TH are not well documented. Takamatsu et al. (1970) proposed a mathematic model which described thermal decomposition of WAS in terms of solubilisation of solid matter into soluble evaporative matter and soluble non-evaporative matter. Performing TH at 170 – 250 °C, the chemical oxygen demand (COD) in sludge solids decreased while COD in the soluble matter increased. Total COD in sludge remained unchanged. Imbierowicz and Chacuk (2012) modelled TH in a lumped kinetic model which assumed that two parallel first-order reactions occurred during heating of WAS. The first described the thermal destruction and solubilisation of sludge particles to organic carbon while the second parallel reaction led to a solid phase, which can be decomposed into CO_2. In the recent review, Barber (2016) surmised that with increasing temperature, a sequence of reactions in sludge would occur as: i) solubilisation of bulk material, ii) release of loosely-bound polysaccharides from extra-cellular polymers (ECP), iii) destruction of tightly bound ECP, degradation of cell walls and eventual rupture, iv) release of intracellular proteins, which eventually the interaction between polysaccharides and proteins led to producing non-biodegradable high molecular weight products.

The solubilisation of organic compounds in sludge has been reflected as an increase in COD in the soluble phase of sludge (Farno et al., 2015; Li and Noike, 1992). Li and Noike (1992) reported that the soluble COD

of WAS was considerably high after thermal treatment at 120 – 175 °C. This was considered due to particulate organics being hydrolysed into soluble matter by thermal treatment. Bougrier et al. (2008) also reported COD solubilisation after thermal treatment (90 – 210 °C), which increased linearly with treatment temperature. Perez et al. (2010) reported an increase in soluble COD after thermal treatment (170 °C, 30 minutes) and considers that this was due to the lysis of cells and destruction of floc structure in sludge. The hydrolysed sludge was also dewatered more easily. Appels (2010) reported increased soluble COD in the water phase after sludge was thermally treated (70 – 90 °C). This was found to be due to disruption of chemical bonds of the cell walls and membranes of microorganisms in the sludge, which releases intracellular organic material into the water phase. Morgan-Sagastume (2011) found that soluble COD increased greatly after TH (160 °C) and viscosity was also decreased. Furthermore, it was found that the total COD of sludge were relatively constant after TH, suggesting that degradation of organic matter was not significant.

In the above-mentioned studies, all rheological characterisations had been performed at ambient conditions after TH, which does not consider changes as a result of the sludge being cooled down after TH. Limited studies are available where sludge rheological measurement was performed under TH conditions. Farno et al. (2015) studied the rheological behaviour of WAS under thermal treatment temperature. However, the temperatures investigated (50 – 80 °C) were much lower than those typically encountered in TH. It was also found that the yield stress and infinite shear viscosity of sludge decreased linearly with increasing treatment temperature and logarithmically decreased over time at constant temperature. Furthermore, the rate of decrease of yield stress and infinite shear viscosity was found to be linearly proportional to the rate of solubilisation of organic matter in the sludge. As a result, it was suggested that rheological measurements can be used to predict organic matter solubilisation in the sludge. However, no study has shown whether this linear relationship is applicable for high pressure and high temperature thermal treatment.

The current study aims to investigate the rheological changes in thickened WAS under high temperature (80 – 145 °C) and high pressure (5 bar) conditions during 60 minutes of TH treatment. The aim is to study the rheological changes in sludge as TH progresses while the changes in organic matter solubilisation (sCOD) was simultaneously monitored to study their correlation.

4.3 MATERIALS AND METHODS

4.3.1 WASTE ACTIVATED SLUDGE

Waste activated sludge for the experiments was collected from Mount Martha wastewater treatment plant in Victoria, Australia. The collected sludge was thickened by dissolved air flotation in the treatment plant without any polymer dosing. The sludge had an initial solids concentration of 3.5 wt% at the time of collection and was stored at 4 °C for up to 30 days before use. This was done in order to minimize changes in the sludge due to biological activity and to help ensure the stability and consistency between samples during measurement (Curvers et al., 2009). A centrifuge was used to thicken the sludge to 7 wt% solids concentration at 9,000 rpm (~13,700 G) for 20 minutes. The sludge concentration was adjusted by diluting the centrifuge thickened sludge with the non-centrifuged sludge until the desired concentration was obtained. The solids concentration was determined by drying the sludge in an oven at 105 °C for over 24 hours until constant mass was obtained (APHA, 1992).

4.3.2 RHEOLOGICAL MEASUREMENTS

Rheological measurements were conducted using a stress-controlled rheometer (DHR3, TA Instruments). The rheometer is equipped with a pressure cell where the temperature can be monitored and controlled via a water-cooled Peltier jacket. The pressure cell operates based on a cup-and-bob geometry, with bob diameter of 26 mm and cup diameter of 28 mm. For rheology measurement, 10 mL of sludge sample was introduced into the pressure cell at room temperature. Nitrogen gas was used to purge air out of the system. The pressure cell was then sealed, and a syringe pump was used to pressurize the cell to 5 bar using nitrogen gas. Air was removed from the system in order to limit any oxidation reactions which may occur due to presence of oxygen gas. The pressure applied (5 bar) also ensures that sludge remains in the liquid phase during measurement at elevated temperatures, mimicking conventional TH processes. A shear rate of 10 s^{-1} was applied on the sludge for 3 minutes in order to homogenize the sample in the pressure cell. Then a shear rate of 675 s^{-1} was applied for 20 minutes on the sludge as a pre-shearing step in order to erase any shear history on the sample. The shear rate of 675 s^{-1} was the maximum shear rate limit of the pressure cell setup. An equilibrium period of 2 minutes with zero shear rate was then applied. Following that, a flow curve was generated for the sludge at 25 °C (i.e. untreated sludge). The sludge was then heated to the desired experiment temperature (80, 90, 100, 120, 130, 145 °C), with heating times averaging between 10 to 15 minutes, depending on the target temperature. Once the temperature was

reached, the pre-shearing step was applied again with shear rate of 675 s-1 for 2 minutes, followed by 1 minute of equilibration. This was done in order to erase the shear history during the previous flow curve measurements and heating time. The sludge would then remain at the target temperature for a period of 60 minutes, over which time, a series of flow curve measurements was carried out periodically. The same pre-shearing procedure (675 s^{-1} for 2 minutes followed by 1-minute equilibrating) was applied prior to each flow curve measurement. The flow curve measurements were done by performing a logarithmic sweep of decreasing shear rates (600 – 0.1 s^{-1}, 10 data points per decade) in 120 seconds. This way, flow curves could be generated to depict the periodic changes in sludge rheological behaviour during 60-minute TH under elevated temperature and pressure conditions.

The starting point for measurements was defined as the moment when the sample has reached the desired experiment temperature. The measured sample remained in the closed rheometer system throughout the entire measurement period. This was done to observe the sludge rheological changes under conditions mimicking TH processes, as it progresses over time.

4.3.3 CHEMICAL OXYGEN DEMAND

Changes in the chemical oxygen demand (COD) in the soluble phase of sludge were investigated in a separate reactor, using similar conditions as the rheological measurements. Using a 100 mL high pressure reactor (Parr Instrument Company), sludge samples were subjected to thermal hydrolysis treatment at 100, 120, 130, and 145 °C. Sludge was introduced into the reactor which was then purged with nitrogen gas to remove excess air. The reactor was sealed and pressurized to 5 bar using a syringe pump. The reactor was heated via a heating jacket up to the desired target temperature, with an average heating time of 10 minutes. Once the target temperature was reached, the sludge was held at constant temperature for 60 minutes. Periodically, 5 – 10 mL samples of the sludge were collected for COD analysis via a sampling tube. The reactor was permanently connected to the syringe pump for the duration of the test, which ensured that the pressure remained constant in the reactor. The sludge samples were collected in sealed tubes which were quickly cooled by dipping in an ice bath. The hydrothermally treated sludge samples were then centrifuged at 10,000 rpm (12,100 G) for 20 minutes, and the centrate was filtered through mixed cellulose ester membranes (0.45 μm pore size) for soluble COD (sCOD) measurement. Chemical oxygen demand measurement in the filtered centrate was performed following HACH procedure (using COD high range plus reagents, DR5000 Spectrophotometer and DRB200 reactor). The increase in soluble COD (rsCOD) in the sludge was defined as follows:

$$rsCOD = \frac{(sCOD_T - sCOD_0)}{sCOD_0} \qquad Eq.4.1$$

where $sCOD_T$ represents the soluble COD (mg/L) of the sludge collected any point during thermal hydrolysis treatment and $sCOD_0$ represents the soluble COD (mg/L) of the sludge prior to any thermal hydrolysis treatment, measured at 25 °C.

4.4 RESULTS AND DISCUSSION

4.4.1 FLOW BEHAVIOUR

Flow curves were generated at various time intervals during 60 min TH of 7 wt% WAS at different temperatures. Figure 4.1 shows the impact of temperature (a) and treatment time (b) on the shear stress – shear rate response of sludge during TH. Figure 4.1-a shows individual flow curves for sludge under different treatment temperatures, measured at 30 minutes. The sludge exhibits shear-thinning behaviour at all temperatures investigated. By increasing temperature, the shear stress response at any given shear rate was reduced, showing that sludge became less resistant to flow. Figure 4.1-b shows flow curves of sludge treated at constant temperature of 120 °C for different time intervals, up to 1 hour of treatment. As treatment time progresses, the sludge also became less resistant to flow. In general, with increasing treatment temperature, the apparent viscosity of sludge decreases, and at constant treatment temperature it decreases over time. This suggests that physico-chemical changes due to TH may continue to occur progressively over time, rather than instantaneously upon reaching treatment temperature. This is interesting because there are contradictory opinions on the treatment time requirements in TH. Some studies suggested long reaction times are necessary, while others opposed that (Barber, 2016).

All flow curves generated at the investigated temperatures at any treatment time (Figure 4.1), or at different treatment time at any studied temperatures, as in Figure 4.2, could best be described by the Herschel-Bulkley model:

$$\sigma = \sigma_c + k\dot{\gamma}^n \qquad Eq.4.2$$

Where σ is the shear stress (Pa); σ_c is the yield stress (Pa); $\dot{\gamma}$ is the shear rate (s^{-1}); k is the consistency index ($Pa.s^n$); and n is the flow index.

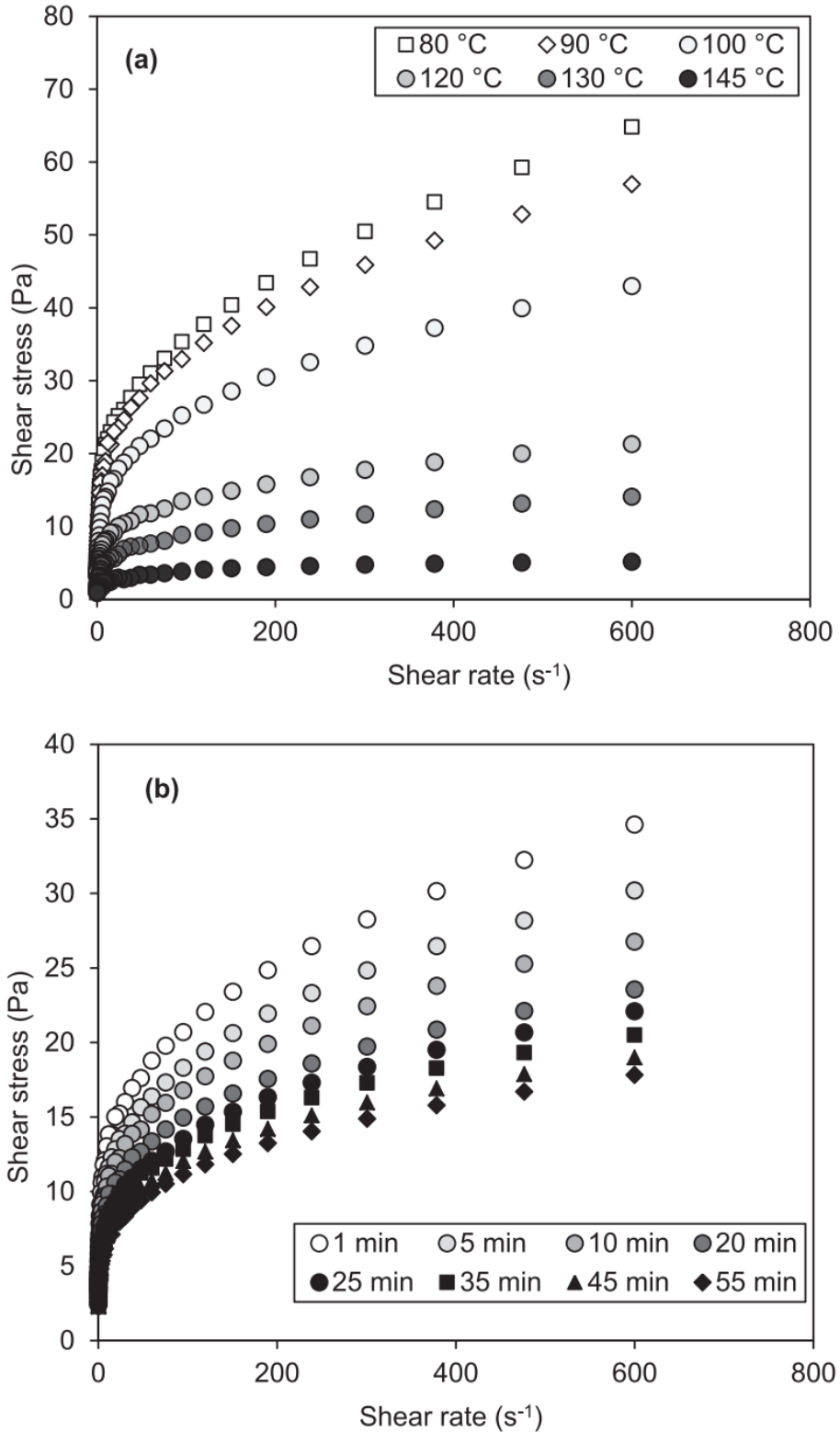

Figure 4. 1 – Flow curves of 7 % WAS (a) at various thermal hydrolysis temperatures upon 30 min treatment and (b) at different times during thermal hydrolysis at 120 °C treatment temperature.

At all different temperatures investigated, it was found that the sludge flow curves followed the same curvature even at different times across the 60-minutes treatment period. This indicated that the same physical phenomenon governs at different temperatures and treatment time. As such, a master flow curve was generated to encapsulate all flow curves obtained from the different temperatures and times of treatment. The aim was to obtain a single equation useful for design purposes. The master curve was then developed using a dimensionless form of the Herschel-Bulkley fluid model:

$$\sigma/\sigma_c = 1 + \beta\Gamma^n \qquad Eq.4.3$$

where

$$\Gamma = \left(\eta/\sigma_c\right).\dot{\gamma} \qquad Eq.4.4$$

$$\beta = \left(k/\sigma_c\right) \cdot \left(\sigma_c/\eta\right)^n \qquad Eq.4.5$$

Where Γ and σ/σ_c are the dimensionless shear rate and shear stress, and η is a measure of the apparent viscosity and equals 1 Pa.s.

Using the dimensionless Herschel-Bulkley model allows all flow curves to be more precisely compared between one another. The shear stress values have been scaled according to the yield stress, which describes the particle interaction network strength of the sludge at rest, thus normalizing all flow curves to the same point of reference. To maintain consistent comparisons, a dimensionless form for shear rates was used, and defined as in equation 4. Here, η represents the viscosity of an equivalent suspension of force-free particles in water, which can be assumed to have a value of 1 Pa.s (Baudez et al., 2004; Coussot, 1995).

One flow curve from the measured data was chosen as a reference curve. In this case, the flow curve generated for sludge treated at 80 °C measured at 1 minute during thermal treatment was chosen as the reference curve. The Herschel-Bulkley parameters (k, σ_c, and n) for the reference curve were determined via iterative calculation (for shear rates 10 – 600 s^{-1}) such that the error between values predicted by the Herschel-Bulkley parameters and the measured data were minimized. For the reference curve, the Herschel-Bulkley parameters were found to be as: yield stress, σ_c = 20.38 Pa, consistency index, k = 2.04 Pa.s^n, and flow index, n = 0.5. The other flow curves representing the sludge rheology at various points in time during 60-minutes thermal hydrolysis at different treatment temperatures (80 – 145 °C) were scaled such that they superimposed onto the reference curve. This was achieved by dividing the shear stress and shear rate values for each curve by a certain value. The factor by which the flow curves were scaled along

the shear stress axis (y-axis) is defined as S_y, and along shear rate axis (x-axis), it is defined as S_x. S_y and S_x are referred as the y and x axis shift factors, respectively. The consistency index and yield stress for the flow curve of sludge at different temperature and treatment time were then determined based on the shift factor values and master curve parameters (Eshtiaghi et al., 2016) as the following:

$$k = k_{master}\left(\frac{S_y}{S_x^n}\right) \qquad Eq.4.6$$

$$\sigma_c = \sigma_{c(master)} \cdot S_y \qquad Eq.4.7$$

It is worth noting, the yield stress being reported in the present study refers to the dynamic yield stress of the sludge at steady flow conditions. This means the yield stress was obtained via curve-fitting of flow curve data, measured at decreasing shear rates, to the Herschel-Bulkley model. Figure 4.2 shows the master flow curve representing rheological behaviour of 7 wt% WAS at 5-minute time intervals across 60-minutes TH for different treatment temperatures (80, 90, 100, 120, 130 and 145 °C.), as well as for untreated sludge at 25 °C. Using the master flow curve, the Herschel-Bulkley parameters for sludge (k and σ_c) at specific treatment temperature and time interval can be determined using corresponding shift factors presented in Table 4.1. Note that in Fig. 2, all flow curves were not shifted along the X-axis, so S_x = 1 for any given time and treatment temperature.

Table 4. 1 - Shift factors in the Y-axis, Sy, for the master flow curve (Fig. 2); shift factor in the X-axis, Sx = 1 for all curves.

Time (min)	80 °C	90 °C	100 °C	120 °C	130 °C	145 °C
Shift factor in the Y-axis, Sy						
(Untreated)*	2.16	2.15	2.06	2.07	2.03	2.14
1	1.00	0.91	0.76	0.47	0.35	0.20
5	0.95	0.88	0.73	0.41	0.31	0.16
10	0.91	0.84	0.67	0.38	0.27	0.13
15	0.89	0.82	0.62	0.34	0.24	0.12
20	0.87	0.80	0.59	0.33	0.22	0.10
25	0.86	0.78	0.58	0.30	0.21	0.09
30	0.85	0.76	0.58	0.29	0.19	0.08
35	0.84	0.75	0.56	0.29	0.19	0.07
40	0.83	0.74	0.55	0.27	0.18	0.07
45	0.82	0.72	0.54	0.27	0.17	0.06
55	0.82	0.68	0.54	0.25	0.16	0.06
60	0.82	0.66	0.55	0.25	0.16	0.05
65	0.81	0.65	0.52	0.24	0.15	0.04
Cooled**	1.49	1.18	1.25	0.90	0.59	0.25

** "Untreated" sludge refers to the initial condition of sludge measured at 25 °C, prior to heating.*
*** "Cooled" sludge refers to sludge following 1-hour thermal hydrolysis*

The calculated Herschel-Bulkley parameters of yield stress, σ_c (Pa) and consistency index, k (Pa.s^n) at different treatment times and different treatment temperatures are shown in Table 4.2. The goodness of fit of the Herschel-Bulkley model and corresponding parameters in describing each flow curve was assessed using a Chi-Square test ($\alpha = 0.05$). This was done by comparing the shear stress values observed from experimental data with the shear stress values calculated from the model at shear rates 10 – 600 s^{-1}. No significant difference was shown between the estimated values and experimental data. The mean absolute percentage error between experimental data and values estimated from the Herschel-Bulkley parameters corresponding to the respective sludge treatment conditions are shown in Table 4.2. Table 4.2 also shows HB parameters of the sludge measured at 25 °C (untreated sludge), prior to heating, and the parameters for the sludge, after 1-hour TH and cooling down to 25 °C.

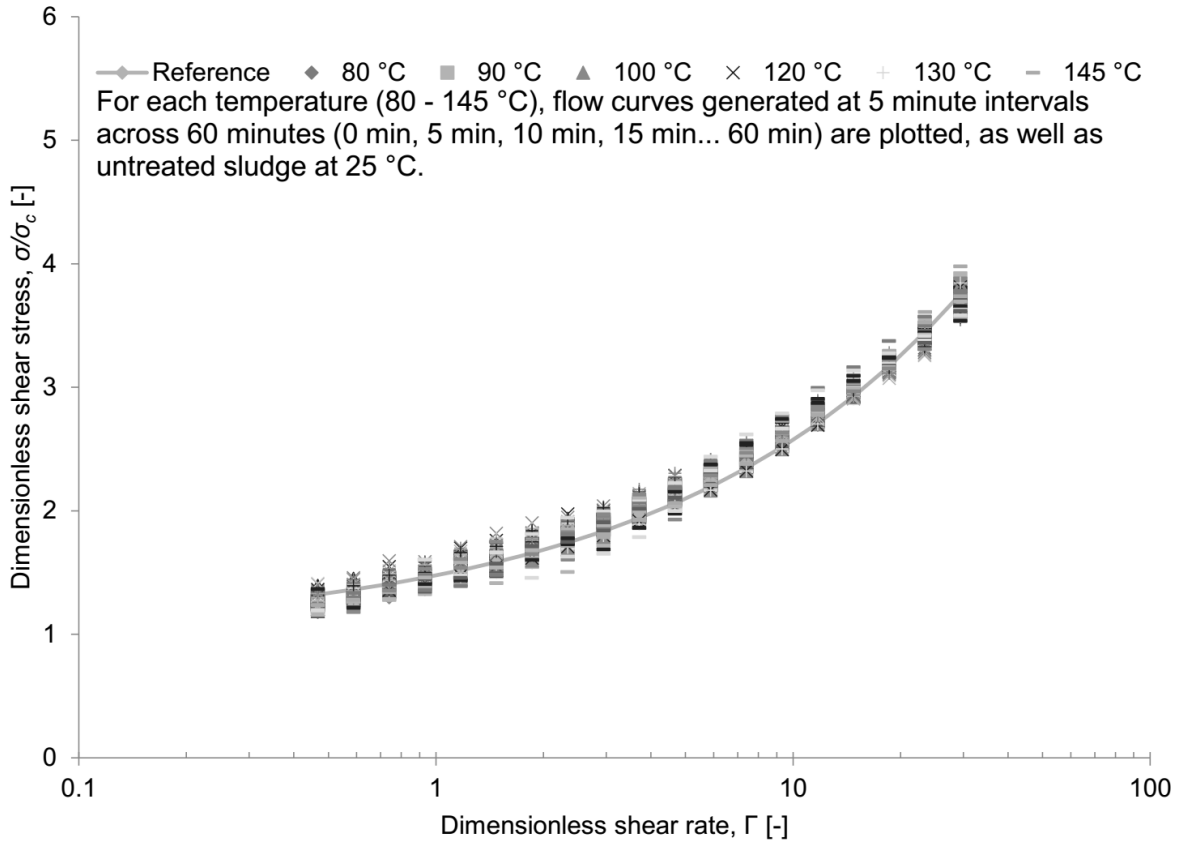

Figure 4. 2 - Master flow curve for 7 % WAS during 60 minute thermal hydrolysis at different temperatures (80 - 145 °C) and various time (Note: the flow curve for sludge at 1 min during 80 °C thermal hydrolysis was used as the reference curve; parameters for the master curve equation are: k = 2.04 Pa.s, σ_c = 20.38 Pa, n = 0.5, η = 1.0 Pa.s).

Table 4. 2– Calculated Herschel-Bulkley parameters for individual flow curves of 7 % WAS treated at different temperatures over time.

Time (min)	80 °C			90 °C			100 °C			120 °C			130 °C			145 °C		
	k (Pa.s)	σ_c (Pa)	*Error* (%)	*k* (Pa.s)	σ_c (Pa)	*Error* (%)	*k* (Pa.s)	σ_c (Pa)	*Error* (%)	*k* (Pa.s)	σ_c (Pa)	*Error* (%)	*k* (Pa.s)	σ_c (Pa)	*Error* (%)	*k* (Pa.s)	σ_c (Pa)	*Error* (%)
(Untreated)*	4.42	44.07	2.1	4.39	43.82	3.5	4.20	41.89	2.4	4.24	42.25	1.7	4.15	41.44	2.1	4.38	43.66	3.2
1	2.04	20.38	3.6	1.86	18.55	0.9	1.56	15.55	3.3	0.96	9.58	4.0	0.72	7.20	4.4	0.41	4.06	3.8
5	1.94	19.36	3.6	1.79	17.84	1.4	1.49	14.84	2.0	0.84	8.34	4.3	0.63	6.26	5.8	0.33	3.30	2.9
10	1.86	18.55	3.6	1.72	17.12	1.1	1.37	13.68	2.1	0.75	7.52	4.9	0.55	5.48	5.9	0.27	2.69	4.4
15	1.82	18.14	3.5	1.67	16.61	1.4	1.27	12.64	2.5	0.68	6.83	3.8	0.49	4.85	4.3	0.24	2.38	3.8
20	1.78	17.73	3.5	1.63	16.31	2.2	1.21	12.03	3.1	0.66	6.58	4.7	0.44	4.40	6.4	0.21	2.08	4.8
25	1.76	17.53	3.4	1.59	15.86	2.6	1.19	11.88	3.1	0.61	6.11	4.2	0.42	4.20	4.1	0.19	1.90	5.1
30	1.73	17.26	3.8	1.55	15.51	2.4	1.19	11.82	2.8	0.59	5.89	6.5	0.39	3.87	5.3	0.17	1.69	4.7
35	1.72	17.12	3.8	1.53	15.23	2.5	1.15	11.50	3.3	0.57	5.73	5.0	0.39	3.85	5.2	0.15	1.49	6.3
40	1.70	16.92	4.0	1.50	14.98	2.6	1.12	11.15	3.1	0.55	5.44	3.3	0.37	3.71	4.6	0.15	1.47	2.8
45	1.68	16.71	4.5	1.47	14.66	2.6	1.11	11.03	3.3	0.53	5.30	4.4	0.35	3.51	5.5	0.13	1.26	4.6
55	1.68	16.71	4.3	1.38	13.78	3.3	1.10	10.93	3.1	0.49	4.93	4.1	0.32	3.24	5.4	0.11	1.14	5.7
60	1.67	16.67	4.0	1.35	13.43	3.4	1.12	11.15	2.8	0.49	4.91	6.0	0.32	3.18	5.8	0.10	0.96	5.7
65	1.65	16.49	4.4	1.33	13.23	4.1	1.06	10.56	3.2	0.48	4.81	7.3	0.31	3.14	5.9	0.09	0.86	7.8
Cooled**	3.13	31.23	6.9	2.40	23.95	4.2	2.65	26.46	5.2	1.91	19.06	8.9	1.22	12.21	11.5	0.51	5.10	17.5

Error (%) refers to the mean absolute percentage error between experimental data and Herschel-Bulkley model-estimated values, using the tabulated parameters.

** "Untreated" sludge refers to the initial condition of sludge measured at 25 °C, prior to heating.*

*** "Cooled" sludge refers to sludge following 1-hour thermal hydrolysis.*

Figure 4.3 shows the impact of treatment temperature on the high-shear viscosity (a) and yield stress (b) of sludge. The high-shear viscosity, η_{∞}, describes the apparent viscosity of the sludge measured at 600 s^{-1} shear rate. This shear rate was the maximum limit of the pressure cell attachment used for measurement on the rheometer. At high shear rates, the hydrodynamic interactions are predominant which tends to a more Newtonian behaviour. At this shear rate, a better comparison can be made across the different samples. During treatment, the in-situ yield stress, $\sigma_{c,I}$, and in-situ high-shear viscosity, $\eta_{\infty,i}$ decreased linearly with increasing sludge temperature. Following TH at various temperatures, $\eta_{\infty,f}$ and $\sigma_{c,f}$ were determined. These represent the high-shear viscosity and yield stress of the sludge after being cooled down to 25 °C, following 60-minute TH. For the treated sludge, $\eta_{\infty,f}$ and $\sigma_{c,f}$ decreased linearly with increasing treatment temperature. Comparing the high-shear viscosity of sludge before and after 60-minute TH, the high-shear viscosity decreased irreversibly by 28%, 38%, 53%, 70% and 87% for treatment temperatures of 80, 100, 120, 130 and 145 °C respectively. Similarly, yield stress of sludge was also reduced irreversibly by 29%, 37%, 55%, 71% and 89% following 60 minutes TH at 80, 100, 120, 130 and 145 °C respectively.

On the other hand, it is also apparent that for all TH temperatures investigated, the high-shear viscosity and yield stress is lower when measured, in-situ, at TH conditions ($\eta_{\infty,i}$ and $\sigma_{c,i}$) compared to measuring the samples after cooling down to room temperature ($\eta_{\infty,f}$ and $\sigma_{c,f}$). The high-shear viscosity in the reactor was less than the high-shear viscosity of cooled sludge after TH by 48%, 61%, 77%, 77% and 86% at 80, 100, 120, 130 and 145 °C, respectively. The yield stress of sludge would also be less during TH compared to cooled, treated sludge by 47%, 60%, 74%, 74%, and 82% at 80, 100, 120, 130 and 145 °C respectively. This suggests that rheological data measured for cooled sludge after undergoing TH does not directly reflect the behaviour of sludge during TH. Knowing this, the actual value of $\eta_{\infty,i}$ and $\sigma_{c,i}$ during TH at various treatment temperatures could be estimated based on cooled, post-treatment sludge measurements (at room temperature).

$$\Delta\eta_{\infty} = \frac{\eta_{\infty,i} - \eta_{\infty,f}}{\eta_{\infty,f}} = -0.006\,T + 0.059 \qquad Eq.\,4.8$$

$$\Delta\sigma_{c} = \frac{\sigma_{c,i} - \sigma_{c,f}}{\sigma_{c,f}} = -0.006\,T + 0.043 \qquad Eq.\,4.9$$

Where $\eta_{\infty,i}$ and $\eta_{\infty,f}$ (Pa.s) are the high-shear viscosity measured at the treatment temperature, and at 25 °C after TH, respectively; $\sigma_{c,i}$ and $\sigma_{c,f}$ are the yield stress (Pa) measured at treatment temperature, and yield stress (Pa) measured at 25 °C after TH, respectively. T stands for treatment temperature (°C).

These results agree with findings of Farno et al. (2016), where the yield stress and apparent viscosity of cooled sludge also decreased with increasing treatment temperature (50 – 80 °C) as a result of thermal treatment compared to the initial untreated sludge. However, they reported a more significant yield stress reduction for 7 wt% WAS following thermal treatment at 80 °C. The yield stress reduced by 68% (106 Pa to 33.6 Pa after TH) as opposed to 29% reduction (45 Pa to 31 Pa after TH) observed in the present study. This difference is possibly due to different sample preparation methods. In the present study, the sludge samples were thickened via centrifuge which may cause differences in floc or network structure of the untreated sludge. Besides, the dynamic yield stress is being presented in the current study, as opposed to static yield stress in the aforementioned study. The yield stress of a material which describes the minimum stress that must be applied to induce a continuous flow in material is an indication of the structure and network strength of sludge (Eshtiaghi et al., 2013). So, by decreasing yield stress due to thermal hydrolysis, this could indicate changes to the structural integrity of the sludge at elevated temperatures. On the other hand, Urrea (2015) reported for a 2.33 wt% WAS with initial yield stress of 3.7 Pa, the yield stress was reduced to zero almost immediately upon reaching TH temperature. However, this may be due to the lower sludge solids concentration used in their study and the higher TH temperature employed (160 °C).

The evolution of the sludge Herschel-Bulkley parameters with treatment time were investigated at different treatment temperatures. Figure 4.4-a shows the evolution of k_i/k_0 with time at different TH temperatures. Here, k_i is the consistency index of the sludge at the measured treatment temperature and time whereas k_0 is the consistency of the sludge before TH, measured at 25 °C. For all treatment temperatures, k_i/k_0 decreased gradually over the 60-minute TH period. The same behaviour is observed for the $\sigma_{c,i}/\sigma_{c,0}$ as shown in Figure 4.4-b, where $\sigma_{c,i}$ is the yield stress of sludge measured at the treatment temperature and specific treatment time and $\sigma_{c,0}$ is the original yield stress of sludge before TH, measured at 25 °C. For each treatment temperature, both the yield stress and consistency index showed a more rapid logarithmic decrease in the initial 5 - 10 minutes of treatment time, before becoming more gradual. Similarly, figure 4.4-c shows the change in high-shear viscosity of sludge (over 1-hour TH at different temperatures. Here, $\eta_{\infty,i}$ is the apparent viscosity of sludge measured at shear rate of 600 s^{-1} during TH, whereas $\eta_{\infty,0}$ is the apparent viscosity of sludge at 600 s^{-1} shear rate measured at 25 °C before heating (untreated sludge).

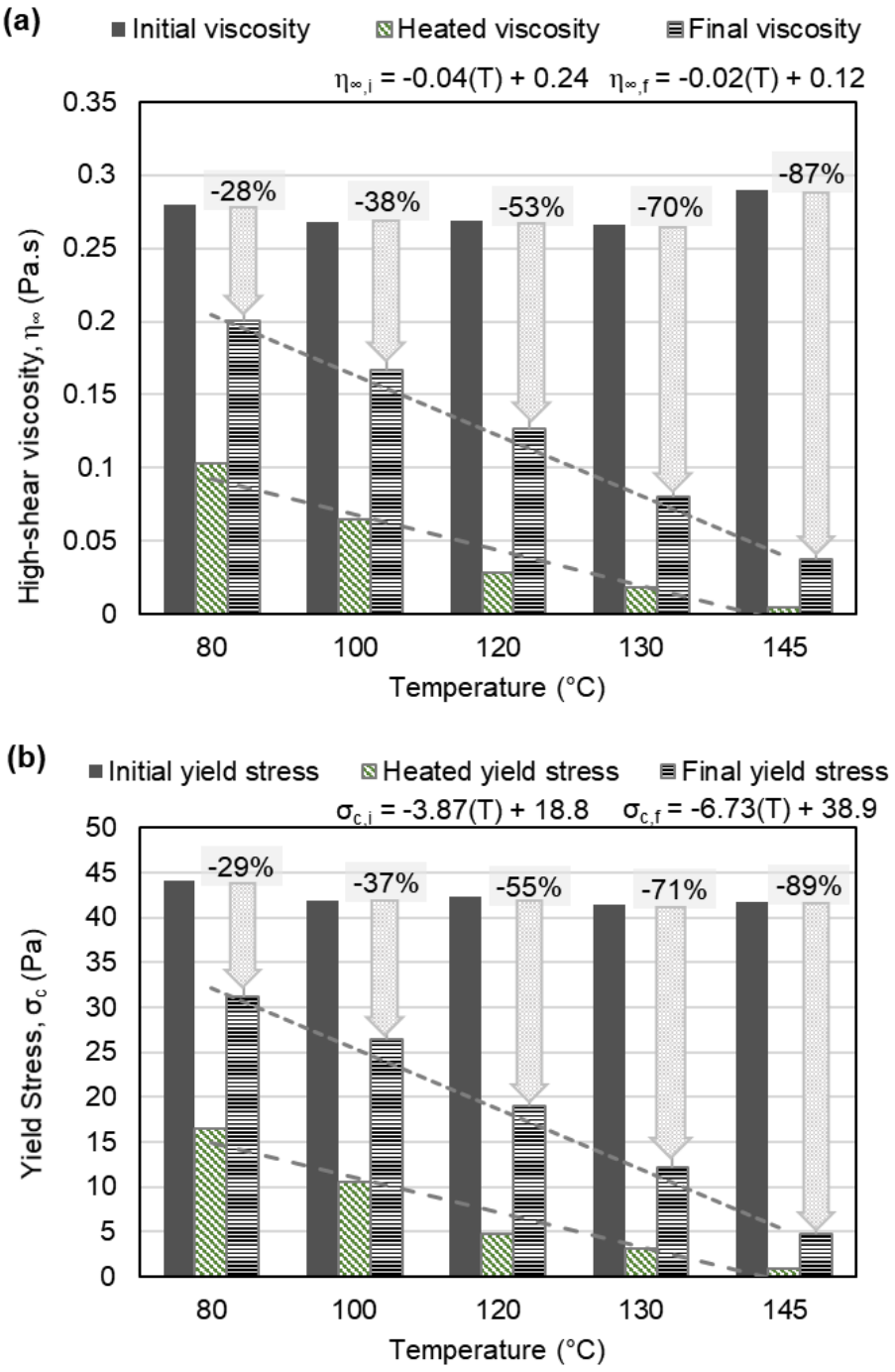

Figure 4. 3 - Impact of different thermal hydrolysis temperatures (80-145°C) on (a) the apparent viscosity measured at 600 s^{-1} and (b) yield stress of 7 % WAS after 60 minutes treatment (in-situ viscosity, $\eta_{\infty,i}$; in-situ yield stress, $\sigma_{c,i}$) and after sample is cooled down from treatment temperature to 25 °C (Final viscosity, $\eta_{\infty,f}$; Final yield stress, $\sigma_{c,f}$).

Multiple regression analysis was performed to generate equations for describe the changes in these parameters due to treatment temperature and time:

$$k_i/k_0 = 0.94 - 0.006\,T - 0.026\,Ln(t) \qquad Eq.4.10$$

$$\sigma_{c,i}/\sigma_{c,0} = 0.94 - 0.006\,T - 0.026\,Ln(t) \qquad Eq.4.11$$

$$\eta_{\infty,i}/\eta_{\infty,0} = 0.92 - 0.006\,T - 0.026\,Ln(t) \qquad Eq.4.12$$

Where *T* is treatment temperature (°C) and *t* is treatment time (min), starting from when the sludge reaches steady treatment temperature.

4.4.2 COD SOLUBILISATION

The impact of TH treatment at different temperatures (100 °C, 120 °C, 130 °C, and 145 °C) on the soluble COD was investigated. Figure 4.5 shows the increase of soluble COD (rsCOD) in sludge at different treatment temperatures during TH. Here, the data shown describes the rsCOD change across the entire TH process, starting from room temperature. In other words, the data describes the changes occurring during the heating phase of the process as well as during the constant temperature treatment phase. Depending on treatment temperature, sludge heating took 10-15 min. This was followed by 60 min at constant temperature. The rsCOD increased rapidly during the heating phase (represented as the initial 10- 15 minutes) in Fig. 5. After that, the rsCOD increased gradually at constant temperature. This suggests the rsCOD change is strongly influenced by temperature. It is reasonable to assume that at the TH conditions investigated (80-145 °C, 5 bar, no oxygen), destruction of organic material does not occur and the total COD in the sludge remains unaltered by TH (Aggrey et al., 2012; Imbierowicz & Chacuk, 2012; Morgan-Sagastume et al., 2011).

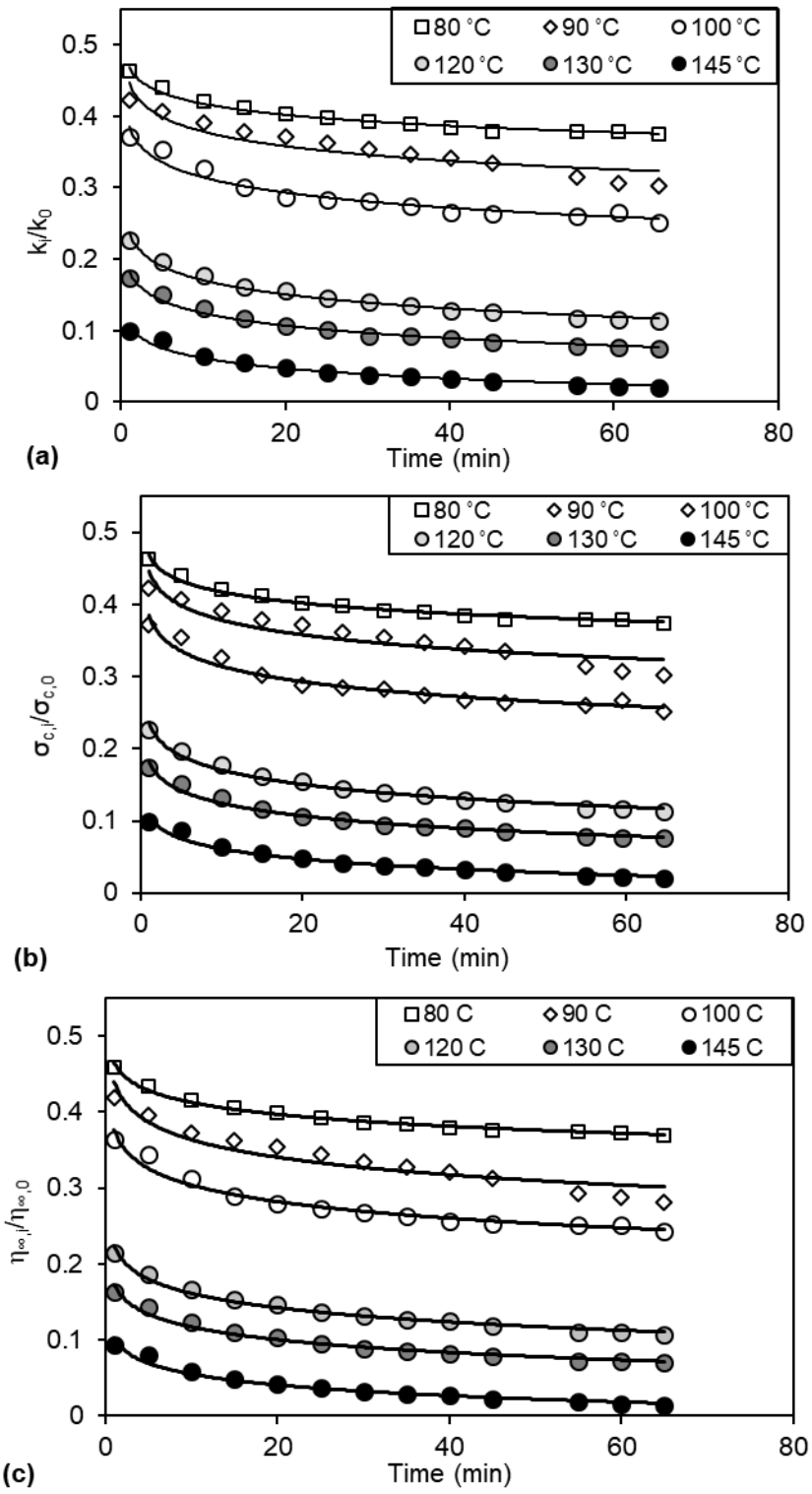

Figure 4. 4 - Evolution of (a) consistency index, (b) yield stress and (c) high-shear viscosity of 7 wt% WAS during 60 min of thermal hydrolysis treatment at various temperatures.

Omitting the data for the heating phase, Figure 4.5 (inset) shows only the rsCOD change at constant temperature, once the desired temperature was reached. At constant temperature, the increase of rsCOD with time follows a logarithmic trend for all temperatures investigated. The rsCOD was also found to increase linearly with increasing treatment temperature at fixed time. At constant temperature, the rsCOD continues to increase gradually with time over 60 minutes. Multiple regression analysis was performed to generate an equation for predicting the rsCOD (excluding heating phase) as a function of treatment temperature and treatment time:

$$rsCOD = 0.19\,Ln(t) + 0.015\,T - 0.71 \qquad Eq.4.13$$

Where *T* is treatment temperature (°C) and *t* is duration of treatment time (min) at the set temperature (excluding heating time).

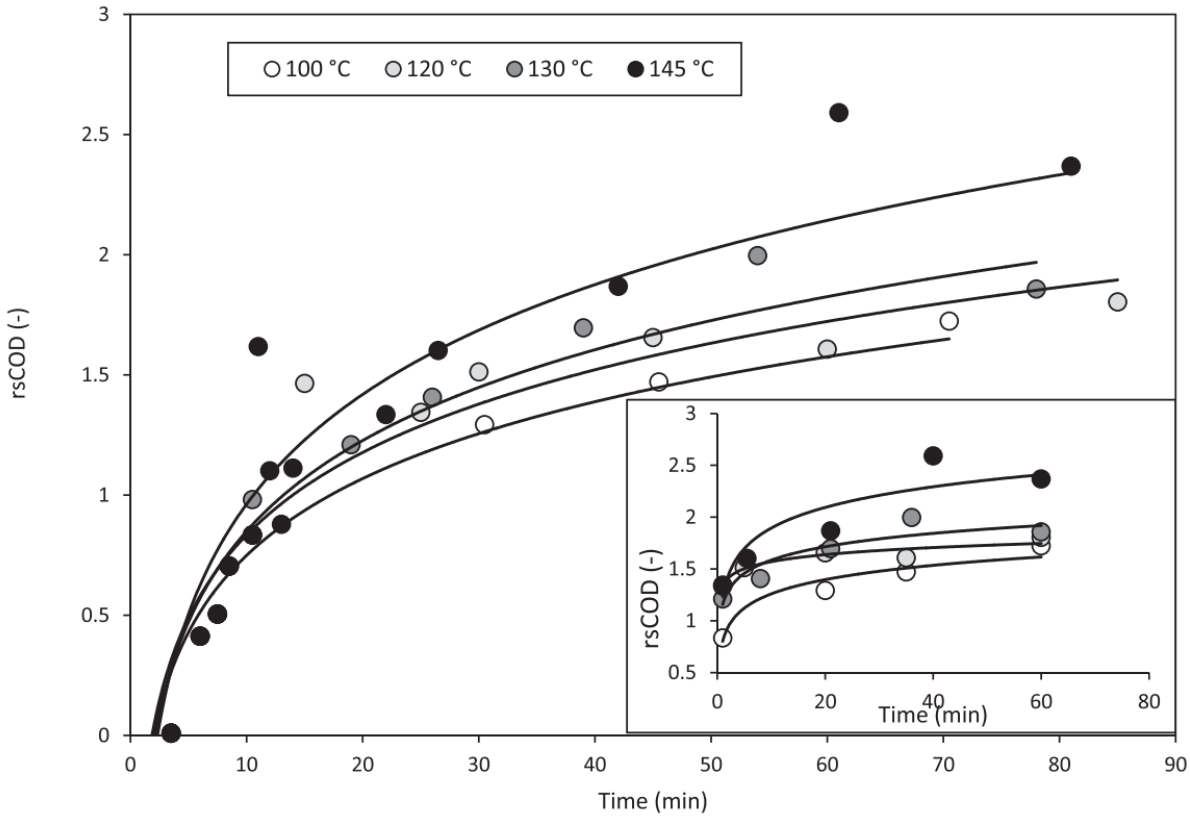

Figure 4. 5 – Impact of thermal hydrolysis temperature and treatment time on the released soluble COD (rsCOD) of 7 % WAS during TH process. The initial 10 – 15 minutes represents the sample heating phase. Inset shows the same figure, omitting sample heating phase, with sample at constant temperature.

The behaviour observed here is comparable to that found in literature. Everett (1972) reported that the concentration of dissolved volatile solids, which can be related with sCOD, increased with increasing treatment time and temperature (150–190 °C). Valo et al. (2004) reported an increase in sCOD with increasing temperature (130 – 150 °C) but found that increasing treatment time only produced gradual increases in sCOD during 60-minute treatment. Qiao et al. (2011) also reported slight increase in sCOD over time during 60-minute treatment (120 – 190 °C). On the other hand, Donoso-Bravo et al. (2011) reported a continuous increase in sCOD during initial 15 minutes of TH (170 °C) of sludge, after that the value remained constant upwards to 30 minutes. Imbierowicz & Chacuk (2012) reported an increase of total organic carbon in the liquid phase (TOC_L) during TH of WAS (150 – 220 °C). It was found that for 2 h thermal hydrolysis at 150 and 170 °C, the TOC_L increased rapidly during the initial 20 minutes, after which it became more gradual. In the current study, it is noted that COD analysis is unable to perform measurements at high precision. Therefore, minute variations in COD during TH may be undetectable, owing to the variable nature of the sludge samples and errors inherent the COD analysis method itself. However, it is known that TH leads to solubilisation of particulate organic compounds in WAS and is reflected as changes in sCOD. In turn, the changes in sCOD could be a further indication of the physical changes occurring in the sludge.

It is notable that in the present study, the significant portion of rsCOD increase also mainly occurs within 20 minutes of reaching steady TH temperature, similar to those reported in other studies. Major changes in the yield stress and viscosity were also primarily observed during the initial 10 – 20 minutes of reaching constant temperature. The rheological changes due to TH observed in the current study, which can generally be described as a reduction in the resistance to flow, is most likely a result several changes occurring in the sludge due to the impact of TH. It is known that during TH, the cell walls of microorganism which make up a large portion of WAS are destroyed, releasing soluble cell contents (Everett, 1972). Insoluble proteins are also broken down into soluble amino acids. The EPS and large sludge particles, which contribute to the floc structure of sludge and its ability to retain water, are also broken down (Bougrier et al., 2008; Neyens et al., 2004). The EPS has been found to correlate strongly with the rheological behaviour of sludge (Feng et al., 2016) and it is very likely that floc structure and sludge particle sizes also contribute to the sludge rheology. As the EPS is solubilised and floc structure is broken down, accompanied by the destruction of sludge particles and release of bound water, these changes are reflected in the rheological changes observed. Furthermore, these changes are also reflected as an increase in soluble COD, as a portion of organic compounds constituting a solid phase become more solubilised (Imbierowicz & Chacuk, 2012). From the experimental results (Figure 4.4-a & b), the apparent

viscosity, yield stress and consistency index decrease rapidly at first (5 – 10 minutes) and then reduces gradually over the treatment period. On the other hand, the sCOD was found to increase rapidly initially before becoming more gradual during constant temperature treatment (Fig.5). Both behaviours were found to follow logarithmic trends. Comparing the rsCOD data to the rheological data, Figure 4.6 shows the correlation between rsCOD to $\sigma_{c,i}/\sigma_{c,0}$ and $\eta_{\infty,i}/\eta_{\infty,0}$. It can be seen that rsCOD is linearly proportional to both parameters, whereby an increase in the soluble COD correlates to a decrease in yield stress and apparent viscosity for the sludge. Farno et al. (2015), also reported that change rsCOD had a strong linear proportionality to change in yield stress and apparent viscosity for WAS thermally treated at low temperature (50 – 80 °C). However, the present study was not able to reproduce as strong of a linear fit as observed in Farno et al. (2015). This is most likely a result of the complicated methodology required for sampling and analysing of sludge COD at much higher treatment temperature and pressure conditions leading to high variability in results. However, it is reasonable to expect that the same correlation would also exist at the higher temperature conditions used in the present study, since it has been shown that the removal of total COD from sludge is minimal even at 150 °C and the solubilisation of sludge is the primary outcome of TH (Imbierowicz & Chacuk, 2012). This correlation suggests that the potential exists for using on-line rheological measurements as a tool for monitoring the performance of TH processes at high temperature and pressure conditions in terms of the solubilisation of sludge.

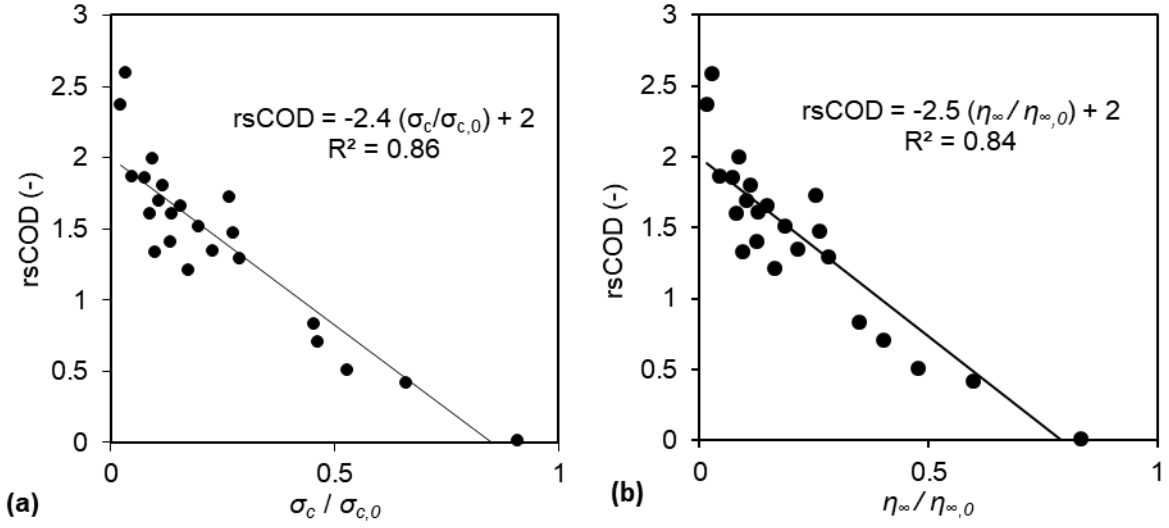

Figure 4. 6 – Linear relationship between the increase in soluble COD in sludge (rsCOD) and the reduction of dimensionless yield stress (a) and high-shear viscosity (at 600 s^{-1}) (b) of sludge during 60-minute thermal hydrolysis at various temperatures (100, 120, 130 and 145 °C). Data points include sample heating phase as well as after sample has reached constant treatment temperature.

4.5 CONCLUSION

Thermal hydrolysis significantly impacts the physical properties of WAS. After 60-minute TH at 80 – 145 °C, the yield stress and apparent viscosity of sludge is irreversibly altered. The yield stress and apparent viscosity of treated sludge decreased linearly with increasing treatment temperature. Over the course of TH, WAS behaved as a shear-thinning fluid with yield stress which could be described by the Herschel-Bulkley model. This was true at any time during 60-minutes TH at the temperatures studied. A master flow curve was developed which can be used to describe the rheological behaviour of sludge at the TH conditions investigated. Furthermore, the rheological changes were found to occur dynamically over the course of the treatment period. The yield stress and apparent viscosity of WAS decreased linearly with increasing treatment temperature. At constant temperature, the yield stress and apparent viscosity decreased logarithmically with time, with the majority of changes occurring within the first 10 minutes upon reaching treatment temperature. Similarly, during TH at constant temperature, soluble COD of sludge was also found to increase logarithmically with treatment time which the majority of increase happened within the initial 10 – 20 minutes.

It was also found that a linear correlation exists between increasing soluble COD with the decreasing yield stress and apparent viscosity of sludge. This suggests that there is potential for using on-line rheological measurement as a tool for monitoring the performance of TH.

REFERENCES

Abe, N., Tang, Y.Q., Iwamura, M., Morimura, S., Kida, K., 2013. Pretreatment followed by anaerobic digestion of secondary sludge for reduction of sewage sludge volume. Water Sci. Technol. 67, 2527–2533. doi:10.2166/wst.2013.154

Aggrey, A., Dare, P., Lei, R., Gapes, D., 2012. Evaluation of a two-stage hydrothermal process for enhancing acetic acid production using municipal biosolids. Water Sci. Technol. 65, 149–155. doi:10.2166/wst.2011.848

APHA, Standard Methods for the Examination of Water and Wastewater, in: A. P.H. Association (Ed.), 1992. Washington, DC.

Appels, L., Baeyens, J., Degrève, J., Dewil, R., 2008. Principles and potential of the anaerobic digestion of waste-activated sludge. Prog. Energy Combust. Sci. 34, 755–781. doi:10.1016/j.pecs.2008.06.002

Appels, L., Degrève, J., Van der Bruggen, B., Van Impe, J., Dewil, R., 2010. Influence of low temperature thermal pre-treatment on sludge solubilisation, heavy metal release and anaerobic digestion. Bioresour. Technol. 101, 5743–5748. doi:10.1016/j.biortech.2010.02.068

Barber, W. P. F. (2016). Thermal hydrolysis for sewage treatment: A critical review. Water Research, 104, 53-71.

Baudez, J. C., Ayol, A., & Coussot, P. 2004. Practical determination of the rheological behavior of pasty biosolids. *Journal of environmental management*, *72*(3), 181-188.

Bougrier, C., Albasi, C., Delgenès, J.P., Carrère, H., 2006. Effect of ultrasonic, thermal and ozone pre-treatments on waste activated sludge solubilisation and anaerobic biodegradability. Chem. Eng. Process. Process Intensif. 45, 711–718. doi:10.1016/j.cep.2006.02.005

Bougrier, C., Delgenès, J.P., Carrère, H., 2008. Effects of thermal treatments on five different waste activated sludge samples solubilisation, physical properties and anaerobic digestion. Chem. Eng. J. 139, 236–244. doi:10.1016/j.cej.2007.07.099

Camacho, P., Ewert, W., Kopp, J., Panter, K., Perez-Elvira, S.I., Piat, E., 2008. Combined experiences of thermal hydrolysis and anaerobic digestion – latest thinking on thermal hydrolysis of secondary sludge only for optimum dewatering and digestion. Proc. Water Environ. Fed. 2008, 1964–1978. doi:10.2175/193864708788733972

Carrère, H., Dumas, C., Battimelli, A., Batstone, D.J., Delgenès, J.P., Steyer, J.P., Ferrer, I., 2010. Pretreatment methods to improve sludge anaerobic degradability: A review. J. Hazard. Mater. 183, 1–15. doi:10.1016/j.jhazmat.2010.06.129

Carvajal, a., Peña, M., Pérez-Elvira, S., 2013. Autohydrolysis pretreatment of secondary sludge for anaerobic digestion. Biochem. Eng. J. 75, 21–31. doi:10.1016/j.bej.2013.03.002

Coussot, P. 1995. Structural similarity and transition from Newtonian to non-Newtonian behavior for clay-water suspensions. *Physical review letters*, *74*(20), 3971.

Curvers, D., Saveyn, H., Scales, P.J., Van der Meeren, P., 2009. A centrifugation method for the assessment of low pressure compressibility of particulate suspensions. Chem. Eng. J. 148, 405–413. doi:10.1016/j.cej.2008.09.030

Dohányos, M., Zábranská, J., Kutil, J., Jeníček, P., 2004. Improvement of anaerobic digestion of sludge. Water Science and Technology. Water Sci. Technol. 49, 89–96.

Donoso-Bravo, A., Pérez-Elvira, S., Aymerich, E., Fdz-Polanco, F., 2011. Assessment of the influence of thermal pre-treatment time on the macromolecular composition and anaerobic biodegradability of sewage sludge. Bioresour. Technol. 102, 660–666. doi:10.1016/j.biortech.2010.08.035

Eshtiaghi, N., Markis, F., Zain, D., & Mai, K. H. 2016. Predicting the apparent viscosity and yield stress of digested and secondary sludge mixtures. *Water research*, *95*, 159-164.

Eshtiaghi, N., Markis, F., Yap, S.D., Baudez, J.C., Slatter, P., 2013. Rheological characterisation of municipal sludge: A review. Water Res. 47, 5493–5510. doi:10.1016/j.watres.2013.07.001

Everett, J.G., 1972. Dewatering of wastewater sludge by heat treatment. Water Pollut. Control Fed. 92–100.

Farno, E., Baudez, J.C., Parthasarathy, R., Eshtiaghi, N., 2016. Impact of thermal treatment on the rheological properties and composition of waste activated sludge: COD solubilisation as a footprint of rheological changes. Chem. Eng. J. 295, 39–48. doi:10.1016/j.cej.2016.03.022

Feng, G., Liu, L., Tan, W., 2014. Effect of thermal hydrolysis on rheological behavior of municipal sludge. Ind. Eng. Chem. Res. 53, 11185–11192. doi:10.1021/ie501488q

Feng, X., Tang, B., Bin, L., Song, H., Huang, S., Fu, F., Ding, J., Chen, C., Yu, C., 2016. Rheological behavior of the sludge in a long-running anaerobic digestor: Essential factors to optimize the operation. Biochem. Eng. J. 114, 147–154. doi:10.1016/j.bej.2016.06.022

Frølund, B., Palmgren, R., Keiding, K., Nielsen, P.H., 1996. Extraction of extracellular polymers from activated sludge using a cation exchange resin. Water Res. 30, 1749–1758. doi:10.1016/0043-1354(95)00323-1

Gavala, H.N., Yenal, U., Skiadas, I. V., Westermann, P., Ahring, B.K., 2003. Mesophilic and thermophilic anaerobic digestion of primary and secondary sludge. Effect of pre-treatment at elevated temperature. Water Res. 37, 4561–4572. doi:10.1016/S0043-1354(03)00401-9

Hammadi, L., Ponton, A., Belhadri, M., 2012. Effects of Heat Treatment and Hydrogen Peroxide (H2O2) on the Physicochemical and Rheological Behavior of an Activated Sludge from a Water Purification Plant. Procedia Eng. 33, 293–302. doi:10.1016/j.proeng.2012.01.1207

Hii, K., Baroutian, S., Parthasarathy, R., Gapes, D.J., Eshtiaghi, N., 2014. A review of wet air oxidation and Thermal Hydrolysis technologies in sludge treatment. Bioresour. Technol. 155, 289–299. doi:10.1016/j.biortech.2013.12.066

Imbierowicz, M., Chacuk, A., 2012. Kinetic model of excess activated sludge thermohydrolysis. Water Res. 46, 5747–5755. doi:10.1016/j.watres.2012.07.051

Kepp, U., Machenbach, I., Weisz, N., Solhelm, O.E., 2000. Enhanced stabilisation of sewage sludge through thermal hydrolysis - Three years of experience with full scale plant BT - Disposal and Utilisation of Sewage Sludge: Treatment Methods and Application Modalities, October 13, 1999 - October 15, 1999 42, 89–96.

Konigsberg, D., Nicholson, T. M., Halley, P. J., Kealy, T. J., & Bhattacharjee, P. K. (2013). Online process rheometry using oscillatory squeeze flow. *Applied Rheology*, *23*(3).

Li, D.-H., Ganczarczyk, J.J., 1990. Structure of activated sludge flocs. Biotechnol. Bioeng. 35, 57–65. doi:10.1002/bit.260350109

Li, Y.-Y., Noike, T., 1992. Upgrading of Anaerobic Digestion of Waste Activated Sludge by Thermal Pretreatment. Water Sci. Technol. 26, 857–866.

Morgan-Sagastume, F., Pratt, S., Karlsson, A., Cirne, D., Lant, P., Werker, A., 2011. Production of volatile fatty acids by fermentation of waste activated sludge pre-treated in full-scale thermal hydrolysis plants. Bioresour. Technol. 102, 3089–3097. doi:10.1016/j.biortech.2010.10.054

Neyens, E., Baeyens, J., 2003. A review of thermal sludge pre-treatment processes to improve dewaterability. J. Hazard. Mater. 98, 51–67. doi:10.1016/S0304-3894(02)00320-5

Neyens, E., Baeyens, J., Dewil, R., De Heyder, B., 2004. Advanced sludge treatment affects extracellular polymeric substances to improve activated sludge dewatering. J. Hazard. Mater. 106, 83–92. doi:10.1016/j.jhazmat.2003.11.014

Perez-Elvira, S.I., Fdz-Polanco, M., Fdz-Polanco, F., 2010. Increasing the performance of anaerobic digestion: Pilot scale experimental study for thermal hydrolysis of mixed sludge. Front. Environ. Sci. Eng. China 4, 135–141. doi:10.1007/s11783-010-0024-5

Pérez-Elvira, S.I., Fernández-Polanco, F., Fernández-Polanco, M., Rodríguez, P., Rouge, P., 2008. Hydrothermal multivariable approach. Full-scale feasibility study. Electron. J. Biotechnol. 11. doi:10.2225/vol11-issue4-fulltext-14

Qiao, W., Peng, C., Wang, W., Zhang, Z., 2011. Biogas production from supernatant of hydrothermally treated municipal sludge by upflow anaerobic sludge blanket reactor. Bioresour. Technol. 102, 9904–9911. doi:10.1016/j.biortech.2011.08.037

Slatter, P., 2011. The Engineering Hydrodynamics of Viscoplastic Suspensions. Part. Sci. Technol. 29, 139–

150. doi:10.1080/02726351.2010.527429

Valo, A., Carrère, H., Delgenès, J.P., 2004. Thermal, chemical and thermo-chemical pre-treatment of waste activated sludge for anaerobic digestion. J. Chem. Technol. Biotechnol. 79, 1197–1203. doi:10.1002/jctb.1106

Zhou, Y., Takaoka, M., Wang, W., Liu, X., Oshita, K., 2013. Effect of thermal hydrolysis pre-treatment on anaerobic digestion of municipal biowaste: A pilot scale study in China. J. Biosci. Bioeng. 116, 101–105. doi:10.1016/j.jbiosc.2013.01.014

CHAPTER 5:

IN-SITU RHEOLOGICAL CHARACTERIZATION OF THICKENED WASTE ACTIVATED SLUDGE DURING THERMAL HYDROLYSIS PROCESSES: INFLUENCE OF SOLIDS CONCENTRATION, TREATMENT TEMPERATURE, AND TIME

This chapter was published jointly with Chapter 6 in Water Research Journal

(Vol: 156, pp: 445-455, 2019)

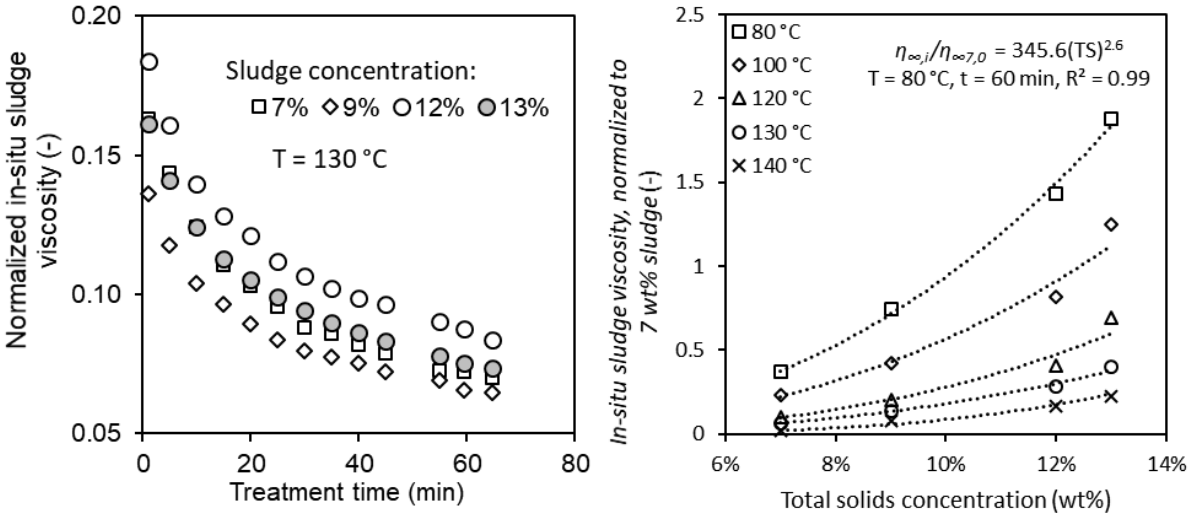

Keywords: Thermal hydrolysis; solids concentration; yield stress; apparent viscosity; waste activated sludge.

Hii, K, Farno, E, Baroutian, S, Parthasarathy, R, Eshtiaghi, N., 2019, Rheological characterization of thermal hydrolysed waste activated sludge, Water Research Journal 156: 445-477

5.1 ABSTRACT

Thermal hydrolysis (TH) is a promising pre-treatment method for the anaerobic digestion of sewage sludge involving the solubilization of sludge at elevated temperature conditions. However, rheological studies on sludge at TH conditions are relatively scarce, while most available studies were performed on treated sludge after it was cooled to ambient temperatures. Furthermore, increasingly thicker sludge types are being used in TH, so the impact of higher sludge concentrations will also be of interest. The flow behaviour of waste activated sludge (WAS) at various solids concentrations (7 – 13 wt.%) was studied under elevated temperature conditions (80 – 140 °C) such as those found during TH processes. During 60–minutes TH at constant temperature, WAS rheological behaviour was best described by the Herschel-Bulkley model at all conditions studied. The apparent viscosity, yield stress and consistency index showed logarithmic relationship with treatment time. At constant time and solids concentration, linear relationship was observed between treatment temperature and apparent viscosity, yield stress and consistency index. With increasing solids concentration, the apparent viscosity, yield stress and consistency index increased following a power law at all temperatures and time studied. This power-law relationship between rheological parameters and sludge concentration existed despite elevated temperature conditions of TH. Results also suggested that the proportion of sludge solubilization and its rate were unaffected by varying sludge concentration. Linear proportionality existed between the extent of sludge solubilisation and rheological parameters. The evolution of rheological parameters in-situ during TH were described by regression models.

5.2 INTRODUCTION

Today, anaerobic digestion remains a promising technique for sewage sludge treatment owing to its potential for energy recovery in the form of biogas production (Appels et al., 2008; Zhen et al., 2017). The large quantity of sewage sludge produced has led to continuous development of different sludge pre-treatment strategies (Ariunbaatar et al., 2014; Zhen et al., 2017). A pre-conditioning step is now also viewed as an essential component in anaerobic digesters, whereby a pre-treatment process makes the incoming sludge more amenable to digestion, greatly improving anaerobic digestion performance. Among the pre-treatment techniques, hydrothermal methods such as thermal hydrolysis (TH) have shown favourable outcomes and received wide industrial applications, with commercial examples such as full-scale CambiTHP™ and Biothelys® processes (Barber, 2016; Sapkaite et al., 2017; Zhen et al., 2017).

Thermal hydrolysis involves subjecting sludge to high temperatures conditions for fixed time in order to solubilize sludge contents and improve its digestibility. The high temperatures applied cause cell membranes to disintegrate and results in the solubilization of sludge particles and organic compounds (Ariunbaatar et al., 2014; Suárez-Iglesias et al., 2017). Thermal hydrolysis processes typically occur in the temperature range of 100 – 200 °C (Hii et al., 2014). In the case of TH, most studies have found the optimal temperature to be around 170 °C, with treatment times of 30 – 60 minutes (Zhen et al., 2017). However, lower temperature thermal pre-treatment processes (<100 °C) have also shown to be promising (Liao et al., 2016; Nazari et al., 2017).

Waste activated sludge (WAS) is the main sludge type primarily handled in TH processes. It has been shown that the effects of TH are more pronounced on WAS due to its high carbohydrate and protein content (Barber, 2016; Wilson and Novak, 2009). Waste activated sludge is a biological suspension consisting of organic particulates and bacteria held together in flocs by gel-like biofilm matrices called extracellular polymeric substances (EPS) (Neyens et al., 2004). The EPS represents up to 80% of its mass (Frølund et al., 1996) and plays a key part in the structural integrity and dewatering characteristics in WAS (Zhang et al., 2017). The EPS has also been found to contribute to the rheological behaviour of WAS (Feng et al., 2014a, 2016), and the removal of EPS has been shown to reduce WAS viscosity (Sanin, 2002).

The rheological behaviour of WAS is complex, but it is generally accepted that WAS behaves as a non-Newtonian, shear-thinning fluid. The Herschel-Bulkley model is commonly used to describe the behaviour of concentrated WAS (Baudez et al., 2011; Eshtiaghi et al., 2013; Khalili Garakani et al., 2011). It has been shown to exhibit thixotropic properties (Guibaud et al., 2004) and many studies identify the presence of a yield stress (Farno et al., 2015; Markis et al., 2014; Ratkovich et al., 2013). The presence of yield stress was explained by a transition of the WAS from a solid-like to fluid-like behaviour due to rupture in the alignment of flocs (Yang et al., 2009). It is also generally understood that the rheological properties of WAS become more significant with increasing solids concentration. Many studies have reported increasing sludge viscosity and consistency index due to increasing solids concentration (Eshtiaghi et al., 2013; Forster, 2002; Laera et al., 2007; Mori et al., 2006; Sanin, 2002). It is suggested that inter-particle interactions become stronger at higher solids content due to larger sizes and closer proximity of particles, leading to increased apparent viscosity in sludge (Eshtiaghi et al., 2013). The effect of solids concentration on sludge viscosity and consistency index has been shown to follow an exponential function (Guibaud et al., 2004; Markis et al., 2014; Tixier et al., 2003) or power law model (Lotito et al., 1997; Markis et al.,

2014; Sanin, 2002; Tixier et al., 2003). The yield stress of WAS also tends to increase with higher solids concentration. Mori et al. (2006) observed an exponential increase of yield stress for WAS when solids concentration increased from 27 to 57 g/L similar to other researchers (Battistoni et al., 1993; Riley and Forster, 2001). On the other hand, Forster et al. (2002) showed that WAS exhibited yield stress which followed a power relationship with solids content (10 – 50 g/L), although at low solids concentrations (<9 - 11 g/L) the yield stress becomes negligible. Lotito et al. (1997) similarly reported power relationship between yield stress and solids concentration of WAS (0.3 – 5.4 % total solids) and found that rheological parameters strongly depended on solids concentration and sludge type and suggested that the presence of EPS leads to higher viscosities generally observed in WAS. Sanin et al. (2002) found that increasing solids concentration (2,000 – 18,000 mg/L) led to decreasing flow index. Mori et al. (2006) similarly reported flow index decreasing linearly with increasing solids content, suggesting that concentrated sludge became increasingly shear thinning. However, these studies are only concerned with the WAS rheology at ambient to moderate temperatures.

Limited studies are available regarding the rheology of sludge during high temperature processes such as TH (Barber, 2016). A better understanding of sludge rheology during TH will be beneficial towards optimizing these energy-demanding processes. It is generally accepted that TH greatly alters sludge rheology. However, detailed rheology studies are relatively scarce, and most studies are performed on post-treatment sludge at ambient temperature, which may not always be representative of the sludge during TH. Dote et al. (1993) showed the apparent viscosity of thermally treated sludge depended on the measurement temperature. Ruffino et al. (2015) performed low temperature TH (90 °C, 3 hours) and found that thermally treated sludge exhibited apparent viscosity which was equal to that of untreated sludge with half the solids content. Bougrier et al. (2008) showed that the apparent viscosity of treated WAS was reduced compared to untreated sludge, and the reduction in apparent viscosity increased with increasing TH temperature up to 150 °C. Increasing TH temperature beyond 150 °C did not lead to further reduction in apparent viscosity, suggesting a threshold temperature for changes in sludge physical characteristics.

Feng et al. (2014a) compared the rheological behaviour of untreated WAS and treated WAS after TH (170 °C, 60 minutes) at various solids concentrations. They reported that shear-thinning behaviour was still exhibited by treated sludge and its non-Newtonian characteristics increased with increasing solid content. They showed that the Herschel-Bulkley model was appropriated for untreated and treated sludge, but expressed that the Newtonian fluid model would also be suitable for treated sludge with solid

concentrations below 187 g/L. For both treated (54 – 187 g/L) and untreated sludge (20 – 120 g/L), the consistency index and apparent viscosity increased with increasing solid content following an exponential relationship, but no correlation was found for flow index. They also found that effect of increasing solids content on apparent viscosity was more pronounced in untreated sludge than treated sludge, due to a higher exponent value. On the other hand, Feng et al. (2014b) compared the rheological behaviour of untreated and treated WAS (5.4 wt% solids content) after 170 °C and 60 minutes by fitting various rheological models. They expressed that the Newtonian fluid model accurately described the treated sludge due to high determination coefficient values (R^2), whereas untreated sludge was described by the Herschel-Bulkley and power law models. However, for treated sludge, the R^2 value was comparable between the Herschel-Bulkley model (R^2 = 0.94) and Newtonian model (R^2 = 0.95). The authors attributed the increased fluidity in treated sludge to the destruction of floc structure and network strength within the sludge.

Urrea et al. (2015) investigated the rheology of WAS (23.3 g/L total suspended solids) sampled at different times during TH (160 – 200 °C). Flow curves were generated at 25 °C for collected samples. They observed different types of flow in the sludge during TH. Initially, the untreated sludge was reported to behave as a Bingham plastic fluid with yield stress (σ_c) of 3.7 Pa, consistency index (*k)* of 0.075 Pa.s, and flow index (*n)* of 1. As the sludge was heating up, *k* increased while n decreased. However, as constant temperature is reached, σ_c and *k* decreased, whereas *n* increased. The final treated sludge was found to behave as a Newtonian liquid. They attributed these changes to the reduced interaction between particles and polymers due to their decrease in size and quantity. They reported that the total suspended solids (TSS) was reduced by 50% after TH and σ_c was correlated exponentially with increasing TSS (10 – 23 g/L) while *k* and *n* were fitted to a polynomial function of third and second order, respectively.

Recently, Hii et al. (2017) studied WAS rheology in-situ at TH conditions (80 – 145 °C) and found that yield stress and apparent viscosity of sludge decreased linearly with increasing temperature, whereas at constant temperature the apparent viscosity, consistency index and yield stress decreased with a logarithmic relationship with time. It was also shown that the viscosity and yield stress of sludge during TH deviate by 40 - 80% with respect to the measurement at ambient temperature. Hence, in situ characterization is of interest as it offers the accurate sludge rheology in the real TH processes, potentially used for better process design. However, the study was limited to a single concentration of WAS, which did not consider the effect of using thicker sludges. Furthermore, there has been great interest for using more concentrated sludge during anaerobic digestion (Zhang et al., 2017) due to rheological

enhancements caused by TH (e.g. reducing sludge viscosity) (Morgan-Sagastume et al., 2011). The current study investigates the rheological behaviour in various concentrations of thickened WAS under elevated temperature conditions like those encountered during TH. It also presents correlations for the change of Herschel-Bulkley parameters with temperature and time and the extent of organic matter solubilization.

5.3 MATERIALS AND METHODS

5.3.1 WASTE ACTIVATED SLUDGE

Waste activated sludge (WAS) originated from Mount Martha wastewater treatment plant in Victoria, Australia, which was thickened by dissolved air flotation without polymer dosing. At the time of collection, the original solids concentration of the sludge was 3.5 wt%. The sludge was stored at 4 °C for 30 days before use, which was done to ensure minimal changes in sludge due to biological activity and help maintain the stability and consistency between samples during experimentation (Curvers et al., 2009). Sludge was thickened via centrifugation at 9000 rpm (13,700 G). Sludge samples consisting of different total solids concentration (TS) were prepared by diluting the centrifuge-thickened sludge using non-centrifuged sludge to achieve 7, 9, 12, and 13 wt% sludge. The TS of sludge was defined as the percentage mass of dried sludge over the mass of the original sludge. The mass of dried sludge was determined by drying the sludge samples to constant mass in an oven at 105 °C (APHA, 1992).

5.3.2 CHEMICAL ANALYSIS

The chemical oxygen demand in the soluble phase (sCOD) of the sludge samples was determined for the WAS samples. Sludge samples were centrifuged (13,700 G) for 20 minutes, then the centrate was collected and filtered through mixed cellulose ester membranes (0.45 µm pore size) via vacuum filtration. Chemical oxygen demand in the filtered sludge liquor was performed following the HACH procedure (COD high range plus reagents, DR6000 Spectrophotometer and DRB200 reactor). The COD measurements were performed in triplicate. The released COD content in the soluble phase due to TH was defined rsCOD according to Equation 4.1.

5.3.3 IN-SITU RHEOLOGICAL MEASUREMENT

Rheological measurements were performed using a pressure cell-equipped, stress-controlled rheometer, employing cup-and-bob geometry. Rotational tests were performed to generate flow curves following protocols that was established in Chapter 4.3.2. After sludge samples were introduced, nitrogen gas was used to purge air and pressurize the system to 5 bar prior to measurements. This ensures oxidation reactions and evaporation of samples does not occur during measurements. Prior to measurement, the samples were initially pre-sheared at 675 s-1 (maximum shear rate producible from the rheometer with pressure cell attachment) for 20 minutes followed by 2 minutes equilibration at rest to erase sample shear history. Flow curves were first generated at 25 °C for untreated samples, and then the samples were heated to the desired temperatures (80, 100, 120, 130 and 140 °C). The average heating time to reach target temperature was between 10 and 15 minutes. Temperature was held constant at target temperature for 60 minutes and flow curves were generated periodically at 5-minute intervals during this period. Pre-shearing was applied between generation of each flow curve (675 s-1 shearing for 2 min, followed by 1 min equilibration). Samples were then allowed to cool to 25 °C, and flow curve for treated sludge was generated. Flow curves were generated by applying a logarithmic sweep of decreasing shear rates (600 – 0.1 s-1) in 120 s. The raw outputs from the rheometer are published at (Hii and Eshtiaghi, 2017).

5.3.4 MASTER CURVE DEVELOPMENT

A master flow curve was generated to characterize the full range of sludge concentrations and experimental conditions investigated, as described in Chapter 4.4.1. The master curve was developed using a dimensionless form of the Herschel-Bulkley fluid model (Eq. 4.3). The flow curve for 12 wt% WAS at 80 °C measured during the first minute of TH was used as the reference curve. Herschel-Bulkley parameters for this curve were determined via least squares iterative calculation. In this study, only data corresponding to the shear rate range 10 – 600 s^{-1} was considered due to limited accuracy of the rheometer setup for measuring lower shear rates. For the reference curve, yield stress, σ_c = 81.33 Pa, consistency index, k = 19.97 Pa.s, and flow index, n = 0.4. Note, here σ_c is the dynamic yield stress of the sludge, measured in steady-shear flow; it was mathematically derived by fitting of flow curve data to the Herschel-Bulkley model. It is only representative of the true stress limit below which no steady state flow occurs (i.e. static yield stress). All the flow curves generated from the different experimental conditions were scaled until they superimposed onto the reference curve. This was achieved by dividing each set of

shear stress and shear rate values for each flow curve by a fixed value, referred to as the shift factors (Table A.5.1 – A.5.2). Along the y-axis (shear stress), the flow curves were scaled by a factor S_y, whereas along the x-axis (shear rate) they were scaled by a factor, S_x. The yield stress and consistency index for each flow curve were then determined using the shift factors and master curve parameters, which in this case is equivalent to the Herschel-Bulkley parameters previously calculated for the reference curve. This was achieved using equations 4.6 and 4.7.

5.4 RESULTS AND DISCUSSION

The flow curves for WAS measured in situ during TH are shown in Figure 5.1. The impact of treatment duration on the sludge flow behaviour are can be seen in Figure 5.1a which shows sludge flow curves at the beginning (1 min) and end (60 min) of TH. At constant temperature, the stress-response of the sludge decreased evidently after 60-minutes treatment. The extent of decrease was consistent despite varying sludge concentrations. Despite elevated temperatures (80 – 140 °C), WAS behaviour was best described by the Herschel Bulkley model (Eq. 4.2). Shear-thinning, yield stress behaviour was exhibited during the entirety of 1-hour TH. Newtonian behaviour was not observed at the end of the treatment period, contrary to some of the observations reported in literature (Feng et al., 2014b; Urrea et al., 2015). This may be due to the range of temperatures used in the current study being relatively low compared to the TH temperature conditions (160 – 200 °C) reported those studies. Higher sludge concentrations were also being used in the current study, which tends to increase non-Newtonian behaviour (Slatter, 1997). During TH, it is believed the elevated temperature conditions results in the destruction of floc structure and solubilization of organic matter, which is inferred from the increase in the soluble fraction of COD and other macromolecular components such as soluble proteins and polysaccharides (Hii et al., 2017; Wilson and Novak, 2009; Zhang et al., 2017). As seen in Figure 5.1b, there is distinct difference between the flow curves of 80 °C and 130 °C, at the same solid concentration. This solubilization destroys the structural integrity of the sludge and releases bound water (Neyens et al., 2004) which to contributes to the rheological changes observed. Then, Figure 5.1a affirms this solubilization effect is time dependent.

Since the general flow behaviour of the WAS during TH was similar across the experimental conditions studied, it was possible to develop a master curve (Figure 5.2) to describe the in-situ WAS flow behaviour across the wide range of sludge concentrations, temperature and treatment times investigated, as well as for untreated and treated sludge measured at 25 °C. Using the master curve, Herschel-Bulkley

parameters for WAS could be estimated for any TH conditions and sludge concentrations within the range of conditions studied.

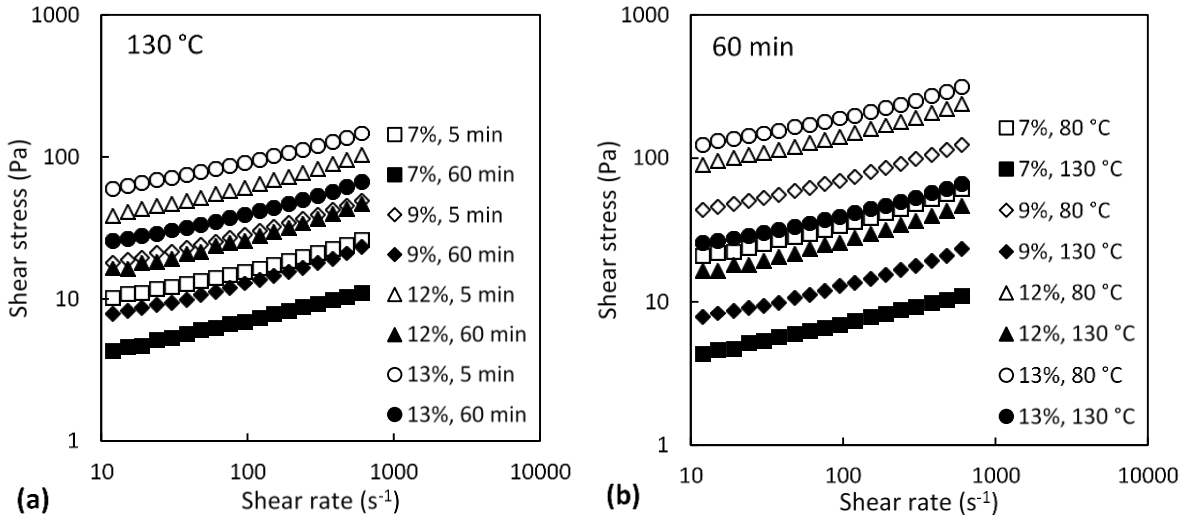

Figure 5. 1 – a) In-situ flow curves of 7 - 13 wt% WAS at 130 °C measured at beginning and end of 60-minutes TH, and b) Impact of TH temperature on in-situ flow curves of 7 - 13 wt%, at treatment time of 60 min.

In this case it is considered that the flow index, n = 0.4 since it was observed that all the flow curves obtained adequately follows the same curvature in the master curve. The validity of the calculated Herschel-Bulkley parameters obtained from Equations 4.6 and 4.7 was assessed by goodness of fit using a Chi-Square test ($\alpha = 0.05$). The shear stress values obtained experimentally were compared against those estimated using the calculated Herschel-Bulkley parameters. There was no significance in difference between the experimental data and estimated values. This means that the Herschel-Bulkley parameters derived from the master curve could accurately describe the experimental results. Using the parameters derived from the master curve also allows the results to be better compared between the different samples due to normalization.

In order to study the impact of the TH parameters on the sludge rheological behaviour, the Herschel-Bulkley parameters: σ_c and k were derived using Equation 4.6 and 4.7 based on the Master curve (Fig. 5.2). Here, σ_c and k represent the dynamic yield stress and consistency index respectively. The evolution of

WAS viscosity during TH is shown in Figure 5.3. Here, $\eta_{\infty,i}$ is the apparent viscosity of sludge measured in situ at shear rate of 600 s^{-1} (maximum shear rate limit of the pressure cell). Since sludge exhibited shear-thinning behaviour, it was important to compare only the non-shear rate dependent viscosity values between different sludge samples. At 600 s^{-1}, the apparent viscosity approaches a plateauing value and is reasonably assumed to approximate the infinite shear viscosity (i.e. limiting viscosity at infinite shear rate). At constant temperature, $\eta_{\infty,i}$ decreased rapidly initially (10 – 15 minutes) then gradually plateauing towards the end of the treatment period. This trend was best described as a logarithmic decrease, similar to previously shown for 7% WAS (Chapter 4.4.1). Notably, the same curve trends were observed for all sludge concentrations studied. This is seen clearer in Figure 5.3 (inset), showing the normalized apparent viscosity ($\eta_{\infty,i}/\eta_{\infty,0}$) for different concentrations (7 – 13%). The same observation was also valid for the Herschel-Bulkley parameters k and σ_c (not shown). A Chi-square test was performed on $\eta_{\infty,i}/\eta_{\infty,0}$, k_i/k_0, and $\sigma_{c,i}/\sigma_{c,0}$ at constant time and temperature, comparing between different sludge concentrations and it showed insignificant difference of the values between sludge concentrations ($\alpha = 0.05$, $p = 0.99$). This suggests the rate and extent of solubilization in the sludge was constant and independent of concentration. This is consistent with Imbierowicz and Chacuk (2012), who showed the kinetics of sludge solubilization are independent of concentration. Higher sludge concentrations only lead to higher internal friction, and hence greater shear stresses observed. Additional figures showing the time-dependent evolution of the in-situ $\eta_{\infty,i}$, k_i, and $\sigma_{c,i}$ during TH at various temperatures and sludge concentrations are presented in supplementary Figures S.5.1 – S.5.3.

At constant treatment time, sludge rheological parameters were described by linear relationship with temperature. An Arrhenius-style relationship was considered unsuitable since it assumes constant activation energy, which would not be the case in time-dependent sludge thermal treatment (Baudez et al., 2013; Farno et al., 2014). As shown in Figure 5.4 (inset), $\eta_{\infty,i}$ of WAS decreased linearly at all studied concentrations; the same was also observed for k_i and $\sigma_{c,i}$ (refer to Supplementary Figure S.5.4). In fact, the impact of temperature on the extent of $\eta_{\infty,i}$, k_i, and $\sigma_{c,i}$ reduction were comparable for all studied concentrations, showing nearly constant curve slopes in Figure 5.4. This suggests sludge concentration did not control the extent of sludge solubilization. This was verified using a Chi-square test ($\alpha = 0.05$) to compare the decrease in $\eta_{\infty,i}/\eta_{\infty,0}$, k_i/k_0, and $\sigma_{c,i}/\sigma_{c,0}$ as a function of temperature between different sludge concentrations, showing insignificant variation ($p = 0.99$ across all comparisons). Comparison between the $\eta_{\infty,i}/\eta_{\infty,0}$, k_i/k_0, and $\sigma_{c,i}/\sigma_{c,0}$ at different sludge concentrations is shown in the appendix Tables A.5.4 – A.5.6 with standard deviation values.

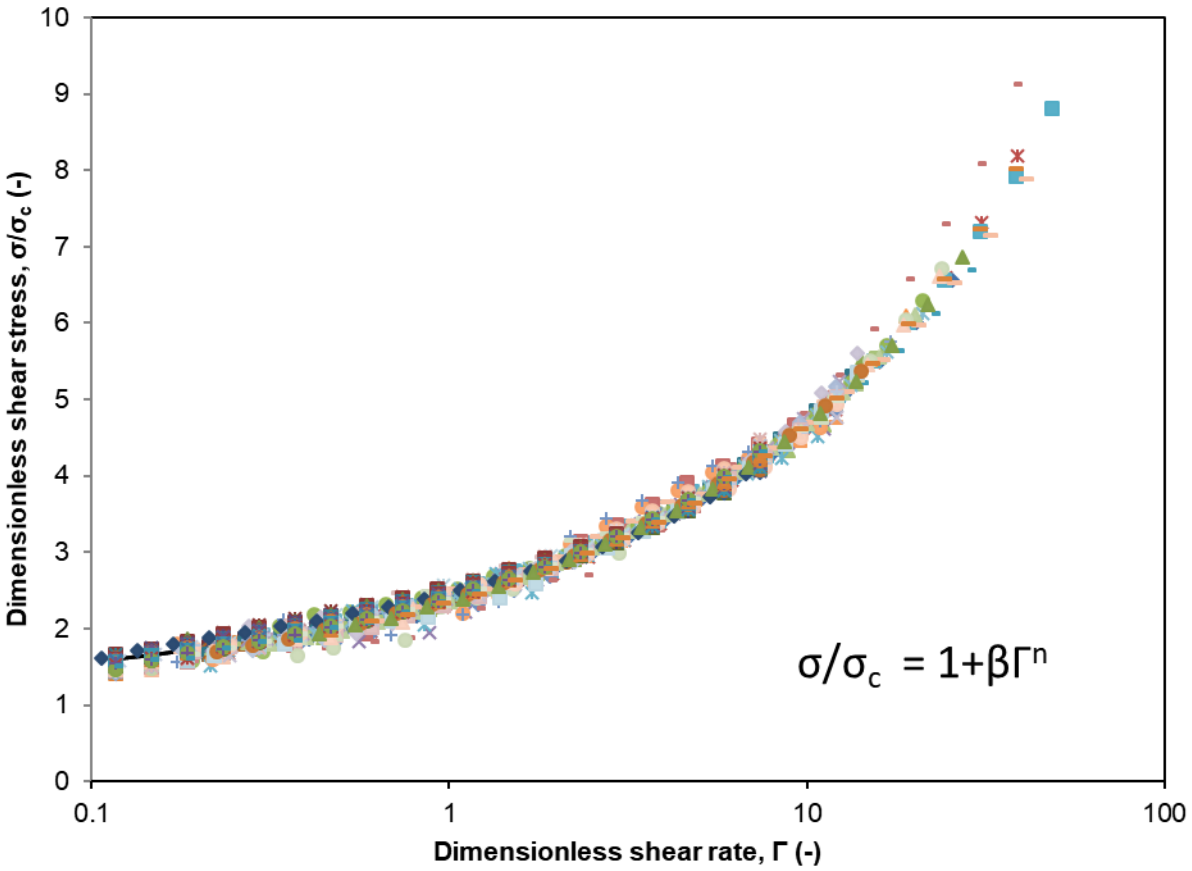

Figure 5. 2 – Master flow curve for WAS during thermal hydrolysis, depicting in-situ sludge flow behaviour at different concentrations (7, 9, 12, 13 wt%) and different temperatures (80, 100, 120, 130, 140 °C) measured at various times, as well as untreated and thermally-treated sludge at 25 °C. Master curve equation is $\sigma/\sigma_c = 1+\beta\Gamma^n$*; where* $\Gamma = (\eta/\sigma_c).\dot{\gamma}$ *and* $\beta = (k/\sigma_c).(\sigma_c/\eta)^n$*; k is the consistency index (Pa.s*^{n}*),* σ_c *is the yield stress (Pa),* $\dot{\gamma}$ *is the shear rate (s*$^{-1}$*), n is the flow index (-) and η is a measure of the apparent viscosity and equals 1 Pa.s. Master curve parameters are: k = 19.97 Pa.s*^{n}*,* σ_c *= 81.33 Pa, and n = 0.4 which yields the following equation:* $\sigma=81.33 +19.97\ \dot{\gamma}^{0.4}$ *.*

At constant temperature and treatment time, the increasing trends of $\eta_{\infty,i}$, k_i, and $\sigma_{c,i}$ with sludge concentration were described by power-law relationship. This is shown for the normalized $\eta_{\infty,i}$, and $\sigma_{c,i}$ in Figure 5.5. Additional figures showing this relationship for non-normalized values of $\eta_{\infty,i}$, k_i, and $\sigma_{c,I}$ are available in the supplementary material (Figure S.5.5) Before and after TH, total solids concentration of WAS was measured, verifying that it remained constant which was expected since only solubilization reactions were expected for TH conditions under nitrogen atmosphere (Hii et al., 2014). Although Figure 5.5 only showed rheological data measured at 60 minutes, the same power-law relationship was observed at any time during TH. Furthermore, this relationship was also true for untreated sludge and thermally-

treated sludge measured at room temperature as well (Figure S.5.6). This is consistent with the power-law relationship observed for ambient WAS reported in literature (Forster, 2002; Lotito et al., 1997; Markis et al., 2014; Sanin, 2002; Tixier et al., 2003). This means the impact of increasing sludge concentration on its rheology are not diminished, despite elevated TH temperatures. It is suspected, with increasing sludge concentration, the fundamental actions governing the intensification of viscous forces (e.g. viscosity and yield stress) remain the same between untreated WAS at ambient conditions and WAS during TH at elevated temperatures. Here, it can be summarised that the role of TS on the sludge rheology remains unchanged during TH. As sludge solids content increased, the increasing strength of particle interactions lead to higher viscous forces (Markis et al., 2016).

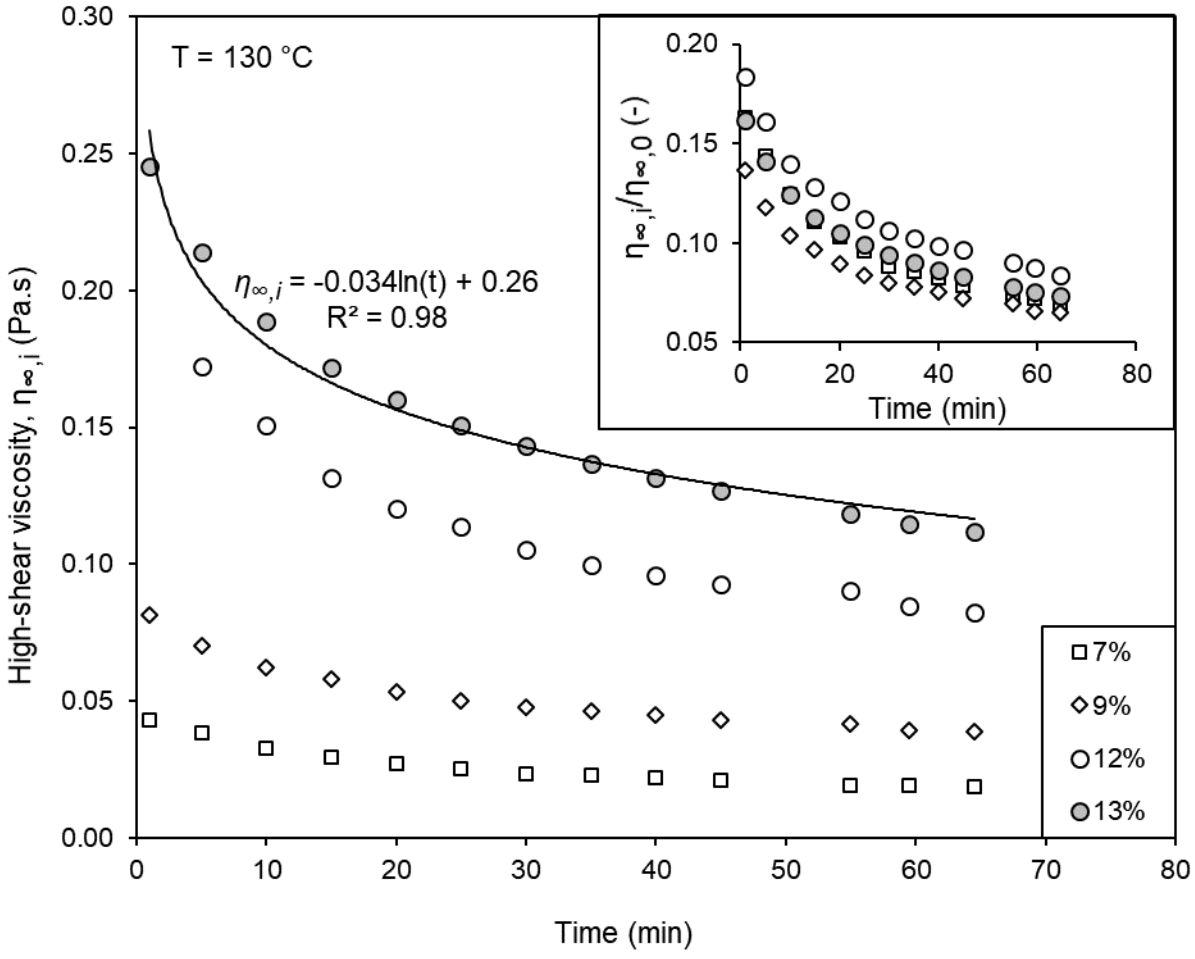

Figure 5. 3 – Time-dependent logarithmic reduction of the in-situ high-shear viscosity, $\eta_{\infty,i}$ (apparent viscosity measured at 600 s^{-1}) and normalized in-situ high-shear viscosity $\eta_{\infty,i}/\eta_{\infty,0}$ (inset) of 7 - 13 wt% WAS during TH at constant temperature (130 °C), where $\eta_{\infty,0}$ is the high-shear viscosity of the sample before TH (at 25 °C).

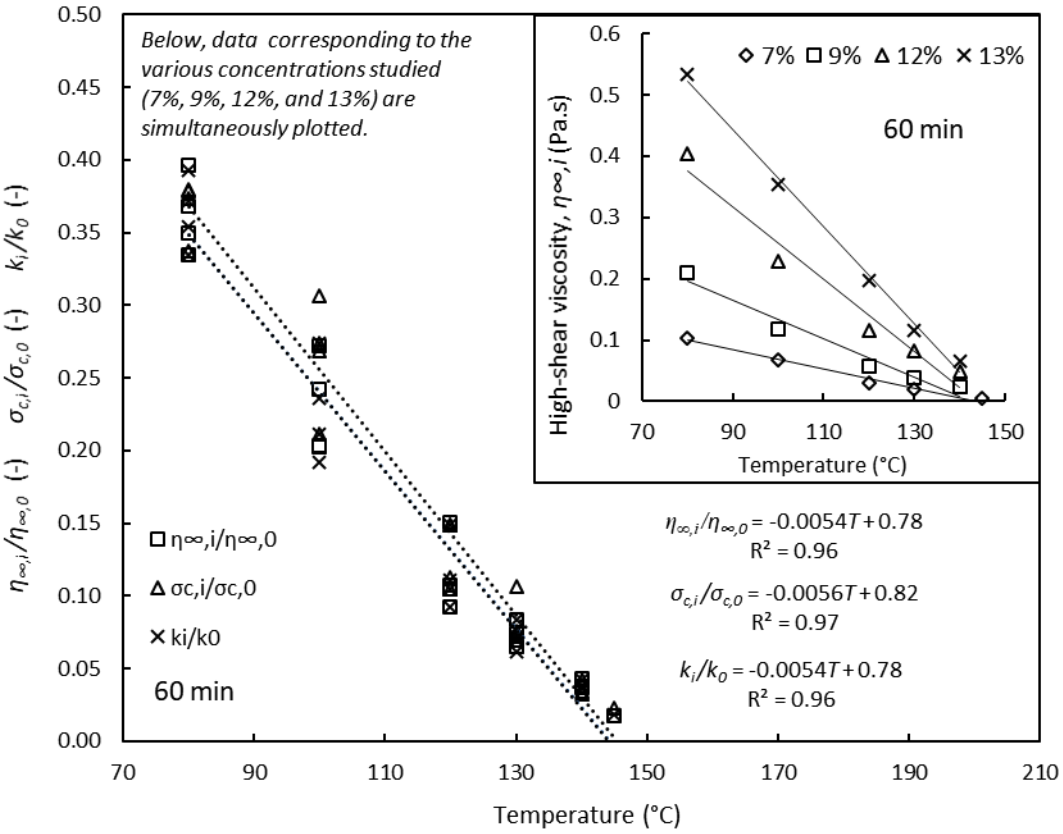

Figure 5. 4 – Linear decreasing relationship with temperature of normalized high-shear viscosity, normalized yield stress, and normalized consistency index at fixed treatment time (60 min) for all studied sludge concentrations (7 – 13 wt%); $\eta_{\infty,i}$, $\sigma_{c,i}$, and k_i correspond to the high-shear viscosity, yield stress and consistency index of samples, respectively, measured in situ at fixed treatment time (60 min); $\eta_{\infty,0}$, $\sigma_{c,0}$, and k_0 correspond to the high-shear viscosity, yield stress and consistency index of corresponding samples with the same solid concentration before TH (i.e. untreated samples). Inset compares the impact of temperature on the raw values of the in-situ high shear viscosity (at 60 minutes) between different sludge concentrations.

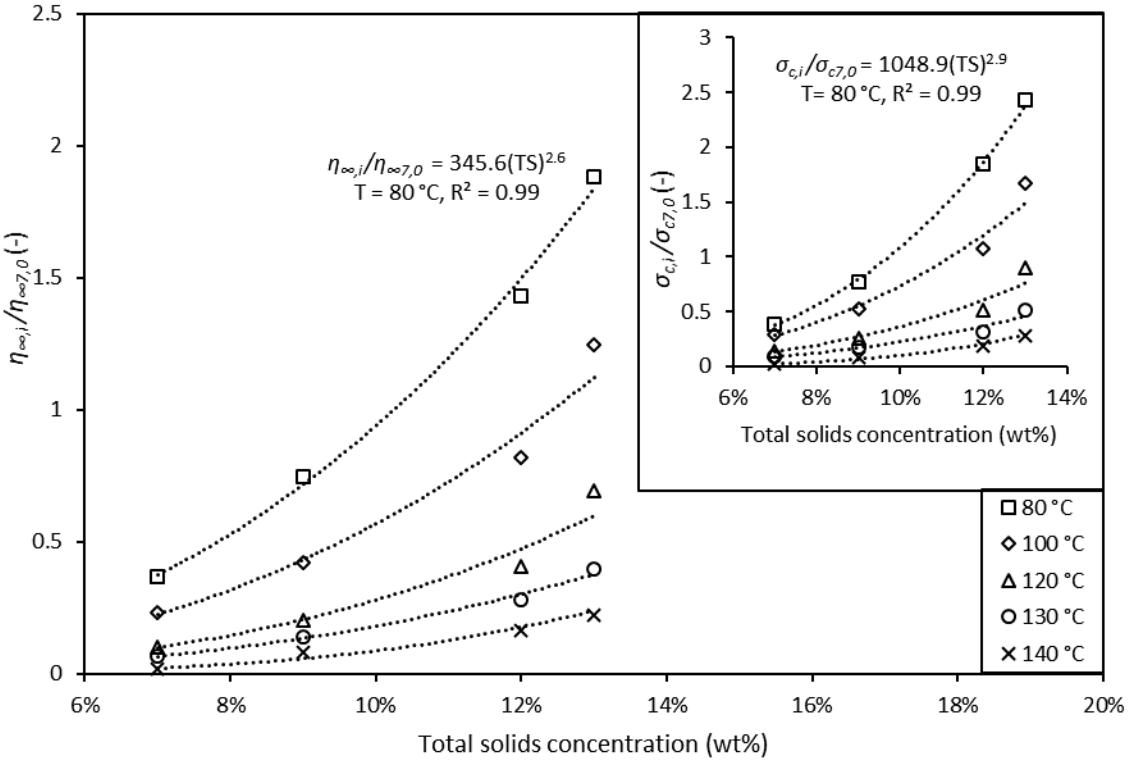

Figure 5. 5 – Impact of increasing total solids concentration of WAS (7 - 13 wt%) on normalized high-shear viscosity, and (inset) normalized yield stress, measured in situ, during TH at various temperatures and constant treatment time (60 min); $\eta_{\infty7,0}$ and $\sigma_{c7,0}$ are the high-shear viscosity and yield stress of untreated 7 wt% WAS, measured at 25 °C, respectively.

The in-situ values of $\eta_{\infty,i}$ (Pa.s), k_i (Pa.s^n) and $\sigma_{c,i}$ (Pa), at any temperature and time during 60-minute TH can be described as follows, considering the logarithmic time-dependent behaviour and linear relationship with temperature:

$$\eta_{\infty,i}/\eta_{\infty7,0} = -A_1(T) - B_1\ln(t) + C_1 \qquad (Eq.\,5.1)$$

$$k_i/k_{7,0} = -A_2(T) - B_2\ln(t) + C_2 \qquad (\text{Eq. } 5.2)$$

$$\sigma_{c,i}/\sigma_{c7,0} = -A_3(T) - B_3\ln(t) + C_3 \qquad (\text{Eq. } 5.3)$$

Where T is the sludge temperature (°C), t is the treatment time (min); $\eta_{\infty7,0}$ is the high-shear viscosity of 7 wt% untreated WAS measured at 600 s^{-1}, at 25 °C; $k_{7,0}$ is the consistency index of 7 wt% untreated WAS at 25 °C; $\sigma_{c7,0}$ is the yield stress of 7 wt% untreated WAS at 25 °C; and $A_{1\text{-}3}$ *and* $B_{1\text{-}3}$ are fitting parameters and C_1, C_2, and C_3 are the $\eta_{\infty,i}/\eta_{\infty7,0}$, $k_i/k_{7,0}$, and $\sigma_{c,i}/\sigma_{c7,0}$, respectively, at time = 0 minutes (i.e. when sludge just

reaches treatment temperature). $A_{1\text{-}3}$, $B_{1\text{-}3}$, *and* $C_{1\text{-}3}$ can be related to the solids concentration of sludge using the following equation:

$$F(\varphi) = y \times \varphi^{z} \quad \text{(Eq. 5.4)}$$

Where *F(φ)* can represent any of the coefficients $A_{1\text{-}3}$, $B_{1\text{-}3}$, B_2, *and* $C_{1\text{-}3}$; φ is the solids concentration of sludge (wt/wt); *y* and *z* are power-law fitting parameters which can be taken from Table 5.1.

The coefficients $A_{1\text{-}3}$, $B_{1\text{-}3}$, B_2, *and* $C_{1\text{-}3}$ showed power-law relation with solids concentration. This is consistent with the power-law relationship for the Herschel-Bulkley parameters with sludge concentration observed in Figure 5.5. Equations 5.1 – 5.3 can be used to estimate in situ the apparent viscosity and Herschel-Bulkley parameters of WAS (7 – 13 wt%) during TH at different time of treatment based on untreated 7% WAS at 25°C. Regression statistics and correlation analysis of parameters are presented in Table A.5.3.

Table 5. 1 – Fitting Parameters of Eq. 5.4 for determining the coefficients of Eq.s 5.1 – 5.3

	A_1	A_2	A_3	B_1	B_2	B_3	C_1	C_2	C_3
y	6	5	18	40	50	73	1024	975	2710
z	2.6	2.6	3	2.8	2.8	3	2.6	2.6	3

The accuracy was higher in the range of 80 – 130 °C, with 4 – 12% mean percentage error (MAPE) of estimated values across this temperature range, but the accuracy decreased significantly at 140 °C. This is because at 140 °C, rheological changes were seemingly less time-dependent compared to the lower temperatures (80 – 130 °C). That is, rheological values plateaued much earlier. Therefore, the logarithmic coefficients in Equations 5.1 – 5.3 would underestimated at 140 °C. Zhang et al. (2017) have shown for low-temperature TH (<100 °C), treatment time was the dominant factor influencing sludge rheological behaviour, while the temperature was the dominant factor for high-temperature TH (>100 °C). Furthermore, Bougrier et al. (2008) suggested that a threshold temperature (150 °C) existed, whereby increasing TH temperatures beyond 150 °C would cause insignificant apparent viscosity reduction of sludge. As such, the rheological changes have likely approached a limit; the impact of raising treatment temperature to 140 °C was also diminished.

The variation between rheological measurements performed in situ and measurement performed at ambient conditions is evaluated in Table 5.2. Here, in-situ values were taken after 60 minutes treatment time (i.e. plateau values), whereas the ambient values were taken after the samples cooled to 25 °C. In all cases, in-situ values were 50 – 80% lower than respective ambient counterparts, depending on TH temperature. This means ambient rheological measurements of treated sludge may be scaled accordingly to represent in-situ values. Notably, the extent of reduction from ambient values to in-situ values remained relatively constant at varying sludge concentrations. For example, the in-situ high-shear viscosity of 7 – 13 wt% sludge at 100 °C was between 0.4 – 0.5 of ambient values. Equations 5.5 and 5.6 correlate the in-situ η_∞, and σ_c to ambient values. This allows quick estimation of in-situ rheological properties based on ambient measurements of TH sludge when on-line rheological measurements are not possible.

$$\eta_{\infty,i} = \eta_{\infty,f}(-0.0055\,T + 1) \quad ; \quad RMSE = 0.06 \qquad (Eq.\,5.5)$$

$$\sigma_{c,i} = \sigma_{c,f}(-0.0036\,T + 1) \quad ; \quad RMSE = 0.08 \qquad (Eq.\,5.6)$$

Where $\eta_{\infty,i}$ is the in-situ high-shear viscosity (Pa.s) of WAS at 60 minutes treatment time; $\eta_{\infty,f}$ is the high-shear viscosity (Pa.s) of ambient WAS after thermal hydrolysis measured at 25 °C; $\sigma_{c,i}$ is the in situ yield stress (Pa), and $\sigma_{c,f}$ is the yield stress of thermally-treated WAS measured at 25 °C. Equation 5.5 can also be used to estimate the consistency index by replacing $\eta_{\infty,i}$ and $\eta_{\infty,f}$ with the in-situ consistency index, k_i, and the consistency index of thermally-treated WAS measured at 25 °C, k_f, respectively.

It has previously been shown for 7 wt% sludge that the reduction in rheological parameters had a linear correlation with an increase of sCOD content (Hii et al., 2017). This correlation was examined here for the higher sludge concentrations. The sCOD content of WAS (7, 9, 12 wt%) before and after 60–minute TH at various temperatures (80, 100, 120, 130, 140 °C) was measured. The extent of COD solubilisation (rsCOD) was correlated with the extent of rheological changes due to TH (Figure 5.6). Here, the rheological parameters were normalized whereby $\eta_{\infty,f}$, k_f and $\sigma_{c,f}$ of thermally treated sludge were divided by the corresponding untreated sludge values, $\eta_{\infty,0}$, k_0 and $\sigma_{c,0}$, at the same sludge concentration.

Linear correlation was observed between rsCOD and the rheological parameters. The apparent viscosity, consistency index, and yield stress decreased proportionally with the extent of sludge solubilization, regardless of sludge concentration and treatment temperature. This linear correlation indicates that the changes in sludge rheology due to TH are likely caused by modification in sludge structure resulting from

solubilization of sludge components and macromolecules (Bougrier et al., 2008). These structural modifications are related to solubilization of EPS, which are capable of binding large volumes of water (Neyens et al., 2004) and contributes to sludge structural integrity (Feng et al., 2016). The solubilization of EPS leads to a proportional increase in sCOD and flowability of the sludge. The yield stress represents the solid-like characteristics in WAS. Its reduction indicates a breakdown of the floc structure in WAS, which is reflected in the proportional solubilization in COD. Since the sludge concentration remained unchanged after TH it is reasonably concluded that the rheological changes in WAS due to TH are primarily contributed by changes in floc structure and composition of the sludge.

Table 5. 2 – *Ratio of rheological parameters of thermally-treated sludge measured in situ vs. at ambient conditions.*

	7 wt%	**9 wt%**	**12 wt%**	**13 wt%**
t = 60 minutes		$\eta_{\infty,i}/\eta_{\infty,f}$		
80 °C	0.52	0.54	0.61	0.62
100 °C	0.39	0.45	0.52	0.52
120 °C	0.23	0.33	0.43	0.52
130 °C	0.23	0.31	0.32	0.34
140 °C	0.18	0.25	0.27	0.26
t = 60 minutes		$\sigma_{c,i}/\sigma_{c,f}$		
80 °C	0.64	0.62	0.72	0.62
100 °C	0.60	0.64	0.60	0.54
120 °C	0.46	0.61	0.60	0.67
130 °C	0.49	0.46	0.53	0.56
140 °C	0.27	0.31	0.55	0.49

$\eta_{\infty,i}$ and $\sigma_{c,i}$ are the high-shear viscosity and yield stress, respectively, of sludge measured in-situ at various temperatures and constant time (60 minutes); $\eta_{\infty,f}$ and $\sigma_{c,f}$ is the high-shear viscosity and yield stress, respectively, of thermally-treated sludge after 60-minute TH, measured once the sample is cooled to ambient temperature (25 °C).

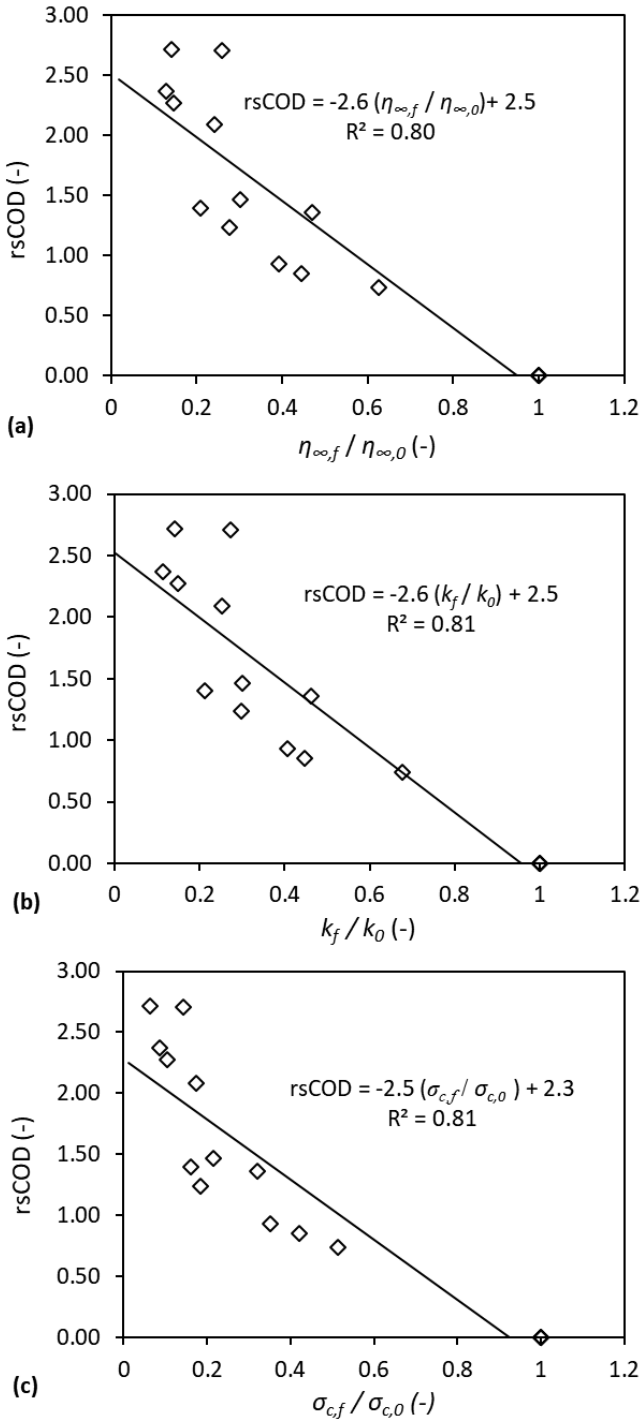

Figure 5. 6 – Linear proportionality between the increase in soluble COD in WAS and the reduction of WAS rheological parameters (7 – 12 wt%) after 60-minutes TH. Data corresponding to all treatment temperatures (80 – 140 °C) are simultaneously plotted. Here, rsCOD is the released soluble COD; $\eta_{\infty,f}$, k_f and $\sigma_{c,f}$ are the high-shear viscosity, consistency index, and yield stress, respectively, of thermally-treated sludge at 25 °C; $\eta_{\infty,0}$, k_0 and $\sigma_{c,0}$ are the high-shear viscosity, consistency index, and yield stress, respectively, of untreated sludge at 25 °C.

5.5 CONCLUSION

The flow behaviour of various concentrations of WAS (7 – 13 wt%) was studied during TH at various temperatures (80 – 140 °C). At all treatment conditions, WAS exhibited shear-thinning behaviour at despite elevated TH temperatures. The flow behaviour of the sludge was best described by the Herschel-Bulkley model for untreated sludge, sludge during TH, and cooled, treated sludge. The impact of treatment temperature, duration of treatment, and sludge concentration on η_∞, k, and σ_c was described by linear, logarithmic, and power-law relationships, respectively. The power-law relationship between sludge concentration and rheological parameters was valid for untreated in-situ, and post-thermally treated sludge. Therefore, the impact of increasing sludge concentrations is not diminished during TH, despite the elevated treatment conditions. However, increasing sludge concentrations did not impact the extent of sludge solubilization since the extent of rheological changes due TH were largely constant across the different sludge concentrations. This means the actions governing the intensification of viscous forces due to increasing sludge concentrations is unchanged at elevated TH conditions. Then, reduction of these forces due to TH is primarily a result of solubilization of the structural components in sludge (e.g. sludge flocs and EPS). This is indicated by the linear correlation between the reduction of rheological parameters and increase in soluble COD content of sludge, suggesting rheological changes due to TH were primarily a result of sludge solubilization.

APPENDIX

Table A.5. 1 – *Shift factors in the Y-axis, Sy, for the master curve in Figure 5.2.*

	80 °C				100 °C				120 °C				130 °C				140 °C			
Time (min)	7 wt%	9 wt%	12 wt%	13 wt%	7 wt%	9 wt%	12 wt%	13 wt%	7 wt%	9 wt%	12 wt%	13 wt%	7 wt%	9 wt%	12 wt%	13 wt%	7 wt%	9 wt%	12 wt%	13 wt%
Shift factor in Y-axis, Sy																				
Untreated*	0.38	0.79	2.07	2.43	0.36	0.74	1.93	2.30	0.36	0.86	1.85	2.29	0.31	0.86	1.61	2.69	0.35	0.96	2.08	2.56
1	0.18	0.42	1.00	1.29	0.17	0.31	0.62	1.03	0.10	0.19	0.39	0.57	0.08	0.14	0.30	0.44	0.04	0.09	0.23	0.34
5	0.17	0.40	0.93	1.21	0.16	0.28	0.55	0.91	0.09	0.16	0.32	0.50	0.07	0.12	0.26	0.38	0.03	0.08	0.19	0.28
10	0.16	0.37	0.86	1.11	0.14	0.26	0.49	0.79	0.08	0.15	0.29	0.45	0.06	0.11	0.23	0.34	0.03	0.07	0.16	0.23
15	0.16	0.36	0.81	1.07	0.13	0.24	0.48	0.74	0.07	0.13	0.27	0.43	0.05	0.10	0.21	0.30	0.02	0.06	0.15	0.20
20	0.16	0.34	0.79	1.04	0.13	0.23	0.46	0.73	0.07	0.13	0.25	0.41	0.05	0.09	0.20	0.28	0.02	0.05	0.13	0.18
25	0.15	0.33	0.77	1.05	0.13	0.22	0.45	0.72	0.07	0.12	0.23	0.41	0.04	0.09	0.18	0.26	0.02	0.05	0.12	0.17
30	0.15	0.33	0.75	1.03	0.12	0.22	0.44	0.70	0.06	0.11	0.22	0.40	0.04	0.08	0.17	0.25	0.02	0.05	0.11	0.16
35	0.15	0.32	0.74	1.01	0.12	0.22	0.43	0.69	0.06	0.11	0.21	0.39	0.04	0.08	0.16	0.24	0.01	0.04	0.09	0.15
40	0.15	0.32	0.73	0.99	0.12	0.21	0.41	0.69	0.06	0.11	0.20	0.38	0.04	0.08	0.16	0.23	0.01	0.04	0.09	0.13
45	0.15	0.32	0.72	0.97	0.11	0.21	0.41	0.67	0.06	0.10	0.21	0.37	0.04	0.08	0.14	0.22	0.01	0.04	0.09	0.13
55	0.15	0.31	0.72	0.95	0.11	0.20	0.41	0.65	0.05	0.10	0.20	0.36	0.03	0.07	0.14	0.20	0.01	0.04	0.08	0.12
60	0.15	0.30	0.71	0.94	0.11	0.20	0.41	0.63	0.05	0.10	0.19	0.35	0.03	0.07	0.12	0.20	0.01	0.03	0.08	0.11
65	0.14	0.29	0.70	0.92	0.11	0.20	0.41	0.63	0.05	0.10	0.19	0.34	0.03	0.06	0.12	0.19	0.01	0.03	0.07	0.11
Treated**	0.23	0.47	0.97	1.48	0.18	0.31	0.68	1.16	0.11	0.16	0.32	0.51	0.07	0.14	0.23	0.35	0.03	0.10	0.13	0.22

Values of yield stress, σ_c (Pa), and consistency index, k (Pa), derived from above shift factors carry a relative standard deviation of 1 – 9% based on inherent sample variability.

** "Untreated" sludge refers to the untreated sludge measured at 25 °C.*

*** "Treated" sludge refers to treated sludge measured at 25 °C.*

Table A.5. 2 – Shift factors in the X-axis, Sx, for the master curve in Figure 5.2.

	80 °C				100 °C				120 °C				130 °C				140 °C			
Time (min)	7 wt%	9 wt%	12 wt%	13 wt%	7 wt%	9 wt%	12 wt%	13 wt%	7 wt%	9 wt%	12 wt%	13 wt%	7 wt%	9 wt%	12 wt%	13 wt%	7 wt%	9 wt%	12 wt%	13 wt%
Shift factor in X-axis, Sx																				
Untreated*	0.52	0.47	0.98	1.09	0.52	0.43	1.00	1.00	0.48	0.60	1	1	0.35	0.61	1	1	0.39	0.78	1	1
1	0.55	0.62	1	1	1	1	1	1	1	1	1	1	1	1	1	1	0.61	0.66	1	1
5	0.55	0.62	1	1	1	1	1	1	1	1	1	1	1	1	1	1	0.61	0.66	1	1
10	0.55	0.62	1	1	1	1	1	1	1	1	1	1	1	1	1	1	0.61	0.66	1	1
15	0.55	0.62	1	1	1	1	1	1	1	1	1	1	1	1	1	1	0.61	0.61	1	1
20	0.55	0.62	1	1	1	1	1	1	1	1	1	1	1	1	1	1	0.61	0.61	1	1
25	0.55	0.62	1	1	1	1	1	1	1	1	1	1	1	1	1	1	0.61	0.61	1	1
30	0.55	0.62	1	1	1	1	1	1	1	1	1	1	1	1	1	1	0.61	0.61	1	1
35	0.55	0.62	1	1	1	1	1	1	1	1	1	1	1	1	1	1	0.63	0.61	0.70	1
40	0.55	0.62	1	1	1	1	1	1	1	1	1	1	1	1	1	1	0.66	0.61	0.64	1
45	0.55	0.62	1	1	1	1	1	1	1	1	1	1	1	1	0.78	1	0.66	0.53	0.69	1
55	0.55	0.62	1	1	1	1	1	1	1	1	0.89	1.00	1	1	0.79	1	0.69	0.53	0.74	1
60	0.55	0.54	1	1	1	1	1	1	1	1	1	1	1	1	0.73	1	0.68	0.53	0.78	1
65	0.55	0.54	1	1	1	1	1	1	1	1	1	1	1	1	0.77	1	0.68	0.53	0.77	1
Treated**	0.29	0.35	0.61	1.00	0.26	0.37	0.70	1.00	0.19	0.18	0.39	0.52	0.15	0.31	0.20	0.27	0.19	0.32	0.13	0.19

Values of yield stress, σ_c (Pa), and consistency index, k (Pa), derived from above shift factors carry a relative standard deviation of 1 – 9% based on inherent sample variability.

** "Untreated" sludge refers to the untreated sludge measured at 25 °C.*

*** "Treated" sludge refers to treated sludge measured at 25 °C.*

Table A.5. 3 – Regression p, R^2 values and correlation analysis results between dependent variables and independent variables (temperature and time) of equations 5.1 – 5.3.

		7 wt%	9 wt%	12 wt%	13 wt%
$\eta_{\infty,i}/\eta_{\infty 7,0}$			**p-values**		
	A_1	1.9E-55	6.2E-45	1.1E-42	6.7E-64
	B_1	2.7E-18	3.3E-12	2.5E-12	1.7E-28
	C_1	6.8E-61	2.3E-50	1.8E-48	2.4E-70
			R^2		
		0.98	0.96	0.96	0.96
			Pearson's coefficient*, r		
	T	-0.97	-0.96	-0.95	-0.97
	Ln(t)	-0.21	-0.21	-0.23	-0.24
$k_i/k_{7,0}$			**p-values**		
	A_2	3.5E-65	4.7E-42	5.7E-44	7.4E-64
	B_2	1.6E-25	2.8E-10	5.2E-13	4.6E-29
	C_2	1.9E-70	3.4E-47	1.3E-49	3.2E-70
			R^2		
		0.99	0.95	0.96	0.99
			Pearson's coefficient*, r		
	T	-0.97	-0.95	-0.95	-0.96
	Ln(t)	-0.20	-0.21	-0.23	-0.25
$\sigma_{c,i}/\sigma_{c7,0}$			**p-values**		
	A_3	1.1E-54	1.4E-61	5.7E-45	1.8E-64
	B_3	7.1E-21	1.5E-26	5.3E-14	1.1E-29
	C_3	5.4E-60	8.6E-68	1E-50	6E-71
			R^2		
		0.98	0.99	0.96	0.99
			Pearson's coefficient*, r		
	T	-0.96	-0.96	-0.95	-0.96
	Ln(t)	-0.18	-0.24	-0.24	-0.25

**Degrees of freedom = 63*

Table A.5. 4 – Normalized in-situ yield stress at different times and temperature of TH.

	$\sigma_{c,i}/\sigma_{c,0}$					
Time (min)	Temperature (°C)	7 wt%	9 wt%	12 wt%	13 wt%	Standard Deviation
1	80 °C	0.467	0.531	0.483	0.531	0.033
4		0.449	0.503	0.448	0.498	0.030
9		0.430	0.474	0.414	0.458	0.027
14		0.417	0.452	0.390	0.441	0.028
19		0.412	0.434	0.384	0.426	0.022
29		0.398	0.415	0.363	0.423	0.027
39		0.388	0.405	0.354	0.407	0.025
54		0.388	0.399	0.346	0.391	0.024
60		0.383	0.381	0.342	0.386	0.021
Cooled	25 °C	0.594	0.597	0.470	0.609	0.066
1	100 °C	0.462	0.413	0.319	0.448	0.064
4		0.435	0.374	0.283	0.396	0.064
9		0.393	0.347	0.252	0.343	0.059
14		0.368	0.323	0.247	0.322	0.050
19		0.357	0.312	0.240	0.317	0.048
29		0.340	0.298	0.230	0.304	0.046
39		0.329	0.285	0.214	0.299	0.049
54		0.318	0.272	0.213	0.284	0.044
60		0.318	0.269	0.212	0.275	0.043
Cooled	25 °C	0.513	0.421	0.352	0.503	0.076
1	120 °C	0.280	0.220	0.208	0.249	0.032
4		0.249	0.190	0.175	0.220	0.033
9		0.227	0.169	0.155	0.198	0.032
14		0.207	0.156	0.144	0.186	0.029
19		0.199	0.147	0.133	0.179	0.030
29		0.179	0.132	0.117	0.172	0.030
39		0.165	0.123	0.109	0.164	0.029
54		0.148	0.115	0.105	0.158	0.025
60		0.148	0.114	0.104	0.152	0.024
Cooled	25 °C	0.319	0.184	0.173	0.223	0.067
1	130 °C	0.248	0.164	0.187	0.163	0.040
4		0.215	0.139	0.162	0.142	0.035
9		0.190	0.124	0.141	0.125	0.031
14		0.167	0.116	0.129	0.113	0.025
19		0.154	0.104	0.121	0.104	0.024
29		0.135	0.096	0.106	0.093	0.019
39		0.125	0.092	0.099	0.084	0.018
54		0.109	0.084	0.084	0.076	0.015
60		0.109	0.077	0.077	0.074	0.017
Cooled	25 °C	0.215	0.161	0.143	0.130	0.038
1	140 °C	0.108	0.096	0.108	0.132	0.015
4		0.088	0.081	0.091	0.109	0.012
9		0.071	0.069	0.078	0.091	0.010
14		0.063	0.058	0.070	0.079	0.009
19		0.054	0.056	0.062	0.071	0.008
29		0.046	0.048	0.053	0.061	0.007
39		0.040	0.043	0.042	0.052	0.006
54		0.031	0.039	0.037	0.045	0.006
60		0.026	0.032	0.037	0.043	0.007
Cooled	25 °C	0.085	0.104	0.063	0.086	0.017

Table A.5. 5 – Normalized in-situ consistency index at different times and temperatures of TH.

	k_i/k_0					
Time (min)	Temperature (°C)	7 wt%	9 wt%	12 wt%	13 wt%	Standard Deviation
1	80 °C	0.457	0.477	0.479	0.550	0.041
4		0.439	0.452	0.444	0.516	0.036
9		0.421	0.426	0.411	0.475	0.029
14		0.408	0.406	0.387	0.457	0.030
19		0.403	0.390	0.380	0.442	0.027
29		0.390	0.373	0.360	0.438	0.034
39		0.380	0.364	0.351	0.422	0.031
54		0.380	0.358	0.344	0.406	0.027
60		0.374	0.361	0.339	0.400	0.025
Cooled	25 °C	0.751	0.674	0.568	0.631	0.077
1	100 °C	0.356	0.294	0.319	0.448	0.067
4		0.335	0.267	0.283	0.396	0.058
9		0.303	0.247	0.252	0.343	0.046
14		0.283	0.230	0.247	0.322	0.041
19		0.275	0.222	0.240	0.317	0.042
29		0.262	0.213	0.230	0.304	0.040
39		0.253	0.203	0.214	0.299	0.043
54		0.245	0.194	0.213	0.284	0.039
60		0.245	0.192	0.212	0.275	0.037
Cooled	25 °C	0.677	0.447	0.406	0.503	0.119
1	120 °C	0.209	0.179	0.208	0.249	0.029
4		0.186	0.155	0.175	0.220	0.027
9		0.169	0.138	0.155	0.198	0.026
14		0.155	0.127	0.144	0.186	0.025
19		0.148	0.120	0.133	0.179	0.026
29		0.134	0.107	0.117	0.172	0.029
39		0.123	0.101	0.109	0.164	0.028
54		0.111	0.094	0.110	0.158	0.028
60		0.111	0.093	0.104	0.152	0.026
Cooled	25 °C	0.463	0.298	0.252	0.289	0.094
1	130 °C	0.163	0.135	0.187	0.163	0.021
4		0.142	0.115	0.162	0.142	0.020
9		0.125	0.102	0.141	0.125	0.016
14		0.110	0.095	0.129	0.113	0.014
19		0.101	0.086	0.121	0.104	0.015
29		0.089	0.079	0.106	0.093	0.011
39		0.082	0.076	0.099	0.084	0.010
54		0.072	0.069	0.092	0.076	0.010
60		0.072	0.064	0.088	0.074	0.010
Cooled	25 °C	0.301	0.212	0.272	0.219	0.043
1	140 °C	0.090	0.102	0.108	0.132	0.017
4		0.074	0.087	0.091	0.109	0.014
9		0.059	0.073	0.078	0.091	0.013
14		0.052	0.064	0.070	0.079	0.011
19		0.045	0.062	0.062	0.071	0.011
29		0.038	0.053	0.053	0.061	0.010
39		0.032	0.047	0.050	0.052	0.009
54		0.025	0.045	0.042	0.045	0.010
60		0.021	0.038	0.040	0.043	0.010
Cooled	25 °C	0.113	0.149	0.140	0.166	0.022

Table A.5.6 – Normalized in-situ high-shear viscosity (measured at 600 s^{-1}) at different times and temperatures of TH.

	$\eta_{\infty,i}/\eta_{\infty,0}$					
Time (min)	Temperature (°C)	7 wt%	9 wt%	12 wt%	13 wt%	Standard Deviation
1	80 °C	0.459	0.484	0.479	0.537	0.033
4		0.435	0.451	0.442	0.504	0.032
9		0.416	0.421	0.412	0.473	0.029
14		0.406	0.405	0.391	0.449	0.025
19		0.398	0.390	0.378	0.443	0.028
29		0.386	0.374	0.362	0.437	0.033
39		0.379	0.364	0.349	0.421	0.031
54		0.375	0.357	0.342	0.410	0.029
60		0.372	0.353	0.337	0.402	0.028
Cooled	25 °C	0.715	0.652	0.548	0.637	0.069
1	100 °C	0.364	0.304	0.308	0.453	0.069
4		0.344	0.274	0.272	0.396	0.060
9		0.312	0.253	0.243	0.342	0.047
14		0.290	0.239	0.235	0.322	0.042
19		0.280	0.232	0.228	0.315	0.041
29		0.268	0.221	0.222	0.305	0.041
39		0.256	0.213	0.207	0.295	0.041
54		0.251	0.205	0.205	0.282	0.038
60		0.252	0.202	0.203	0.276	0.037
Cooled	25 °C	0.625	0.446	0.392	0.523	0.101
1	120 °C	0.215	0.180	0.201	0.247	0.028
4		0.187	0.156	0.172	0.219	0.027
9		0.166	0.139	0.153	0.198	0.025
14		0.153	0.128	0.141	0.185	0.024
19		0.146	0.121	0.132	0.179	0.025
29		0.132	0.109	0.118	0.172	0.028
39		0.125	0.102	0.110	0.165	0.028
54		0.111	0.095	0.109	0.158	0.027
60		0.111	0.094	0.106	0.153	0.026
Cooled	25 °C	0.471	0.277	0.242	0.288	0.103
1	130 °C	0.163	0.136	0.184	0.161	0.019
4		0.144	0.118	0.161	0.141	0.018
9		0.124	0.104	0.140	0.124	0.015
14		0.111	0.097	0.128	0.113	0.013
19		0.103	0.089	0.121	0.105	0.013
29		0.088	0.080	0.106	0.094	0.011
39		0.082	0.075	0.099	0.086	0.010
54		0.073	0.069	0.090	0.078	0.009
60		0.072	0.066	0.088	0.076	0.009
Cooled	25 °C	0.301	0.209	0.258	0.214	0.043
1	140 °C	0.088	0.102	0.108	0.130	0.017
4		0.071	0.086	0.092	0.110	0.016
9		0.057	0.073	0.078	0.092	0.014
14		0.050	0.063	0.070	0.081	0.013
19		0.044	0.060	0.063	0.073	0.012
29		0.036	0.052	0.054	0.062	0.011
39		0.031	0.047	0.049	0.054	0.010
54		0.023	0.043	0.041	0.047	0.011
60		0.020	0.039	0.040	0.045	0.011
Cooled	25 °C	0.128	0.147	0.141	0.165	0.015

SUPPLEMENTARY FIGURES

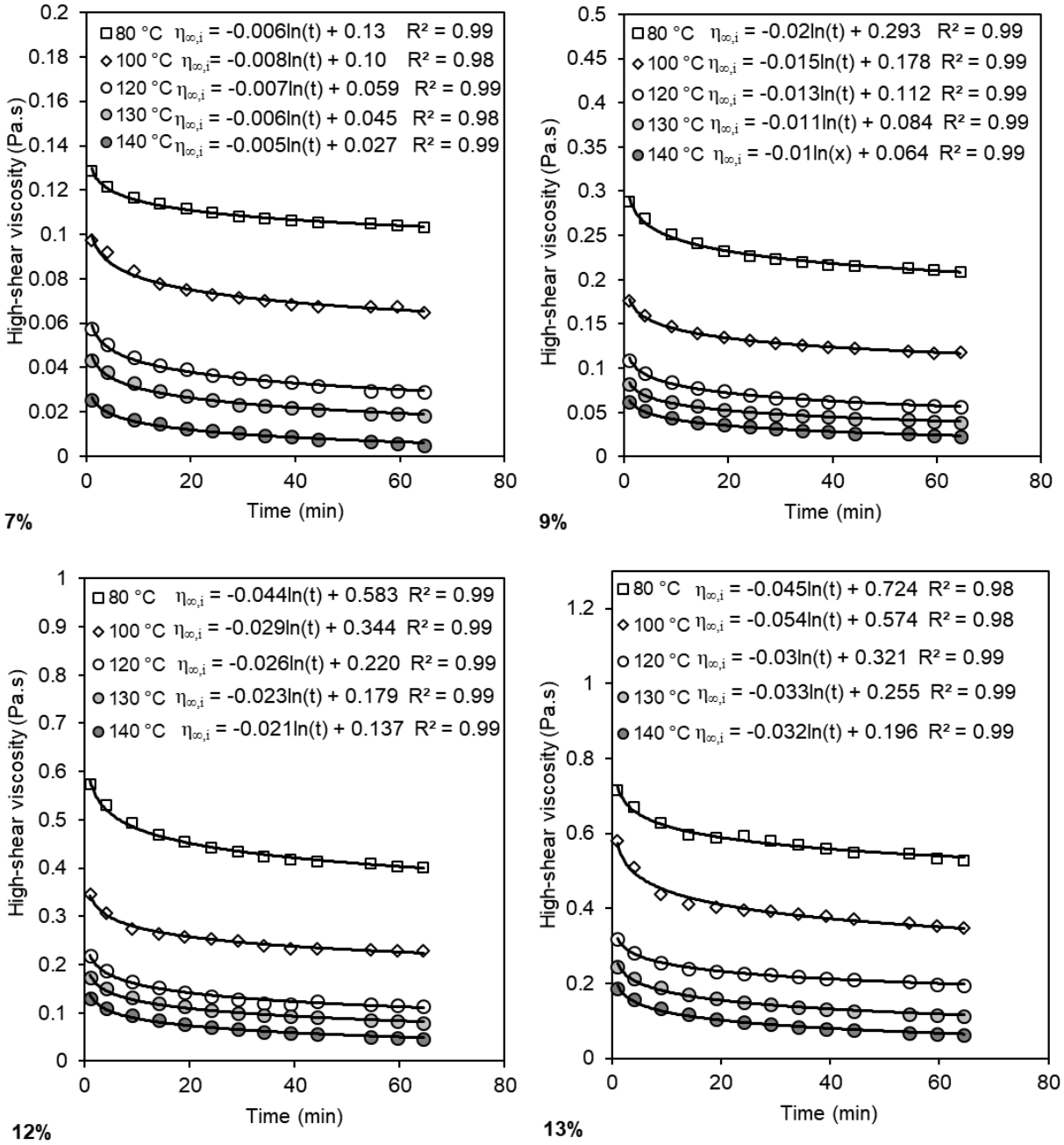

Figure S.5. 1 – Impact of treatment time on apparent viscosity (measured at 600 s^{-1}) of various concentrations (7-13 wt%) of WAS during TH at various temperatures (80-140°C).

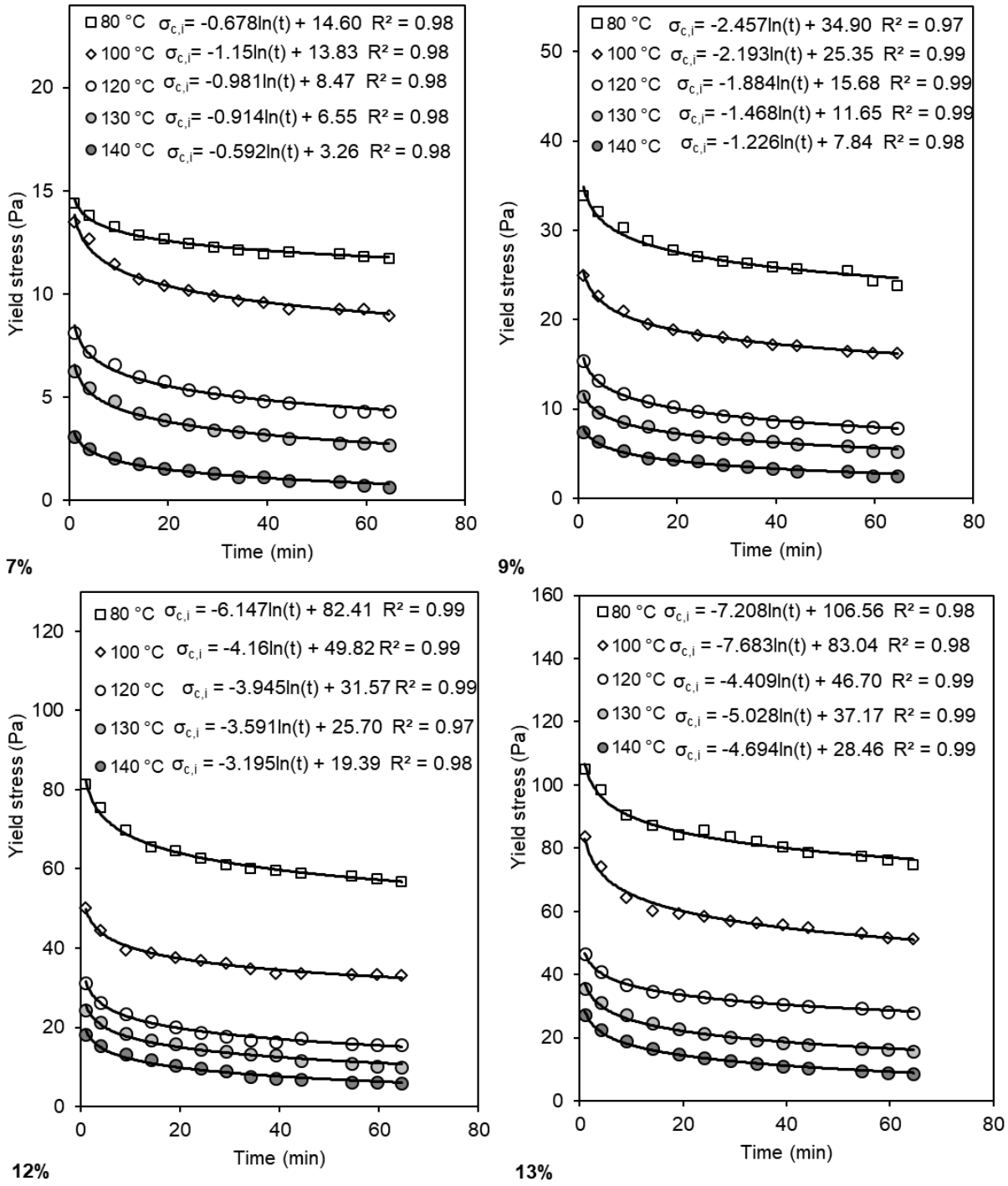

Figure S.5. 2 – Impact of treatment time on yield stress of WAS during TH at various solids concentrations (7-13 wt%) and treatment temperatures (80-140°C).

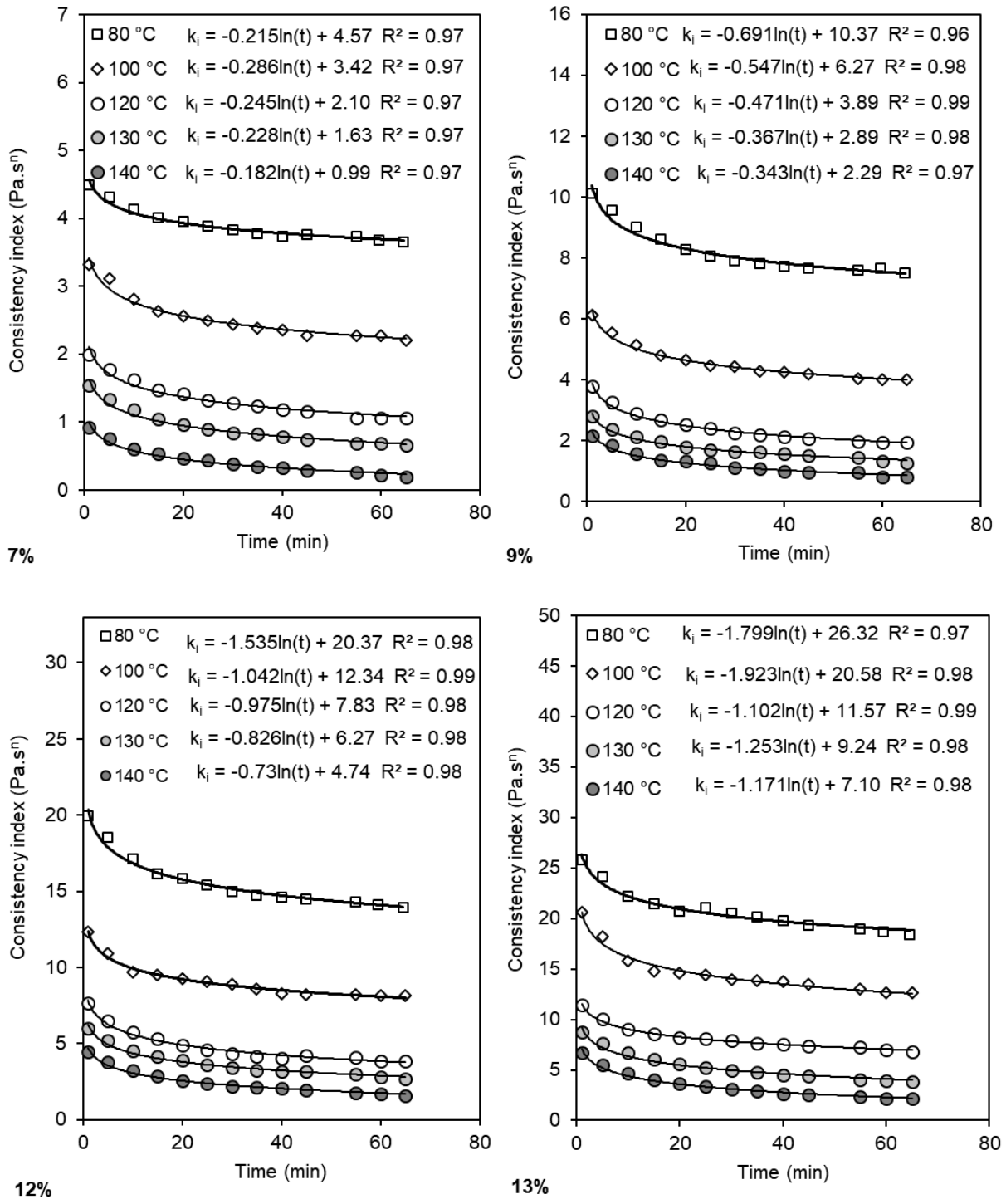

Figure S.5. 3 – Impact of treatment time on consistency index of WAS during TH at various solids concentrations (7 - 13 wt%) and treatment temperatures (80 - 140 °C).

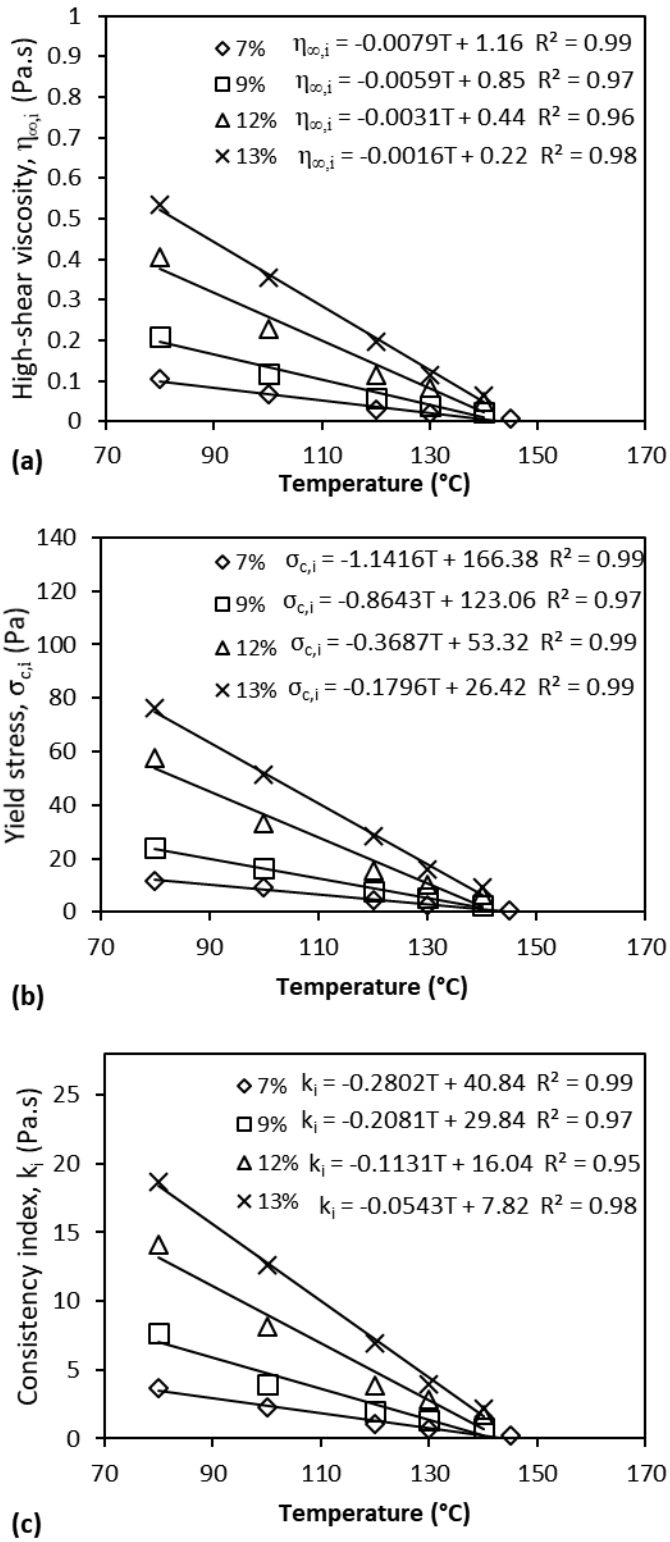

Figure S.5. 4 – Impact of temperature on in-situ (a) high shear viscosity, (b) yield stress, and (c) consistency index of 7 – 13 wt% WAS during TH at constant time (60 min).

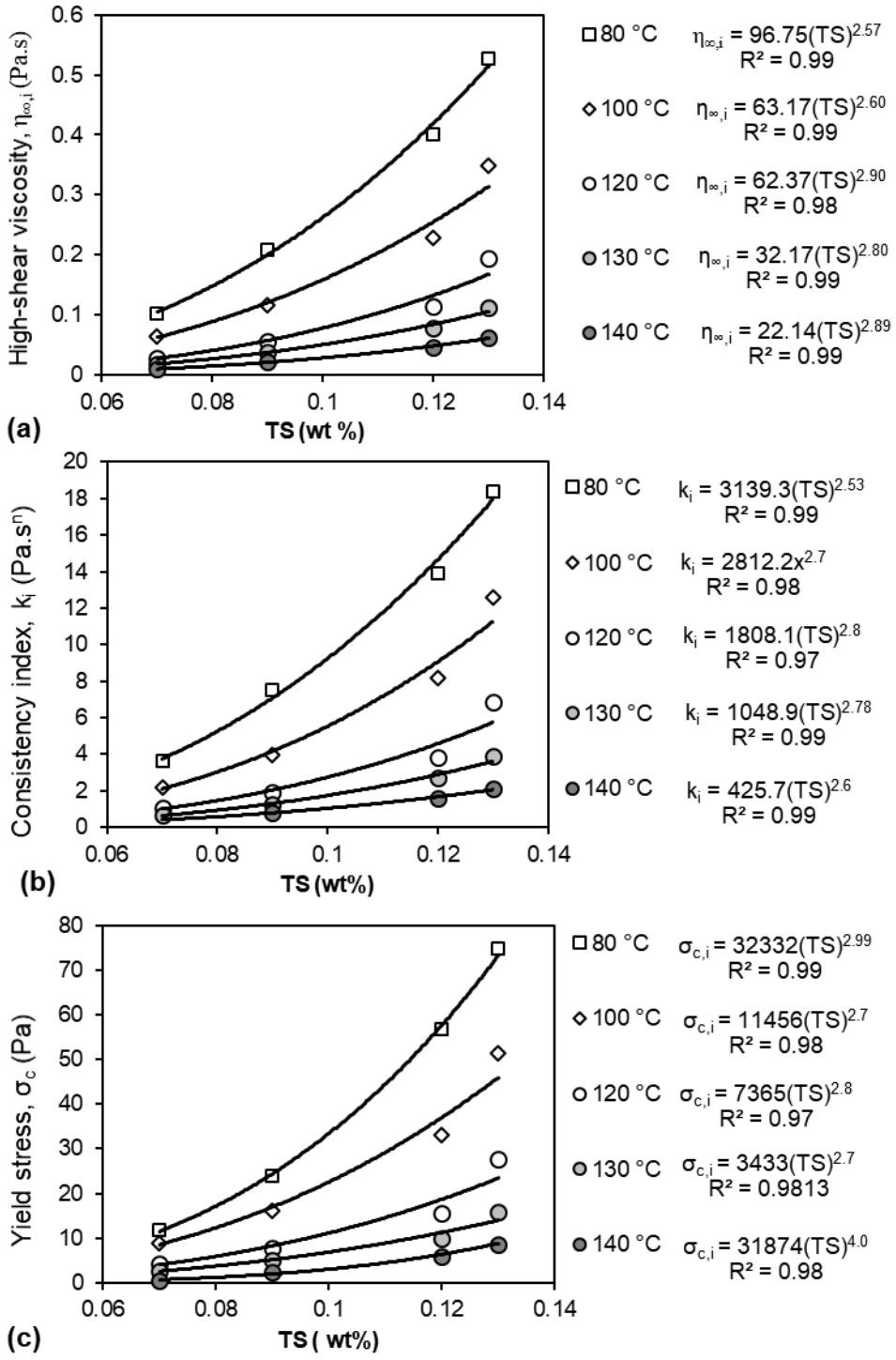

Figure S.5. 5 – Impact of increasing solids concentration of WAS (7 - 13 wt% TS) on the in-situ (a) high shear viscosity (b), consistency index (c), and yield stress during TH at constant time (60 min).

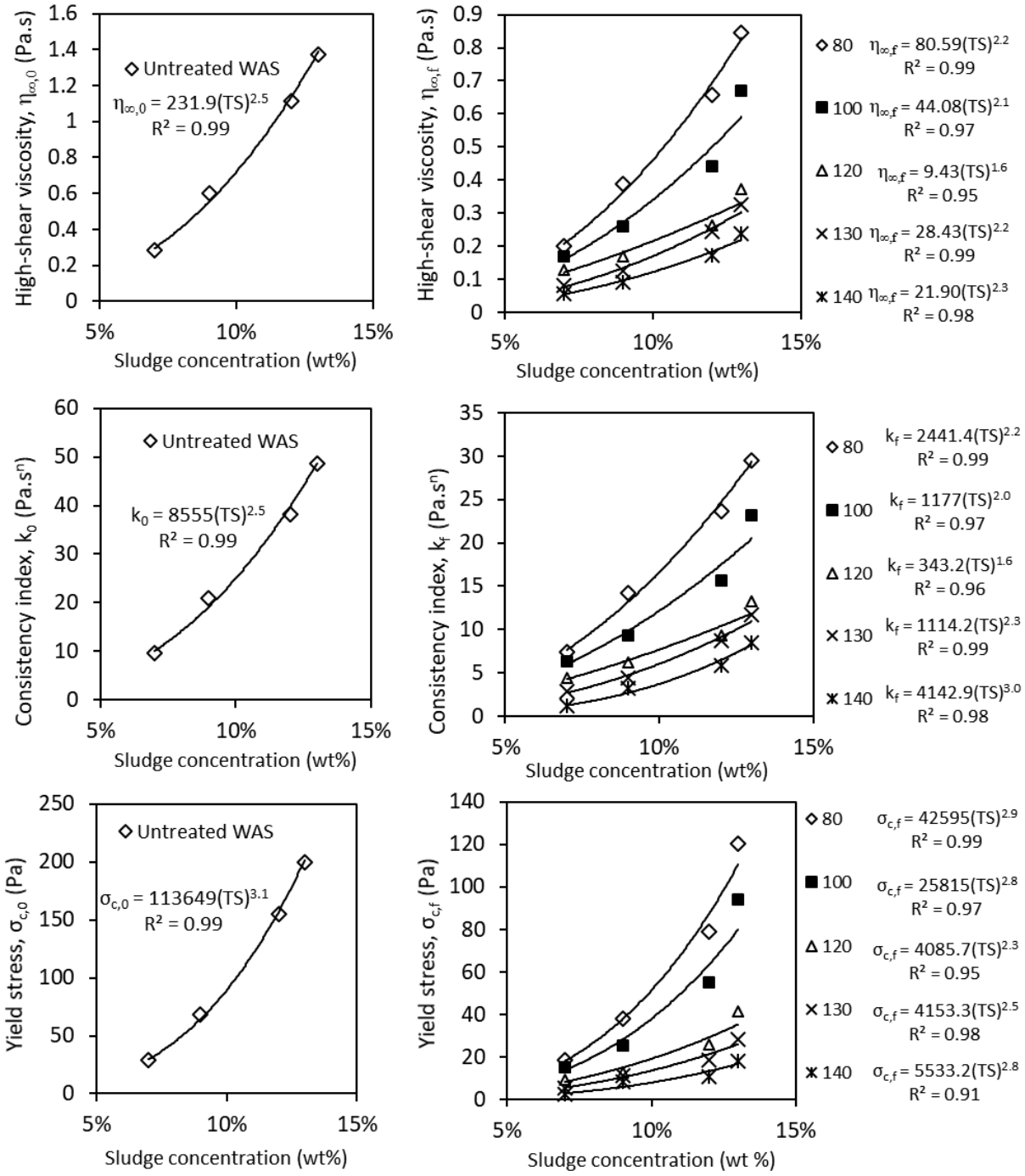

Figure S.5. 6 – Impact of solids concentration (wt%) on apparent viscosity, consistency and yield stress of untreated WAS at 25 °C and thermally-treated WAS at various temperatures (80 – 140 °C) after cooling down to 25 °C.

REFERENCES

APHA, 1992. Standard Methods for the Examination of Water and Wastewater.

Appels, L., Baeyens, J., Degrève, J., Dewil, R., 2008. Principles and potential of the anaerobic digestion of waste-activated sludge. Prog. Energy Combust. Sci. 34, 755–781. doi:10.1016/j.pecs.2008.06.002

Ariunbaatar, J., Panico, A., Esposito, G., Pirozzi, F., Lens, P.N.L., 2014. Pretreatment methods to enhance anaerobic digestion of organic solid waste. Appl. Energy 123, 143–156. doi:10.1016/j.apenergy.2014.02.035

Barber, W.P.F., 2016. Thermal hydrolysis for sewage treatment: A critical review. Water Res. 104, 53–71. doi:10.1016/j.watres.2016.07.069

Battistoni, P., Fava, G., Stanzini, C., Cecchi, F., Bassetti, A., 1993. Feed characteristics and digester operative conditions as parameters affecting the rheology of digested municipal solid wastes. Water Sci. Technol. 27, 37–45.

Baudez, J.C., Markis, F., Eshtiaghi, N., Slatter, P., 2011. The rheological behaviour of anaerobic digested sludge. Water Res. 45, 5675–5680. doi:http://dx.doi.org/10.1016/j.watres.2011.08.035

Baudez, J.C., Slatter, P., Eshtiaghi, N., 2013. The impact of temperature on the rheological behaviour of anaerobic digested sludge. Chem. Eng. J. 215–216, 182–187. doi:10.1016/j.cej.2012.10.099

Bougrier, C., Delgenès, J.P., Carrère, H., 2008. Effects of thermal treatments on five different waste activated sludge samples solubilisation, physical properties and anaerobic digestion. Chem. Eng. J. 139, 236–244. doi:10.1016/j.cej.2007.07.099

Curvers, D., Saveyn, H., Scales, P.J., Van der Meeren, P., 2009. A centrifugation method for the assessment of low pressure compressibility of particulate suspensions. Chem. Eng. J. 148, 405–413. doi:10.1016/j.cej.2008.09.030

Dote, Y., Yokoyama, S.-Y., Minowa, T., Masuta, T., Sato, K., Itoh, S., Suzuki, A., 1993. Thermochemical liquidization of dewatered sewage sludge. Biomass and Bioenergy 4, 243–248. doi:http://dx.doi.org/10.1016/0961-9534(93)90081-E

Eshtiaghi, N., Markis, F., Yap, S.D., Baudez, J.C., Slatter, P., 2013. Rheological characterisation of municipal sludge: A review. Water Res. 47, 5493–5510. doi:10.1016/j.watres.2013.07.001

Farno, E., Baudez, J.C., Parthasarathy, R., Eshtiaghi, N., 2014. Rheological characterisation of thermally-treated anaerobic digested sludge: Impact of temperature and thermal history. Water Res. 56, 156–161. doi:10.1016/j.watres.2014.02.048

Farno, E., Baudez, J.C., Parthasarathy, R., Eshtiaghi, N., 2015. Impact of temperature and duration of thermal treatment on different concentrations of anaerobic digested sludge: Kinetic similarity of organic matter solubilisation and sludge rheology. Chem. Eng. J. 273, 534–542. doi:10.1016/j.cej.2015.03.097

Feng, G., Liu, L., Tan, W., 2014a. Effect of thermal hydrolysis on rheological behaviour of municipal sludge. Ind. Eng. Chem. Res. 53, 11185–11192. doi:10.1021/ie501488q

Feng, G., Tan, W., Zhong, N., Liu, L., 2014b. Effects of thermal treatment on physical and expression dewatering characteristics of municipal sludge. Chem. Eng. J. 247, 223–230. doi:10.1016/j.cej.2014.03.005

Feng, X., Tang, B., Bin, L., Song, H., Huang, S., Fu, F., Ding, J., Chen, C., Yu, C., 2016. Rheological behaviour of the sludge in a long-running anaerobic digestor: Essential factors to optimize the operation. Biochem. Eng. J. 114, 147–154. doi:10.1016/j.bej.2016.06.022

Forster, C.F., 2002. The rheological and physico-chemical characteristics of sewage sludges. Enzyme Microb. Technol. 30, 340–345. doi:10.1016/S0141-0229(01)00487-2

Frølund, B., Palmgren, R., Keiding, K., Nielsen, P.H., 1996. Extraction of extracellular polymers from activated sludge using a cation exchange resin. Water Res. 30, 1749–1758. doi:10.1016/0043-1354(95)00323-1

Guibaud, G., Dollet, P., Tixier, N., Dagot, C., Baudu, M., 2004. Characterisation of the evolution of activated sludges using rheological measurements. Process Biochem. 39, 1803–1810. doi:10.1016/j.procbio.2003.09.002

Hii, K., Baroutian, S., Parthasarathy, R., Gapes, D.J.D.J., Eshtiaghi, N., 2014. A review of wet air oxidation and Thermal Hydrolysis technologies in sludge treatment. Bioresour. Technol. 155, 289–299. doi:10.1016/j.biortech.2013.12.066

Hii, K., Eshtiaghi, N., 2017. Waste activated sludge (7 - 13 wt%) flow curves at elevated temperature conditions (80 - 140 °C). doi:10.6084/m9.figshare.5477212.v1.

Hii, K., Parthasarathy, R., Baroutian, S., Gapes, D.J.D.J., Eshtiaghi, N., 2017. Rheological measurements as a tool for monitoring the performance of high pressure and high temperature treatment of sewage sludge.

Water Res. 114, e3–e27. doi:10.1016/j.watres.2017.02.031

Imbierowicz, M., Chacuk, A., 2012. Kinetic model of excess activated sludge thermohydrolysis. Water Res. 46, 5747–5755. doi:10.1016/j.watres.2012.07.051

Khalili Garakani, A.H., Mostoufi, N., Sadeghi, F., Hosseinzadeh, M., Fatourechi, H., Sarrafzadeh, M.H., Mehrnia, M.R., 2011. Comparison between different models for rheological characterization of activated sludge. Iran. J. Environ. Heal. Sci. Eng. 8, 255–264.

Laera, G., Giordano, C., Pollice, A., Saturno, D., Mininni, G., 2007. Membrane bioreactor sludge rheology at different solid retention times. Water Res. 41, 4197–4203. doi:http://dx.doi.org/10.1016/j.watres.2007.05.032

Liao, X., Li, H., Zhang, Y., Liu, C., Chen, Q., 2016. Accelerated high-solids anaerobic digestion of sewage sludge using low-temperature thermal pretreatment. Int. Biodeterior. Biodegradation 106, 141–149. doi:10.1016/j.ibiod.2015.10.023

Lotito, V., Spinosa, L., Mininni, G., Antonacci, R., 1997. The rheology of sewage sludge at different steps of treatment. Water Sci. Technol. 36, 79–85. doi: 10.1016/S0273-1223(97)00672-0

Markis, F., Baudez, J.C., Parthasarathy, R., Slatter, P., Eshtiaghi, N., 2014. Rheological characterisation of primary and secondary sludge: Impact of solids concentration. Chem. Eng. J. 253, 526–537. doi:10.1016/j.cej.2014.05.085

Markis, F., Baudez, J.C., Parthasarathy, R., Slatter, P., Eshtiaghi, N., 2016. Predicting the apparent viscosity and yield stress of mixtures of primary, secondary and anaerobically digested sewage sludge: Simulating anaerobic digesters. Water Res. 100, 568–579. doi:10.1016/j.watres.2016.05.045

Morgan-Sagastume, F., Pratt, S., Karlsson, a., Cirne, D., Lant, P., Werker, a., 2011. Production of volatile fatty acids by fermentation of waste activated sludge pre-treated in full-scale thermal hydrolysis plants. Bioresour. Technol. 102, 3089–3097. doi:10.1016/j.biortech.2010.10.054

Mori, M., Seyssiecq, I., Roche, N., 2006. Rheological measurements of sewage sludge for various solids concentrations and geometry. Process Biochem. 41, 1656–1662. doi:10.1016/j.procbio.2006.03.021

Nazari, L., Yuan, Z., Santoro, D., Sarathy, S., Ho, D., Batstone, D., Xu, C.C., Ray, M.B., 2017. Low-temperature thermal pre-treatment of municipal wastewater sludge: Process optimization and effects on solubilization and anaerobic degradation. Water Res. 113, 111–123. doi:10.1016/j.watres.2016.11.055

Neyens, E., Baeyens, J., Dewil, R., De Heyder, B., 2004. Advanced sludge treatment affects extracellular polymeric substances to improve activated sludge dewatering. J. Hazard. Mater. 106, 83–92. doi:10.1016/j.jhazmat.2003.11.014

Ratkovich, N., Horn, W., Helmus, F.P., Rosenberger, S., Naessens, W., Nopens, I., Bentzen, T.R., 2013. Activated sludge rheology: A critical review on data collection and modelling. Water Res. 47, 463–482. doi:10.1016/j.watres.2012.11.021

Riley, D.W., Forster, C.F., 2001. The physico-chemical characteristics of thermophilic aerobic sludges. J. Chem. Technol. Biotechnol. 76, 862–866. doi:10.1002/jctb.456

Ruffino, B., Campo, G., Genon, G., Lorenzi, E., Novarino, D., Scibilia, G., Zanetti, M., 2015. Improvement of anaerobic digestion of sewage sludge in a wastewater treatment plant by means of mechanical and thermal pre-treatments: Performance, energy and economical assessment. Bioresour. Technol. 175, 298–308. doi:10.1016/j.biortech.2014.10.071

Sanin, D.F., 2002. Effect of solution physical chemistry on the rheological properties of activated sludge. Water SA 28, 207–212. doi:10.4314/wsa.v28i2.4886

Sapkaite, I., Barrado, E., Fdz-Polanco, F., Pérez-Elvira, S.I., 2017. Optimization of a thermal hydrolysis process for sludge pre-treatment. J. Environ. Manage. 192, 25–30. doi:10.1016/j.jenvman.2017.01.043

Suárez-Iglesias, O., Urrea, J.L., Oulego, P., Collado, S., Díaz, M., 2017. Valuable compounds from sewage sludge by thermal hydrolysis and wet oxidation. A review. Sci. Total Environ. 584–585, 921–934. doi:10.1016/j.scitotenv.2017.01.140

Tixier, N., Guibaud, G., Baudu, M., 2003. Determination of some rheological parameters for the characterization of activated sludge. Bioresour. Technol. 90, 215–220. doi:http://dx.doi.org/10.1016/S0960-8524(03)00109-3

Urrea, J.L., Collado, S., Laca, A., Díaz, M., 2015. Rheological behaviour of activated sludge treated by thermal hydrolysis. J. Water Process Eng. 5, 153–159. doi:10.1016/j.jwpe.2014.06.009

Wilson, C.A., Novak, J.T., 2009. Hydrolysis of macromolecular components of primary and secondary wastewater sludge by thermal hydrolytic pretreatment. Water Res. 43, 4489–4498. doi:10.1016/j.watres.2009.07.022

Yang, F., Bick, A., Shandalov, S., Brenner, A., Oron, G., 2009. Yield stress and rheological characteristics of

activated sludge in an airlift membrane bioreactor. J. Memb. Sci. 334, 83–90. doi:10.1016/j.memsci.2009.02.022

Zhang, J., Xue, Y., Eshtiaghi, N., Dai, X., Tao, W., Li, Z., 2017. Evaluation of thermal hydrolysis efficiency of mechanically dewatered sewage sludge via rheological measurement. Water Res. 116, 34–43. doi:10.1016/j.watres.2017.03.020

Zhen, G., Lu, X., Kato, H., Zhao, Y., Li, Y.Y., 2017. Overview of pretreatment strategies for enhancing sewage sludge disintegration and subsequent anaerobic digestion: Current advances, full-scale application and future perspectives. Renew. Sustain. Energy Rev. 69, 559–577. doi:10.1016/j.rser.2016.11.187

CHAPTER 6:

VISCOELASTIC CHARACTERIZATION OF THERMAL HYDROLYSED WASTE ACTIVATED SLUDGE

This chapter was published jointly with Chapter 6 in Water Research Journal

(Vol: 156, pp: 445-455, 2019)

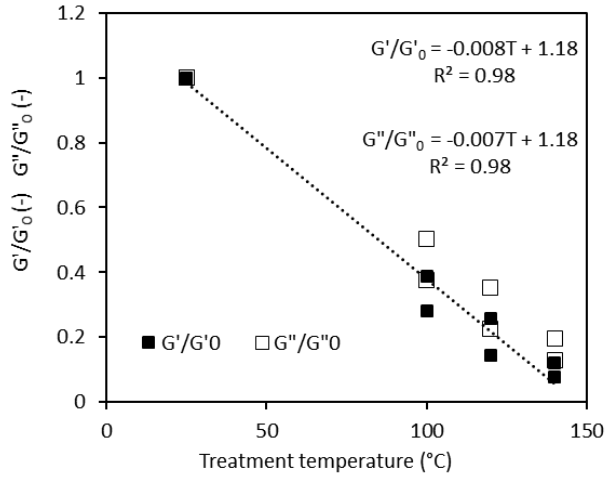

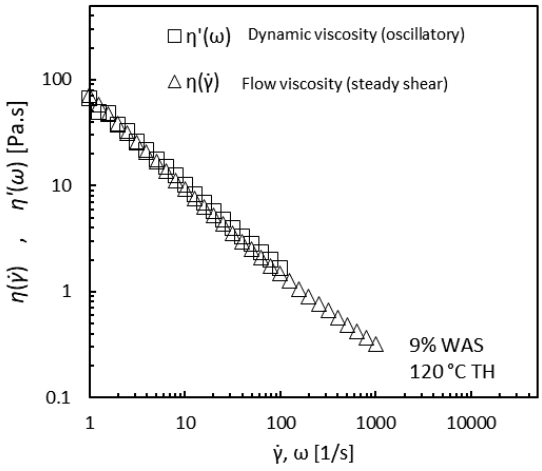

Keywords: Thermal hydrolysis; sludge concentration; yield stress; viscoelasticity; Cox-Merz; fractional Kelvin-Voigt

Hii, K, Farno, E, Baroutian, S, Parthasarathy, R, Eshtiaghi, N., 2019, Rheological characterization of thermal hydrolysed waste activated sludge. Water Research Journal 156: 445-455.

6.1 ABSTRACT

Dynamic measurements were performed to describe the viscoelastic properties of thickened raw and thermally hydrolysed waste activated sludge (WAS). Amplitude sweep results revealed gel-like characteristics in both the raw and thermally treated sludges; the storage modulus (*G'*) was greater than loss modulus (*G"*). Due to thermal hydrolysis (TH), *G'* and *G"* decreased linearly with TH temperature. This suggests thermally treated sludge structure was increasingly weakened, as reflected by linear proportionality between G' and G" with values of energy of cohesion, E_c. Frequency and creep response of the sludge were described using a fractional derivatives Kelvin-Voigt model (FKV), which had not previously been attempted for thermally hydrolysed sludge. The FKV model parameters revealed increasingly viscous characteristics in the treated sludge. Results obtained from oscillatory measurements can also approximate steady-shear behaviour by comparing dynamic viscosity, $\eta'(\omega)$, and steady-shear viscosity, $\eta(\dot{\gamma})$, whose values were very similar. This enables convenient estimation of steady-shear behaviour of sludge from oscillatory measurments which is found to be a non-destructive technique for measurning flow behaviour of highly concentrated sludge. Yield stress can also be predicted from the product of modified Cox-Merz shift factors and storage modulus (*G'*).

6.2 INTRODUCTION

Thermal hydrolysis (TH) is a processing technique involving usage of high temperatures (100 – 200 °C) to achieve desirable physical or chemical changes in wastewater sludge. One major application is in anaerobic digestion, where TH is used as pre-treatment to overcome the rate-limiting hydrolysis step, showing favourable results and successful industrial-scale application (Barber, 2016; Carrère et al., 2010; Sapkaite et al., 2017; Zhen et al., 2017). In these processes, particulate organic matter is solubilized through application of heat for a defined period. This disintegrates cellular material to release organic compounds, which improves microorganism access to them, thus enhancing anaerobic digestion performance (Ariunbaatar et al., 2014; Suárez-Iglesias et al., 2017). Besides that, TH leads to advantageous rheological enhancements. For example, the viscosity of thermally-treated sludge is greatly reduced, which improves the efficiency of pumping, mixing, heating, digester loading, and sludge dewaterability (Farno et al., 2017; Morgan-Sagastume et al., 2011; Pérez-Elvira et al., 2008; Pérez-Elvira and Fdz-Polanco, 2012; Zhou et al., 2013). Rheology plays an important role in the design and operation of sludge handling systems (Dentel, 1997; Eshtiaghi et al., 2013). Despite extensive research on sludge TH, detailed studies

related to its rheology are scarce (Barber, 2016). Accordingly, detailed rheological characterization of sludge and its viscoelastic properties are of interest and can lead to better implementation of TH processes.

Waste activated sludge (WAS) is the main sludge-type handled in TH processes; its rheology at ambient conditions has been well researched (Eshtiaghi et al., 2013; Ratkovich et al., 2013). WAS rheology is generally accepted to behave as a non-Newtonian, shear-thinning fluid, commonly described by the Herschel-Bulkley model. It exhibits thixotropic properties (Guibaud et al., 2004) and many studies identified the presence of yield stress (Farno et al., 2015; Markis et al., 2014; Ratkovich et al., 2013). Besides, WAS exhibits viscoelasticity, meaning that it initially shows solid-like behaviour under stress but liquid-like behaviour upon breakdown of floc structure.

A few studies have characterized viscoelastic properties of sludge. Ayol et al (2006) performed dynamic measurements on anaerobically digested sludge conditioned with acrylamide polymers and showed that storage modulus (*G'*) was greater than loss modulus (*G"*) in the linear viscoelastic (LVE) region. However, this did not consider unconditioned WAS. Baudez et al. (2011) similarly identified linear viscoelastic behaviour of digested sludge at low stresses. Elastic and loss moduli were constant in the LVE range with *G'>G"* but *G"* reaches a peak value at the cross-over strain. Then *G'<G"*, which was identified as being a feature of soft-glassy materials. Yuan and Wang (2013) and Yuan et al. (2017) identified solid-like characteristics in raw WAS (54 g/L TSS) where *G'>G"*. This was still valid even after extraction of extracellular polymeric substances (EPS) from the sludge. However, these studies were limited to low WAS concentrations.

Viscoelastic properties have been reported for thermally treated WAS. Generally, *G'* and *G"* reduced as a result of TH, and *G'>G"* (Farno et al., 2016a; Feng et al., 2014a; Zhang et al., 2017), although some studies also suggest *G">G'* at low concentrations (< 0.8 wt%) (Feng et al., 2014a, 2014b). However, Feng et al. (2014a) and Feng et al. (2014b) did not examine the impact of varying treatment temperature whereas Farno et al. (2016b) was related to low temperature (50 – 80 °C) thermal sludge processing. Zhang et al. (2017) characterized the viscoelastic properties of WAS (14.2 and 18.2 wt%) after low (60 – 90 °C) and high temperature (120 – 180 °C) TH. A Kay-Bernstein-Kearsley-Zappa (KBKZ) model described the viscoelastic properties. However, their study was concerned with polyacrylamide (PAM) conditioned sludge, which alters flocculation and network structure (Chen et al., 2005). Furthermore, Farno et al. (2018) have shown that a fractional derivatives Kelvin-Voigt model was more representative for sludge

viscoelasticity but was limited to lower thermal treatment temperatures (<80 °C) and sludge concentrations (<6.1 wt%).

The current study investigates the viscoelastic properties of the raw and thermally-treated WAS. The results from viscoelastic measurements are fitted to a fractional derivates Kelvin-Voigt model, which has not been attempted before for high-temperature thermally treated sludge. Finally, the adaptability of dynamic measurements to obtaining steady shear data is evaluated, assessing its potential for overcoming the practical challenges related to the steady shear flow measurement of highly concentred sludge.

6.3 MATERIALS AND METHODS

6.3.1 WASTE ACTIVATED SLUDGE

Samples of WAS were collected at initial solids concentration 3.5 wt.% from Mount Martha wastewater treatment plant in Victoria, Australia, where dissolved air flotation without polymer dosing is used to thickened sludge. The sludge was stored at 4 °C for 30 days before use to ensure minimal changes due to biological activity during experiments, and to help maintain the stability and consistency between samples (Curvers et al., 2009). To achieve different concentrations, sludge was first thickened via centrifugation at 9000 rpm (13,700 G). Then it was diluted to 7, 9, and 13 wt% by mixing the centrifuged sludge with the original sludge. Total solids concentration (wt%) was determined gravimetrically by drying samples to constant mass at 105 °C (APHA, 1992).

6.3.2 OSCILLATROY VISCOELASTIC MEASUREMENT

In-situ measurements produced unreliable results when using the pressure cell in dynamic mode. This was likely caused by high inertial forces produced in the bob, which connects to the rheometer via magnetic coupling. Therefore, viscoelastic analysis was carried out using parallel plate geometry (40 mm diameter, 1 mm gap, 25 °C) on untreated and post-thermal treatment sludge (7, 9 and 12 wt%). Strain sweep tests were performed at 10 rad/s. Frequency sweep tests were performed at angular frequency range 1 – 100 rad/s at constant 0.1% strain, which was within the linear viscoelastic region (LVE) for all samples tested. Creep tests were performed by applying step stress and recording the strain over 180 s. Flow curves were also generated, and stress ramps were performed to determine the static yield stress of samples via the tangent cross-over method (Farno et al., 2016a; Mezger, 2006). Prior to each

measurement, samples were pre-sheared at 1000 s^{-1} for 5 mins followed by 2 minutes equilibration at rest. Parallel plates were lined with sandpaper (400 grit) to eliminate slippage, and thermally treated samples were obtained using a separate 100 mL reactor (Parr Instrument Company). Rheometer raw data for oscillatory measurements are published in (Hii and Eshtiaghi, 2018).

6.3.3 VISCOELASTIC MODELLING

A fractional derivatives Kelvin-Voigt (FKV) model was fitted to viscoelastic data to allow calculation of viscoelastic parameters. This model has so far been used to describe thermally treated sludge, but only at low treatment temperatures below 80 °C (Farno et al., 2018):

$$\sigma_t(t) = E_1\tau_1^{\alpha}\frac{d^{\alpha}\gamma(t)}{dt^{\alpha}} + E_2\gamma(t) \quad , \quad 0 < \alpha < 1 \qquad (Eq.6.1)$$

where σ (Pa) is stress, γ (-) is strain; E_1 (Pa.s$^{\alpha}$) and α are constants related to the fractional element, and τ_1 is the corresponding characteristic time; E_2 (Pa) is the spring constant representing the elastic element. In this system, G' and G'' moduli are related to frequency, ω (rad/s), as:

$$G'(\varpi) = E_1\varpi^{\alpha}\cos\left(\frac{\pi}{2}\alpha\right) + E_2 \qquad (Eq.6.2)$$

$$G''(\varpi) = E_1\varpi^{\alpha}\sin\left(\frac{\pi}{2}\alpha\right) \qquad (Eq.6.3)$$

The strain response to step stress is given (Schiessel et al., 1995):

$$\gamma(t) = \frac{\sigma}{E}\left(1 - E_{\alpha}\left(-\left(\frac{t}{\tau}\right)^{\alpha}\right)\right) \qquad (Eq.6.4)$$

where E_{α} is a generalized Mittag-Leffler function of order α; $E = E_1(\tau_1/\tau)^{\alpha}$; $\tau = (E_1\,\tau_1^{\alpha}/E_2)^{1/\alpha}$. Experimental data were fitted to the FKV models via MATLAB, using the non-linear least squares function. The Mittag-Leffler function was evaluated using MATLAB protocols extracted from (Garrappa, 2015).

6.4 RESULTS AND DISCUSSION

6.4.1 VISCOELASTIC BEHAVIOUR

Strain sweep results (Figure 6.1) compare deformation behaviour before and after TH, as well as changes in G' and G'' moduli. For both untreated and thermally treated samples, WAS exhibited linear viscoelastic deformation at low strain values with $G'>G''$, indicating gel-like behaviour. Then, with increasing strain the rate of change in G' and G'' became increasingly strain-dependent, where both moduli decreased rapidly

until a crossover point was reached, then *G"*>*G'*. The viscous characteristics of the sludge are then dominant, and sludge exhibits irreversible deformation, or flow. This general behaviour was observed for all concentrations (7 – 12 wt%) of untreated and thermally treated (100 – 140 °C) WAS examined. These results are consistent with those reported in Farno et al. (2016b) and Zhang et al. (2017) for different sludge concentrations and treatment conditions. Interestingly, the abovementioned studies reported presence of a *G"*-peak, which was largely absent in the current study. Instead, the *G"*-curves for all untreated and thermally treated sludge transitioned smoothly into the viscous region without rising above its plateau values. This difference compared to Farno et al. (2016b) is likely due to the higher sludge concentrations used in the current study as compared to theirs (3.5 – 6.1 wt%). On the other hand, the sludge used by Zhang et al. (2017) had higher concentration(14.2 and 18.2 wt%) but was conditioned with PAM, which significantly affects its network structure (Wang et al., 2017).

In those studies, the *G"* curve first rises to a local maximum near the cross-over point before decreasing smoothly with increasing strain. This phenomenon was attributed to be a feature of soft-glassy materials and was believed to be an indication of the breakdown of the sludge's internal structure. Essentially, *G"* represented the non-recoverable deformation energy. Then, at increasing strain values beyond the LVE range, the rising G" curve could be interpreted as the gradual collapse in the network structure of the sludge which was initially present at rest (Mezger, 2006). Furthermore, it was reported in both studies that the height of the *G"*-peak was reduced by thermal treatment.

However, in the current study, this phenomenon was not pronounced. In the case of thermally treated sludge, only a small rise in the G" curve was observed in the flow transition range of strain. This increasing G" only becomes apparent when presented on a linear-log scale, as shown in figure 6.1(b). Still, the peak G" value for all cases of untreated sludge was no more than 10% greater than its plateau values in the LVE region, whereas in Farno et al. (2016b), this was upwards of 40% for thermally treated sludge. One possible reason is that the sludge used in the current study was of a much higher solids concentration. In the case of Farno et al. (2016b), the sludge used in their study was more dilute (3.5 – 6.1 wt%), meaning that the fraction of continuous medium (sludge liquor) was greater. This possibly allowed the dispersed phase (sludge flocs) to be distributed further apart. It has been shown that WAS is composed of filamentous material, besides EPS and bacteria (Koivuranta et al., 2015; Perez et al., 2006), which serve as the "backbone" of the microbial flocs (Jenkins et al., 2003). Then, the filaments may become more readily entangled due to the larger inter-particle spaces between flocs, forming a gel network. Therefore, as the

sludge is deformed beyond the LVE region, this disentangling gel-network would be detected as a rising G" curve.

On the other hand, sludge used in the current study has higher solids content exhibiting a pasty appearance – especially for 12% untreated sample. This means the sludge flocs are likely to be more tightly packed together and the filamentous substances may not be as free to entangle in the continuous medium. Thus, as the sludge is deformed, the particles in the sludge are likely just sliding past one another, such as in the case of simple thickened particle suspension systems. In this case, the loss of deformation energy due to the gradual breakage of the sludge network may be comparatively undetectable. Then, the rising G"-curve is not observed.

In the case of thermally treated sludge, the network structure has been largely destroyed due to solubilization of flocs and sludge particulates. Therefore, some network structure still remains, while the particles and flocs are also able to flow more freely due to their reduced size. Then, the dissipation of energy due to breakage of sludge network during deformation is detectable, but small due to an already weakened network. In the case of Zhang et al. (2017), highly concentrated sludges (14.2 and 18.2 wt%) was studied but they also detected the presence of a G"-peak. However, it is noted that in their study the sludge samples have been conditioned with PAM which is a flocculant used to form network structures within the sludge (Chen et al., 2005). Therefore, breakage of the PAM network during deformation beyond the LVE range may have contributed to the G"-peaks observed in their study.

Although gel-like characteristic (G'>G") was present in all samples of untreated and thermally treated sludge, treated samples showed larger portions of viscous deformation. This is indicated by higher G" values in the LVE region. Figure 6.2 compares the loss factor (tanδ = G"/G') for untreated and thermally treated samples. Increasing tanδ values indicate a higher portion of non-recoverable deformation energy. Generally, tanδ increased with treatment temperature but reduced with sludge concentration. This means sludge exhibited more elastic characteristics with sludge concentration, but this becomes diminished due to TH. At increasing sludge concentrations, interactions between the sludge particles and its gel-like network are strengthened (Markis et al., 2016), resulting in the observed higher elastic properties. But as a result of TH, the polymeric network structures are destroyed due to solubilization of sludge components. Then, the increasing tanδ suggests a greater extent of network destruction occurred at higher treatment temperatures.

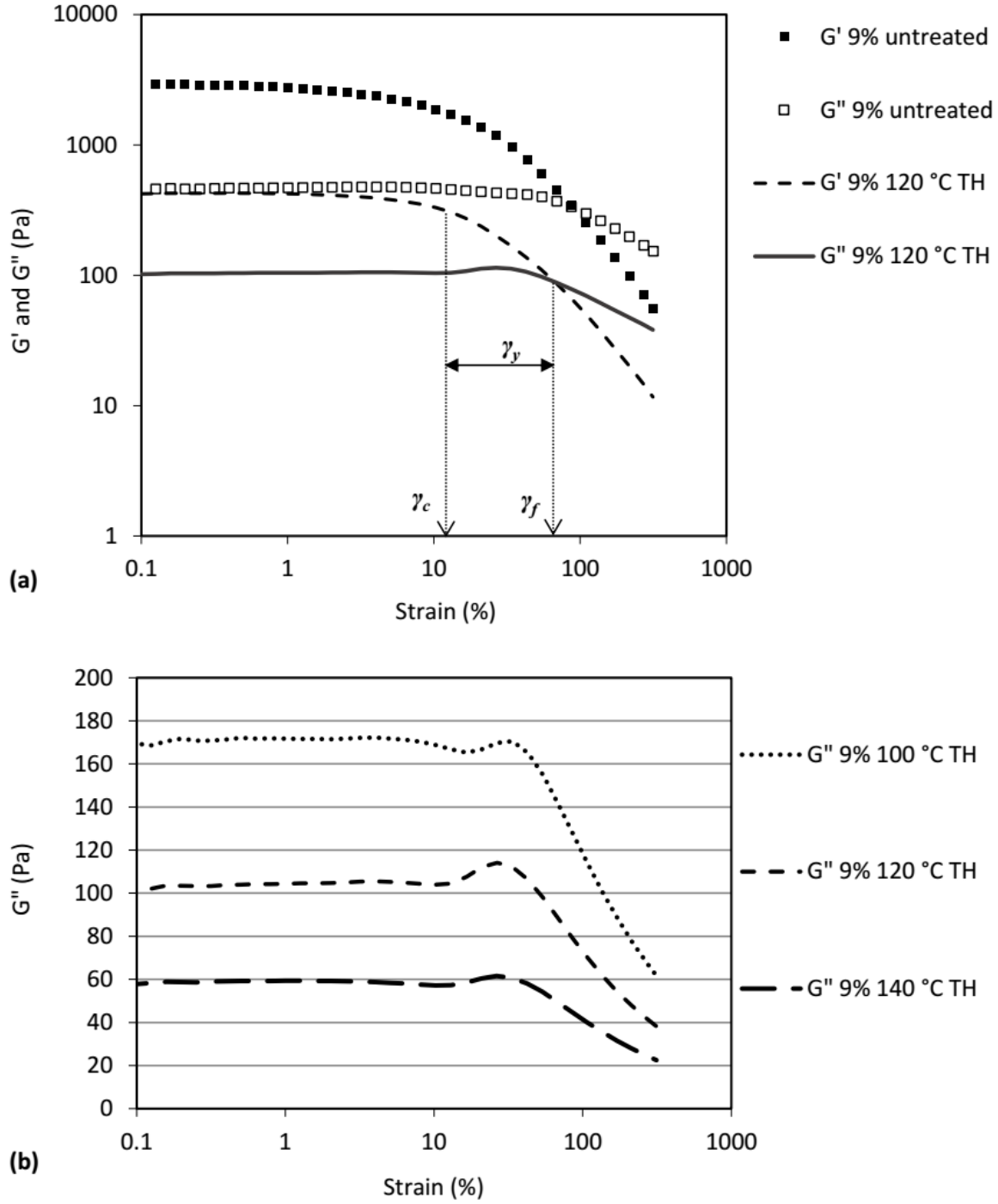

Figure 6. 1 – (a) Strain sweep results for 9% untreated WAS and 9% thermally treated WAS (120 °C, 1 hour), measured at 25 °C and constant oscillation frequency of 10 rad/s. (b) G" curves on linear-log scale for 9% thermally treated WAS (100 – 140 °C, 1 hour), measured at 25 °C and constant oscillation frequency of 10 rad/s.

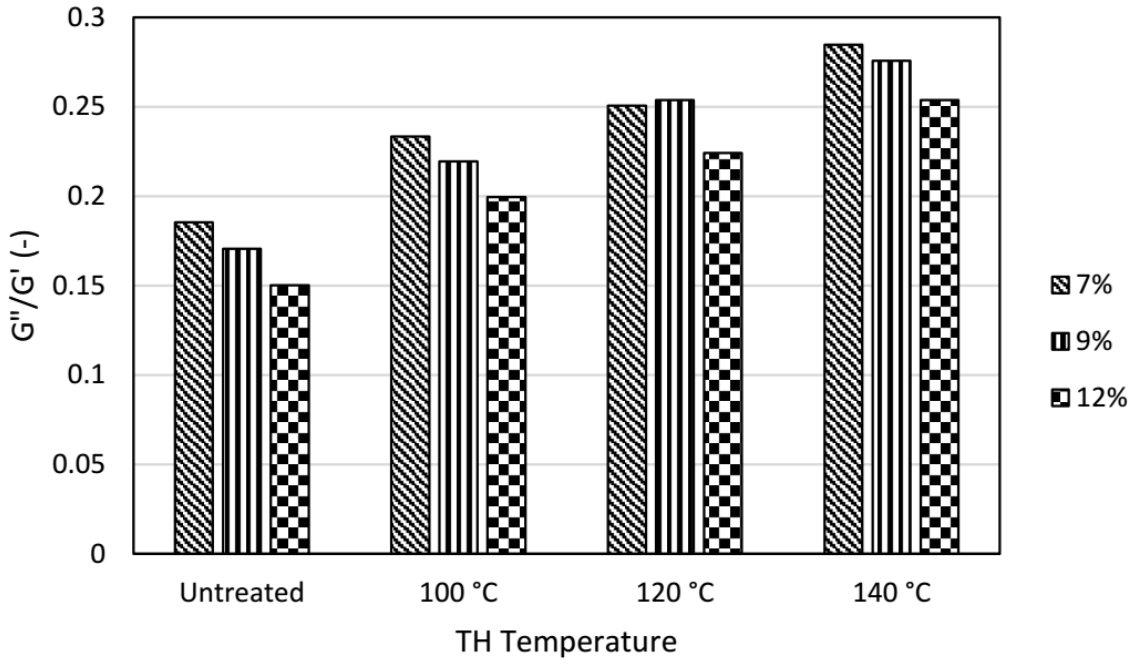

Figure 6. 2 – Loss factor, tanδ = G"/G', for untreated and thermally treated WAS in the LVE region (<1% strain) measured at 25 °C, 10 rad/s.

The critical strain values, γ_c (%), of the LVE region remain largely unchanged for all untreated and thermally treated sludge samples, regardless of treatment temperature. Here, γ_c was defined as the strain value at which G' deviated by at least 5% compared its previous measuring point at decreasing strain (i.e. when G' deviates significantly from the plateau LVE values; refer Figure 6.1a). In most cases, γ_c was 6 – 12% strain, below which the sludge showed LVE behaviour. No discernible pattern was observed between γ_c and TH conditions or sludge concentration. This is consistent with (Mori et al., 2006) who reported that critical strain values largely remained constant for different concentrations of WAS (2.7 – 5.7 wt% total suspended solids) and was independent of sludge concentration.

Shrinkage of the LVE region due to TH (170 °C, 60 min) has been reported in treated sludge (Feng et al., 2014b). This was indicated by a reduction in the crossover strain value, γ_f, (where G' = G"). A similar observation was made in the current study for 7 wt% and 9 wt% sludge, where γ_f was reduced after TH. Here, a "yielding range of strain" can be defined: $\gamma_y = \gamma_f - \gamma_c$, which describes the size of the strain values for which sludge begins to exhibit irreversible deformation, but the gel-like behaviour still exists. Figure 6.3 shows the reduction in γ_y is linearly correlated with increasing treatment temperature, which reflects

the temperature-dependent solubilization of the gel network. Thus, thermally treated sludge was less able to recover deformation energy, hence flowed more readily at the lower strain. Accordingly, a value representing the energy of cohesion of the three-dimensional network of the sludge, E_c (J/mol), can be calculated (Mori et al., 2006):

$$E_c = \frac{1}{2}\sigma_c\gamma_c \tag{12}$$

Here, γ_c (%) is the critical strain value as previously defined, and σ_c (Pa) is the corresponding critical stress. As shown in Figure 6.3a, E_c is reduced with treatment temperature, indicating a reduction in the degree of interparticle interaction and strength of flocs. Furthermore, G' and G" also decreased linearly with treatment temperature and showed linear proportionality with E_c (Figure 6.3a and b), which affirms the decrease in sludge's deformation resistance is due to the breakdown of structural integrity.

G' and *G"* exhibited minor frequency dependence in the LVE region, showing slight increase with angular velocity, as seen in Figure 6.4. Across the whole frequency range, *G'>G"* for all concentrations of sludge, regardless of thermal treatment. The moduli do not cross over at any point in the range of frequencies examined. In fact, the loss factor (*tanδ = G"/G')* largely remained constant. This behaviour is characteristic of weak gels (Rao and Cooley, 1992) and reflects the presence of biopolymers in sludge. This means in the LVE range, sludge exhibited physical network structure (Mezger, 2006), which remained relatively constant in the entire frequency range. Due to TH, the gel network of biopolymers is deteriorated which leads to reduction in *G'* and *G"* (Figure 6.3a), but a gel network remained, regardless.

Zhang et al. (2017) used KBKZ to describe the viscoelastic behaviour of thermally treated sludge. However, Farno et al. (2018) showed the FKV model can be more realistic and accurate due to the fractional element in the model, which describes the intermediate characteristics between purely viscous and purely elastic elements. Here, frequency sweep results could be very well described by the FKV model (Equations 6.2 and 6.3), with fitting curves predicting experimental data shown as continuous lines in Figure 6.4. The corresponding fitting parameters, as well as fitting error, are presented in Table 6.1.

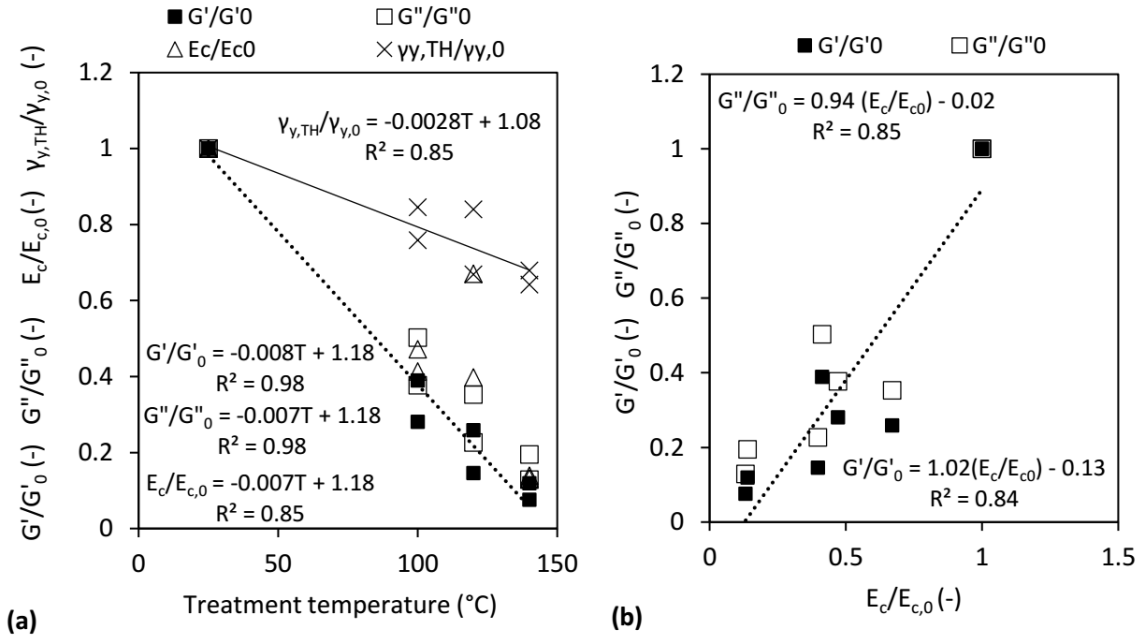

Figure 6. 3 – (a) Impact of TH temperature on the normalized yielding strain range, γ_y (%), normalized energy of cohesion, E_c (J/m^3), normalized storage modulus, G' (Pa), and the normalized loss modulus, G" (Pa) of treated WAS. Here, $\gamma_{y,TH}$ (%) is the difference between the modulus cross-over strain and the critical strain ($\gamma_y = \gamma_f - \gamma_c$) for thermally treated sludge, and $\gamma_{y,0}$ (%) is the corresponding value for untreated sludge; $E_{c,0}$, G'_0, and $G"_0$, are the energy of cohesion, storage modulus and loss modulus, respectively, of the untreated sample. (b) Linear proportionality between normalized G' and G" with E_c. Data is shown for 7 wt% and 9 wt%.

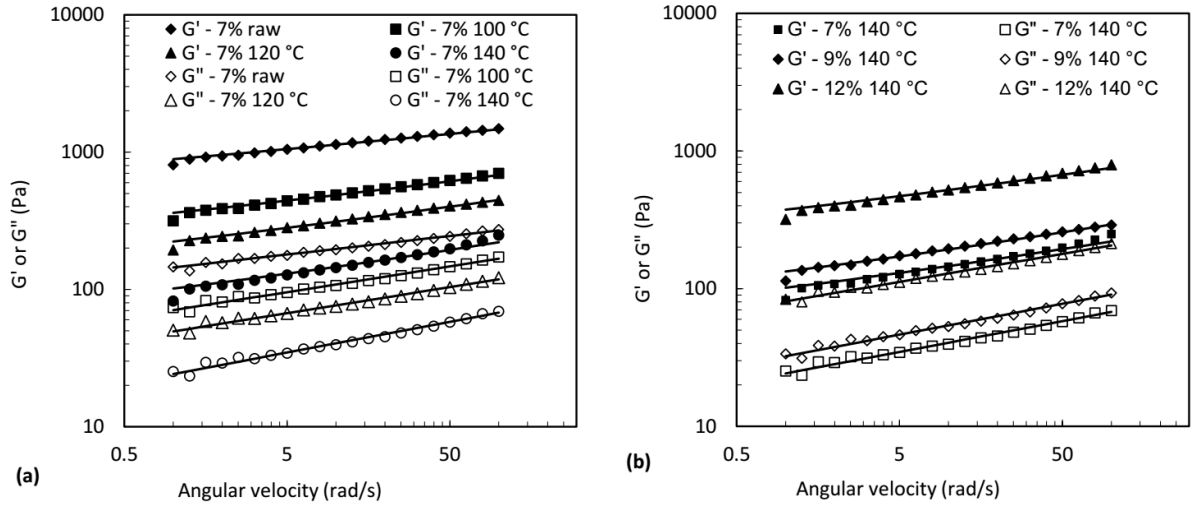

Figure 6. 4 – Frequency sweep results showing impact of (a) treatment temperature on 7 wt% untreated and thermally treated WAS after TH, and (b) sludge concentration (7 – 12 wt%) on thermally treated WAS (140 °C). Continuous lines represent model fitting via FKV model.

Table 6. 1 – Fitting parameters of fractional Kelvin-Voigt model (Eqs. 3 and 4) to describe frequency sweep experimental results obtained for untreated and thermally treated WAS.

		E_1	E_2	α	G' error	G" error
7%	25 °C	217.14	686.69	0.14	1.53%	1.20%
	100 °C	128.18	243.51	0.19	1.98%	2.31%
	120 °C	62.09	168.49	0.19	1.77%	2.12%
	140 °C	35.59	70.24	0.22	3.97%	2.94%
9%	25 °C	610.30	1584.80	0.13	1.44%	1.63%
	100 °C	231.56	422.96	0.18	1.93%	2.16%
	120 °C	102.45	210.95	0.20	2.50%	2.28%
	140 °C	45.27	93.72	0.22	1.91%	2.81%
12%	25 °C	10.00	21,650.00	0.09	1.52%	2.10%
	100 °C	622.19	916.93	0.17	2.09%	2.50%
	120 °C	282.11	490.45	0.19	2.52%	1.99%
	140 °C	130.93	257.10	0.20	3.02%	2.26%

G' and G" error (%) refers to the mean absolute percentage error (MAPE) between experimental data and corresponding values obtained via the FKV model. The 25 °C value denotes untreated sludge.

E_1 and E_2 are model constants representing responses of the fractional and elastic elements in Equation 6.1, respectively. It was described for biological soft tissues (Nicolle et al., 2010) that the fractional portion was analogous to the gel-like behaviour of the filamentous cytoskeleton inside cellular material, whereas the elastic portion represented the elastic response of permanent structures such as the cell wall. Both E_1 and E_2 linearly decreased with treatment temperature, except for 12 wt% untreated sludge (25 °C). In the case of 12 wt% untreated sludge, E_1 was inconsistently low, and E_2 was exceedingly high. On one hand, this may be an indication that untreated 12% sludge behaviour could be predominantly described as an elastic solid than a weak gel compared to other sludge. This is plausible as the untreated 12% sludge sample exhibited a thicker, paste-like appearance as opposed the other less concentrated and thermally treated samples. On the other hand, the inconsistent values observed for 12% untreated sample may also be a result of unsuitability of the current measurement methods being adopted for higher concentrations of untreated WAS, since it was observed that this sample tended to exhibit signs bifurcation and edge effects during repeated measurements. Indeed, thickened sludge types (15 – 30 wt%) have been considered as soft solids, rather than weak gels. (Baudez et al., 2016). However, for all other sludge samples the linear reduction of E_1 and E_2 with treatment temperature indicate weakening of sludges' structural strength after TH. Furthermore, α also increased linearly with treatment temperature. This means the sludge exhibited higher viscous characteristics after TH since Equation 6.1 reduces to the classical Kelvin-Voigt model when $\alpha = 1$ (Farno et al., 2018).

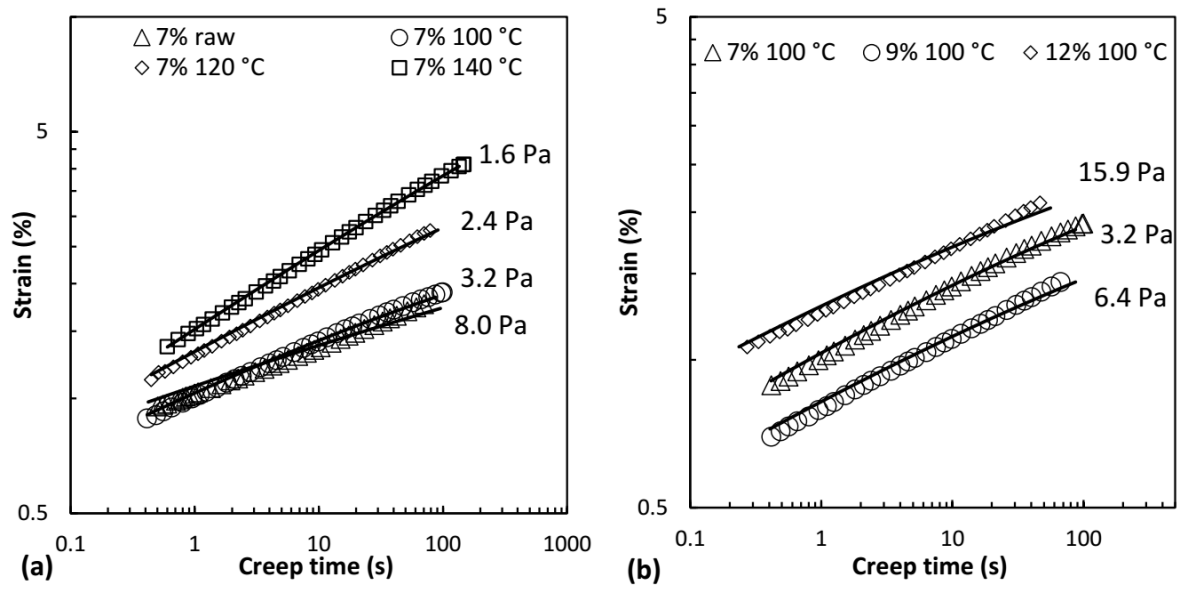

Figure 6. 5 – Strain response to input stress over time taken from creep test results for (a) untreated and thermally treated 7% WAS and (b) 7 – 12% thermally treated WAS (100 °C, 1hour). Continuous lines represent model fitting via FKV model.

Table 6. 2 – Fitting parameters for FKV model (Eq. 5) describing creep response of 7 – 12% untreated and thermally treated WAS.

		Stress (Pa)	***E (Pa)***	***1/τ (s^{-1})***	***α***	***MAPE***
7%	Raw	7.96	139.39	1.2E-05	0.14	3.38%
	100 °C	3.18	70.96	9.7E-04	0.19	1.57%
	120 °C	2.39	17.86	5.6E-06	0.19	1.55%
	140 °C	1.59	6.76	4.2E-06	0.22	0.66%
9%	Raw	31.83	461.33	7.3E-03	0.13	1.60%
	100 °C	6.37	170.58	4.9E-04	0.18	2.09%
	120 °C	3.18	67.08	9.7E-04	0.20	2.15%
	140 °C	3.98	3.78	2.6E-07	0.22	3.20%
12%	Raw	-	-	-	-	-
	100 °C	15.92	340.30	2.4E-03	0.18	2.35%
	120 °C	6.37	100.25	1.2E-04	0.19	3.28%
	140 °C	3.18	52.50	2.5E-04	0.20	2.98%

MAPE refers to the mean absolute percentage error (%) between experimental data and corresponding values obtained via the FKV model.

The creep data and FKV model fitting are presented by markers and continuous lines in Figure 6.5, respectively. Fitting parameters of the model (Equation 6.4) are presented in Table 6.2. Similar to Farno et al. (2018), α was obtained from fitting of the FKV model (Equation 6.2 and 6.3) to frequency sweep data (listed in Table 6.1). This was described as an advantage of the FKV model over classical Kelvin-Voigt model since α is not an arbitrarily derived value, but derived from frequency sweep results, reducing the number

of unknown parameters in Equation 6.4 to two and improving reliability of the FKV model fitting. Another advantage of the FKV model is that it features a single τ value, as opposed to other models which consider a spectrum of τ values, such as the generalized Kelvin-Voigt model or the KBKZ model (Zhang et al., 2017). This becomes useful in process design cases; for example, in mixing of viscoelastic fluids, where relevant equations require discrete τ values (Xu et al., 2018).

Increasing treatment temperature, E is reduced for all concentrations of sludge, indicating lower strain resistance. The respondence time, τ (s), does not exhibit any apparent relationship with treatment temperature but for all samples, were large. This reveals highly viscoelastic behaviour in sludge as a long time is required to reach its final deformation at given input stress. As described for the Kelvin-Voigt model, τ is infinite for purely viscoelastic materials by definition, and zero for purely elastic materials, whereas it is undefined for purely viscous materials since they do not exhibit strain (Tschoegl, 2012). As shown in Figure 6.5, the FKV model can adequately describe the viscoelastic characteristics of thermally treated sludge (error values for fitting presented in Table 6.2). However, 12 wt% untreated sludge could not be reliably described, likely due to its pasty characteristics as previously speculated. It is recommended that further research be done to examine more appropriate models for thick, pasty sludges.

6.4.2 EVALUATING STEADY SHEAR FLOW PARAMETERS FROM OSCILLATORY MEASUREMENTS

It was of interest whether viscoelastic data could approximate steady-shear flow properties of sludge. Such correlation would be useful in applications where steady-shear measurements are not readily producible. For example, online process rheometers which operate by dynamic measurements (Konigsberg et al., 2013). Besides that, it was observed in the current study that steady-shear measurements of thickened WAS (12 wt% untreated) tended to exhibit edge effects and bifurcation phenomena. The challenges associated with rheological measurement of highly concentrated sludge are highlighted in many works (Baudez et al., 2016; Mouzaoui et al., 2018). Potentially, such issues could be overcome by approximating steady-shear properties from dynamic measurements since it produces low sample strains.

As described by Cox-Merz analogy, $\eta^*(\omega) = \eta(\dot{\gamma})|_{\omega=\dot{\gamma}}$ where η^* is the complex viscosity (Pa.s) and ω is the angular velocity (rad/s), from dynamic measurements, whereas η is the steady-shear apparent viscosity (Pa.s) and $\dot{\gamma}$ is the shear rate (s^{-1}), from rotational measurements. Traditionally, Cox-Merz analogy is not

applicable for dispersion systems (e.g. sludge). However, a modified Cox-Merz rule was applied to correlate complex viscosity *(η*)* and dynamic viscosity *(η')* to steady-shear viscosity of semi-solid foods (Bistany and Kokini, 1983):

$$\eta^*, \eta'(\omega) = C[\eta(\dot{\gamma})]^s \qquad (Eq. 6.5)$$

According to Equation 6.5, the plot of $\eta(\dot{\gamma})$ is effectively shifted until it superimposed with the plot of $\eta^*(\omega)$ or $\eta'(\omega)$. This modified Cox-Merz rule was applied to the untreated and thermally treated sludge here, based on measurements employing parallel plate geometry. As shown in Figure 6.6 (a), $\eta^*(\omega)$ does not readily superimpose with the unshifted $\eta(\dot{\gamma})$ curve. This confirms traditional Cox-Merz analogy is not valid, even for thermally-treated sludge. Interestingly, the $\eta'(\omega)$ plot closely resembled the $\eta(\dot{\gamma})$ plot even without shifting, as shown in Figure 6.6 (b). The dynamic viscosity, $\eta'(\omega)$, describes the real portion of the complex viscosity (i.e. $\eta^* = \eta' - i\eta''$) and represents the energy lost during deformation.

Table 6.3 shows shift factors for Equation 6.5, as well as error between the steady-shear and oscillatory values after shifting. Besides that, the error between the unshifted $\eta(\dot{\gamma})$ and $\eta'(\omega)$ curves are also shown. Notably, the *s*-values nearly equal 1 in all cases. This means the curve trends for $\eta^*(\omega)$, $\eta'(\omega)$, and $\eta(\dot{\gamma})$ were already initially very similar. Then, a simple vertical or horizontal shift can reliably superimpose $\eta(\dot{\gamma})$ to the $\eta^*(\omega)$ and $\eta'(\omega)$ curves. On the other hand, *C*-values showed that unshifted $\eta^*(\omega)$ values were at least 5 times greater than $\eta(\dot{\gamma})$ in all cases, but $\eta'(\omega)$ and $\eta(\dot{\gamma})$ were nearly equal. The *C*-values did not show a clear relationship with the sludge concentration or treatment temperature, but generally decreased with temperature and increased with concentration. This suggests that the pastier samples tend to show greater deviation between their oscillatory and steady shear viscosity values.

Since the shift factor values corresponding to $\eta'(\omega)$ were very close to 1 in all cases, this suggests the following, based on the correlation by Spriggs et al. (1966):

$$\eta'(\omega) \approx \eta(\dot{\gamma})|_{\dot{\gamma}=\omega} \qquad (Eq. 6.6)$$

Equation 6.6 Error values for this approximation are in the range of 9 – 20% for thermally treated samples (Table 6.3). For untreated sludge, this error increased likely due to bifurcation and edge effect phenomena. Possibly, the higher error values are likely due to inherent flaws of the steady shear method, since dynamic measurement did not exhibit abovementioned phenomena. This was especially apparent in 12 wt% sludge which exhibited obvious sample fractures and edge effects during repeated steady-shear measurements, as reflected by inconsistently high error value and shift factors.

From a practical standpoint, Equation 6.6 allows quick, simple approximation of sludge's steady-shear viscosity using frequency sweep data. Sludge's shear-thinning behaviour can also be determined from either $\eta^*(\omega)$ or $\eta'(\omega)$ since they followed nearly identical curve trends with $\eta(\dot{\gamma})$. If a single $\eta(\dot{\gamma})$ value can be determined, then the $\eta(\dot{\gamma})$ curve over a range of shear rates can be predicted. Alternatively, shift factors in Table 6.3 can be used to transform $\eta^*(\omega)$ or $\eta'(\omega)$ plots from frequency sweep tests to produce $\eta(\dot{\gamma})$ plots. Shift factor values for intermediate conditions between those presented in Table 6.3 may also be interpolated. Along with Equations 5.1 – 5.3, the above observations allow process monitoring in TH using either steady-shear or dynamic measurements in real time. Furthermore, it offers potential application in qualitative determination of flow properties of thicker sludge using non-destructive oscillatory methods.

Table 6. 3 – Empirical shift factors for Cox-Merz rule

		$\eta^*(\omega) = C[\eta(\dot{\gamma})]^s\|_{\dot{\gamma}=\omega}$			$\eta'(\omega) = C'[\eta(\dot{\gamma})]^{s'}\|_{\dot{\gamma}=\omega}$			$\eta'(\omega) = \eta(\dot{\gamma})\|_{\dot{\gamma}=\omega}$
		C	***s***	***MAPE***	***C'***	***s'***	***MAPE***	***MAPE***
7%	Raw	6.88	0.98	5%	1.12	1.00	9%	22%
	100 °C	5.39	0.97	3%	1.10	0.99	8%	18%
	120 °C	5.04	0.96	4%	1.14	0.99	6%	20%
	140 °C	3.31	0.95	4%	0.84	0.99	9%	8%
9%	Raw	8.33	0.98	4%	1.25	1.00	8%	35%
	100 °C	5.81	0.97	3%	1.10	0.99	9%	20%
	120 °C	4.35	0.96	4%	0.97	0.99	10%	9%
	140 °C	4.14	0.95	4%	1.03	0.99	10%	15%
12%	Raw	16.43	0.99	3%	2.38	1.01	2%	134%
	100 °C	6.42	0.98	3%	1.09	1.00	12%	23%
	120 °C	5.92	0.97	4%	1.18	0.99	10%	30%
	140 °C	5.09	0.96	4%	1.16	0.99	9%	27%

MAPE refers to the mean absolute percentage error (%) between the complex or dynamic viscosity values and the steady-shear viscosity values as shifted by applying the modified Cox-Merz rules.

Equation 6.5 imposes a vertical shift of the viscosity plots. However, a horizontal shift is also valid here since the *s*-values in Table 6.3 nearly equal to 1. Then, a linear relationship exists between $\eta^*(\omega)$ and $\eta(\dot{\gamma})$, and it can be written: $\eta^*(H \times \omega) = \eta(\dot{\gamma})|_{\dot{\gamma}=\omega}$, where *H* is a horizontal shift factor applied to superimpose both curves. This horizontal shift factor, *H*, has been used to derive the yield stress of concentrated, non-Newtonian suspensions (Canet et al., 2005). This was achieved by multiplying *H* with *G'* at the critical strain. In the current study, a better approximation of yield stress was obtained by multiplying *H* with the plateau *G'* (obtained from strain sweep results, as in Figure 6.1). The yield stress values derived from *G' x H* are compared against those derived from flow curve fitting (dynamic yield stress), as well as direct measurement (static yield stress) in Table 6.4. Notably, the *G' x H* values come very close to approximating

the yield stress as derived from flow curve fitting, and in most cases fall within the same order of magnitude. This becomes very useful as it allows for a quick approximation of the yield stress when direct measurement methods may not be available. However, the theoretical or physical basis behind this approximation will require further investigation.

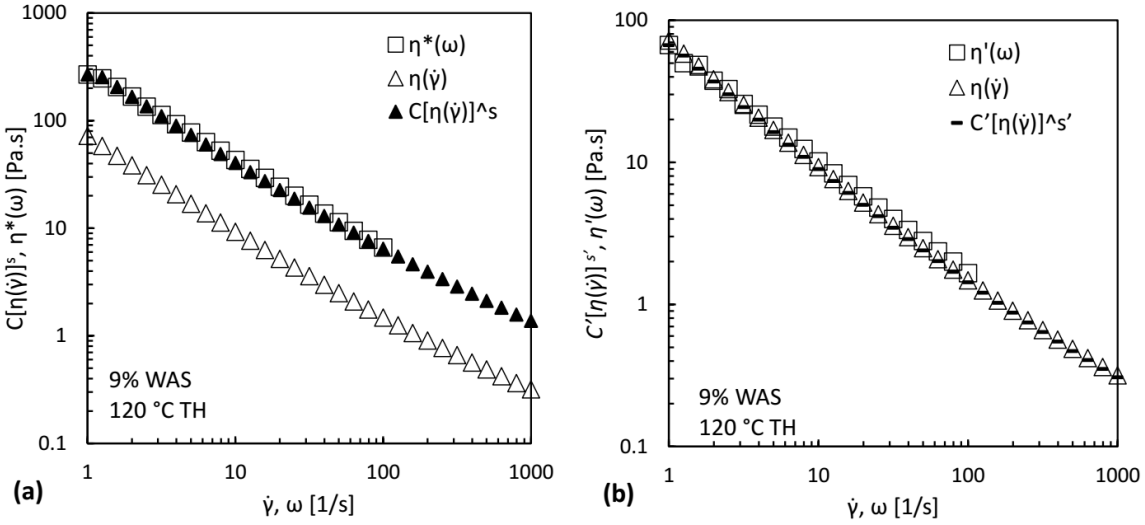

Figure 6. 6 – Comparison of (a) complex viscosity, η(ω), to steady shear viscosity, η(γ̇), and shifted steady shear viscosity, $C[\eta(\dot{\gamma})]^{s}$ and (b) dynamic viscosity, η'(ω), to steady shear viscosity and shifted steady shear viscosity, $C'[\eta(\dot{\gamma})]^{s'}$ of thermally treated (120 °C, 1 hour) 9% WAS.*

Table 6. 4 – Comparison of yield stress values obtained using different methods

		Yield stress (Pa)			
		Herschel-Bulkley	**Stress Ramp**	***G' x H***	***H***
7 wt%	Raw	127.6	175.7	135.8	0.11
	100 °C	60.4	69.3	62.5	0.13
	120 °C	39.8	36.8	44.7	0.14
	140 °C	27.1	15.9	34.1	0.23
9 wt%	Raw	255.1	376.0	253.1	0.09
	100 °C	100.2	117.0	104.4	0.13
	120 °C	63.8	46.6	66.2	0.16
	140 °C	29.7	21.9	36.7	0.17
12 wt%	Raw	1262.8	1064.9	937.6	0.045
	100 °C	215.5	257.2	231.0	0.11
	120 °C	115.1	179.9	121.1	0.13
	140 °C	67.9	88.5	76.5	0.14

6.5 CONCLUSION

Thermally treated and untreated sludges exhibited gel-like viscoelastic behaviour in low strain values (<12%). The frequency dependence of the storage (*G'*) and loss (*G"*) moduli were well described by the FKV viscoelastic model, as well as the strain response to a step stress during creep. The FKV model parameters (E_1, E_2, and α) revealed that the viscoelastic properties of thermally treated sludges were increasingly described by viscous characteristics at higher treatment temperatures, which suggests the destruction of structural components in the sludge, such as polymeric substances and EPS due to solubilization. This is reflected in the decreasing energy of cohesion values, E_c, which describe the strength of the three-dimensional sludge network. Strain sweep results did not exhibit a rising G" value near critical strain values in the G" curve, suggesting that the deformation behaviour thicker sludges may be closer to simple thick suspension systems than soft-glassy materials, as in dilute sludges. The dynamic rheological measurements are adaptable to describing steady shear results using a modified Cox-Merz rule. Since the curve trends for complex and dynamic viscosity are virtually identical, a simple horizontal shift factor can superimpose the two curves. On the other hand, the dynamic viscosity can approximate steady shear viscosity (to within 20% error) for thermally treated sludges without shifting. On the other hand, horizontal shift factors for superimposing complex viscosity and steady shear viscosity curves can be used to approximate yield stress values of the sludge to within the same order of magnitude as compared to yield stress values obtained by other methods. These open up more alternative options for in situ monitoring of TH processes via different rheometric techniques. From a practical viewpoint, the above outcomes mean that TH sludge should not be handled as a Newtonian material. This is especially the case as process parameters tend towards thicker sludge types and more economically desirable moderate TH temperatures. As sludge exhibited yield stress and viscoelastic properties at rest, appropriate consideration should be taken in the design and operation of TH processes as these rheological properties can affect the mixing, heating, and pumping performance, and subsequently cost of these processes.

REFERENCES

APHA, 1992. Standard Methods for the Examination of Water and Wastewater.

Ariunbaatar, J., Panico, A., Esposito, G., Pirozzi, F., Lens, P.N.L., 2014. Pretreatment methods to enhance anaerobic digestion of organic solid waste. Appl. Energy 123, 143–156. doi:10.1016/j.apenergy.2014.02.035

Ayol, A., Filibeli, A., Dentel, S.K., 2006. Evaluation of conditioning responses of thermophilic-mesophilic anaerobically and mesophilic aerobically digested biosolids using rheological properties. Water Sci. Technol. 54, 23–31. doi:10.2166/wst.2006.543

Barber, W.P.F., 2016. Thermal hydrolysis for sewage treatment: A critical review. Water Res. 104, 53–71. doi:10.1016/j.watres.2016.07.069

Baudez, J.C., Markis, F., Eshtiaghi, N., Slatter, P., 2011. The rheological behaviour of anaerobic digested sludge. Water Res. 45, 5675–5680. doi:http://dx.doi.org/10.1016/j.watres.2011.08.035

Baudez, J.C., Megnien, J.C., Guibelin, E., 2016. Pumping of dewatered sludge: Slipping or flowing behavior? Chem. Eng. J. 295, 494–499.

Bistany, K.L., Kokini, J.L., 1983. Dynamic viscoelastic properties of foods in texture control. J. Rheol. (N. Y. N. Y). 27, 605–620.

Canet, W., Álvarez, M.D., Fernández, C., Luna, P., 2005. Comparisons of methods for measuring yield stresses in potato puree: effect of temperature and freezing. J. Food Eng. 68, 143–153.

Carrère, H., Dumas, C., Battimelli, A., Batstone, D.J., Delgenès, J.P., Steyer, J.P., Ferrer, I., 2010. Pretreatment methods to improve sludge anaerobic degradability: A review. J. Hazard. Mater. 183, 1–15. doi:10.1016/j.jhazmat.2010.06.129

Chen, B.-H., Lee, S.-J., Lee, D.J., 2005. Rheological characteristics of the cationic polyelectrolyte flocculated wastewater sludge. Water Res. 39, 4429–4435.

Curvers, D., Saveyn, H., Scales, P.J., Van der Meeren, P., 2009. A centrifugation method for the assessment of low pressure compressibility of particulate suspensions. Chem. Eng. J. 148, 405–413. doi:10.1016/j.cej.2008.09.030

Dentel, S.K., 1997. Evaluation and role of rheological properties in sludge management. Water Sci. Technol. 36, 1–8. doi:https://doi.org/10.1016/S0273-1223(97)00662-8

Eshtiaghi, N., Markis, F., Yap, S.D., Baudez, J.C., Slatter, P., 2013. Rheological characterisation of municipal sludge: A review. Water Res. 47, 5493–5510. doi:10.1016/j.watres.2013.07.001

Farno, E., Baudez, J.C., Eshtiaghi, N., 2018. Comparison between classical Kelvin-Voigt and fractional derivative Kelvin-Voigt models in prediction of linear viscoelastic behaviour of waste activated sludge. Sci. Total Environ. 613–614, 1031–1036. doi:10.1016/j.scitotenv.2017.09.206

Farno, E., Baudez, J.C., Parthasarathy, R., Eshtiaghi, N., 2017. Net positive energy wastewater treatment plant via thermal pre-treatment of sludge: A theoretical case study. J. Environ. Sci. Heal. Part A 52, 429–432.

Farno, E., Baudez, J.C., Parthasarathy, R., Eshtiaghi, N., 2016a. Impact of thermal treatment on the rheological properties and composition of waste activated sludge: COD solubilisation as a footprint of rheological changes. Chem. Eng. J. 295, 39–48. doi:10.1016/j.cej.2016.03.022

Farno, E., Baudez, J.C., Parthasarathy, R., Eshtiaghi, N., 2016b. The viscoelastic characterisation of thermally-treated waste activated sludge. Chem. Eng. J. 304, 362–368. doi:10.1016/j.cej.2016.06.082

Farno, E., Baudez, J.C., Parthasarathy, R., Eshtiaghi, N., 2015. Impact of temperature and duration of thermal treatment on different concentrations of anaerobic digested sludge: Kinetic similarity of organic matter solubilisation and sludge rheology. Chem. Eng. J. 273, 534–542. doi:10.1016/j.cej.2015.03.097

Feng, G., Liu, L., Tan, W., 2014a. Effect of thermal hydrolysis on rheological behavior of municipal sludge. Ind. Eng. Chem. Res. 53, 11185–11192. doi:10.1021/ie501488q

Feng, G., Tan, W., Zhong, N., Liu, L., 2014b. Effects of thermal treatment on physical and expression dewatering characteristics of municipal sludge. Chem. Eng. J. 247, 223–230. doi:10.1016/j.cej.2014.03.005

Garrappa, R., 2015. Numerical evaluation of two and three parameter Mittag-Leffler functions. SIAM J. Numer. Anal. 53, 1350–1369.

Guibaud, G., Dollet, P., Tixier, N., Dagot, C., Baudu, M., 2004. Characterisation of the evolution of activated sludges using rheological measurements. Process Biochem. 39, 1803–1810. doi:10.1016/j.procbio.2003.09.002

Hii, K., Eshtiaghi, N., 2018. Measuring the viscoelastic properties of thermally treated waste activated sludge (7 - 12 wt%). doi:10.6084/m9.figshare.7245161

Jenkins, D., Richard, M.G., Daigger, G.T., 2003. Manual on the causes and control of activated sludge bulking, foaming, and other solids separation problems. Crc Press.

Koivuranta, E., Stoor, T., Hattuniemi, J., Niinimäki, J., 2015. On-line optical monitoring of activated sludge floc morphology. J. Water Process Eng. 5, 28–34. doi:https://doi.org/10.1016/j.jwpe.2014.12.009

Konigsberg, D., Nicholson, T.M., Halley, P.J., Kealy, T.J., Bhattacharjee, P.K., 2013. Online process rheometry using oscillatory squeeze flow. Appl. Rheol. 23.

Markis, F., Baudez, J.C., Parthasarathy, R., Slatter, P., Eshtiaghi, N., 2016. The apparent viscosity and yield stress of mixtures of primary and secondary sludge: Impact of volume fraction of secondary sludge and total solids concentration. Chem. Eng. J. 288, 577–587. doi:10.1016/j.cej.2015.11.107

Markis, F., Baudez, J.C., Parthasarathy, R., Slatter, P., Eshtiaghi, N., 2014. Rheological characterisation of primary and secondary sludge: Impact of solids concentration. Chem. Eng. J. 253, 526–537. doi:10.1016/j.cej.2014.05.085

Mezger, T.G., 2006. The Rheology Handbook: For Users of Rotational and Oscillatory Rheometers, Coatings compendia. Vincentz Network.

Morgan-Sagastume, F., Pratt, S., Karlsson, a., Cirne, D., Lant, P., Werker, a., 2011. Production of volatile fatty acids by fermentation of waste activated sludge pre-treated in full-scale thermal hydrolysis plants. Bioresour. Technol. 102, 3089–3097. doi:10.1016/j.biortech.2010.10.054

Mori, M., Seyssiecq, I., Roche, N., 2006. Rheological measurements of sewage sludge for various solids concentrations and geometry. Process Biochem. 41, 1656–1662. doi:10.1016/j.procbio.2006.03.021

Mouzaoui, M., Baudez, J.-C., Sauceau, M., Arlabosse, P., 2018. Experimental rheological procedure adapted to pasty dewatered sludge up to 45% dry matter. Water Res. 133, 1–7.

Nicolle, S., Vezin, P., Palierne, J.F., 2010. A strain-hardening bi-power law for the nonlinear behaviour of biological soft tissues. J. Biomech. 43, 927–932. doi:10.1016/j.jbiomech.2009.11.002

Pérez-Elvira, S.I., Fdz-Polanco, F., 2012. Continuous thermal hydrolysis and anaerobic digestion of sludge. Energy integration study. Water Sci. Technol. 65, 1839–1846. doi:10.2166/wst.2012.863

Pérez-Elvira, S.I., Fernández-Polanco, F., Fernández-Polanco, M., Rodríguez, P., Rouge, P., 2008. Hydrothermal multivariable approach. Full-scale feasibility study. Electron. J. Biotechnol. 11. doi:10.2225/vol11-issue4-fulltext-14

Perez, Y.G., Leite, S.G.F., Coelho, M.A.Z., 2006. Activated sludge morphology characterization through an image analysis procedure. Brazilian J. Chem. Eng. 23, 319–330.

Rao, M.A., Cooley, H.J., 1992. Rheological behavior of tomato pastes in steady and dynamic shear. J. Texture Stud. 23, 415–425.

Ratkovich, N., Horn, W., Helmus, F.P., Rosenberger, S., Naessens, W., Nopens, I., Bentzen, T.R., 2013. Activated sludge rheology: A critical review on data collection and modelling. Water Res. 47, 463–482. doi:10.1016/j.watres.2012.11.021

Sapkaite, I., Barrado, E., Fdz-Polanco, F., Pérez-Elvira, S.I., 2017. Optimization of a thermal hydrolysis process for sludge pre-treatment. J. Environ. Manage. 192, 25–30. doi:10.1016/j.jenvman.2017.01.043

Schiessel, H., Metzler, R., Blumen, A., Nonnenmacher, T.F., 1995. Generalized viscoelastic models: their fractional equations with solutions. J. Phys. A. Math. Gen. 28, 6567.

Spriggs, T.W., Huppler, J.D., Bird, R.B., 1966. An experimental appraisal of viscoelastic models. Trans. Soc. Rheol. 10, 191–213.

Suárez-Iglesias, O., Urrea, J.L., Oulego, P., Collado, S., Díaz, M., 2017. Valuable compounds from sewage sludge by thermal hydrolysis and wet oxidation. A review. Sci. Total Environ. 584–585, 921–934. doi:10.1016/j.scitotenv.2017.01.140

Tschoegl, N.W., 2012. The phenomenological theory of linear viscoelastic behavior: an introduction. Springer Science & Business Media.

Wang, H.-F., Wang, H.-J., Hu, H., Zeng, R.J., 2017. Applying rheological analysis to understand the mechanism of polyacrylamide (PAM) conditioning for sewage sludge dewatering. RSC Adv. 7, 30274–30282.

Xu, Q., Bhattacharjee, P.K., Allitt, D., Eshtiaghi, N., Parthasarathy, R., 2018. Evolution of flow regimes in non-Newtonian liquids under gas sparging. Chem. Eng. Sci. 176, 153–156. doi:10.1016/j.ces.2017.10.034

Yuan, D., Wang, Y., 2013. Influence of extracellular polymeric substances on rheological properties of activated sludge. Biochem. Eng. J. 77, 208–213.

Yuan, D., Wang, Y., Qian, X., 2017. Variations of internal structure and moisture distribution in activated sludge with stratified extracellular polymeric substances extraction. Int. Biodeterior. Biodegradation 116, 1–9.

Zhang, J., Xue, Y., Eshtiaghi, N., Dai, X., Tao, W., Li, Z., 2017. Evaluation of thermal hydrolysis efficiency of mechanically dewatered sewage sludge via rheological measurement. Water Res. 116, 34–43. doi:10.1016/j.watres.2017.03.020

Zhen, G., Lu, X., Kato, H., Zhao, Y., Li, Y.Y., 2017. Overview of pretreatment strategies for enhancing sewage sludge disintegration and subsequent anaerobic digestion: Current advances, full-scale application and future perspectives. Renew. Sustain. Energy Rev. 69, 559–577. doi:10.1016/j.rser.2016.11.187

Zhou, Y., Takaoka, M., Wang, W., Liu, X., Oshita, K., 2013. Effect of thermal hydrolysis pre-treatment on anaerobic digestion of municipal biowaste: A pilot scale study in China. J. Biosci. Bioeng. 116, 101–105. doi:10.1016/j.jbiosc.2013.01.014

CHAPTER 7:

PRACTICAL ENGINEERING IMPLICATIONS

7.1 INTRODUCTION

Hydrothermal processing markedly alters the rheology of waste activated sludge (WAS). Compared to untreated sludge, the high-shear viscosity ($600s^{-1}$) and yield stress of thermally treated sludge at 25 °C was 14-72% and 9-60% of their original values at 25 °C (Figure 4.3), respectively, depending on treatment temperature within the range of 80-140°C. The G' and G" of treated sludge were also 8-39% and 13-50% their original values (Figure 6.3), respectively, for the range of temperatures studied. These rheological parameters would decrease even further in situ at treatment temperature, as previously shown by equations 5.5 and 5.6. Indeed, the pronounced rheological changes demonstrated in the preceding chapters highlight the significance of considering rheological parameters as a part of the efficient design and operation of high-temperature sludge-handling processes. It also reveals areas for optimization in hydrothermal processing in sludge treatment systems. For example, studies on the energy balance around TH systems have shown that hydrothermal processing of sludge is a net positive energy process (Barber, 2016; Pilli et al., 2015), even without considering additional savings which could be achieved in the ancillary processes, such as mixers and pumps, due to sludge rheological enhancements. This chapter explores some practical implications of the findings in this thesis and their significance for engineering applications.

7.2 DISCUSSION

The results from this thesis can be applied to several practical engineering applications. A few note-worthy areas are explored below with examples. These include applications in pump design, heat exchanger design, process monitoring, the impact of sludge concentration and its viscoelastic properties, and the potential research implications for using oscillatory rheological measurements to approximate steady-shear measurements.

7.2.1 PUMP DESIGN

In pumping operations, the frictional head losses are dependent upon sludge viscosity and yield stress (Anderson et al., 2008). Then, the reduction of yield stress and viscosity due to thermal treatment of sludge can lead to reduced pumping cost (Farno et al., 2017). The sludge yield stress is used in the Reynolds-3 friction loss model to determine the transition pipe flow velocity from laminar to turbulent (Slatter, 2008). These rheological parameters that are of high significance for sizing pump power, can be acquired using the equations presented in this study. For example, given a thermal hydrolysis (TH) pre-

treatment process (130 °C and 60 minutes) treating waste activated sludge (WAS) of 10 wt% solids content, the frictional head losses for pumping incoming (feed) and exiting (thermally treated) sludge from the TH reactor can be estimated. Assumptions for this calculation is presented in Table 7.1:

Table 7. 1 – Example parameters for calculating pump requirements.

	Incoming	Exiting
Temperature	25 °C	130 °C
Density (Honey and Pretorius, 2000)	1015 kg/m^3	1015 kg/m^3
Sludge concentration	10 wt%	10 wt%
Pipe diameter (Anderson et al., 2008)	200 mm	200 mm
Pipe length	100 m	100 m

Since sludge is relatively thickened, settling is unlikely to occur; laminar pipe flow is reasonable for pumping thickened sludge (Anderson et al., 2008). Furthermore, Herschel-Bulkley fluids are seldom operated in turbulent regime owing to high pressure drops which subsequently results in high pumping power (Swamee and Aggarwal, 2011). Then, the critical velocity for onset of transition to turbulent flow region can be determined using the proposed Reynolds-3 friction loss model as follows (Slatter, 2008):

$$Re_3 = \frac{8\rho V_{ann}^2}{\left(\sigma_c + k\left(\frac{8V_{ann}}{D_{shear}}\right)^n\right)} \qquad (Eq.7.1)$$

Where ρ (kg/m^3) is the sludge density, V_{ann} (m/s) is the sludge annular velocity, D_{shear} (m) is the diameter of the sheared-zone of the fluid, σ_c (Pa), k (Pa.s^n) and n (-) are the Herschel-Bulkley parameters, yields stress consistency index and flow index. It is assumed that transitional pipe flow occurs at Re_3 = 2100 similar to thickened mineral slurries. To solve Eq. 7.1, the Herschel-Bulkley parameters for the incoming and exiting sludge must be determined.

For incoming sludge (10 wt%, untreated, 25 °C), σ_c and k can be approximated using the master curve parameters (Figure 5.2, Tables A.5-1 and A.5-2) and equations 4.6 and 4.7. Firstly, master curve shift factors S_y and S_x were determined for 9 wt% sludge as the closest approximation. From Table A.5-1, 130 °C untreated, 9 wt%, S_y=0.96; from Table A.5-2, 130 °C untreated, 9 wt%, S_x=0.78. Then, from equations 4.6 and 4.7:

$$k = 19.97\left(\frac{0.86}{0.61^{0.4}}\right) = 20.9\ Pa.s^n$$

$\sigma_c = 81.33 * 0.86 = 69.9\ Pa$

Alternatively, using the power-law relationship with solids concentration for untreated sludge (Figure S.5.6), the *k* and σ_c of 10 wt% untreated sludge can be approximated:

$k_0 = 8555(0.1)^{2.5} = 27.1\ Pa.s^n$

$\sigma_{c,0} = 113469(0.1)^{3.1} = 90.1\ Pa$

Then, to obtain the critical velocity which transition happens in pipe flow Re_3 can be used,

$$Re_3 = 2100 = \frac{8 * 1015 * V_{ann}^2}{90.1 + 27.1\left(\frac{8 * V_{ann}}{D_{shear}}\right)^{0.4}}$$

Detailed steps for solving Re_3 is presented in Appendix 7.1, but for Re_3 = 2100, the following parameters are true:

$V_{ann} = 10.43\ \frac{m}{s}$

$D_{shear} = 0.16\ m$

$V_{critical} = 10.62\ \frac{m}{s}$

The critical velocity for transitional pipe flow of 10 wt% WAS at 25 °C is rather high. In practical terms, this means the thickened raw WAS is unlikely to reach transitional or turbulent flow at the given pipe diameter (200 mm) under common sludge pumping velocities of around 4 m/s (Anderson et al., 2008). This is reasonable given the pasty nature of thickened WAS.

For the exiting sludge, post-thermal treatment it is assumed the sludge concentration remains unchanged. Then, σ_c and *k* can be determined using Eq. 5.2 and Eq. 5.3:

$$k_i \Big/ k_{7,0} = -A_2(130) - B_2 \ln(60) + C_2$$

Here, $k_{7,0}$ = 9.86 Pa was determined using the master curve, following the procedures described above, for untreated sludge at 25 °C with 7 wt% solids concentration.

A_2, B_2, and C_2 are determined for 10 wt% WAS using Eq. 5.4:

$A2=5 \times 0.12.6 A_2 = 5\ \times\ 0.1^{2.6} = 0.0126$

$$B_2 = 50 \times 0.1^{2.8} = 0.079$$

$$C_2 = 975 \times 0.1^{2.6} = 2.45$$

Then,

$$k_i/_{9.86} = 0.49$$

Then k_i = 4.83 Pa was calculated.

Similarly, σ_c is determined:

$$\sigma_{c,i}/_{\sigma_{c7,0}} = -A_3(130) - B_3 \ln(60) + C_3$$

Such that σ_c = 2.19 Pa. Then, solving for Re_3, the velocity for transitional pipe flow is determined (example calculations in Appendix 7.1):

$$V_{critical} = 3.05 \frac{m}{s}$$

This means the critical velocity for transitional pipe flow is reduced to one third of its value compared to untreated sludge. Pumping thermally-treated sludge exiting the TH reactor at velocities greater than 3.05 m/s may be desirable to assist heat transfer, as well as reduce the likelihood of solids settling in the pipes.

Subsequently, the pumping requirements for the incoming and exiting sludge to the TH reactor can be calculated, given the conditions in Table 7.1.

For the incoming sludge, since it is quite thickened (10 wt%) and rheological parameters are quite high, particle settling is not a likely concern. Then, sludge should be pumped at velocities below V_c = 10.62 m/s to maintain laminar flow and reduce head losses.

For laminar flow of Herschel-Bulkley fluids, pumping power requirements can be determined (Swamee and Aggarwal, 2011):

$$P = \frac{8fL\rho}{\pi^2 D^5} Q^3 \qquad (Eq. 7.2)$$

Where f is the friction factor, L (m) is pipe length, Q (m^3/s) is flow rate. The friction factor, f, can be calculated from (Swamee and Aggarwal, 2011):

$$f \times Re = 64 + 64\left(\frac{He}{\left(36 + \left(\frac{1.5}{n}\right)^{2.46}\right)^{0.5} Re}\right)^{\frac{0.958n}{2-n}} \quad (Eq.7.3)$$

, where *He* is the Hedstrom number and *Re* is the generalized Reynolds given by:

$$Re = \frac{8D^n V^{2-n}\rho}{k}\left(\frac{0.5n}{1+3n}\right)^n \quad (Eq.7.4)$$

$$He = \frac{D^2\rho}{k}\left(\frac{\sigma_c}{k}\right)^{\frac{2-n}{n}} \quad (Eq.7.5)$$

To maintain laminar flow conditions, assume the incoming sludge is pumped at 5 m/s. Then the following parameters are calculated:

$$Re = \frac{8(0.2)^{0.4}(5^{2-0.4})(1015)}{27.1}\left(\frac{0.5 \times 0.4}{1+3\times 0.4}\right)^{0.4} = 792.1$$

$$He = \frac{0.2^2(1015)}{27.1}\left(\frac{90.1}{27.1}\right)^{\frac{2-0.4}{0.4}} = 183.05$$

$$f \times Re = 64 + 64\left(\frac{183.05}{\left(36 + \left(\frac{1.5}{0.4}\right)^{2.46}\right)^{0.5} 792.1}\right)^{\frac{0.958\times 0.4}{2-0.4}} = 91.5$$

$$f = \frac{91.5}{792.1} = 0.12$$

Then, pumping power for untreated sludge is:

$$P = \frac{8fL\rho}{\pi^2 D^5}Q^3 = \frac{8(0.12)(100)(1015)}{\pi^2(0.2)^5}(5 \times \pi\left(\frac{0.2}{2}\right)^2)^3 = 119.58\ kW$$

For the exiting sludge, it is assumed turbulent conditions are required, so sludge is pumped at V = 5 m/s which is greater than the critical velocity of 3.05 m/s.

For turbulent conditions, the friction factor can be calculated (Slatter, 2001):

$$\frac{1}{\sqrt{f}} = \frac{4}{n^{0.75}}\log\left(Re_{MR} \times f^{\left(\frac{2-n}{2}\right)}\right) - \frac{0.4}{n^{1.2}} \quad (Eq.7.6)$$

$$Re_{MR} = \frac{8\rho V^2}{k\left(\frac{8V}{D}\right)^n} \qquad (Eq.\,7.7)$$

And pump power can be determined (Swamee and Aggarwal, 2011):

$$P = Q\Delta p \qquad (Eq.\,7.8)$$

Where Q is the mass flow rate (m^3/s) and the pressure drop, Δp (Pa), can be determined (Anderson et al., 2008):

$$\Delta p = \frac{2f\rho LV^2}{D} \qquad (Eq.\,7.9)$$

Then, the following are calculated:

$$Re_{MR} = \frac{8(1015)(5)^2}{4.83\left(\frac{8\times 5}{0.2}\right)^{0.4}} = 5048.2$$

$$\frac{1}{\sqrt{f}} = \frac{4}{0.4^{0.75}}\log\left(5048.2 \times f^{\left(\frac{2-0.4}{2}\right)}\right) - \frac{0.4}{0.4^{1.2}}$$

$$f = 0.0015$$

$$\Delta p = \frac{2(0.0015)(1015)(100)(5)^2}{0.2} = 38062.5\ Pa$$

$$P = 5\left(\pi \times \left(\frac{0.2}{2}\right)^2\right)(38062.5) = 5.98\ kW$$

From above calculations, the pumping power required to transport untreated sludge was 119.58 kW, whereas for thermally-treated sludge it was 5.98 kW. Given that the pipe dimensions and velocity were kept constant between the two conditions and the only difference was in rheological parameters of the sludge, it is apparent that the pumping of thermally-treated sludge was tremendously reduced. As demonstrated, these values were determined reliably based on the availability of required rheological parameters.

7.2.2 HEAT EXCHANGER DESIGN

Typically, it is desirable to utilise high temperature of thermally treated sludge to heat feed sludge as it travels between the TH reactor and subsequent anaerobic digester (Pilli et al., 2015). As the treated sludge

is cooled across the temperature gradient of the heat-exchange surface, it is reasonable to expect its viscosity and yield stress to increase gradually. For example, the apparent viscosity and yield stress of treated WAS at 140 °C was only about 10% its value at 80 °C. Since rheological parameters are related to a fluid's velocity profile and residence time in a heat exchanger (Tucker, 2017), variation in sludge rheological parameters due to temperature changes will affect the heat-transfer performance. Then, heat exchangers must be designed accordingly to accommodate these variations. The relationships presented earlier (e.g. Eq. 5.3) help to estimate correct values of rheological parameters, with respect to temperature, useful in design. For example, heat transfer equations for heat transfer coefficients in non-Newtonian fluids requires values for the fluid viscosity (Peixinho et al., 2008):

$$\frac{hD}{\kappa} = 0.0152 \times \left(\frac{\rho V D}{\eta_w}\right)^{0.845} \times \left(\frac{\nu}{\kappa}\right)^{\frac{1}{3}} \qquad (Eq. 7.10)$$

Where h is the heat transfer coefficient ($Wm^{-2}K^{-1}$), κ is the thermal conductivity of the fluid ($Wm^{-1}°C^{-1}$), η_w is the fluid viscosity at the wall (Pa.s), and ν is the kinematic viscosity (m^2s^{-1}).

Assuming the same conditions as the example from 7.1.1 of thermally-treated sludge (130 °C, 10 wt%) exiting the TH reactor and assuming temperature at the pipe wall to be 120 °C, the apparent viscosity at the pipe wall can be determined. Assuming sludge travelling at velocity of 5 m/s, the apparent wall shear-rate is calculated:

$$\frac{8V}{D} = \frac{8(5)}{0.2} = 200\ s^{-1}$$

Then, from figure S5.5 the flow curve parameters for 10 wt% WAS at 120 °C is determined:

$$k_i = 1808.1(0.1)^{2.8} = 2.87\ Pa.s^n$$

$$\sigma_{c,i} = 7365(0.1)^{2.8} = 11.7\ Pa$$

Then, the flow curve representing the 10 wt% WAS at 120 °C is:

$$\sigma = 11.7 + 2.87(\dot{\gamma})^{0.4}$$

The apparent viscosity at the wall is determined:

$$\sigma = 11.7 + 2.87(200)^{0.4} = 35.6\ Pa$$

$$\eta_w = \frac{\sigma}{\dot{\gamma}} = \frac{35.6}{200} = 0.18\ Pa.s$$

Then, the heat transfer coefficient can be determined from Eq.7.10:

Assuming thermal conductivity equal to water, κ = 0.677 $Wm^{-1}K^{-1}$,

$$\frac{h(0.2)}{(0.677)} = 0.0152 \times \left(\frac{(1015)(5)(0.2)}{0.18}\right)^{0.845} \times \left(\frac{\frac{0.18}{1015}}{0.677}\right)^{\frac{1}{3}}$$

$$h = 4.87\frac{W}{m^2K}$$

Then, assuming the sludge is cooled to ambient conditions (25 °C) by the end of the heat exchanger, the flow curve parameters for the cooled, thermally treated sludge can be determined from Equations 5.5 and 5.6:

$$11.7 = \sigma_{c,f}(-0.0036\ (120) + 1)$$

$$\sigma_{c,f} = 20.6\ Pa$$

$$2.87 = k_f(-0.0055\ (120) + 1)$$

$$k_f = 8.44\ Pa.s^n$$

Then, the flow curve describing 10 wt% WAS thermally-treated at 120 °C but cooled to 25 °C is:

$$\sigma = 20.6 + 8.44(\dot{\gamma})^{0.4}$$

Similarly, the apparent viscosity is determined as above:

$$\eta_w = \frac{\sigma}{\dot{\gamma}} = \frac{99.2}{200} = 0.5\ Pa.s$$

Then, calculating heat transfer coefficient as described above yields:

$$h = 2.89\frac{W}{m^2K}$$

Then, as the sludge cools along the heat exchanger, it becomes increasingly viscous and the heat transfer coefficient is similarly reduced.

Given the rheological parameters of the cooled sludge have changed compared to when it first exited the TH reactor, a check for turbulent flow conditions can be performed as previously described for Re_3. Assuming sludge still flows at 5 m/s velocity:

$$Re_3 = 2064$$

Since Re_3 of the cooled thermally-treated sludge is reduced (compared to Re_3 = 4913 for thermally treated sludge at 130 °C when exiting the reactor) and less than 2100, there is likelihood it will flow under laminar conditions at the exit of the pipe. Using the calculations above, the pumping velocity can be adjusted to achieve the desired flow conditions, as the examples here have demonstrated.

7.2.3 PROCESS PERFORMANCE MONITORING

Besides above examples, equations 5.1-5.4 allow quick estimation of in-situ WAS rheology at various treatment conditions. Having in-situ WAS rheological parameters is useful in monitoring TH performance). Also, as discussed in Chapter 5, the in-situ measurements suggest that sludge concentration does not impact the effectiveness of TH, as the extent and rate of rheological changes was almost equal at different concentrations (Figure 5.3 inset). This new information provides engineers with a certain degree of flexibility in choosing sludge concentrations for TH, since varying sludge concentration would not negatively impact its solubilization effectiveness. This information is useful when there is a need to vary sludge concentration in order to maximize biogas production while also maintain a good heating efficiency (Barber, 2016). Furthermore, as there is minimal rheological changes at treatment times beyond 30 minutes (Figures S.5.1 – S.5.3) and organic matter solubilisation, TH treatment time can be optimised to reduce heating cost and increase sludge throughput based on observed sludge rheological behaviours and its link to solubilisation. In addition, in Chapter 4, a linear relationship was shown between changes of the amount of organic matter solubilisation and changes of rheological properties. So, monitoring process performance via rheological properties is possible instead of time consuming and offline measurements of the amount of solubilisation of organic matter via COD test.

An example is presented here for monitoring the performance of TH processes. Given a TH process was to be carried out at 125 °C on 8 wt% WAS. It was required to optimize the treatment duration by stopping the TH treatment once the sludge reaches minimal changes in solubilization. Assume that the untreated 8 wt% sludge had soluble COD value of sCOD = 3500 mg/L; and when diluted to 7 wt% it has high-shear apparent viscosity (measured at 600 s^{-1} shear rate), $\eta_{\infty,0}$ = 0.3 Pa.s. Then, the extent of solubilization can

be estimated by observing the extent of change in the sludge viscosity during TH. It has been shown that regardless of sludge concentration, the extent of rheological changes was relatively constant (Chapter 5; Tables A.5.4 – A.5.6). Then, equation 4.12 can be used to estimate the extent of viscosity reduction at different times during TH.

Examining treatment time of 5 min, 10 min, 20 min, and 40 min:

$$\eta_{\infty,i}/\eta_{\infty,0} = 0.92 - 0.006\,(125) - 0.026\,Ln(5) = 0.128$$

$$\eta_{\infty,i}/\eta_{\infty,0} = 0.92 - 0.006\,(125) - 0.026\,Ln(10) = 0.110$$

$$\eta_{\infty,i}/\eta_{\infty,0} = 0.92 - 0.006\,(125) - 0.026\,Ln(20) = 0.092$$

$$\eta_{\infty,i}/\eta_{\infty,0} = 0.92 - 0.006\,(125) - 0.026\,Ln(40) = 0.074$$

$$\eta_{\infty,i}/\eta_{\infty,0} = 0.92 - 0.006\,(125) - 0.026\,Ln(60) = 0.064$$

Then, the estimated evolution of $\eta_{\infty,i}/\eta_{\infty,0}$ can be plotted over time (Figure 7.1). Assuming a cut-off point of 3% change in the solubilization of the sludge for efficient process, then from Figure 7.1, it can be seen that limiting values of apparent viscosity reduction have been reached by 20 minutes treatment time. Then, treatment times beyond 20 minutes gave negligible changes which implies suboptimal energy efficiency in terms of sludge solubilisation.

At 20 minutes, the solubilization of COD may be estimated from Figure 4.6:

$$rsCOD = -2.6\left(\eta_{\infty}/\eta_{\infty,0}\right) + 2.5$$

$$rsCOD = -2.6(0.092) + 2.5$$

$$rsCOD = 2.3$$

Then an increase in soluble COD upwards by a factor of 2.3 can be expected due to solubilization at 20 minutes of 125 °C TH treatment.

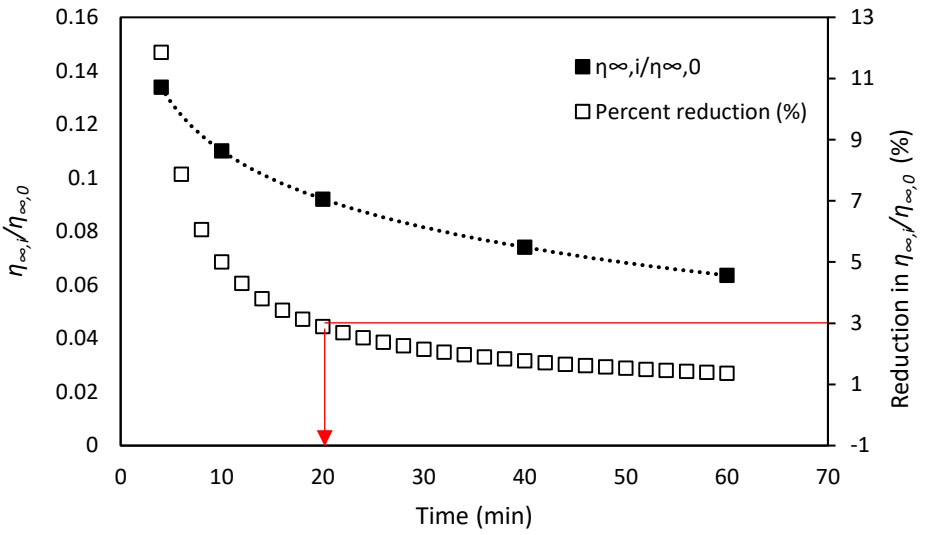

Figure 7. 1 – Estimated evolution of 8wt% WAS apparent viscosity during 125 °C thermal treatment.

7.2.4 IMPACT OF SLUDGE CONCENTRATION

As demonstrated in Chapter 5, the impact of WAS concentration on rheology during TH are significant as in situ measurement is still showing a power-law increase of yield stress with concentration (Figure S.565) and this matter should not be overlooked. In some TH processes, sludge concentration varies as a result of dilution by process steam, as well as by the addition water to dilute the treated sludge (Barber, 2016). Then, in the case of highly concentrated WAS, a significant drop in its yield stress and apparent viscosity should be expected as it becomes diluted. Sludge-handling equipment must be appropriately designed to accommodate these changes in order to maintain the desired flow conditions.

As TH processes is more economical at thicker feed sludges, sludge viscoelastic properties are also important to be considered in process design. Viscoelastic measurements in Chapter 6 showed gel-like, viscoelastic behaviour still existed in thermally-treated WAS despite significant reduction in *G'* and *G"*. This must be taken into consideration when designing mixing systems, since the presence of viscoelasticity determines the mixing power (Reviol et al., 2016). This becomes particularly important in anaerobic digestion where efficient mixing is required to ensure adequate contact between the treated sludge and microorganisms. The viscoelastic parameters *G'*, *G"*, τ, and yield stress plays significant role in the formation of inactive zones during mixing (Bhattacharjee et al., 2017).

An example is shown below to demonstrate the impact of changing sludge concentrations during TH on mixing power requirements.

Given a TH process at 120 °C treating 12 wt% sludge. At the end of treatment, water was added to dilute the sludge to 9 wt% in order to control ammonia inhibition in downstream anaerobic digestion process (Barber,2016). The change in mixing power can be determined. It is assumed the rheological parameters of the untreated sludge, initially at 7 wt%: k = 4.5 Pa.s^n, σ_c = 44 Pa, n = 0.4.

The equation for calculating power consumption in a mixer for power law fluid is given (Shamlou and Edwards, 1985):

$$P = \frac{\pi^2 h D_T^2 N k (4\pi N)^n}{\left(n\left(1-\left(\frac{D_i}{D_T}\right)^{\frac{2}{n}}\right)\right)^n} \qquad (Eq.7.11)$$

Where, P = power input (W); h = impeller height (m); D_T = tank diameter (m); N = impeller rotational speed (rps); D_i = impeller diameter (m).

It is assumed a tank diameter 0.5 m; an agitator height of 0.5 m; agitator diameter of 0.3 m and agitator speed of 2 rps.

To solve Eq. 7.1.1, the consistency index, k, must be determined for 12 wt% sludge at 120 °C and 60 min TH; using Eq. 5.2:

$$k_i/k_{7,0} = -A_2(T) - B_2\ln(t) + C_2$$

$$A_2 = 5 \times 0.12^{2.6} = 0.02$$

$$B_2 = 50 \times 0.12^{2.8} = 0.13$$

$$C_2 = 975 \times 0.12^{2.6} = 3.9$$

$$k_i/k_{7,0} = -0.02(120) - 0.13\ln(60) + 3.9$$

$$k_i/4.5 = 0.97$$

$$k_i = 4.5 * 0.97 = 4.36\ Pa.s^n$$

Similarly, k for 9 wt% sludge due to dilution can be determined at 120 °C and 60 minutes:

$$k_i/k_{7,0} = -A_2(T) - B_2\ln(t) + C_2$$

$A_2 = 5 \times 0.09^{2.6} = 0.01$

$B_2 = 50 \times 0.09^{2.8} = 0.06$

$C_2 = 975 \times 0.09^{2.6} = 1.86$

$$k_i/k_{7,0} = -0.01(120) - 0.06\ln(60) + 1.86$$

$$k_i/_{4.5} = 0.41$$

$k_i = 4.5 * 0.41 = 1.85\ Pa.s^n$

Since all flow curves measured in-situ could be described by a single master curve (Fig 5.2), the *n* = 0.4 value applies at any condition of treatment. Then the power required for mixing prior to sludge dilution:

$$P = \frac{\pi^2(0.5)(0.5^2)(2)(4.36)(4\pi \times 2)^{0.4}}{\left(0.4\left(1 - \left(\frac{0.3}{0.5}\right)^{\frac{2}{0.4}}\right)\right)^{0.4}} = 58.2\ W$$

Then, after sludge was diluted to 9 wt%:

$$P = \frac{\pi^2(0.5)(0.5^2)(2)(1.85)(4\pi \times 2)^{0.4}}{\left(0.4\left(1 - \left(\frac{0.3}{0.5}\right)^{\frac{2}{0.4}}\right)\right)^{0.4}} = 24.7\ W$$

A mixing power reduction of about 60% would occur due to the sludge dilution, which could be determined by estimating changes in rheological parameters during TH, based on varying sludge concentrations. This can help to optimise the required mixing power for when sludge concentration is varied in the reactor, which in turn contributes to electricity cost savings.

7.2.5 VISCOELASTICE BEHAVIOUR OF THERMALLY TREATED SLUDGE

The frequency response (Figure 6.4) revealed gel stability in the treated sludge, since the slope of the G' at different frequencies was relatively small and G' was mostly greater than 100 Pa at low angular velocities. This means the sludge exhibits strong structural strength at rest. Then, the sludge is unlikely to exhibit settling and phase separation (Mezger, 2006). This would imply, at least for the range of sludge concentrations studied, there is not a need to pump sludge under turbulent conditions for the purpose of mitigating blockages due to settling effects. On the other hand, it also validates the observed improved

dewaterability of thermally-treated sludges by other researchers such as Feng et al. (2014b) and Wang et al. (2017) since G' values of treated sludge are significantly reduced compared to untreated sludge. The frequency and creep responses of highly concentred sludge were described for the first time by the FKV model across all treatment conditions studied. The FKV model can be used in CFD programs to reliably design and optimise the efficiency of pumping, mixing systems and heat exchangers.

7.2.6 APPROXIMATING STEADY SHEAR PROPERTIES FROM OSCILLATORY MEASUREMENT

The comparability between dynamic viscosity and steady shear viscosity (Chapter 6.4.2) allows viscoelastic data, as obtained from oscillatory measurements, to approximate steady-shear data.

As sludge handling is being carried out at increasingly higher sludge concentrations, difficulties arise in its reliable rheological measurement in traditional steady-shear methods. This is due to challenges related to overcoming edge effects and cracking of the sample in steady-shear because of the pasty nature of the thickened sludge. Researchers have proposed various methods for characterizing the rheological properties of highly concentrated sludges (15 – 45 wt%) (Baudez et al., 2016; Mouzaoui et al., 2018). However, for sludges of moderately high concentration (<15 wt%) and thermally-treated sludge, the modified Cox-Merz approach (Chapter 6.4.2) offers a much more simple, alternative solution. This method provides a non-destructive measurement technique for collecting sludge flow data through oscillation data. Furthermore, it suggests that online rheometers which operate based on colleting viscoelastic data can potentially be used to generating steady-shear parameters.

An alternative method of calculating yield stress from oscillatory measurement (Table 6.4) was also suggested, which can be a quick way to approximate yield stress values for design calculations such as those examples previously described.

7.3 CONCLUSION

This chapter presented some of the potential areas of applying the knowledge developed within this thesis, particularly in sludge-handling applications and hydrothermal sludge processes. An illustration of how to utilize the developed master flow curve for thermally treated sludge was demonstrated, and how the rheological parameters obtained are essential to correctly sizing pumps and heat transfer units. Usage of

the in-situ equations for estimating sludge rheological parameters during TH from after thermal treatment data were also demonstrated in the examples provided. The significance of sludge concentration with regard to its impact on TH processes and the implications of the viscoelastic properties of thermally-treated sludge were also discussed. Finally, the significance of the oscillatory measurements as a means of approximating steady-shear parameters provides a new way of non-destructive technique for rheological characterisation of highly concentrated sludge.

APPENDIX 7.1 REYNOLDS-3 CALCULATIONS

For Herschel-Bulkley fluids, the transitional pipe flow is determined using the Reynolds-3 number (Slatter, 2008):

$$Re_3 = \frac{8\rho V_{ann}^2}{(\sigma_c + k\left(\frac{8V_{ann}}{D_{shear}}\right)^n)}$$

The rheological parameters of the sludge were determined:

σ_c = 90.1 Pa

k = 27.1 Pa.s^n

n = 0.4

Firstly, a wall shear stress was assumed as some factor of the yield stress:

$\sigma_w = 1.25(\sigma_c) = 1.25*(90.1) = 112.63$ Pa.

Then, sludge velocity was determined using (Slatter, 2008):

$$\frac{8V}{D} = \frac{4n}{k^{\frac{1}{n}}\sigma_c^3}(\sigma_w - \sigma_c)^{\frac{1+n}{n}} \qquad (Eq.7.11)$$

Solving for V gives the fluid velocity:

$$\frac{8V}{0.2} = \frac{4(0.4)}{27.1^{\frac{1}{(0.4)}} \times 90.1^3}(112.63 - 90.1)^{\frac{1+0.4}{0.4}}$$

$$V = 0.003\frac{m}{s}$$

Plug radius is determined:

$$r_{plug} = \left(\frac{D}{2}\right)\left(\frac{\sigma_c}{\sigma_w}\right) = \left(\frac{0.2}{2}\right)\left(\frac{90.1}{112.63}\right) = 0.08\,m$$

Sheared diameter is determined:

$$D_{shear} = D - 2(r_{plug}) = 0.2 - 2(0.08) = 0.04\,m$$

Plug area is determined:

$$A_{plug} = \pi(r_{plug})^2 = 0.02\,m^2$$

Area of sheared annulus is determined:

$$A_{ann} = A - A_{plug} = \pi\left(\frac{0.2}{2}\right)^2 - 0.02 = 0.011\,m^2$$

Plug velocity is determined:

$$V_{plug} = \frac{1}{\left(k^{\frac{1}{n}}\right)\left(\frac{2\sigma_w}{D}\right)}\left(\frac{n}{n+1}\right)(\sigma_w - \sigma_c)^{\frac{n+1}{n}} = \frac{1}{\left(27.1^{\frac{1}{0.4}}\right)\left(\frac{2 \times 112.63}{0.2}\right)}\left(\frac{0.4}{0.4+1}\right)(112.63 - 90.1)^{\frac{0.4+1}{0.4}}$$

$$V_{plug} = 0.0036\frac{m}{s}$$

Then, volumetric flow rate of the plug is determined:

$$Q_{plug} = A_{plug} \times V_{plug} = 0.02(0.0036) = 7.24 * 10^{-5}\,m^3/s$$

Then, flow rate of the annular gap is determined:

$$Q_{ann} = Q - Q_{plug} = 0.003 \times \pi\left(\frac{0.2}{2}\right)^2 - 7.24 * 10^{-5} = 3.1 * 10^{-5}\,m^3/s$$

Then, velocity of the annular gap is determined:

$$V_{ann} = \frac{Q_{ann}}{A_{ann}} = \frac{3.1 \times 10^{-5}}{0.011} = 0.0027\frac{m}{s}$$

Then, Re_3 is solved by replacing known terms:

$$Re_3 = \frac{8(1015)(0.0027)^2}{\left(90.1 + 27.1\left(\frac{8 \times 0.0027}{0.04}\right)^{0.4}\right)} = 0.00055$$

Since this value of Re_3 is very low, the wall shear stress, σ_w, from the first step is re-evaluated by multiplying σ_c with a new factor. The above calculations are repeated until Re_3=2100 is obtained, such that:

σ_w = 5.05(σ_c) = 5.05(90.1) = 455.28 Pa,

V = 10.6 m/s

Re_3 =2100

Then, critical velocity is Vc = 10.6 m/s.

REFERENCES

Anderson, C.N., Hanna, D.J., Brotherton, R.H., Brower, G.R., Carthew, G.A., Mulbarger, M.C., Playford, W.C., 2008. Chapter 19 - System Design for Sludge Pumping, in: Jones, G.M., Sanks, R.L., Tchobanoglous, G., Bosserman, B.E. (Eds.), Pumping Station Design (Third Edition). Butterworth-Heinemann, Burlington, p. 19.1-19.29. doi:https://doi.org/10.1016/B978-185617513-5.50026-3

Baudez, J.C., Megnien, J.C., Guibelin, E., 2016. Pumping of dewatered sludge: Slipping or flowing behavior? Chem. Eng. J. 295, 494–499.

Bhattacharjee, P.K., Kennedy, S.P., Xu, Q., Eshtiaghi, N., Parthasarathy, R., 2017. The influence of injection velocity and relaxation time on the spreading of tracers in viscoelastic liquids agitated by submerged, recirculating jets with low reynolds numbers. AIChE J. 63, 3132–3140.

Honey, H.C., Pretorius, W.A., 2000. Laminar flow pipe hydraulics of pseudoplastic-thixotropic sewage sludges. WATER SA 26, 19–25.

Mouzaoui, M., Baudez, J.-C., Sauceau, M., Arlabosse, P., 2018. Experimental rheological procedure adapted to pasty dewatered sludge up to 45% dry matter. Water Res. 133, 1–7.

Peixinho, J., Desaubry, C., Lebouche, M., 2008. Heat transfer of a non-Newtonian fluid (Carbopol aqueous solution) in transitional pipe flow. Int. J. Heat Mass Transf. 51, 198–209.

Shamlou, P.A., Edwards, M.F., 1985. Power consumption of helical ribbon mixers in viscous Newtonian and non-Newtonian fluids. Chem. Eng. Sci. 40, 1773–1781.

Sinnott, R.K., 2014. Chemical engineering design. Elsevier.

Slatter, P., 2008. Pipe flow of highly concentrated sludge. J. Environ. Sci. Heal. Part A 43, 1516–1520.

Slatter, P.T., 2001. Sludge pipeline design. Water Sci. Technol. 44, 115–120.

Swamee, P.K., Aggarwal, N., 2011. Explicit equations for laminar flow of Herschel–Bulkley fluids. Can. J. Chem. Eng. 89, 1426–1433.

CHAPTER 8: CONCLUSIONS AND RECOMMENDATIONS

8.1 RESEARCH CONCLUSIONS

In this chapter, the key findings, observations, and conclusions in this research work are presented in summary. Additionally, some recommendations for future work are described based on some of the observations which may have been of interest but was outside of the scope of the present study. The primary conclusions in this thesis are:

- Waste activated sludge (WAS) behaves as a non-Newtonian, shear-thinning fluid exhibiting yield stress, described by the Herschel-Bulkley rheological model. This was true for the untreated and thermally-treated (80 – 140 °C) sludge at ambient conditions. More importantly, sludge did not exhibit Newtonian behaviour at any point during thermal hydrolysis (TH), despite being subjected elevated temperature conditions. During TH, the sludge continued to exhibit non-Newtonian behaviour. Therefore, this must be considered during the design and operation of hydrothermal sludge treatment processes. Notably, this is the first time such observation has been made for WAS, since no previous work had measured sludge rheology at the elevated temperature conditions of this study.

- During TH (80 – 140 °C), the apparent viscosity, η, and Herschel-Bulkley rheological parameters (yield stress, σ_c, and consistency index, k) decreased logarithmically with time at constant temperature. This suggested that the solubilisation of sludge organics due to TH was also a time-dependent process. This progressive reduction in σ_c, η, and k during TH had not been shown before in previous works; this observation was made possible through direct measurements in situ carried out in this work. This observation provides additional insight into the kinetics of sludge solubilisation during TH and may be a useful tool in future studies. Furthermore, the η, σ_c, and k followed a linear relationship with temperature at constant treatment time. In-situ values of η, σ_c, and k during TH could be estimated for various treatment conditions using a combined model based on aforementioned relationships.

- The flow behaviour of untreated, thermally-treated, and in-situ WAS at various conditions of TH and sludge concentrations could be described using a single master flow curve. This meant a similar network of physical interactions governing its flow behaviour existed within the sludge, regardless of sludge concentration and thermal treatment condition.

- Due to TH, the η, σ_c, and k of thermally-treated sludge decreased irreversibly by upwards of 89% at ambient conditions compared to their corresponding values of untreated sludge. The extent of this reduction followed a linear relationship with treatment temperature. In all cases, η, σ_c, and k of cooled (25 °C), post-thermally treated sludge was higher than their corresponding values in situ (80 – 140 °C); the extent of this difference followed a linear relationship with temperature.

- The solubilization of sludge organics during TH showed a logarithmic time-dependent behaviour at constant temperature, as determined from measurement of chemical oxygen demand (COD) in the soluble phase of sludge. This reflects the logarithmic time-dependent reduction of η, σ_c, and k during rheological measurements under similar conditions. Accordingly, linear correlation existed between the reduction of rheological parameters (η, σ_c, and, k) and solubilization of COD. Although such correlation had been shown previously for lower-temperature thermal treatment, this was the first time this correlation was examined for TH. This supports the implication that the rheological changes due to TH were a result of disintegration of sludge's network structure. These structural components were believed to be composed of extracellular polymeric substances which are destroyed during TH and transitioned into the soluble phase as soluble COD.

- At increasing sludge concentrations, η, σ_c, and k increased following a power-law relationship. This was true for untreated sludge as well as in-situ TH sludge at all temperatures and times of treatment investigated. The fundamental actions governing the intensification of viscous forces in sludge at higher concentrations remained significant despite solubilisation of sludge components during TH. Furthermore, regardless of sludge concentration the extent and rate of η, σ_c, and k reduction was nearly constant. This means the effectiveness of sludge solubilisation due to TH was not impacted by varying sludge concentrations, which allows for more flexible choice of operating TH at higher concentrations. This has not been discussed before in earlier studies.

- Viscoelastic measurements reveal gel-like characteristics in the sludge before and after TH. However, as a result of TH the structural integrity of the thermally-treated sludge was weakened, as shown by values of storage (G') and loss (G'') moduli which decreased linearly with increasing treatment temperatures. As a result of higher TH temperatures, the loss factor (G"/G') increased which reveals a greater extent of network destruction. The frequency dependence and creep behaviour of the sludges were described using a fractional derivatives Kelvin-Voigt model (FKV)

for the first time in TH sludge. Fitting parameters of the FKV model revealed weakening elastic portion of the sludge at higher treatment temperatures.

- Viscoelastic data which are obtained via oscillatory measurements could be used to represent steady-shear data, which are traditionally obtained via rotational measurements. Plots of the dynamic viscosity, $\eta'(\omega)$, nearly overlaps with plots of the steady shear viscosity, $\eta(\dot{\gamma})$, when assuming the angular velocity was equal to shear rate (i.e. $\omega = \dot{\gamma}$). This highlights the potential for steady-shear data collection of thickened sludges and pasty material based on non-destructive oscillatory measurement. Besides that, it was possible to estimate yield stress values by multiplying G' to shift factors.

- Practical engineering implications of this study's findings were discussed and highlights the importance of careful determination of rheological parameters in optimizing unit operations.

8.2 RECOMMENDATIONS FOR FUTURE STUDIES

- The current study was focused rheological investigation on non-oxidative hydrothermal processes, namely TH. However, oxidative hydrothermal sludge treatment processes are also of interest in sludge treatment processes. These processes, such as wet oxidation, operate similar to non-oxidative processes but involve much higher treatment temperatures and simultaneous oxidation reactions in the sludge. It is of interest whether the same observations made in this study can apply to these more demanding processes. Besides that, advanced TH processes (also termed thermochemical treatment) which involve the addition of chemical reagents in TH are also of interest. These processes operate in the lower range of TH temperatures but are enhanced by chemical addition. It is of interest how these chemicals (which often increases pH) affect sludge rheology. Recent advances in rheometers (for high temperature and pressure measurements) will allow the above studies to be conducted with relative ease.

- The equations for relating the rheological changes in situ during TH were developed empirically only for the limited range of variables examined (treatment temperature, time and sludge concentration). For example, a linear model was used to describe the reduction of sludge apparent viscosity as a function of sludge temperature in this study, but this could only be true in the range of temperature examined. The more fundamental laws governing these interactions

were beyond the scope of this work and were not comprehensively studied. It is of interest whether a more robust model which incorporates fundamental kinetic models for sludge hydrolysis could be developed.

- The current study primarily quantified the organic solubilisation due to TH in terms of the bulk organic matter solubilisation. However, it was difficult to relate these to specific components in the sludge, which may or may not play a major role in sludge's rheological behaviour. It has been shown in literature that extracellular polymeric substances (EPS) plays a major role in sludge viscosity, and this is suspected to also be the case in this study. However, it would be interesting to measure changes in the EPS during TH more directly and relate these changes to rheological observations. Recent studies have shown interesting methods to quantify EPS more descriptively, such as the stratified EPS method (Yuan et al., 2017). It would be interesting to apply these methods to sludge TH.

- The rheological measurement of increasingly thickened sludges presented an ongoing challenge in this current study. Due to the pasty nature of the concentrated sludge, practical issues arose during rotational measurement and, to some extent, in oscillatory measurement. These issues included sample bifurcation and migration, in the case of parallel plate measurement geometries, and wall slippage, shear-banding, rod-climbing, and un-sheared zones, in the case of Couette-type geometries. The current study proposed one method to correlate oscillatory measurements to rotational measurements, while avoiding most of the above practical challenges. Traditionally, a Cox-Merz empirical relation, which states: $\eta^*(\omega) = \eta(\dot{\gamma})$, could be applied to most polymer solutions. As expected, this relation was inapplicable to sludge, which showed gel-like character. However, in the current study it was found an alternative correlation could be made, based on Sprigg's theory: $\eta'(\omega) \approx \eta(\dot{\gamma})$. It is of interest why this correlation is valid instead of the traditional Cox-Merz relation, and whether it also applies to other materials.

- The current study was limited to waste activated sludge, which is highly biological and organic in composition. However, there has been interest in using mixed sludges in hydrothermal processes, especially in oxidative processes. It will be of interest how a varying composition of sludge will affect its rheological behaviour and the reduction of rheological parameters during hydrothermal processing.